THE FRACTIONATION OF DEXTRAN USING ETHANOL

A Thesis submitted by
Kalwant Singh Bhambra, B.Sc.,
for the Degree of Doctor of Philosophy
to the Faculty of Engineering,
University of Aston in Birmingham

February 1985

ACKNOWLEDGEMENT

The author is indebted to the following:

Professor G.V. Jeffreys, the Head of the Department of Chemical Engineering for making available the facilities for research.

Professor P.E. Barker and the late Dr. R. Gibbs of Fisons Ltd., who supervised the work, for their help and guidance throughout this project.

Dr. M. Fidgett and members of the Separation and Purification Group for many invaluable discussions.

Mr. N. Roberts and other members of the technical staff.

Mr. R.M. Alsop, Mr. R. Travis and Mr. G. Butera of Fisons Ltd., Pharmaceutical Division for their technical advice and support.

Dr. K. Kamide of Textile Research Laboratories, Japan and Professor J. Neel of Institut National Polytechnique de Lorraine, France for providing useful literature.

For the provision of a Scholarship by the Science and Engineering Research Council and the Directors of Fisons Ltd., for their financial support.

Miss S. Mehrali of Quest Vitamins (UK) Ltd., for typing this thesis.

Finally and above all, to my family for their support and encouragement.

The University of Aston in Birmingham

The Fractionation of Dextran Using Ethanol

Kalwant Singh Bhambra (B.Sc.) Ph.D. February 1985

Summary

Reviews of molecular weight fractionation based on solubility difference and of gel permeation chromatography theories have been made.

Fractional precipitation with ethanol has to be performed at least twice to obtain clinical dextran, which is a polyglucose, from an aqueous solution of dextran having a broad molecular weight distribution. In the first stage the high molecular weight dextrans precipitate out from the solution as a syrup. In the second stage the lower molecular weight dextrans precipitate out from the remaining supernatant solution, when the ethanol concentration is increased.

For the economic optimisation of dextran fractions, a mathematical model has been proposed based on the Boltzmann equation which predicts the weight percentage dextrans in each of the two stages of fractionation, the Boltzmann equation constants C, E and the volume ratios D,F for the two-phase separation.

The aims of the project were to test this mathematical model on the laboratory-scale ethanol fractionation of dextran and also to use it to predict actual plant fractionations.

In the laboratory-scale ethanol fractionation, the comparison of results on the first stage between the model predictions and experimental values are in very good agreement. On the second stage there is an offset present between the two comparable sets of results over the entire experimental range of values. The model predicts values that are approximately 10 Wt% higher than the experimental values.

A similar pattern to that in the laboratory was found to exist between the two sets of results obtained for the plant fractionations of dextran.

The precipitation of dextran molecules on an industrial-scale was also studied and it was found that the current settling times were inadequate.

It is shown that a company producing 100 batches per annum could increase its cash flow by £200,000 per annum by using the model to predict plant fractionations.

Key Words: Gel Permeation Chromatography, Fractionation, Molecular Weight Distribution, Precipitation, Dextran.

DEDICATION

TO

My Family and my Friends

LIST OF CONTENTS

LIST OF TABLES

LIST OF FIGURES

C H A P T E R O N E

INTRODUCTION

1.0 INTRODUCTION

1.1 DEXTRAN AND ITS USES

The first chemical studies on dextrans were made about a hundred years ago, when it was found that slimes of microbial origin caused much trouble in the sugar industries. In 1874 Scheibler (1,2) found that complete acid hydrolysis of dextrans yielded only glucose and determined its empirical formula as $(C_6H_{10}O_5)_n$. The name was proposed because of the optical dextrorotation found with dextrans. Dextran is a generic name for polymers of glucose in which at least 60% of the glucosidic bonds are of the α-1,6 type.

Dextran is used in the field of medicine as (i) a blood volume restorer, and (ii) for the production of iron dextran, which is used in the treatment of anaemia (3,4).

It was in the 1940's that Ingelman and Grönwall first pioneered the clinical use of dextran as a plasma volume expander. Dextran solution made to a carefully designed specification is used in place of plasma to restore blood volume. In 1947 a 6% solution of dextran with a weight average molecular weight of 70,000, dextran 70, was introduced as a plasma substitute under the trade name Macrodex. A 10% solution of dextran with a weight average molecular weight of 40,000 (dextran 40, Rheomacrodex), was introduced in 1961 which temporarily expands plasma volume, but the main purpose of this product is to reduce blood viscosity and assist blood flow (1,5).

Another dextran fraction of lower molecular weight (2,000-3,000) is also in use. This is dried thoroughly, converted by chlorsulphonic acid to the sulphate and isolated as the sodium salt which has heparin-like anticoagulant activity.

Dextran solutions have three main advantages:

1. Because of their method of manufacture they are virus free, whereas the use of natural plasma for restoring blood volume entails some risk from virus and other infections.
2. Infusion of natural plasma adds some blood components but dextran solutions add only the polymer with glucose or sodium chloride.
3. The life of 6% solution is probably as long as that of the container in which it is stored. (This is an important property for a substance stock-piled by many governments for use in the event of a national disaster). Maycock and Ricketts (6) reported that dextrans made in 1954 had remained stable when tested after 10 years.

1.2 INDUSTRIAL MANUFACTURE OF DEXTRAN

Many different micro-organisms can produce dextrans, which often give rise to substances with differing chemical and physical properties (68). Nevertheless, they are all polyglucoses of high molecular weight.

The coccus, Leuconostoc mesenteroides, is the most commonly used micro-organism for the commercial production of dextran. Of the many different strains of micro-organism,

the Leuconostoc mesenteroides B512 strain is used for production of clinical dextran because of the minimum number of side chains, that is α-1,3 linkages, and thus a high degree of linearity with about 95% α-1,6 linkages (Fig.1.2.1), that means less side effects. Most of the side chains are more than one glucose unit long.

The Leuconostoc mesenteroides B512 bacteria has the ability to convert sucrose to dextran. The synthesis proceeds by the transfer of glucosyl groups from the sucrose to the growing dextran chain, where they are linked by α-1,6 linkages. Hehre (7) showed that the reaction obeyed the equation stoichiometrically:

$$n.\text{Sucrose} \longrightarrow \underset{\text{dextran}}{(\text{Glucose Units})_n} + n.\text{Fructose}$$

As far as is known, only the glucose part of sucrose appears in dextran. Part of the fructose is consumed by the organism, and a large part appears as a by-product. Dextran cannot be produced from glucose alone or from mixtures of glucose and fructose; sucrose is necessary.

Dextran, as produced by the bacterium, is called "native dextran" (Fig.1.2.2) and it cannot be used directly as a plasma expander. Molecular weight of native dextran ranges from several million to several hundred million, whereas material for use as an expander (clinical dextran) must have a narrow molecular weight distribution, hereafter referred to as MWD, because material with too small a molecular weight is rapidly lost from the circulation and is therefore ineffective and material with too high a molecular weight can interfere with normal coagulation

Fig. 1.2.1 Partial Structure of Dextran from L.Mesenteroides B512

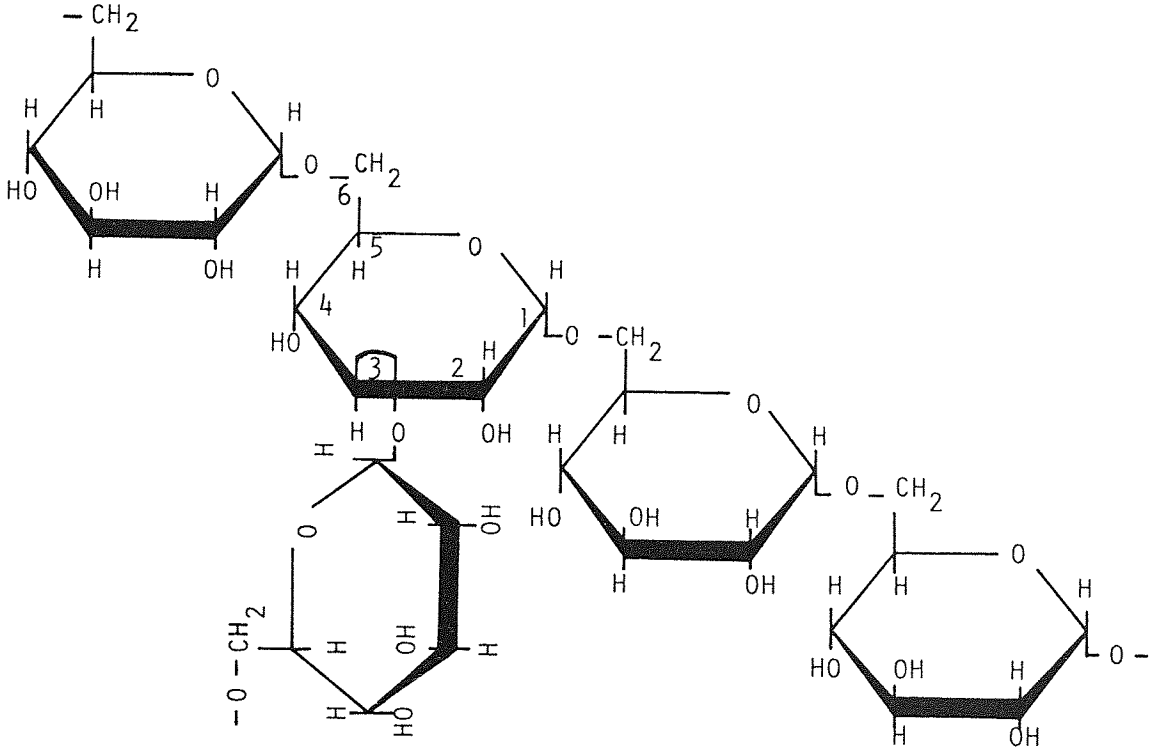

Fig. 1.2.2 Industrial Manufacture of Dextran

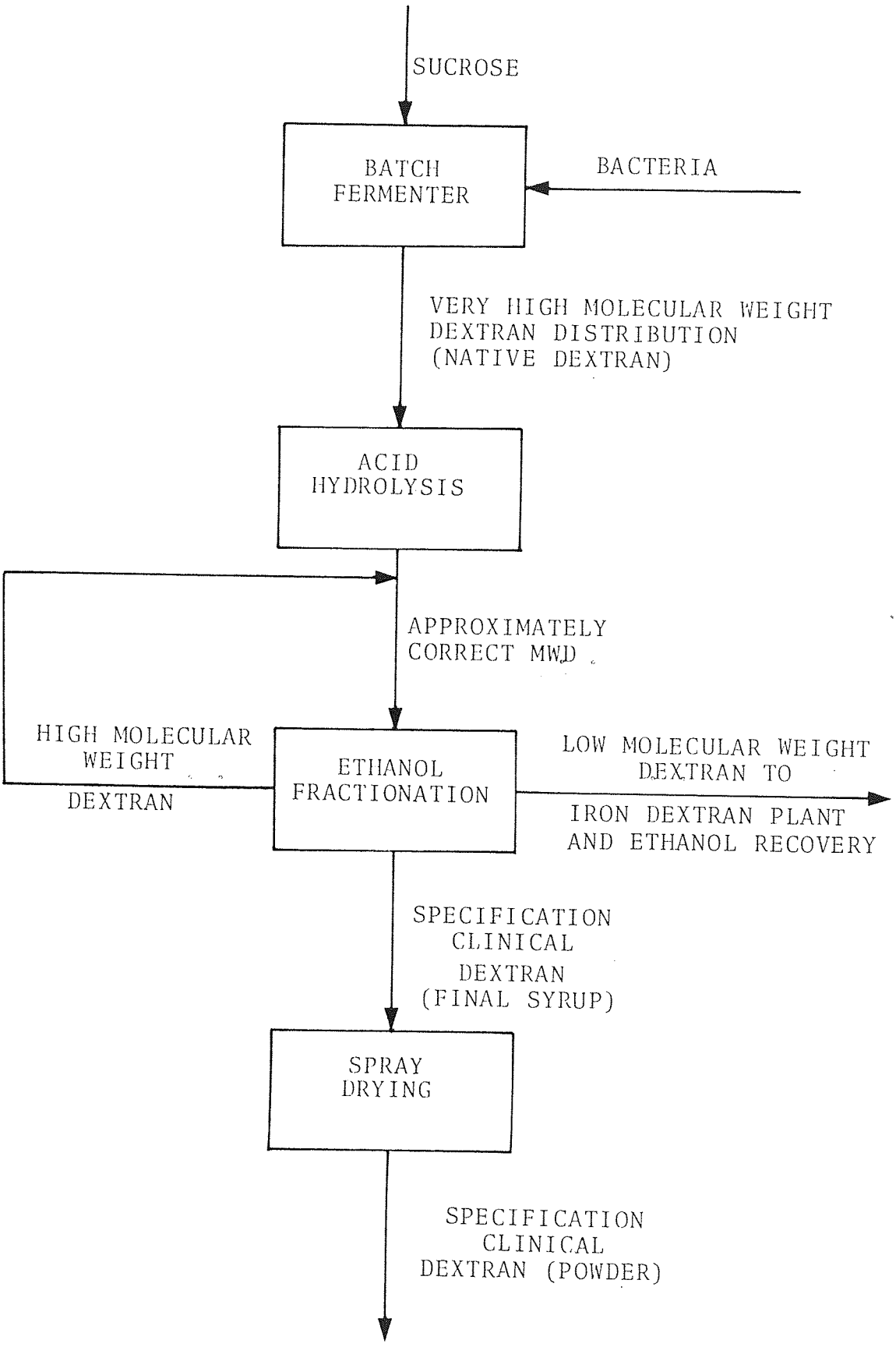

processes of the blood.

This native dextran is subjected to partial acid hydrolysis to split the higher molecular weight material into smaller fragments. Clinical dextran is separated from the hydrolysate by performing fractional precipitation with ethanol at least twice (Fig.1.2.3). Addition of ethanol to an aqueous solution of dextran results in the precipitation of the largest molecules first, the smaller molecules being precipitated when the ethanol concentration is increased. The clinical dextran after being spray-dried is then ready for storage (8-21).

Fig. 1.2.3 Clinical Dextran Separation from the Hydrolysate

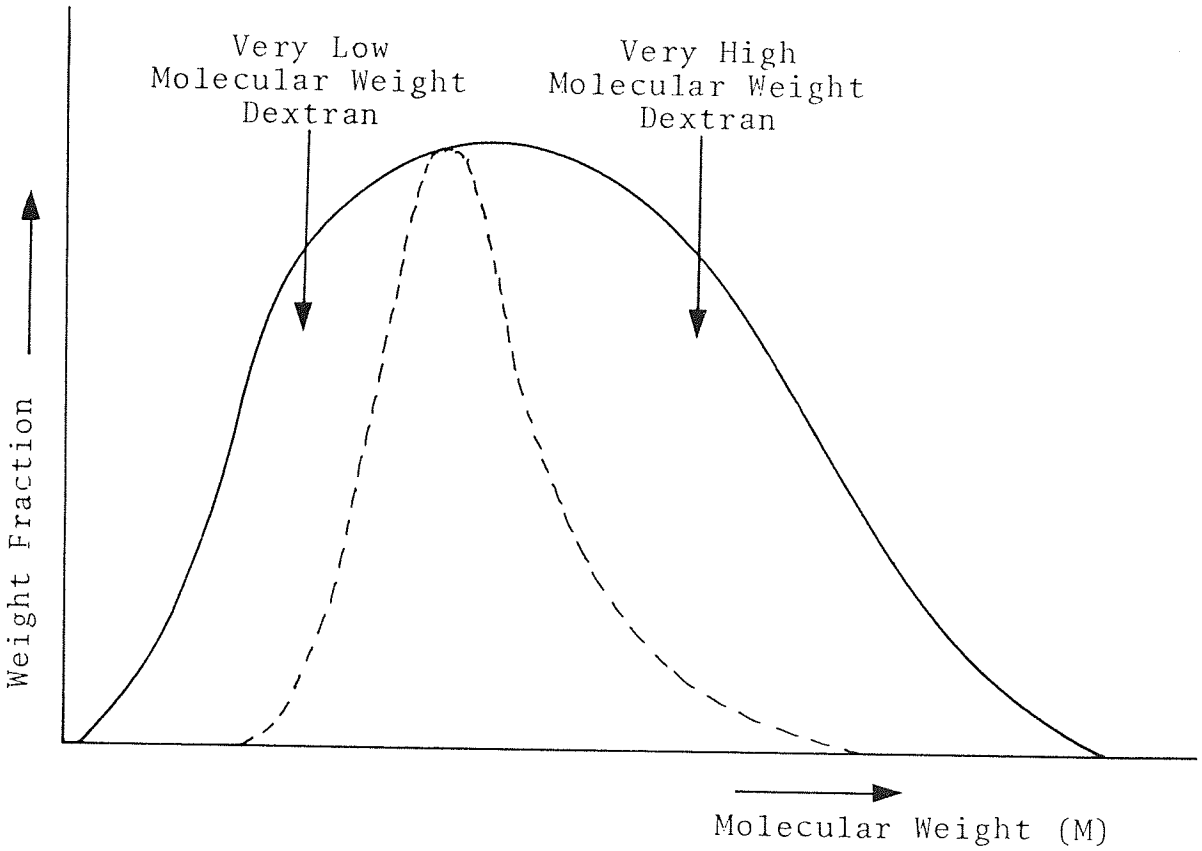

——— Dextran Hydrolysate

------ Clinical Dextran

British Pharmacopoeia Specification of Clinical Dextran 40

Molecular Weight 12,000 < 85% of Dextran < 98,000 Molecular Weight

C H A P T E R T W O

AIMS OF THE PROJECT

2.0 AIMS OF THE PROJECT

Fractional precipitation with ethanol has to be performed at least twice for obtaining clinical dextrans from dextran syrup I, (see Fig.2.1). In the first stage the high molecular weight dextrans precipitate out from the solution as a syrup. A sample of the dextrans remaining in the solution (supernatant) is then examined by Gel Permeation Chromatography (GPC), to check whether the MWD is that required to proceed for the manufacture of clinical dextran. If this is not the case, the alcohol concentration is changed by addition of either alcohol or water and the process repeated until the MWD of dextran in the solution as measured by GPC is satisfactory. The same procedure is carried out for precipitating the lower molecular weights.

It can clearly be seen that the above process is a trial and error method, it also relies on the judgement of a skilled analyst to interpret the chromatographic data and decide when it is justifiable to proceed to the next fractionation. Often more ethanol is used for precipitation than necessary, so that repetition is avoided (this is obviously not economical due to the high cost of ethanol), and also the yield of clinical dextrans is lowered by use of excess ethanol. Another disadvantage is that the MWD's at each stage of the fractionation process have to be determined before the next stage can be started.

For the economic optimisation of dextran fractions, a mathematical model has been proposed by Gibbs (22) which predicts the weight percentage (Wt %) dextrans in each

Fig. 2.1 Fractionation of Dextran using Ethanol

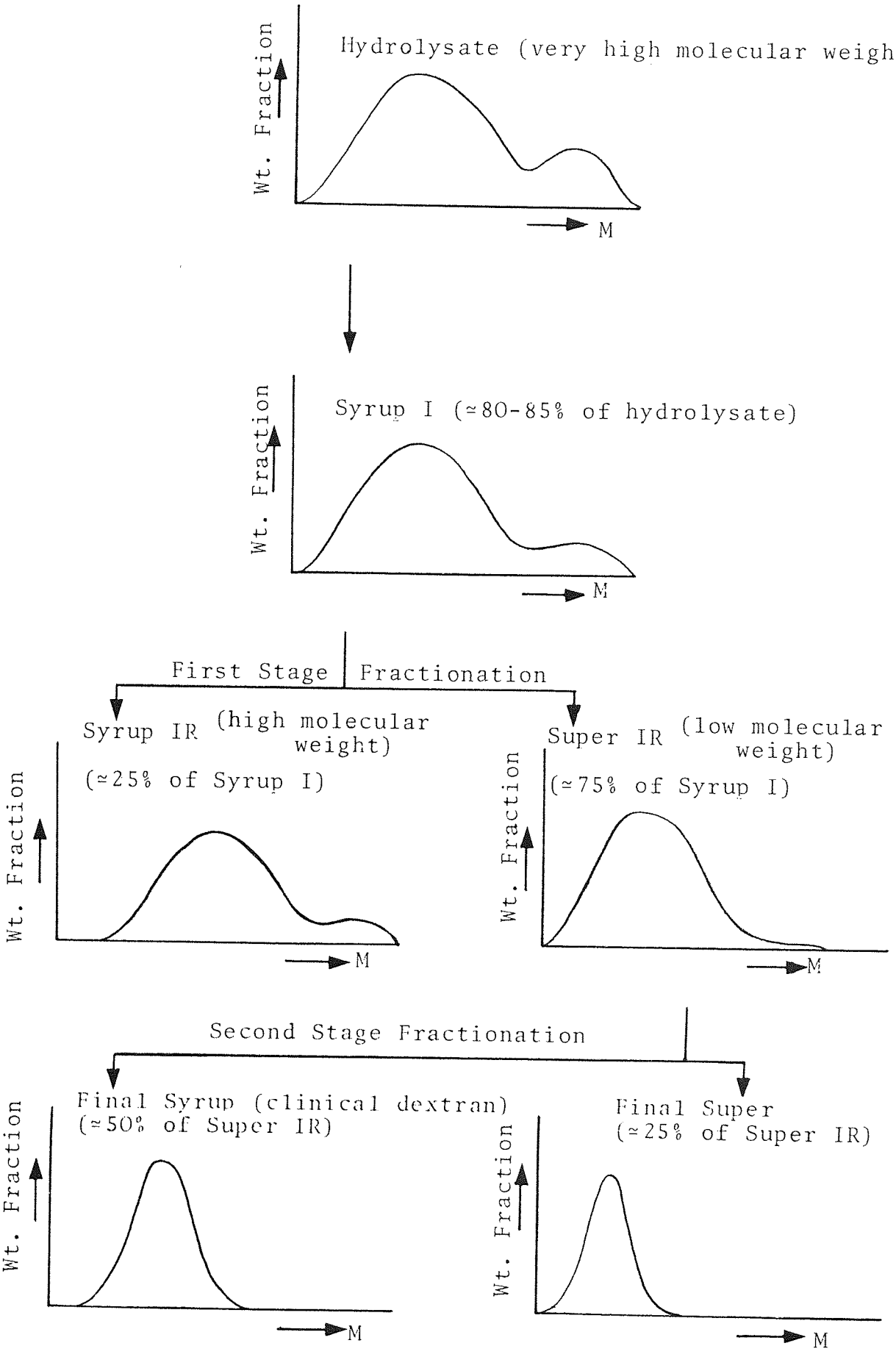

stage of the fractionation and ratios of the volumes for the two-phase separation. The objective of this project was to test this model and use it to predict actual plant fractionations. The model requires only the starting MWD of dextran prior to fractionation measured by GPC and the target MWD of clinical dextran, the latter is known from previous fractionations in which the MWD of clinical dextrans has been measured by GPC.

The use of this mathematical model to simulate the fractionation process would have several advantages:

1. It would remove the need for judgement in deciding how to adjust the fractionation if the MWD by GPC is different to that required.
2. It may remove the requirement to determine the MWD at each stage of the fractionation.
3. It would enable the existing methods of fractionations to be optimised to give the narrowest MWD for the minimum cost.
4. It would enable new methods of fractionation to be investigated, to examine whether yields can be improved and ethanol usage reduced, whilst the molecular weight and MWD remained unchanged.

C H A P T E R T H R E E

LITERATURE SURVEY

3.0 LITERATURE SURVEY

3.1 MOLECULAR WEIGHT FRACTIONATION BASED ON SOLUBILITY DIFFERENCES

A polymer is a compound each molecule of which is formed (except for end groups) of a given number of structural units closely related to the molecules of the monomer (or monomers) from which the polymer is derived. It has, therefore, like other covalent compounds, a molecular weight; if its molecular weight is very large, it is a "high" polymer. Many high-polymeric substances are known, and as a class they are of great and increasing importance; yet high polymers in pure form are not known. Both the natural and synthetic high-polymeric substances are mixtures; individual molecules may differ in size (i.e. in the number of repeating units, or, as it is often called, the degree of polymerisation), in shape (i.e. in the degree of branching or cross-linking), and even in chemical composition.

High-polymeric systems may, however, be homogeneous in all respects but molecular size. The term "homologous polymeric series" had been introduced in the late 1930's for a series of linear (unbranched) polymers whose members differed in the degree of polymerisation but not in chemical composition. Many high-polymeric substances are found to be mixtures of members of such homologous polymeric series.

The fact that high polymers are heterogeneous is of tremendous importance; to their very heterogeneity they owe many of the properties that make them so interesting

and useful. But it is important to realise that, being non-uniform, they are infinitely variable. The MWD of a high polymer, for example, may vary from sample to sample; with natural products it depends on the source of the material, with synthetics on the method of preparation, and with both on previous treatment such as purification, bleaching (of cellulose), or milling (of rubber).

If a polymer is ideally monodisperse, the polydispersity (a measure of the breadth of a MWD) is unity. This value increases as the polydispersity increases. Of course, for a fixed polydispersity, there can be an infinite number of different types of MWD's (103).

Fractionation is carried out to reduce the polydispersity of high polymers, either for the purpose of evaluating the degree of polydispersity or for the preparation of samples of reduced polydispersity. The usual procedures for polymer fractionation involve the distribution of the polymer molecules between two phases. Fractionation results because of differences in the distribution for the molecules of different sizes or structures.

Fractional precipitation, which is now the most widely used fractionation method, was at first used for the purpose of purification and only later for the separation of fractions.

Fractional solution methods, although claimed by some to be superior to precipitation, have never come into such wide use.

Other methods such as those involving ultracentrifugation

or chromatographic adsorption have been used, but they are of much less general applicability. The ultracentrifuge has been shown to be well suited to analytical determination of hetrogeneity, but cost and complexity have limited its use.

The solubility methods for fractionating heterogeneous high-polymeric substances depend on the greater solubility in a given liquid of the lower-molecular weight species, and on the fact that the solvent power of a binary liquid mixture (of solvent and non-solvent) depends on the proportion of the two liquid components. If a non-solvent (also often called the precipitant) is added to a polymer-solvent system, as in fractional precipitation, or a polymer is added to a solvent - non solvent mixture, as in fractional solution, two phases are obtained at equilibrium, if the proportions of the components are properly adjusted. The upper layer is a solution in which the polymer is present in low concentration; the lower layer, or "precipitated" phase, is either a swollen gel or a very viscous liquid, and contains a high proportion of the polymer. The material of higher molecular weight tends to concentrate in the precipitated phase (or the syrup phase), that of lower molecular weight in the supernatant liquid.

One of the earliest theories of solubility fractionation was that of Bronsted (102). He suggested that the distribution of large polymers between two phases would be determined almost entirely by the difference of potential energy between them. The less mobile large molecules collecting in the phase with the lower potential energy

(the precipitated phase), the smaller and more mobile ones in the supernatant liquid. At equilibrium, a relationship between the concentration ratio and difference of potential energy can be expressed as follows:

$$\frac{C_1}{C_2} = \exp\left(\frac{E}{KT}\right) \quad \text{..... 3.1.1}$$

where C_1 and C_2 are the concentrations in the bottom and top phases respectively, E is the difference in potential energy, T the temperature, K the Boltzmann's constant.

Bronsted assumed that the difference in potential energy was proportional to the molecular weight (M) of the polymer. He suggested the following equation:

$$\frac{C_1}{C_2} = \exp\left(\frac{\lambda M}{KT}\right) \quad \text{..... 3.1.2}$$

where λ is a constant characteristic of the solvent-polymer system but independent of M. If M is large it is readily seen that the ratio C_1/C_2 may assume extreme values. Considering λ as continuously variable along a series of liquids, it is clear that, as λ decreases through zero and becomes negative, the distribution undergoes a sudden change of character. With $\lambda>0$, $C_1/C_2 \to \infty$, and the liquid is practically a non-solvent; with $\lambda<0$, $C_1/C_2 \to 0$, and the liquid is a perfect solvent.

Schulz (101,104,105) developed these ideas further by assuming that in the case of binary liquid mixtures λ is a linear function of the liquid composition and showed that the equation

$$\gamma^* = A + B/M \quad \text{..... 3.1.3}$$

adequately expresses the relationship between γ^*, the

"critical" liquid composition at the precipitation point, and the molecular weight, M, of the polymer; A and B are empirical constants. He also applied the theory to heterogeneous polymers, using a rather arbitrary modification of equation 3.1.2, and concluded that the efficiency of fractionation is improved by keeping the concentration of polymer in the supernatant phase as low as possible.

The Bronsted-Schulz theory was remarkably successful in predicting the solubility behaviour of several high-polymer solutions. However, it was soon suspected that the entropy of mixing of polymer and solvent molecules was a factor of importance, which was ignored by Bronsted and Schulz assuming that the free energy changes were determined entirely by the heat term.

The free energy relations of high polymer solutions were first calculated independently by Flory (112,116) and Huggins (113) for the case of a homogeneous chain polymer of uniform molecular weight in a single uniform solvent. In practice, however, one is never dealing with a polymer sample in which all the molecules have the same molecular weight, but rather with a mixture of molecular weights, forming a virtually continuous distribution. If, on the other hand, one intends to extend the treatment of such solutions to the problems of fractionation and precipitation it is of interest to extend the treatment to a solvent medium consisting of a mixture of two pure solvents.

Scott and Magat (114,115) extended the theory to the above two cases and also gave a thermodynamic treatment

of solubility, fractionation and precipitation. They found that the partial molal free energies of mixing of a heterogeneous polymer in a mixture of solvent may be represented as:

$$\overline{\Delta G}_1 = RT\{\ln(1-V_2) + V_2(1-\frac{1}{\bar{x}_n}) + \mu V_2^2\} \quad \ldots\ldots\ldots \quad 3.1.4$$

where

$\overline{\Delta G}_1$ = partial molal free energy of mixing of the solvent

R = gas constant

T = absolute temperature

V_2 = volume fraction of all polymer molecules

$\bar{x}_n$ = number average molecular size (α weight)

μ = constant for any given system, consisting of the heat of mixing and a term from the entropy (polymer/solvent interaction parameter)

$$\overline{\Delta G}_i = RT\{\ln V_i - (x-1) + V_2 x(1-\frac{1}{\bar{x}_n}) + \mu x(1-V_2)^2\} \quad .. \quad 3.1.5$$

where

$\overline{\Delta G}_i$ = partial molal free energy of mixing of the ith fraction of the polymer

V_i = volume fraction of the ith fraction ($V_2=\Sigma V_i$)

x = the ratio of the molecular volume of the polymer molecule of molecular weight M_i and the molecular volume of the solvent $\bar{V}_1$ or $x=M_i/\rho\bar{V}_1$.

If ρ, the density of the polymer is considered as independent of the chain length, then x is, for any given solvent, directly proportional to and therefore a measure of the molecular weight.

The solubility at any other point than the critical may be determined by use of the condition for equilibrium between the two phases - namely, that the partial molal free energy of each constituent is the same in both phases. Using primes to signify quantities referring to the precipitated phase, the conditions for equilibrium can be expressed as follows:

$$\overline{\Delta G}_1 = \overline{\Delta G}_1' \quad \ldots\ldots\ldots\ldots\ldots\ldots\ldots\ldots\ldots\ldots \quad 3.1.6$$

$$\overline{\Delta G}_i = \overline{\Delta G}_i' \quad \ldots\ldots\ldots\ldots\ldots\ldots\ldots\ldots\ldots\ldots \quad 3.1.7$$

Substituting from equations 3.1.4 and 3.1.5 gives

$$\ln(1-V_2)+V_2\left(1-\frac{1}{\bar{x}_n}\right)+\mu V_2^2 = \ln(1-V_2')+V_2'\left(1-\frac{1}{\bar{x}_n'}\right)+\mu V_2'^2 \quad \ldots \quad 3.1.8$$

$$\ln V_i-(x-1)+V_2x\left(1-\frac{1}{\bar{x}_n}\right)+\mu x(1-V_2)^2 = \ln V_i'-(x-1)+V_2'x\left(1-\frac{1}{\bar{x}_n'}\right) + \mu x(1-V_2')^2 \quad \ldots\ldots\ldots \quad 3.1.9$$

Equation 3.1.9 can be written as

$$\ln\left(\frac{V_i'}{V_i}\right) = \alpha x \quad \ldots\ldots\ldots\ldots\ldots\ldots\ldots\ldots\ldots\ldots \quad 3.1.10$$

where

$$\alpha = V_2\left(1-\frac{1}{\bar{x}_n}\right) - V_2'\left(1-\frac{1}{\bar{x}_n'}\right) + \mu\{(1-V_2)^2-(1-V_2')^2\} \quad \ldots\ldots \quad 3.1.11$$

The above equations were also obtained by Flory (117). Equation 3.1.10 was simplified further by Scott (115) by solving for $\ln(V_i'/V_i)$ and substituting from equation 3.1.8, the following expression is obtained.

$$\ln\left(\frac{V_i'}{V_i}\right) = x\{2\mu(V_2'-V_2) - \ln\left(\frac{1-V_2}{1-V_2'}\right)\} \quad \ldots\ldots\ldots\ldots\ldots\ldots \quad 3.1.12$$

$$\text{or} \quad \ln\left(\frac{V_i'}{V_i}\right) = Ax \quad \ldots\ldots\ldots\ldots\ldots\ldots\ldots\ldots\ldots\ldots \quad 3.1.13$$

where

$$A = 2\mu(V_2'-V_2) - \ln\left(\frac{1-V_2}{1-V_2'}\right) \quad \text{..... 3.1.14}$$

These equations were also reported by Sayre (118). The constants α and A from equations 3.1.10 and 3.1.13 respectively are obviously identical. These equations were first proposed theoretically for a polymer-single solvent system but they were found to be also applicable to a polymer-solvent-nonsolvent system (119).

For a homogeneous polymer the partial molal free energies may be represented as (120):

$$\overline{\Delta G}_1 = RT\{\ln(1-V_2) + V_2\left(1-\frac{1}{x}\right) + \mu V_2^2\} \quad \text{..... 3.1.15}$$

which differs from equation 3.1.4 only in the replacement of $\bar{x}_n$ by x. The partial molal free energy of the polymer (N.B. not the ith fraction as in the heterogeneous case) is represented as:

$$\overline{\Delta G}_2 = RT\{\ln V_2-(x-1)(1-V_2) + \mu x(1-V_2)^2\} \quad \text{..... 3.1.16}$$

where

$\overline{\Delta G}_2$ = partial molal free energy of mixing of the polymer. It is interesting to notice that equation 3.1.5 reduces to the homogeneous polymer equation 3.1.16 when $V_i = V_2$ and $\bar{x}_n = x$.

As before the conditions for equilibrium can be expressed as follows:

$$\overline{\Delta G}_1 = \overline{\Delta G}_1' \quad \text{..... 3.1.17}$$

$$\overline{\Delta G}_2 = \overline{\Delta G}_2' \quad \text{..... 3.1.18}$$

the precipitated phase quantities are signified by the primes. Substituting from equations 3.1.15 and 3.1.16 gives:

$$\ln(1-V_2)+V_2(1-\frac{1}{x})+\mu V_2^2 = \ln(1-V_2')+V_2'(1-\frac{1}{x})+\mu V_2'^2 \quad \ldots\ldots \quad 3.1.19$$

$$\ln V_2-(x-1)(1-V_2)+\mu x(1-V_2)^2 = \ln V_2'-(x-1)(1-V_2')+\mu x(1-V_2')^2 \quad \ldots\ldots\ldots\ldots\ldots\ldots \quad 3.1.20$$

Solving for $\ln(V_2'/V_2)$ and substituting from equation 3.1.19, the following expression is obtained:

$$\ln\frac{V_2'}{V_2} = x\{2\mu(V_2'-V_2) - \ln(\frac{1-V_2}{1-V_2'})\} \quad \ldots\ldots\ldots\ldots \quad 3.1.21$$

the right hand side of the above equation is identical with equation 3.1.12 which was derived for a heterogeneous polymer. The only difference in other words is in the left hand side of the equations, for a homogeneous polymer it is expressed by the volume fraction of all polymer molecules (V_2), whereas for a heterogeneous polymer it is expressed by the volume fraction of the ith fraction (V_i).

Kamide and his collaborators (121-126) have studied the successive precipitational, solutional fractionation (SPF & SSF) of macromolecules on the basis of the Flory-Huggins solution theory. The authors have extensively developed a simulative technique for the investigation of the effects of the fractionation conditions, such as the size of the fraction and the initial concentration and of the analytical procedures for evaluating the size distribution in the original polymer from the fractionation data.

The Flory-Huggins theory assumes that the polymer/solvent interaction parameter, μ, is only a function of

temperature and independent of the concentration. Contrary to this assumption, the value of μ obtained from the experiments often depends considerably on the concentration, as suggested by Kamide and co-workers. An attempt has been made to examine the effect of the concentration dependence of μ on phase separation of polydisperse polymers in a single solvent by Kamide et al (121-124).

According to Kamide et al the polymer/solvent interaction parameter, μ, is related to the volume fraction of the polymer (V_2) by the expression:

$$\mu = \mu_o(1 + pV_2) \quad \ldots\ldots\ldots\ldots\ldots\ldots\ldots \quad 3.1.22$$

where

μ_o = a constant

p = a parameter representing concentration dependence of μ

The equations 3.1.4 and 3.1.5 should now be written as:

$$\overline{\Delta G}_1 = RT\{\ln(1-V_2) + V_2(1-\frac{1}{\bar{x}_n}) + \mu_o(1+pV_2)V_2^2\} \quad \ldots\ldots\ldots \quad 3.1.23$$

and

$$\overline{\Delta G}_i = RT\{\ln V_i - (x-1) + V_2 x(1-\frac{1}{\bar{x}_n}) + \mu_o x(1-V_2)^2 + \mu_o px(0.5-1.5V_2^2+V_2^3)\}$$

$$\ldots\ldots\ldots\ldots\ldots\ldots \quad 3.1.24$$

Repeating the process of equations 3.1.6 and 3.1.7 for thermodynamic equilibrium gives:

$$\ln(\frac{V_i'}{V_i}) = \sigma x \quad \ldots\ldots\ldots\ldots\ldots\ldots\ldots \quad 3.1.25$$

where σ is the partition coefficient given by:

$$V_2(1-\frac{1}{\bar{x}_n})-V_2'(1-\frac{1}{\bar{x}_n'})+\mu_o\{2(V_2'-V_2)+V_2^2-V_2'^2\}+\mu_o p\{V_2^3-V_2'^3-1.5(V_2^2-V_2'^2)\}$$

..... 3.1.26

By taking p as zero, from equation 3.1.22 it can be seen that $\mu=\mu_o$, equations 3.1.23 and 3.1.24 therefore reduce to the corresponding well-known equations 3.1.4 and 3.1.5 in which the concentration dependence of μ was completely ignored.

The simulation results of Kamide et al (122-124) agreed well with the experimental results provided the concentration dependence of the thermodynamic interaction parameter in the theory of Flory-Huggins was taken into consideration. It should be however noted that the experimental normalised MWD curves of the fractions separated by SPF & SSF did not agree very well with the theoretical curves, see Fig.20.(122) and Fig.3.(123).

Kamide et al (122) showed that the partition coefficient σ depended slightly on molecular weight. The authors then introduced the concept of molecular weight and concentration-dependence of the polymer/solvent thermodynamic interaction parameter to the previous theory. In this theory the interaction parameter is expressed by:

$$\mu = \mu_{oo}(1+k/x)(1+pV_2) \quad \text{..... 3.1.27}$$

where

μ_{oo} = a constant independent of both polymer molecular weight and concentration

k = the molecular weight dependence coefficients

As before when the two phases are in thermodynamic equilibrium the following expression is obtained:

$$\ln\left(\frac{V_i'}{V_i}\right) = \sigma x \quad \ldots\ldots\ldots\ldots\ldots\ldots\ldots\ldots \quad 3.1.28$$

which is similar to equation 3.1.25 except that σ is a much more complicated parameter expressed as:

$$V_2\left(1-\frac{1}{\bar{x}_n}\right)-V_2'\left(1-\frac{1}{\bar{x}_n'}\right)+\mu_{oo}\{(1+\frac{k}{\bar{x}_n})\{(1-V_2)^2+p(0.5-1.5V_2^2+V_2^3)\}$$

$$-(1+\frac{k}{\bar{x}_n'})\{(1-V_2')^2+p(0.5-1.5V_2'^2+V_2'^3)\}+k(\frac{1}{x}-\frac{1}{\bar{x}_n})\{(1-V_2)+0.5p(1-V_2^2)\}$$

$$-k(\frac{1}{x}-\frac{1}{\bar{x}_n'})\{(1-V_2')+0.5p(1-V_2'^2)\}\} \quad \ldots\ldots\ldots\ldots\ldots\ldots \quad 3.1.29$$

By putting k=0 we obtain the previously derived equation 3.1.26. Kamide et al (125) concluded that the molecular weight dependence of the μ-parameter has only a minor effect when compared with its concentration dependence, on the phase-separation phenomenon of polymer solutions.

Breitenbach and Wolf (127) derived the equation:

$$\ln\left(\frac{V_i'}{V_i}\right) = \ln B_1 + B_2 x \quad \ldots\ldots\ldots\ldots\ldots\ldots\ldots\ldots \quad 3.1.30$$

Comparison of equation 3.1.28 with 3.1.30 leads to:

$$\sigma = B_2 + (\ln B_1)/x \quad \ldots\ldots\ldots\ldots\ldots\ldots\ldots\ldots \quad 3.1.31$$

this equation is principally equivalent to equation 3.1.29.

It must however be mentioned that the solubility equations of these authors have one common characteristic, in that the solubility is proportional to the exponent of molecular weight.

In the field of biochemistry and physiology Albertsson (106-109) has studied the distribution of biological macromolecules and cell particles between the two phases

in mixed polymer systems. For the phase system of dextran, methylcellulose and water, Albertsson (108) showed that the distribution of protein particles approximately followed the Bronsted relation (equation 3.1.2), in the version where the particle surface area was introduced instead of the molecular weight. It was also pointed out by Bronsted (102) that for large particles, e.g. of cellular dimensions, the molecular weight in the formula should then be replaced by the surface area of the particles.

Albertsson found good agreement with theory for globular proteins, the logarithm of the C_1/C_2 value being approximately proportional to molecular weight raised to the two-third power, which in turn is approximately proportional to the surface area of the molecules when the molecular weight in the Bronsted relationship was replaced by the surface area of the molecules (108). The above relationship between molecular weight and surface area was also obtained by Pharmacia Fine Chemicals (111); they found that for globular proteins the Stokes' radius (r) was related to the molecular weight (M) by the following expression:

$$r = 0.4898\ M^{0.378} \quad \ldots\ldots\ldots\ldots\ldots\ldots\ldots\ldots \quad 3.1.32$$

which would therefore make the surface area approximately proportional to $M^{0.756}$. For dextran the Stokes' radius was given by:

$$r = 0.263\ M^{0.48} \quad \ldots\ldots\ldots\ldots\ldots\ldots\ldots\ldots \quad 3.1.33$$

If dextran was to be assumed global (in fact they randomly coiled in solution) then the surface area would be approximately proportional to $M^{0.96}$ (i.e. make little change if the molecular weight was replaced by the surface area).

Frick and Lif (110) found that DNA of different molecular weights prepared from Escherichia coli distribute in agreement with the Bronsted relationship between the phases of a sodium dextran sulfate-methylcellulose aqueous system.

3.2 FRACTIONATION METHODS

Many methods have been used for the fractionation of high-polymeric substances, but some are much more generally useful than others.

Some of the methods available are:

1. Solubility Methods

(a) Fractional Precipitation

This is where the heterogeneous polymer is completely dissolved in a suitable liquid and then partially "precipitated". The precipitated phase, which contains the high-molecular-weight fraction, and the supernatant solution are separated. The procedure is repeated to precipitate more of the polymer.

There are two principal ways in which precipitation can be effected and these will be considered separately: (i) by adding a precipitant (non-solvent) isothermally; (ii) by lowering the temperature, keeping the total composition constant. A combination of the two can, of

course, be used.

(i) Fractional Precipitation by the Addition of a Precipitant

In this method fractionation is effected by adding to a solution of the polymer a suitable amount of precipitant, enough to cause separation into two phases, but not enough to cause precipitation of all the polymer present; the phases are then separated, and the procedure repeated with the supernatant liquid, until all the polymer has been precipitated (material of very low molecular weight may remain in solution even when excess precipitant has been added, but the amount is usually not large).

Dextran is fractionated by this method, the precipitant most often used is ethanol although methanol and acetone have been used before in industry. Ethanol is favoured because of the poisonous property of methanol and high volatility of acetone (3,15-17,20).

(ii) Fractional Precipitation by Cooling

The precipitation point of a polymer-solvent-precipitant system depends very markedly on the temperature; rather careful control of temperature during a fractional precipitation is therefore necessary. This temperature dependence of solubility is used in carrying out fractionations.

(b) Fractional Solution

In this method the polymer is placed in contact with a solvent-non-solvent mixture, and the system is allowed to come to equilibrium; after the supernatant solution is separated, the residue is treated with a fresh mixture, richer in solvent than the first, this process is repeated until the polymer has all dissolved, or until no more will

dissolve. In this way the low-molecular fractions are extracted first, the high-molecular ones last.

(c) Distribution between two Immiscible Solvents

In precipitation and solution methods, the solvent and non-solvent are completely miscible; only the presence of a polymer (in amounts above the critical value) causes a separation into two phases. It is also possible, however, to use a solvent system which is heterogeneous even in the absence of the polymer. The distribution of the polymer molecules in such a system depends on molecular weight, a fractionation can, therefore, be accomplished by varying the composition of one of the phases.

2. Chromatographic Fractionation

Barker and co-workers (33,37,45-48) have been investigating the fractionation of dextran hydrolysate using GPC for the last ten years in association with Fisons Pharmaceutical Division, Holmes Chapel.

GPC is a form of liquid chromatography based on the unique properties of the gels (porous silica, agarose, etc) for separating polymers, primarily on the basis of molecular size. Since dextran molecules are of different sizes, GPC is therefore useful for fractionating dextran.

3. Ultrafiltration (UF)

It is often possible to separate particles of different sizes by ultrafiltration through carefully graded membranes. This separation is based on a sieving action; ideally the pore sizes are chosen in such a way that particles up to certain size can pass, but larger ones cannot.

Vlachogiannis (37,128) used ultrafiltration to remove some of the silica present in the dextran solutions (introduced initially because of the dissolution of the chromatographic packing). It was found that ultrafiltration was not only useful in removing silica but could also be used for the fractionation and concentration of dextran solutions. To meet clinical requirements any remaining silica was successfully removed by appropriate ion exchange media.

4. Combined GPC, UF and Ion Exchange to Fractionate and Concentrate Dextran Polymer Solutions

Alsop et al (129) studied the possibility of a new process to produce clinical dextran 40 from dextran hydrolysate.

The process was one that combined GPC for removing the very high molecular weight dextran, ultrafiltration to remove the very low molecular weight dextran, concentrate the dextran solution and to remove most of the silica present in the final product. Finally to produce a silica-free dextran product a mixed bed ion exchange cartridge was used.

The final product of this process was within the British Pharmacopoeia specification. More than 85% of the material had a molecular weight between 12,000 and 98,000 daltons and the amount of silica present in the final product was negligible.

3.3 ANALYTICAL GEL PERMEATION CHROMATOGRAPHY

3.3.1 INTRODUCTION TO GEL PERMEATION CHROMATOGRAPHY

Gel permeation chromatography was first introduced by Moore (23) in 1964, as a technique for separating synthetic polymers soluble in organic solvents. With this event conventional GPC was born. It was immediately recognised that, with proper calibration, GPC was capable of providing molecular weight and MWD information for synthetic polymers. Since these quantities were difficult to obtain by other methods (i.e. light-scattering, ultra-centrifugation, osmometry and functional group analysis) GPC came rapidly into extensive use (24). GPC has grown at a fast rate both in technical sophistication and in the scope of application when it was made practical around 1964. It has now gained a key position in polymer chemistry.

GPC is the newest of the four modes of elution chromatography (i.e. liquid-liquid, liquid-solid, ion exchange and gel chromatography) and it has been stated to be the easiest to use and to understand (25).

GPC is a form of liquid chromatography where solute molecules are retarded by their ability to permeate into the solvent-filled pores of the packing material. Thus GPC is really a special case of liquid chromatography. The separation is found to be dependent on molecular size, although other more complex physical effects may also be involved to an extent dictated by the nature of the gel system employed and the system of solutes under investigation. Such effects are undesirable and can often, but not always, be minimised by careful design of the

chromatographic system used. Speculation as to the exact mechanism involved in GPC has led to various alternative names, e.g. gel chromatography, gel filtration, exclusion chromatography, molecular sieve chromatography and restricted diffusion chromatography.

3.3.2 THE PRINCIPLE OF GEL PERMEATION CHROMATOGRAPHY

Basically, any soluble molecules can be separated by GPC, small ones of less than 100 molecular weight as well as large ones of several millions molecular weight.

The separation is usually carried out on columns that are tightly packed with a gel or some other porous material (stationary phase) of variable pore size and completely filled with solvent. The same solvent is used to dissolve the sample before introducing it into the column and also for elution (mobile phase or eluent).

The mobile phase flows through the interstitial regions and the solute molecules travel only through the column when they are in these regions. Solute molecules permeating into the pores are retarded, and the more time molecules spend in the pores, the more they are retarded.

Large molecules which are completely excluded are thus eluted first, and small molecules which can penetrate the pores freely are eluted last.

A species is eluted at a volume equal to the volume available to it in the column. For large, completely excluded molecules, the elution volume V_R is equal to the void volume V_o and for small molecules which can completely penetrate all pores of the gel it is equal to the total

liquid volume V_t of the column, i.e. equal to the sum of V_o and the internal (pore) volume V_i. For intermediate molecules the elution volume is dependent on the pore volume accessible to the species, V_{iAcc} and is given by:

$$V_R = V_o + K_d V_i \quad \ldots\ldots\ldots\ldots\ldots\ldots\ldots \quad 3.3.1$$

where K_d is the distribution coefficient, that is defined as:

$$K_d = \frac{V_{iAcc}}{V_i} \quad \ldots\ldots\ldots\ldots\ldots\ldots\ldots \quad 3.3.2$$

Alternatively, Equation 3.3.1 may be written:

$$V_R = V_o + K_d(V_t - V_o) \quad \ldots\ldots\ldots\ldots\ldots\ldots \quad 3.3.3$$

The values of K_d for GPC should ideally be equal to or between 0 and 1.

Equation 3.3.1 is illustrated schematically in Fig.3.3.1.

The height of an equivalent theoretical plate (HETP) and the number of theoretical plates in a column (N) are parameters widely used in chromatography to describe the efficiency of a column. There are several methods available for measuring N defined as V_R^2/σ^2. Calculation of σ^2 is too tedious for hand calculation and usually is best done by computer. However, if the peaks are symmetrical and close to Gaussian shape N can be expressed in variables that are more easily measured experimentally. The most commonly used approximations are:

$$N = 16\left(\frac{V_R}{W_b}\right)^2 \quad \ldots\ldots\ldots\ldots\ldots\ldots\ldots \quad 3.3.4$$

where W_b is the baseline width formed by tangents of the peak intersecting the baseline (approximately 4σ).

Fig. 3.3.1 Illustration of the GPC Fractionation Process

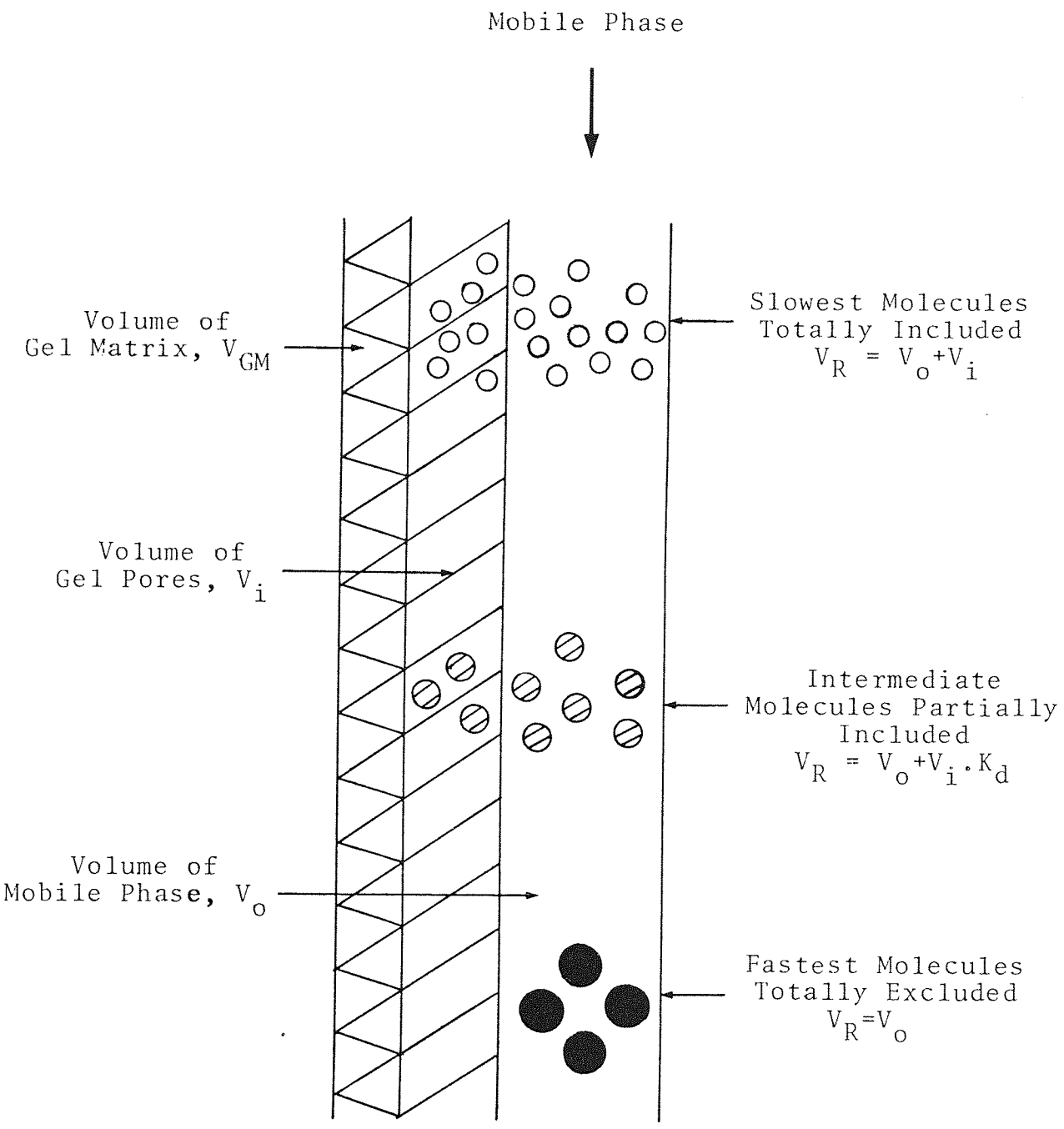

$$N = 5.54\left(\frac{V_R}{W_{\frac{1}{2}}}\right)^2 \quad \text{..... 3.3.4.a}$$

where $W_{\frac{1}{2}}$ is the peak width at one-half the peak height (see Fig.3.3.2).

$$HETP = \frac{L}{N} \quad \text{..... 3.3.5}$$

where L is the length of the packed column.

Another widely used parameter to describe the condition of a column is the asymmetry factor. The asymmetry factor (A_s) of a column is calculated by one-tenth the peak height (see Fig.3.3.2.a).

$$A_s = \frac{b}{a} \quad \text{..... 3.3.6}$$

Giddings (26) developed an expression to give the approximate number of peaks, ϕ, that may be resolved on a column as a function of N:

$$\phi = 1 + 0.2N^{\frac{1}{2}} \quad \text{..... 3.3.7}$$

3.3.3 COLUMN PACKINGS

If optimum results are to be obtained, it is essential that properly designed columns of suitable dimensions are used, and the columns to be packed with the most suitable packing available.

The heart of the GPC instrument is the column bed, since it is within the column that the separation takes place. A variety of porous packing materials are available for GPC.

The packings can be classified by the rigidity of the material: rigid, semi-rigid and soft gels, or they can be divided according to the material from which they are made: organic and inorganic gels. Analytical GPC gels

Fig. 3.3.2 Illustration of Parameters for Determining HETP

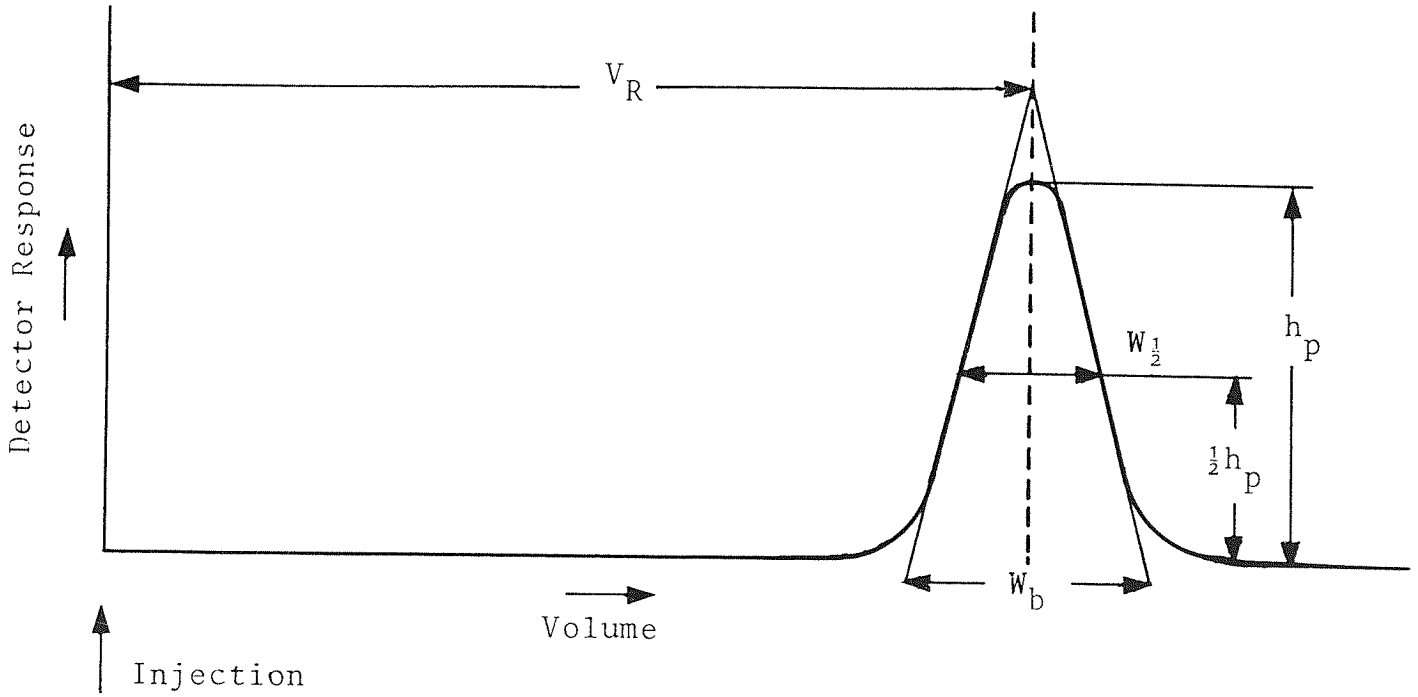

Fig. 3.3.2a Illustration of Parameters for Determining the Asymmetry Factor

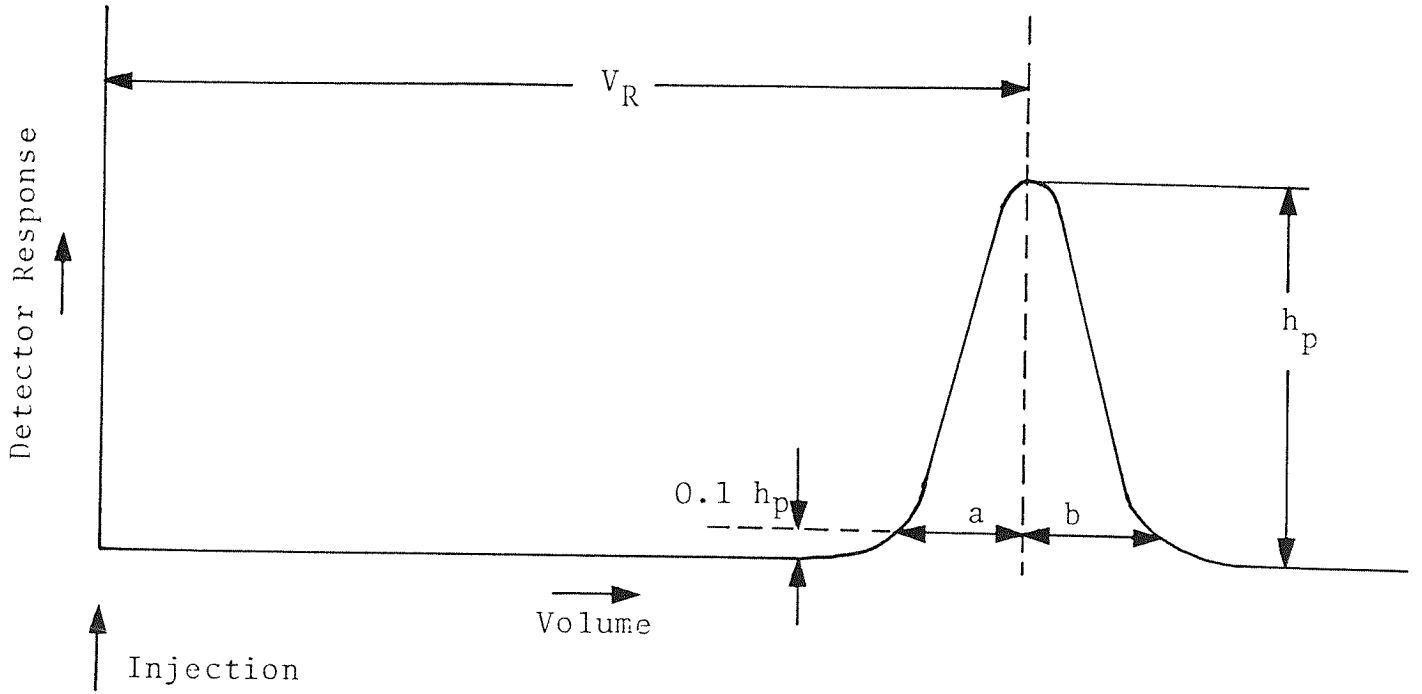

have particle diameters in the range 5-40 μm, larger diameter particle packings are used for preparative GPC and large scale equipment.

I) Conventional Organic-Based Packings

(a) Soft Gels (Aerogels)

Cross-Linked Dextran Gels - Sephadex was the first gel available commercially. Now it is marketed by Pharmacia Fine Chemicals in eight different pore sizes ranging from 20 to 300 μm, the maximum molecular weight exclusion limit is around 200,000 daltons. Sephadex has a high content of hydroxyl groups, the beads therefore swell considerably in water. The gels are stable in the pH range 2-10, the column inlet pressure is limited to $10x10^5$-$15x10^5$ N/m^2 because of their relative softness, therefore low flowrates have to be employed. It is used to fractionate polysaccharides (27,28).

Enzacryl Gels - Cross-linked gels of poly(acryloyl-morpholines), have the interesting property of being compatible with both aqueous and organic phases. However, in aqueous mobile phases, the gels are soft and low flow-rates must be used. In aqueous GPC, applications have included polyethylene glycols, oligometric diols and polysaccharides (29). The exclusion limit of these gels is up to 100,000 daltons, they are marketed by Koch-Light Labs. Ltd.

Sephacryl - Pharmacia Fine Chemicals, the makers of Sephadex gels, introduced a new type of hydrophobic polysaccharide gel Sephacryl S-200 superfine. This gel is prepared by covalently cross-linking allyl dextran with

N,N'-methylenebisacrylamide. Higher flowrates can be employed because of its rigidity compared to Sephadex.

Agarose Gels - These gels are available from several commercial sources: perhaps the best-known are the Sepharose range (Pharmacia Fine Chemicals) and Bio-Gel A range (Bio-Rad Laboratories), which is available in 6 pore sizes, A-0.5 - A-150. These materials are stable in the pH range 4-9 and should be used at temperatures between 0 and 40°C.

An important property of agarose gels, one of considerable advantage in practice, is their flexibility and reversible change of volume in the gel bed. In contrast to other gels, agarose columns do not aggregate under hydrostatic pressure, and when the pressure is released the gel bed recovers its original volume. There is no need to repack the column.

Bio-Gel P - This is a cross-linked polyacrylamide gel produced by Bio-Rad Laboratories. A superior feature of these gels as compared to dextran gels is that, being synthetic, they do not enhance the growth of micro-organisms and are neutral to bacterial attack.

Ten different types are sold, the P-2, P-4, P-6 and P-10 are available in four particle sizes, the rest in three particle sizes. The exclusion limit for polysaccharides is 1.5×10^5 daltons.

Ultrogel - These composite packings were introduced in 1975 and consist of both polyacrylamide and agarose. Therefore these gels have a fractionating range greater than the polyacrylamide gels and they are more rigid than agarose. Owing to their agarose content the gels must be

used between the temperatures of 2 and 36°C. They are sensitive to heat and to reagents prone to destroy the hydrogen bonds (concentrated urea for example) as well as to bacterial effects. Their chemical resistance (between pH3 and 11) is adequate. Ultrogel is marketed by LKB Instruments Ltd (30).

Aquapak - This is a polystyrene gel cross-linked with divinylbenzene marketed by Waters Associates (Instruments) Ltd. Fractionations of dextrans and sodium lignin sulfonates were demonstrated (31) by Waters Associates.

Bio-Beads marketed by Bio-Rad Laboratories Ltd is a similar gel to aquapak.

Cross-Linked Cellulose Gels - The preparation of these gels and their performance compared with the performance of other soft gels are described by Kuga (32).

(b) Semi-Rigid and Rigid Gels

Hydrogel - This is reported to be a highly cross-linked ethylene glycol dimenthacrylate polymer packing. Three pore sizes are available with a molecular weight exclusion limit of 2×10^6 for dextran solutions, pressures of up to 2×10^7 N/m^2 can be used. It was reported that no deterioration in efficiency or change in calibration was observed, over a period of one year, using Hydrogel packed columns for the analysis of dextran solutions (32-34). Unfortunately, the Hydrogel range of GPC packings was withdrawn from the market due to poor batch reproducibility.

Waters Associates now market a new range of Hydrogel packings which is of the type sulfonated cross-linked styrene with divinylbenzene copolymer. The new gels may

show ionic sorption effects and/or hydrolysis on either side of pH7.

Spheron - This is a similar packing to Hydrogel marketed by Koch-Light Labs Ltd. Columns packed with Spheron were used for dextran analysis by (33,34). It was also found by these authors that the packed bed compressed and efficiency was rapidly reduced.

Toyopearl - This is a semi-rigid, spherical hydrophilic polymer (polyvinyl) gel marketed by Toyo Soda Manufacturing Co. Ltd.

Toyopearl is produced in five types (35), each with three different particle sizes ranging from 20 to 100 μm, they are also chemically stable in the pH range 1-14. The maximum molecular weight exclusion limit is about $1x10^7$ daltons for dextran solutions. Low pressures have to be employed (less than $10x10^5$ N/m^2) resulting in slow flow-rates and hence long analysis time (36).

TSK-PW - Marketed again by Toyo Soda Manufacturing Co. Ltd., it is a fully porous, spherical and semi-rigid gel with high porosity. The exact structure of this high-performance polymeric gel has not been published; however it does contain - $CH_2.CHOH.CH_2O$ - groups (37). TSK-PW is available in six types with particle size ranging from 10-25 μm, it has a maximum molecular weight exclusion limit of $2x10^7$ daltons for dextran solutions (35). These packings have wide GPC applications (38-43).

II) Inorganic Packings

Almost all the inorganic packings used for aqueous GPC are made from silica. They are rigid and can withstand

very high pressures.

In aqueous GPC, adsorption can arise from hydrogen bonding, hydrophobic and ionic interactions. For high molecular weight compounds, adsorption can be quite severe when silica gels are used. In addition, with long term use, silica slowly dissolves in the aqueous mobile phase, especially at high pH values. The major thrust in column technology has been to develop deactivated silica packings or rigid cross-linked gels to prevent non-size exclusion effects from occurring.

(a) Unmodified Silica Packings

Spherosil - These are the best known gels, manufactured by Pechiney-Saint-Govain but sold in this country by Waters Associates under the name Porasil (44). It is available in six different pore sizes.

Barker and Others (33,44-54) have tried Porasil as analytical and preparative packings and it was reported that they slowly dissolve in water. For the preparative work the rate of dissolution was sufficiently low, compared to the volume of the columns used, to avoid creating any significant problems.

Porous Glass - This is available from several commercial sources. The CPG10 series advertised as a 'column packing material for glass permeation chromatography' is available in twelve different pore diameters.

CPG packings are widely used for dextran analysis and fractionation (55-60) and they seem to behave similarly to Porasil gels.

Zorbax - Barker et al (33,61) have used DuPont's Zorbax SE and PSM packings for dextran analysis. They noticed a significant drop in column efficiency after a few weeks and assumed that this might have been caused by dissolution of silica.

The SE series come in four different pore diameters whereas for the PSM series only three different pore diameters are available.

LiChrospher - They are totally porous spherical silica microparticles with a range of pore sizes; it is manufactured by E. Merck. These microparticles have a relatively large internal porosity, which provides both good sample capacity and column efficiencies (62).

LiChrospher was used by Buytenhuys (49) on polysaccharides.

(b) Modified Silica Packings

Glycophase-G/GPC - These are irregular siliceous particles which have been modified with a hydrophilic glycol. They are available in six different pore diameters and marketed by Pierce Chemical Co.

The first commercially available packing of this type was SynChropak, which is also marketed under the names of Aquapore and Bio Sil GFC. These packings have been used for the GPC of a wide variety of water soluble polymers including polysaccharides (63).

Bondagel - Marketed by Waters Associates is a porous silica to which an ether functionality has been chemically bonded. This material is offered in four different pore diameters, plus an E-linear column which is a blend of

pore sizes.

Bondagel has been used to characterise a number of water soluble polymers including polysaccharides (64).

TSK-SW - Marketed by Toyo Soda Manufacturing Co. Ltd., it is a rigid, hydrophilic fully porous, spherical gel. They are available in two different particle sizes and have a maximum molecular weight exclusion limit of $4x10^5$ for dextran, used in the 2.5-7.5 pH range (36).

Very little information is available on this packing, but interesting applications have been reported (65-67).

3.3.4 EQUIPMENT

Gel permeation chromatography is normally employed both as an analytical method and as a preparative technique. The experimental arrangement commonly used for analytical work is essentially that given in Fig.3.3.3. The equipment consists of an eluent reservoir, a pump, a pressure indicator, a sample loading device, a packed column, a detector, a chart recorder and a flow measuring device.

In practice a sample of the mixture to be analysed is loaded on to the top of the column, and eluent is pumped through it. For most chromatographic systems, the injection of the sample into the column is either by syringe or injection valve (this is usually carried out manually or automatically). Bristow (69) summarised the advantages and disadvantages of each injection method. Pumps are carefully chosen to ensure constant flowrate, based on either constant pressure or constant flow. The use of constant pressure pumps is not recommended since the flow-

Fig. 3.3.3 Line Diagram of an Analytical GPC System

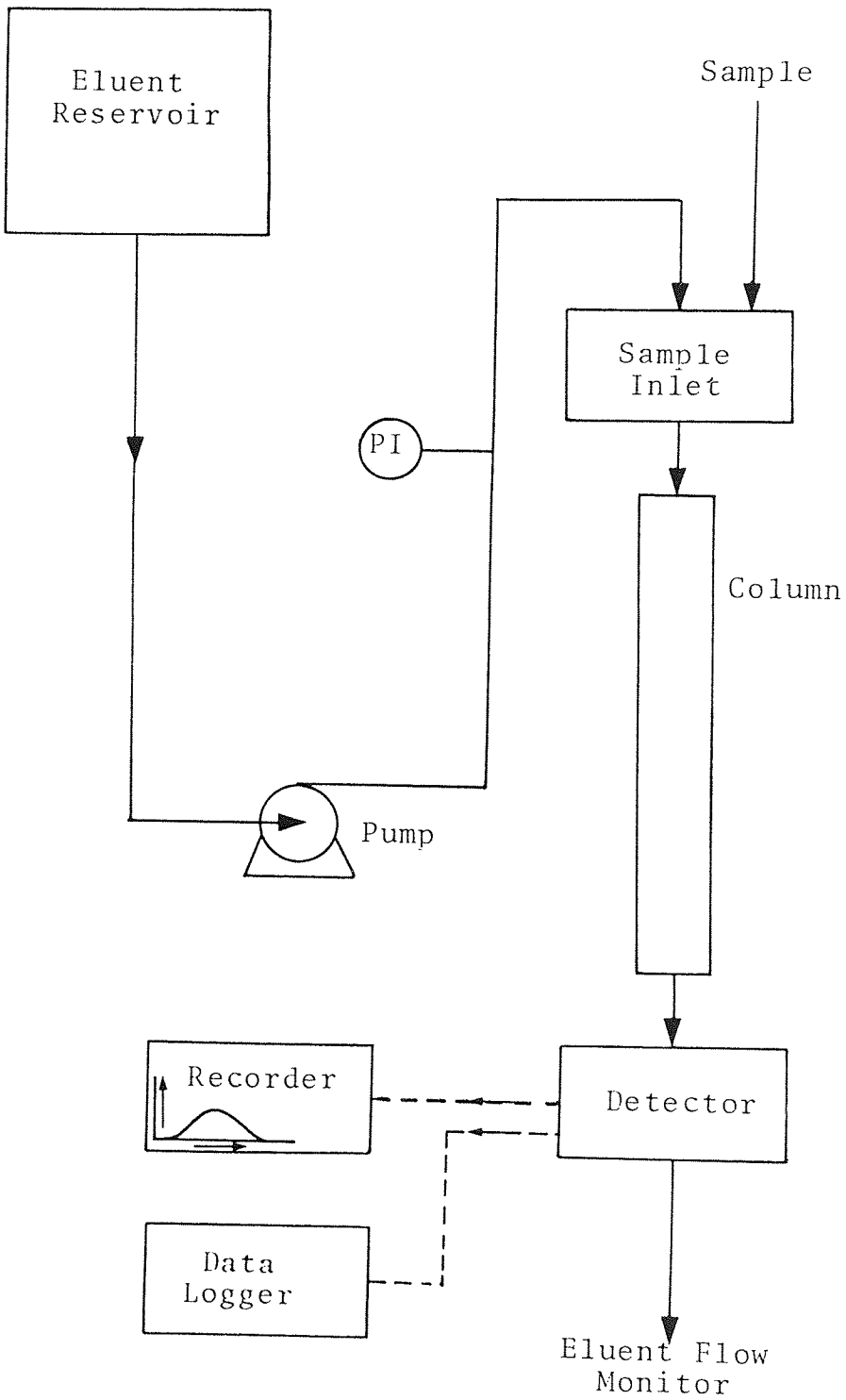

rate depends on the resistance of the column and the viscosity of the eluent. There are two types of constant flow pumps, reciprocating piston pumps and more expensive syringe pumps. The latter should give better flow control since there are no 'working' valves but high quality reciporating pumps should be satisfactory if the eluent is filtered prior to the pump.

After size separation takes place in the packed column, sample detection is usually carried out in one of two ways. The first involves collection of fractions from the column outlet stream followed by analysis of the fractions by one of several techniques. The second method is to monitor the column outlet stream which allows a chromatogram to be produced simultaneously. The detectors that are most commonly used are refractive index detectors and ultraviolet detectors, although other less common detectors have been used and have been reviewed in the literature (69-73).

The most widely used detector in GPC is the differential refractometer (or refractive index detector), this continuously monitors the difference in refractive index between the mobile phase and column eluate. This method is suitable for a wide range of samples, but suffers from the disadvantages of being extremely sensitive to temperature, and sensitive to a lesser degree to flow changes in the system.

General requirements of detectors are low noise and drift, high sensitivity with respect to the measured parameter, low sensitivity to changes in operating

parameters, low 'dead' volume, and a linear relationship between the detector output and solute concentration.

The signal from the detector is transmitted to the chart recorder so that a chromatogram is produced. Finally the flowrate measurement is either carried out manually by weighing a sample collected in a given time interval, or automatically by a siphon arrangement that discharges when full, each discharge sending a signal to the chart recorder hence producing a blip on the chromatogram.

Modern GPC systems (24,74-77) also have a data logger connected to the detector, so that the data can be stored in a computer for later calculations without any manipulation; expensive systems have inbuilt computers.

3.3.5 POLYMER CHARACTERISATION

All polymer molecules, whether natural or synthetic, consist by definition of large numbers of sample repeat units, derived from small molecules and joined together by covalent bonds to form the high molecular weight polymer molecules. In the simplest polymer structure, the linear homopolymer, only one type of repeat unit is present and the units are joined end-to-end to form linear chains. However, even in the simplest cases, it is rare for the repeat units to be distributed equally between all of the polymer molecules. With relatively few exceptions, of biological origin, random processes occurring during polymer synthesis produce chains containing varying numbers of repeat units, so that the polymer contains a distribution

of molecular chain lengths and is said to be polydisperse. A polymer in which all molecules have the same molecular weight is said to be monodisperse (70).

Because of the polydisperse nature of polymers it is not generally possible to characterise a polymer by a single molecular weight and the mass of the polymer molecules can only be completely described by a MWD. A knowledge of this data is essential in explaining or predicting the behaviour of the polymeric system. One method of obtaining this data is GPC, its speed and simplicity, together with the ability to automate the technique, has meant that it is usually the method of choice for determining the MWD.

The MWD may be represented in the form of a histogram (Fig. 3.3.4a), which truly represents the discrete distribution of the system. However, as the polymer usually contains a very large number of different molecular weights, it is often more convenient to treat the distribution as continuous and to represent it as either a differential or integral (cummulative) distribution curve (Figs.3.3.4b and 3.3.4c).

Since no single number can adequately characterise the molecular weight of a polymer, various averages are used. Of the various molecular weight averages the most common are:

$$\text{Number Average, } \bar{M}_N = \frac{\Sigma n_i M_i}{\Sigma n_i} \quad \ldots\ldots\ldots\ldots\ldots\ldots \quad 3.3.8$$

$$\text{Weight Average, } \bar{M}_W = \frac{\Sigma n_i M_i^2}{\Sigma n_i M_i} \quad \ldots\ldots\ldots\ldots\ldots\ldots \quad 3.3.9$$

where n_i = number of molecules of molecular weight M_i.

Molecular Weight Distribution Curves

Fig. 3.3.4a

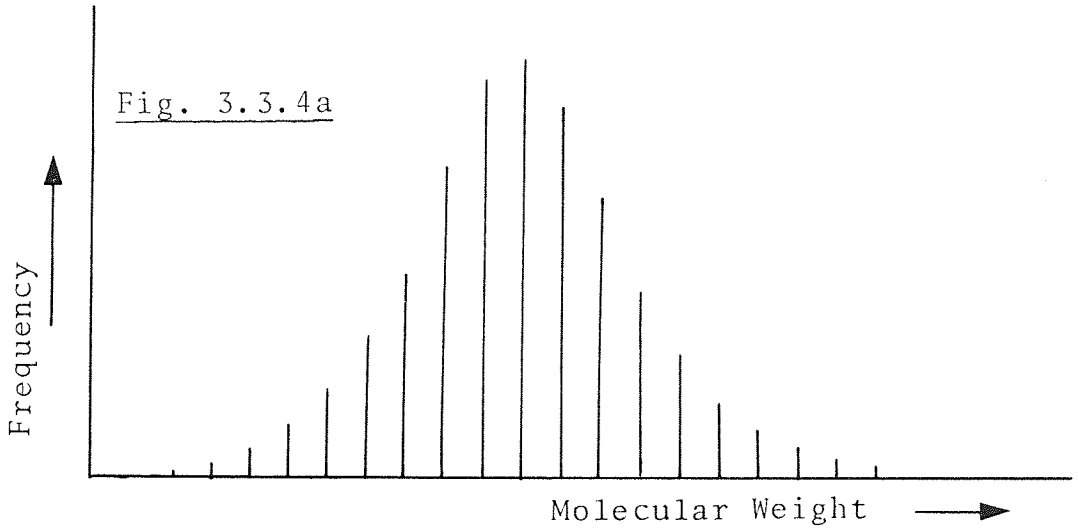

Fig. 3.3.4b

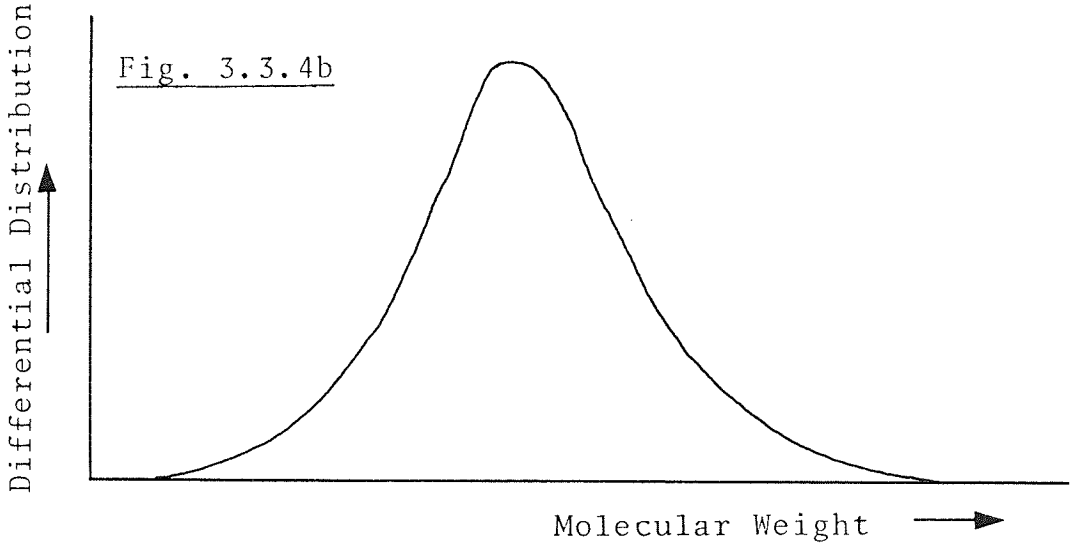

Fig. 3.3.4c

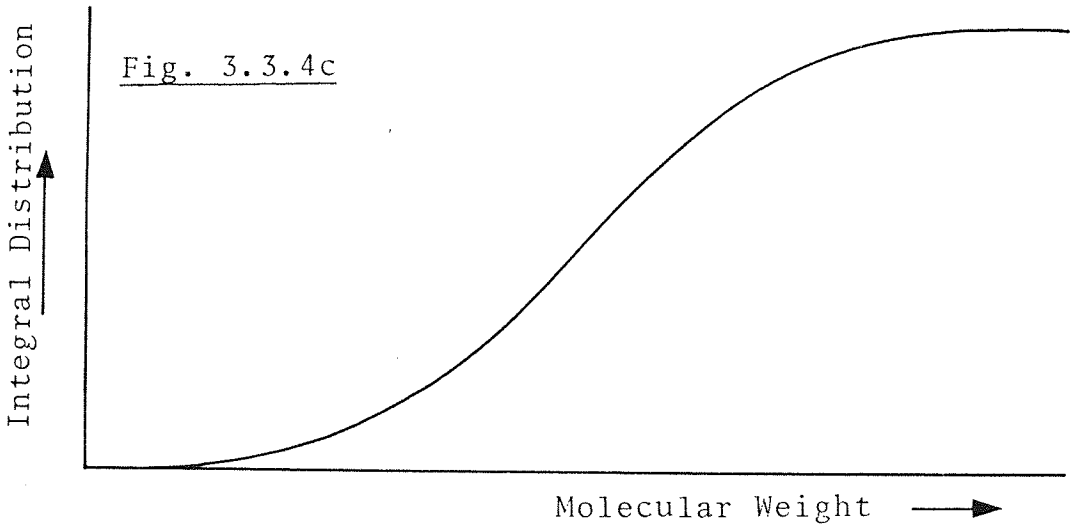

For polydisperse polymers $\bar{M}_W$ is always greater than $\bar{M}_N$ except that the values are identical for a monodisperse system.

The term polydispersity is often used to describe the breadth of the MWD and is defined as:

$$\text{Polydispersity, } \bar{D} = \frac{\bar{M}_W}{\bar{M}_N} \quad \ldots\ldots\ldots\ldots\ldots\ldots \quad 3.3.10$$

This polydispersity ratio is 1.0 for a monodisperse sample, while most commercial synthetic polymers have polydispersity ratios in the range 2-20.

3.3.6 COLUMN CALIBRATION

The complex part of GPC is the production of the final molecular weight distribution curve and the weight average and number average molecular weights from the chromatographic data.

The raw data consists of an elution profile of detector response against elution volume. A typical chromatogram obtained is shown in Fig.3.3.5. The ordinate represents the variable being measured by the detector, but as this is proportional to concentration of polymer present, concentration will be used for convenience. The abscissa is the elution volume, or elution time, the area under the curve represents the weight of sample loaded on the column and the shaded area represents the weight between V_{R_1} and V_{R_2}.

Since the molecular weight of the polymer is a logarithmic function of K_d, itself a function of the elution volume (equation 3.3.1), calibration of the GPC

Fig. 3.3.5 A Typical GPC Polymer Chromatogram

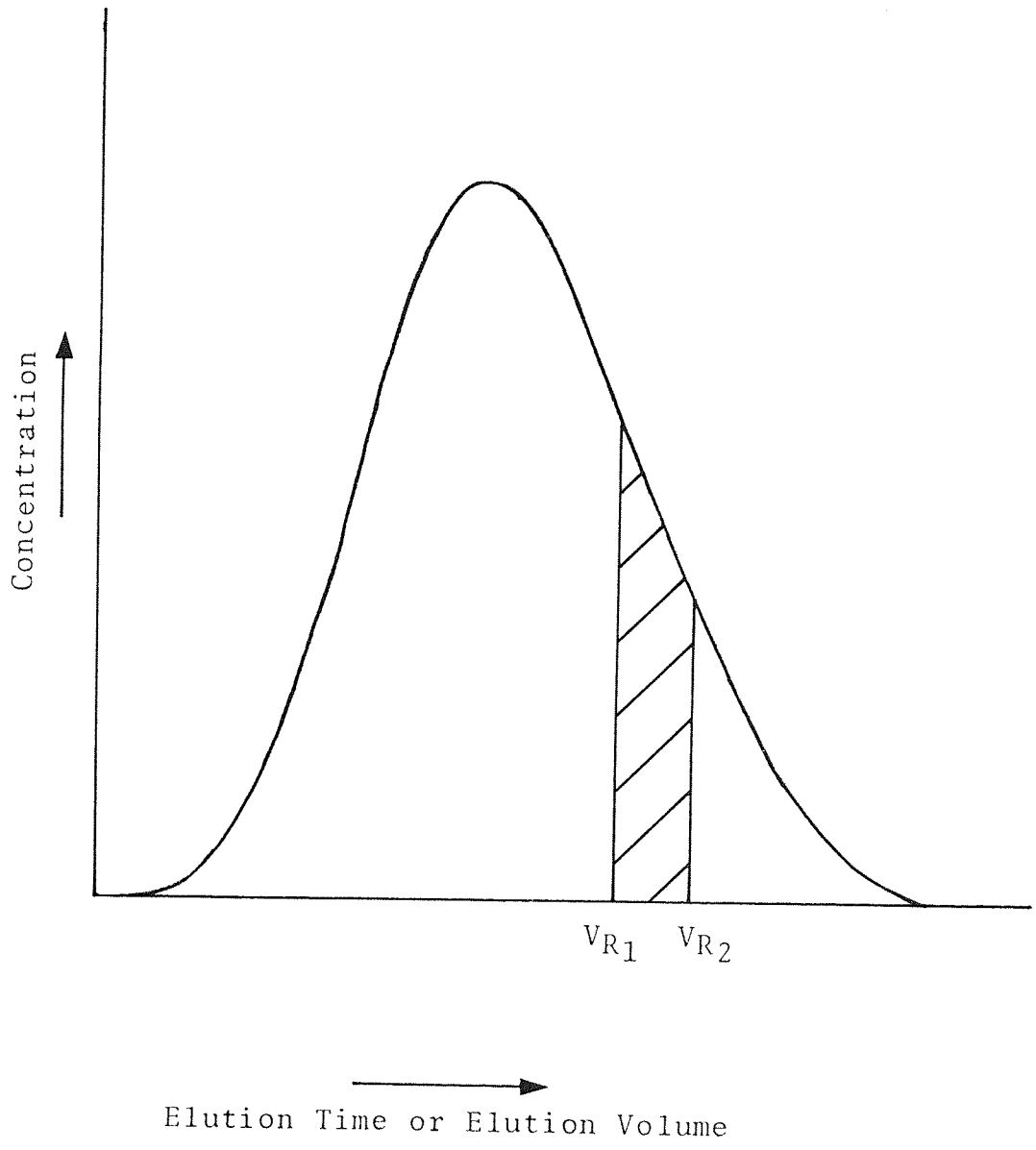

column is necessary in order to relate the elution volume (through K_d) to the molecular weight. This is done by chromatographing standard samples of known molecular weight. Ideally these should be as near monodisperse as possible and should also consist of the same polymer as the one being characterised. The former simplifies the procedure and the latter ensures that no doubt can be expressed concerning the validity of the calibration.

Figure 3.3.6 shows the relationship between molecular weight, or some function thereof relating to the size of the molecule in solution and its retention (elution) volume, V_R on a semi-logarithmic scale. This is a typical S-shaped calibration curve. Five regions of this curve may be identified. Above a certain molecular weight (M_x) no fractionation occurs (Section a-b) as all these molecules are too large to penetrate any of the pores of the packing (K_d=0), and therefore they all elute at the void volume, V_o. Similarly below a certain molecular weight (M_y) the molecules are not fractionated (Section e-f) as they all completely penetrate the pores (K_d=1), and therefore they are the last to elute at a retention volume of the void plus the pore volumes, V_o+V_i. Molecules between these two molecular weight limits are fractionated because they penetrate the pores to varying degrees. With many column packings there is a region where the curve may be represented by a straight line (Section c-d), and one normally chooses a column that fractionates the whole of the unknown sample in this region as the fractionating power of the packing is greatest here; also the subsequent calculations

Fig. 3.3.6 A Typical Calibration Curve for a GPC Column

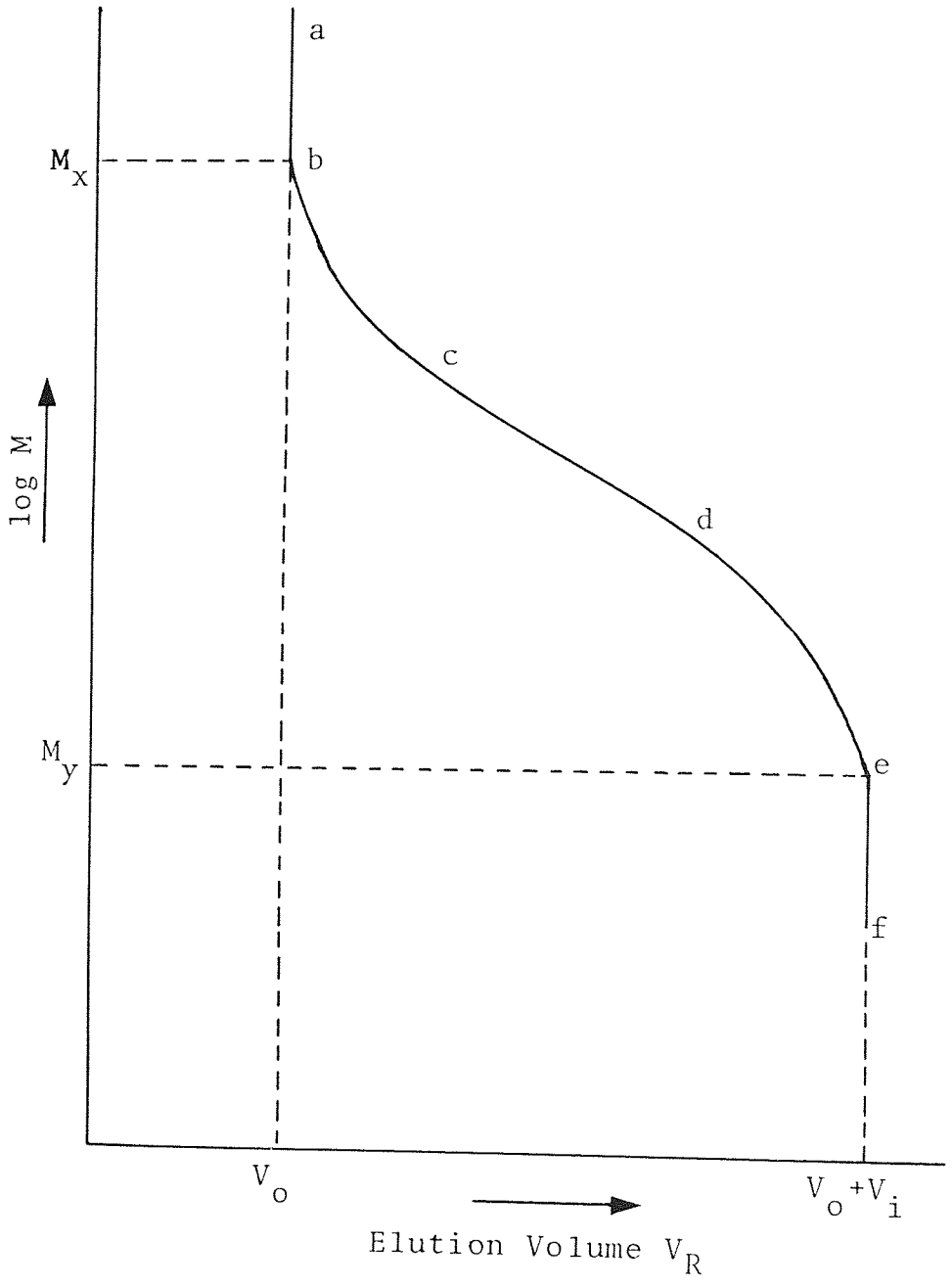

are aided if log M is directly proportional to the retention volume. In Sections b-c and d-e, fractionation is still occurring, but the relationship between log M and V_R is non-linear. However, it is necessary to calibrate over the whole region that is likely to be covered by the unknown samples because extrapolation of calibration curves will give erroneous results.

It is important when accurate MWD data is required that the sample polymers should not contain material with molecular weights outside the fractionation range of the column. The GPC chromatograms of samples which extend past the inclusion or exclusion limits of the packing will frequently exhibit two peaks: one peak is due to the fractionation of the main part of the polymer and the other peak is an artifact caused by the grouping together of molecules in one of the extremes of the elution limits of the column packing and eluting them all at the same retention volume, either the void volume or the void plus pore volumes. This effect is illustrated in Fig.3.3.7.

A widely used approach for calibrating column(s) is to assume that the calibration curve, not necessarily linear, is represented by a mathematical function with two or more unknown parameters. These parameters are then calculated to give a good fit between the molecular weight averages determined from the GPC curves and those measured by independent means, the simplest form of the equation of the calibration curve is:

$$\ln M = a - bV_R \quad \ldots\ldots\ldots\ldots\ldots\ldots\ldots\ldots \quad 3.3.11$$

Fig. 3.3.7 Fractionation of Same Polymer on Packings with Different Calibration Curves

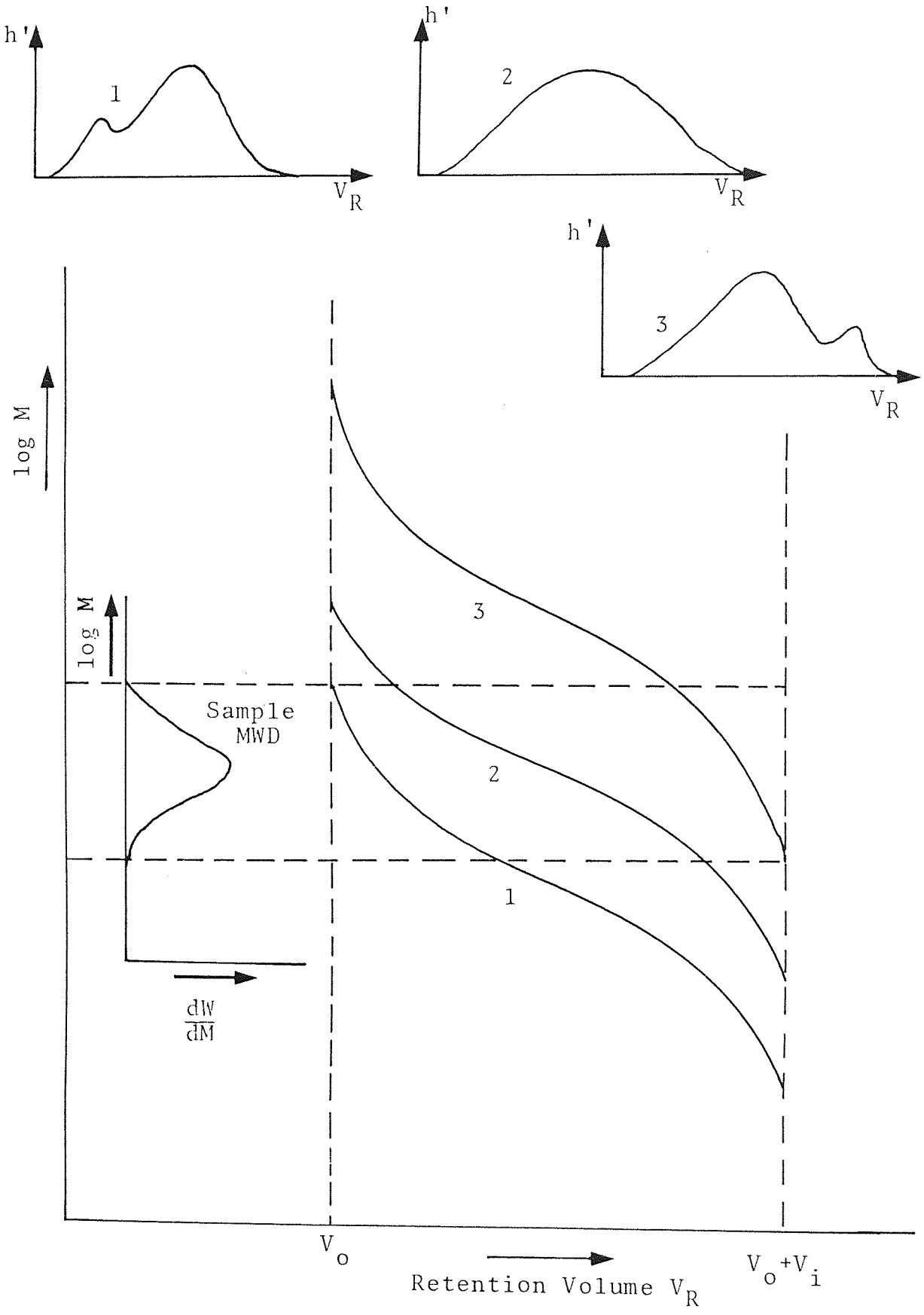

where

M is the molecular weight

a and b are the calibration constants

Frank et al (82) used this technique and they were able to let a and b vary from sample to sample provided both $\bar{M}_W$ and $\bar{M}_N$ were known for each standard. By using this method Balke et al (83) determined the equation of the linear calibration curve with only one or two standards, each of which had two known molecular weight averages. The linear calibration equation was obtained by using a Rosenbrock search (84) to calculate the optimum values for the coefficients a and b.

Many examples of a linearly calibrated column exist; however in cases where this condition is not fulfilled Tung and Runyon (85) have suggested that a considerable error can be introduced. Therefore polynomial equations of the third, fourth and fifth degree are often used to represent the way in which calibration lines are convex in a graphical representation at their higher limit of molecular weight; concave at the lower molecular weight range, and approximately linear in the central portion. Many people (24,86-88) have used non-linear calibration polynomials, generally of the type:

$$\log M = a_o + a_1 V_R + a_2 V_R^2 + \ldots a_n V_R^n \ldots\ldots \quad 3.3.12$$

or its inverse function

$$V_R = C_o + C_1 \log M + C_2 \log^2 M + \ldots C_n \log^n M \ldots \quad 3.3.13$$

where $a_i + C_i$ are experimentally determined constants.

Basedow et al (89) uses the same form as expression (3.3.12) but reduces the retention volume to a canonical form by using the distribution coefficient K_d inplace of V_R, the advantage being that because displacements in the retention volume could easily be corrected in due course without repeating the whole calibration, and that the void volumes of the chromatographic system are avoided.

As the present understanding of the mechanism of GPC is not sufficiently developed to allow direct calculation of calibration curves, it is evident that these curves must be obtained by experimental methods.

In GPC with organic eluents, polystyrene standards with various average molecular weights and very narrow MWD's are commercially available (e.g. from Waters Associates) and are widely used as calibrants for a variety of polymers in addition to polystyrene. This requires the use of the universal calibration (33,70,71,73,78-80), a concept derived from studies on the properties of polymers in dilute solution, which have also thrown light on the mechanism of GPC. The universal calibration method introduced by Benoit et al (81) utilises the concept of the hydrodynamic volume of polymer molecules, the hydrodynamic volume (V_n) can be expressed in terms of the molecular weight and intrinsic viscosity ($\{\eta\}$) according to the following equation:

$$\{\eta\}.M. = \gamma N_o V_n \quad \ldots\ldots\ldots\ldots\ldots\ldots\ldots\ldots \quad 3.3.14$$

where

M is the molecular weight

N_o is the Avogadro's constant

γ is the Simha constant, for spherical molecules it equals 0.025 but is a function of M for non-spherical molecules.

Benoit found that a plot of $\log\{\eta\}.M.$ against V_R for many polymers gave coincident calibration curves when the polymers were fractionated on the same column. Thus two fractions of different polymers, 1 and 2, eluting at the same V_R had molecular weights (M_1 and M_2) related by the expression:

$$\{\eta\}_1.M_1 = \{\eta\}_2.M_2 \quad \ldots\ldots\ldots\ldots\ldots\ldots\ldots \quad 3.3.15$$

If the column had been calibrated with standard fractions of polymer 2, each with known intrinsic viscosity, the molecular weight of the sample polymer, M_1, can be calculated if its intrinsic viscosity is known. Thus a plot of $\log\{\eta\}M$ against V_R has provided a universal calibration curve found to be true for many polymers.

However, polystyrene standards are not suitable for aqueous GPC and for the purpose of this research project dextran is the only satisfactory molecule for calibration. Dextran fractions of low polydispersity are not readily available and have to be produced by fractional precipitation or preparative GPC, normally in the laboratory requiring them. Lansing and Kraemer (90) developed a method in which standards with polydispersity less than 1.1 are first characterised by measuring their $\bar{M}_W$ values by light-scattering and their $\bar{M}_N$ values by end group analysis. A Gaussian distribution (weight vs. log molecular weight)

is then assumed for the fractions and by using their derived equation the theoretical MWD is calculated. The samples are then chromatographed and the characteristics thus obtained equated with those from the calculated MWD. By this means a calibration curve is produced by using a series of suitable standards.

Another method is to fractionate a number of polymers of the same type as the samples under test, which are sufficiently broad enough to cover most of the molecular weight range of interest and also have a well characterised distribution. This technique is of particular use to laboratories dealing exclusively with one polymer type as there is a considerable effort required in characterising the MWD. This broad polymer calibration technique was used by Nilsson and Nilsson (88) who assumed that the molecular weight could be related to K_d by the equation:

$$M = b_5 + \exp\{b_4+b_1(K_d)+b_2(K_d)^2+b_3(K_d)^3\} \quad \ldots\ldots \quad 3.3.16$$

Values of the constants b_1-b_5, which give the optimum agreement between the actual values of $\bar{M}_W$ measured by light scattering for each standard fraction and the calculated values obtained from the chromatogram using equations (3.3.9) and (3.3.16), i refers to the ith vertical section. The optimisation is carried out using Hartley's modification of the Gaussian-Newton method (91).

This is a better calibration procedure since any one set of K_d, M co-ordinates are estimated from the several overlapping profiles of the dextran standards. This calibration procedure can easily be incorporated into an automated calculation.

The various calibration methods are described in detail in several papers and chromatography books (33,71,80,88, 90,92-95).

3.3.7 DATA TREATMENT

The elution curve (chromatogram) of a sample polymer is given by plotting the detector response h' against elution volume V_R, and it may be used to construct a full molecular weight distribution curve, provided that the calibration curve (log M against V_R) for the analytical GPC columns is determined (24,33,70,71,80).

A differential MWD curve may be represented by a plot of dW/d(log M) versus log M, where W is the weight fraction of the sample with molecular weight below M. To convert the GPC chromatogram into the correct MWD the following manipulation of the ordinate has to be made:

$$\frac{dW}{d(\log M)} = \frac{dW}{dV_R} \cdot \frac{dV_R}{d(\log M)} \quad \ldots\ldots\ldots\ldots\ldots\ldots \quad 3.3.17$$

where the term dW/dV_R is the ordinate of the normalised elution curve and $dV_R/d(\log M)$ is the reciprocal of the gradient of the calibration curve.

An alternative differential MWD could be obtained by plotting dW/dM versus dM. The term dW/dM may be expanded to give:

$$\frac{dW}{dM} = \frac{dW}{dV_R} \cdot \frac{dV_R}{d(\log M)} \cdot \frac{d(\log M)}{dM} \quad \ldots\ldots\ldots\ldots\ldots \quad 3.3.18$$

$$= \frac{dW}{dV_R} \cdot \frac{dV_R}{d(\log M)} \cdot \frac{1}{M} \quad \ldots\ldots\ldots\ldots\ldots\ldots \quad 3.3.19$$

This procedure is illustrated by Fig.3.3.8.

Fig. 3.3.8 Summary of Steps in the Conversion of a GPC Chromatogram to a MWD Curve

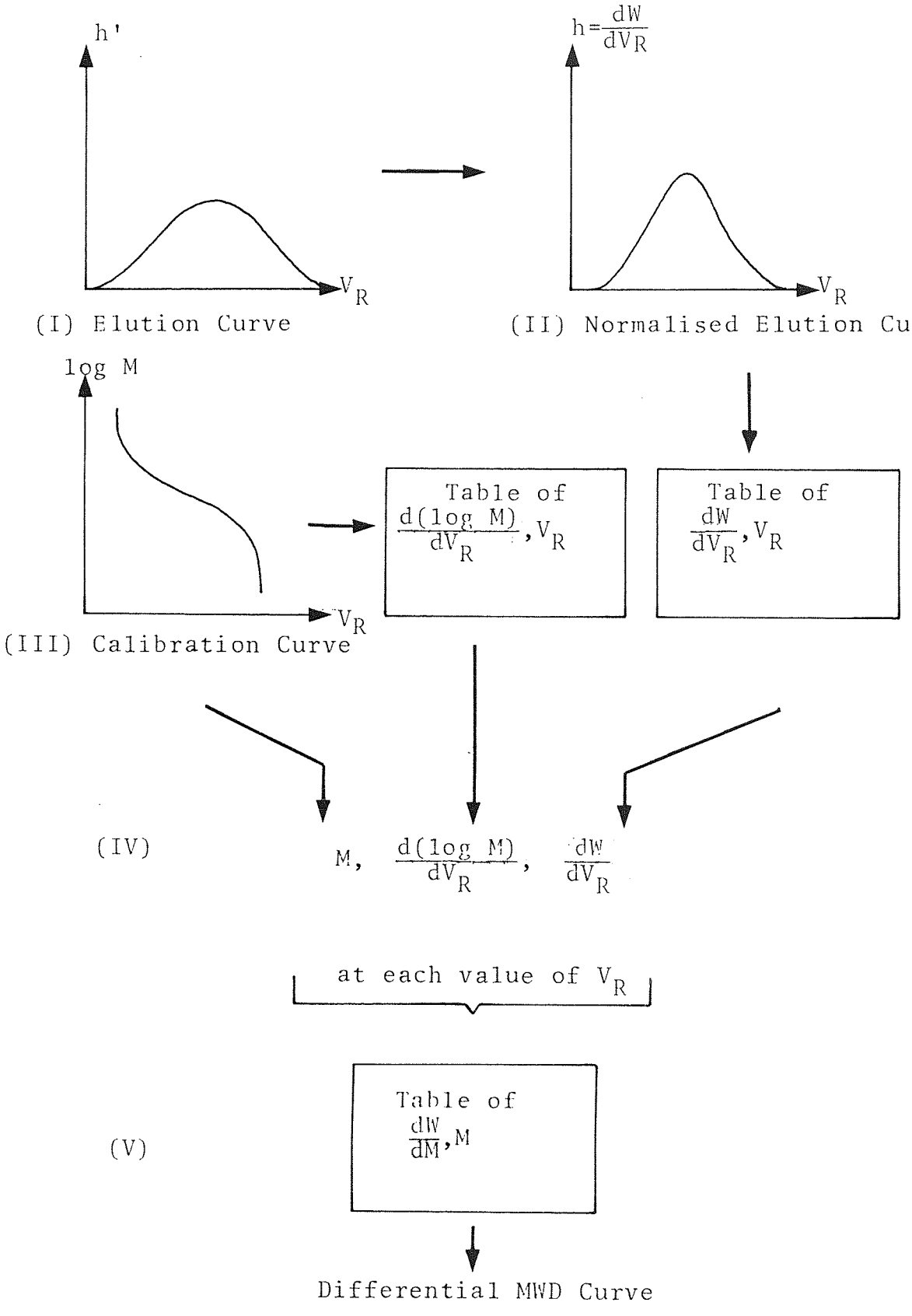

The GPC chromatogram (I) is normalised to give a unit area under the curve. Provided the detector response h' is directly proportional to concentration, it is not necessary to convert the ordinate to concentration units. Heights h_i' are measured at various regular intervals along the V_R axis and each value is divided by $\Sigma h_i'$. The normalised ordinate values $h = dW/dV_R$ are then plotted against V_R to give the normalised elution curve (II) so the value of dW/dV_R can be generated for any value of V_R. Likewise the calibration curve (III) will give a range of values of $d(\log M)/dV_R$ for the same V_R values, and a corresponding range of values for M(IV). Then the values of dW/dM can be calculated from equation 3.3.19 and the normalised weight differential MWD curve can be constructed (V).

The $\bar{M}_W$ and $\bar{M}_N$ values can be calculated from equations

$$\bar{M}_W = \frac{\Sigma n_i M_i^2}{\Sigma n_i M_i} = \frac{\Sigma W_i M_i}{\Sigma W_i} = \frac{\Sigma h_i M_i}{\Sigma h_i} \quad \ldots\ldots\ldots\ldots\ldots\ldots \quad 3.3.20$$

$$\bar{M}_N = \frac{\Sigma n_i M_i}{\Sigma n_i} = \frac{\Sigma W_i}{\Sigma (W_i/M_i)} = \frac{\Sigma h_i}{\Sigma (h_i/M_i)} \quad \ldots\ldots\ldots\ldots \quad 3.3.21$$

where W_i and n_i are the weight and number of molecules of molecular weight M_i respectively.

CHAPTER FOUR

PROPOSED THEORY OF ETHANOL FRACTIONATION

4.0 PROPOSED THEORY OF ETHANOL FRACTIONATION

When ethanol is added to a dextran solution, high molecular weight dextrans preferentially precipitate out of solution and settle to the bottom, this is the syrup phase. The top phase, known as the supernatant, contains the low molecular weight dextrans.

A Brief Study of the Possible Precipitation Process

A partial structure of a dextran molecule with a branching point is shown in Fig.4.1.a as produced by the micro-organism Leuconostoc mesenteroides B512 strain.

When dextran is dissolved in water (Fig.4.1.b), physical bonds are formed between the water and dextran molecules. When ethanol is added to the dextran solution the water molecules are replaced by ethanol molecules $R\text{-}\overset{-}{O}\text{-}\overset{+}{H}$ (Fig.4.1.c).

The alkyl group of ethanol is insoluble in water and therefore precipitates out the dextrans, preference being given to the high molecular weight dextrans because of their long chains creating more chances for the ethanol molecules to replace the water molecules.

The Fractionation of Dextran using Ethanol : A Possible Mechanism

Fig.4.1a

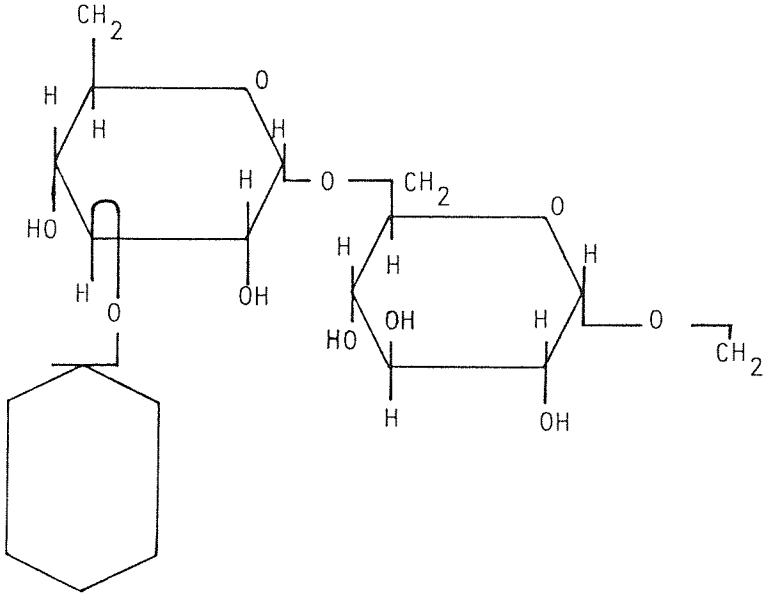

Fig.4.1b

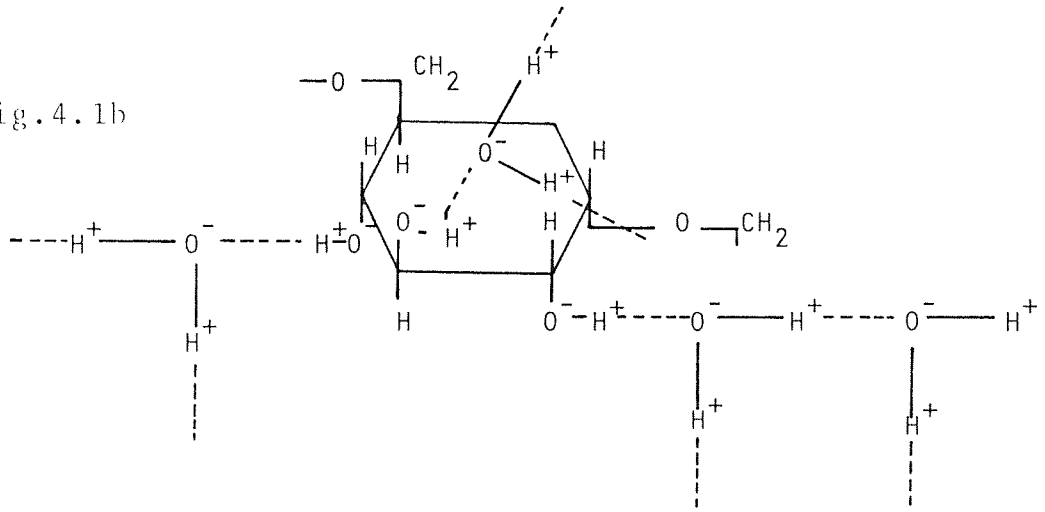

Fig.4.1c

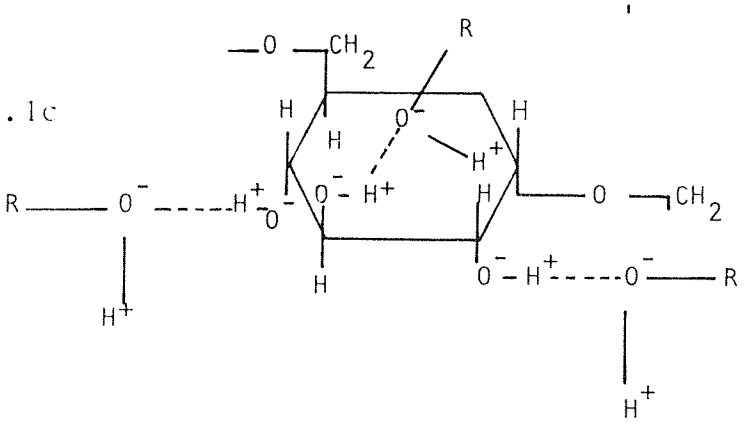

C H A P T E R F I V E

MATHEMATICAL MODELLING OF DEXTRAN FRACTIONATION USING ETHANOL

5.0 MATHEMATICAL MODELLING OF DEXTRAN FRACTIONATION USING ETHANOL

Schulz and Nordt (101) showed that high polymers can be fractionated by distribution between two phases. The equation was derived from purely energetic considerations. If C_1 and C_2 are the concentrations in the bottom and top phases respectively, the distribution of a two-phase system can be described by the Boltzmann equation:

$$\frac{C_1}{C_2} = \exp\left(\frac{E}{KT}\right) \quad \ldots\ldots\ldots\ldots\ldots\ldots\ldots\ldots \quad 5.1$$

in which

E is the difference in potential energy (E_2-E_1)

K is the Boltzmann constant $(1.3805 \times 10^{-26}$ kJ/K)

T is the absolute temperature of fractionation

According to Bronsted (102) for an isochemical substance (that differs in molecular weight only) the potential energy is proportional to the molecular weight (M). The Boltzmann equation therefore can be written as:

$$\frac{C_1}{C_2} = \exp\left(\frac{\lambda M}{KT}\right) \quad \ldots\ldots\ldots\ldots\ldots\ldots\ldots\ldots \quad 5.2$$

where λ is an energetic parameter which depends upon the solvent/monomer segment interactions.

Considering the two stage fractionation described in Chapter 2.0, Gibbs (22) has proposed a mathematical model for multi-stage fractionation based on the above Boltzmann equation as follows:

A polymer (mass m_o) which has a wide MWD is in solution (volume V_o). Ethanol is added until the higher molecular weight molecules (mass m_b, volume V_b) separate as a syrup

and are drawn off. The supernatant phase (volume V_t) containing dextran (mass m_t) is then treated with further ethanol to precipitate the required molecular weight dextran (mass m_f, volume V_f) as a syrup and leaving the small molecules (mass m_s) in the supernatant volume V_s.

For each dextran species with a molecular weight of M_i, the concentration ratio of syrup to supernatant phase in the first ethanol precipitation will be given by:

$$\frac{C_1}{C_2} = \frac{\text{Concentration of species i in syrup IR}}{\text{Concentration of species i in supernatant IR}}$$

$$= \left(\frac{m_{ib}}{V_b}\right) / \left(\frac{m_{it}}{V_t}\right) \quad \ldots\ldots\ldots\ldots\ldots\ldots\ldots\ldots \quad 5.3$$

where

m_{ib} is the mass of species i in the syrup phase of molecular weight M_i

m_{it} is the mass of species i in the supernatant phase of molecular weight M_i

Substituting equation 5.3 into 5.2 gives:

$$\frac{m_{ib}}{m_{it}} = \frac{V_b}{V_t} \exp\left(\frac{\lambda M_i}{KT}\right) \quad \ldots\ldots\ldots\ldots\ldots\ldots\ldots\ldots \quad 5.4$$

at a fixed ethanol strength and temperature

$$\frac{\lambda}{KT} = \text{constant} = C \quad \ldots\ldots\ldots\ldots\ldots\ldots\ldots\ldots \quad 5.5$$

$$\frac{V_t}{V_b} = \text{constant} = D \quad \ldots\ldots\ldots\ldots\ldots\ldots\ldots\ldots \quad 5.6$$

from mass balance

$$m_{ib} = m_{io} - m_{it} \quad \ldots\ldots\ldots\ldots\ldots\ldots\ldots\ldots \quad 5.7$$

where m_{io} is the mass of species i in the starting dextran solution.

Rearranging equation 5.4 after substitution of equations 5.5, 5.6 and 5.7 gives:

$$m_{it} = \frac{D}{D+\exp(CM_i)} \cdot m_{io} \quad \ldots\ldots\ldots\ldots\ldots\ldots 5.8$$

This equation defines the mass (m_{it}) of dextran species with a molecular weight M_i in the supernatant phase in relation to its mass (m_{io}) in the starting dextran solution.

$$\text{Total mass of dextran in super IR} = \sum_{i=1}^{i=n} m_{it} \quad \ldots\ldots 5.9$$

$$= \sum_{i=1}^{i=n} \frac{D}{D+\exp(CM_i)} m_{io}$$

$$\ldots\ldots\ldots\ldots\ldots 5.10$$

$$\text{Total mass of dextran in syrup I} = \sum_{i=1}^{i=n} m_{io} \quad \ldots\ldots 5.11$$

$$\text{Therefore \% dextrans in super IR} = \frac{100 \sum_{i=1}^{i=n} \frac{D}{D+\exp(CM_i)} \cdot m_{io}}{\sum_{i=1}^{i=n} m_{io}}$$

$$\ldots\ldots\ldots\ldots 5.12$$

$$\text{but } m_{io} = m_o \mu_{io} \quad \ldots\ldots\ldots\ldots\ldots\ldots\ldots\ldots 5.13$$

where μ_{io} is the weight fraction of species i in the starting dextran solution.

$$\text{Therefore \% dextrans in super IR} = \frac{100 \sum_{i=1}^{i=n} \frac{D}{D+\exp(CM_i)} \mu_{io}}{\sum_{i=1}^{i=n} \mu_{io}}$$

$$\ldots\ldots\ldots\ldots 5.14$$

For the second stage fractionation since the solvent strength is being altered the solvent/monomer segment

interaction parameter will change from its value of λ when the first syrup was precipitated to λ_1 on precipitation of the second syrup.

Equation 5.2 can be rewritten for the second stage fractionation as:

$$\frac{C_1}{C_2} = \exp\left(\frac{\lambda_1 M_i}{KT}\right) \quad \ldots\ldots\ldots\ldots\ldots\ldots\ldots\ldots \quad 5.15$$

The concentration ratio of syrup to supernatant phase in the second ethanol precipitation will be:

$$\frac{C_1}{C_2} = \frac{\text{Concentration of species i in final syrup}}{\text{Concentration of species i in final supernatant}}$$

$$= \left(\frac{m_{if}}{V_f}\right) / \left(\frac{m_{is}}{V_s}\right) \quad \ldots\ldots\ldots\ldots\ldots\ldots\ldots\ldots \quad 5.16$$

where

m_{if} is the mass of species i in the final syrup of molecular weight M_i

m_{is} is the mass of species i in the final supernatant of molecular weight M_i

Substitution of equation 5.16 into 5.15 gives:

$$\frac{m_{if}}{m_{is}} = \frac{V_f}{V_s} \exp\left(\frac{\lambda_1 M_i}{KT}\right) \quad \ldots\ldots\ldots\ldots\ldots\ldots\ldots\ldots \quad 5.17$$

at a fixed ethanol strength and temperature

$$\frac{\lambda_1}{KT} = \text{constant} = E \quad \ldots\ldots\ldots\ldots\ldots\ldots\ldots\ldots \quad 5.18$$

$$\frac{V_s}{V_f} = \text{constant} = F \quad \ldots\ldots\ldots\ldots\ldots\ldots\ldots\ldots \quad 5.19$$

from mass balance

$$m_{if} + m_{is} = m_{it} \text{ (mass of species i in super IR)}$$

therefore $m_{is} = m_{it} - m_{if}$ 5.20

Substituting equations 5.18, 5.19 and 5.20 into equation 5.17 gives on rearranging

$$m_{if} = \frac{\exp(EM_i)}{F+\exp(EM_i)} m_{it} \quad \text{..... 5.21}$$

Substituting equation 5.8 for m_{it} into the above equation gives:

$$m_{if} = \frac{D.\exp(EM_i)}{(F+\exp(EM_i))(D+\exp(CM_i))} m_{io} \quad \text{..... 5.22}$$

This equation describes the mass distribution of the final syrup (m_{if}) in terms of the mass distribution of syrup I (m_{io}).

Total mass of dextran in final syrup = $\sum_{i=1}^{i=n} m_{if}$ 5.23

Therefore % dextrans in final syrup

$$= 100 \frac{\sum_{i=1}^{i=n} \frac{D.\exp(EM_i)}{(F+\exp(EM_i))(D+\exp(CM_i))} \cdot m_{io}}{\sum_{i=1}^{i=n} m_{io}} \quad \text{..... 5.24}$$

On substitution of equation 5.13, $m_{io} = m_o \mu_{io}$

% dextrans in final syrup

$$= 100 \frac{\sum_{i=1}^{i=n} \frac{D.\exp(EM_i)}{(F+\exp(EM_i))(D+\exp(CM_i))} \cdot \mu_{io}}{\sum_{i=1}^{i=n} \mu_{io}} \quad \text{..... 5.25}$$

To determine the percentages of super IR and final syrup, values of the constant parameters C,D,E and F have to be found; this is achieved by the following procedure.

It has been shown that $m_{io} = m_o \mu_{io}$, similarly the mass of species i in the final syrup can be defined as:

$$m_{if} = m_f \mu_{if} \quad \ldots\ldots\ldots\ldots\ldots\ldots\ldots\ldots \quad 5.26$$

$$\text{let} \quad P = \frac{m_f}{m_o} \quad \ldots\ldots\ldots\ldots\ldots\ldots\ldots\ldots \quad 5.27$$

where P is the weight fraction of dextrans precipitated in the final syrup.

Equation 5.26 can now be rewritten as:

$$m_{if} = P m_o \mu_{if} \quad \ldots\ldots\ldots\ldots\ldots\ldots\ldots\ldots \quad 5.28$$

Substituting m_{io} and m_{if} from equations 5.13 and 5.28 into 5.22 gives:

$$\mu_{if} = \frac{D.\exp(EM_i)}{P(F+\exp(EM_i))(D+\exp(CM_i))} \cdot \mu_{io} \quad \ldots\ldots \quad 5.29$$

From Gel Permeation Chromatography the MWD of syrup I is known (i.e. μ_{io} at all values of M_i), also known is the MWD of the final syrup (μ'_{if} at all values of M_i).

Using a modified Marquardt method, a computer program (Appendix A3) has been used, which from initial estimates finds the best values of C,D,E,F and P to satisfy equation 5.29 at all values of μ_{io},M_i such that the sum

$$S = \sum_{i=1}^{i=n} (\mu'_{if} - \mu_{if})^2 \text{ is a minimum} \quad \ldots\ldots\ldots \quad 5.30$$

where S is the residual sum of squares.

CHAPTER SIX

ANALYTICAL GPC

6.0 ANALYTICAL GPC

6.1 ANALYTICAL EQUIPMENT

The experimental arrangement used for the analytical work was essentially that given in Fig.6.1.1. The equipment basically consisted of an eluent reservoir, water bath, thermoregulator, microfilter, pump, a sample introduction valve, fractionating columns, hot water circulator, glass column, detector, chart recorder and a PET computer.

The eluent used was a 0.02% w/v solution of sodium azide in distilled water. The sodium azide solution was used to prevent bacterial growth in the columns. The samples to be injected were made up to a concentration of 2% w/v dextran and 0.02% w/v sodium azide, the latter to prevent the presence of any negative (absence of sodium azide) peaks on the chromatogram.

The eluent was pumped with a positive displacement pump (series II, Metering Pumps Ltd., London, U.K.). This pump has recently been changed to a more accurate dual piston, low pulsation pump (model 1330, Bio-Rad Laboratories, Watford, U.K.). Samples were injected using a six-port sample injection valve (type 30.100) supplied by Spectroscopic Accessory Co., London, and fitted with a constant volume (100 µl) sample loop. All the samples before being injected into the columns were filtered using a disposable syringe filter of 0.45 µm mesh supplied by Millipore, London.

The fractionating columns used will be described in detail in Section 6.2. The columns were enclosed in a

Fig. 6.1.1 Schematic Diagram of the Analytical System

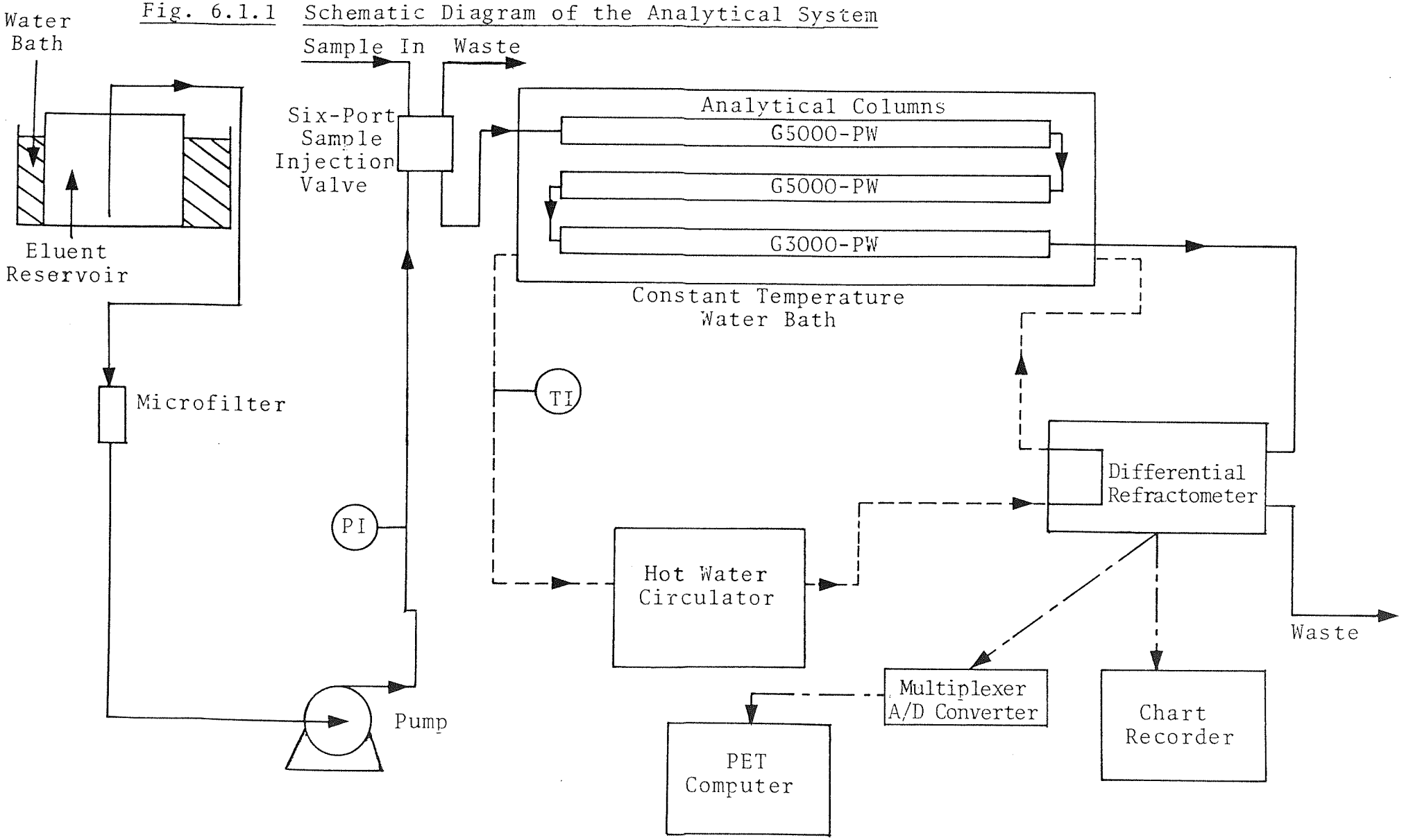

large glass column (70 cm long x 7.5 cm ID, Corning Glass) filled with water and heated by passing it through a hot water circulator (C-400, Techne, Cambridge, U.K.), so that the operating temperature of the columns was kept constant.

The eluate from the columns passed into a differential refractometer (R401, Waters Associates Ltd.), and the resulting change in the eluate concentration was registered first on a flat-bed, potentiometric chart recorder (Venture Servoscribe, RE541.20, Smiths Ltd.), and secondly on a multiplexer (Model PCI 1001, CIL Electronics Ltd., Sussex) to convert the signal from the differential refractometer into a digital mode. The data was then stored and printed (Appendix A4) on a PET Computer (CBM Model 4032, 32K bytes, with CBM Model 4022P printer, Commodore, U.K.). After minor corrections to the raw data the MWD and average molecular weights were computed (Appendix A2) on the CBM 4032.

6.2 FRACTIONATING COLUMNS

The fractionating columns used during this research project were the TSK-PW type marketed by Toyo Soda Manufacturing Co. Ltd., Tokyo, Japan.

The system used for dextran analysis consisted of two G5000 PW columns and one G3000 PW column. The G5000 PW column has a particle size of 17 $\pm$ 2 μm and fractionates dextran in the molecular weight range of 10,000-2×10^6 whereas the G3000 PW has a particle size of 13 $\pm$ 2 μm and fractionates dextran up to a molecular weight of 10,000. The columns were of 60 cm length x 0.75 cm ID,

connected in series in sequence of descending pore size. The operation of these columns was kept at 35°C so that the pressure drop across the columns was lower than at ambient temperature and also better resolution was obtained. The eluent reservoir was kept at a constant temperature of 40°C, the water bath heated by a thermo-regulator (TE-4, Techne, Cambridge, U.K.). The reason for the eluent reservoir being at a higher temperature than the columns was to avoid any de-gassing of the eluent in the columns.

The flowrate through the columns was 1.0 cm^3/min and the analysis time for dextran-glucose solutions was approximately one hour.

Fisons Ltd., Pharmaceutical Division, Holmes Chapel, Cheshire (96) own about four sets of these columns, one set has been in use for more than two years in their Quality Control Department without any significant problems. Some of the dextran samples in this research work have been analysed at their Works Technical Department (97). The GPC equipment of the latter department has been described in detail by Alsop et al (24,98) and Vlachogiannis (37).

In January 1984 the columns at Aston showed signs of deterioration after three and a half years of intensive use therefore a new set of these columns were ordered and installed at Aston. The number of theoretical plates (N) and the asymmetry factor (A_s) of the old and new set of columns were calculated using equations 3.3.4.a and 3.3.6. The results are given in Fig.6.2.1 for a 1% w/v

Fig. 6.2.1 Results of Theoretical Plates and Asymmetry Factors for TSK-PW Columns

Column Type	Toyo Soda Quality Specifications		Aston Analysis	
	N/Metre	A_S	N/Metre	A_S
G5000-PW OLD I	10000	0.7∿1.6	3732	2.52
G5000-PW OLD II	10000	0.7∿1.6	9098	1.28
G3000-PW OLD	16000	0.7∿1.6	14508	1.70
G5000-PW NEW I	10000	0.7∿1.6	16083	0.94
G5000-PW NEW II	10000	0.7∿1.6	16667	1.01
G3000-PW NEW	16000	0.7∿1.6	19777	1.08

ethylene glycol solution; operation of the columns was at ambient temperature.

6.3 ANALYTICAL TECHNIQUES

The preparation of a sample to be injected on the analytical columns fell into one of two categories.

These were:

(a) The preparation of 2% w/v dextran solutions of known average molecular weights for the calibration of the TSK columns. The above solutions were prepared by dissolving a known amount of dextran powder of known average molecular weights in a precise volume of 0.02% w/v sodium azide aqueous solution. Glucose and very high molecular weight dextran markers were added to these solutions to indicate the total inclusion and exclusion volumes respectively.

(b) The experimental and plant samples had to be distilled (Quick Fit kit) due to the presence of ethanol. The sample solutions were therefore usually too concentrated hence dilution was required to make it a 2% w/v dextran solution. The concentrations were measured by a pocket sugar refractometer (0-50%, Bellingham and Stanley Ltd., Kent, England). All sample solutions were made up to 0.02% w/v concentration of sodium azide. Glucose was used as a marker.

The samples were filtered and then injected into a six port injection valve with a constant volume sample loop.

The differential refractometer had a full scale deflection of 10mv, the chart recorder and the multiplexer

also had to be adjusted to the above value. The zeroing of the chart recorder and the differential refractometer is explained by Smiths (99) and Waters Associates (100) respectively.

The eluent flowrates through the columns were measured by weighing the eluate collected in a known period of time. The interstitial volume was taken to be at the peak maximum of the high molecular weight dextran (V_o) marker chromatogram. The total liquid volume for the columns was marked by the peak maximum of the glucose chromatogram.

6.4 DATA CONVERSION

6.4.1 CALIBRATION

To convert the chromatograms into a molecular weight distribution it was necessary to calibrate the column packings. The Nilsson and Nilsson (88) approach was used to calibrate the TSK-PW type columns.

A polynomial of the type

$$M = b_5+\exp\{b_4+b_1(K_d)+b_2(K_d)^2+b_3(K_d)^3\} \quad \ldots\ldots\ldots \quad 3.3.16$$

was used. The distribution coefficient (K_d) is related to the elution volume (V_R) according to the equation:

$$V_R = V_o + K_d V_i \quad \text{or} \quad K_d = \frac{V_R - V_o}{V_i} \quad \ldots\ldots\ldots\ldots \quad 3.3.1$$

The values of the calibration constants b_1-b_5 were obtained by the following procedure.

(a) A series of chromatograms were obtained for several Pharmacia dextran T-fractions whose weight average molecular weights, $\bar{M}_W$'s had been measured previously by light-

scattering. The eluent flowrate for each chromatogram was measured.

(b) The heights, elution volumes (converted to K_d values) and $\bar{M}_W$ (measured by light-scattering) of the T-fraction chromatograms together with guessed values of the calibration constants b_1-b_5 were entered into the computer calibration program (Appendix A1). The Hartley's modification of the Gaussian-Newton method was used to calculate the new values of the calibration constants b_1-b_5, which gave the optimum agreement between the actual values of $\bar{M}_W$ measured by light-scattering (L.S.) from each T-fraction and the calculated values obtained from the GPC elution profiles.

(c) The resulting calibration curve was checked by analysing a dextran T-40 sample (batch BT1J, $\bar{M}_W$ 41,500 by L.S.) and comparing the values of the $\bar{M}_W$'s between light-scattering and GPC. The dextran T-40 sample BT1J was analysed frequently as a check on the calibration.

During this research work two calibrations were carried out, one on the old set and one on the new set of the TSK columns. The results of the calibration 'CD5E' on the old columns are given in Figs.6.4.1 and 6.4.2 and of the new columns 'CD6E' in Figs.6.4.3 and 6.4.4.

The Nordic Pharmacopoeia requires that all of the calibration standards shall have individual molecular weights obtained by GPC within 90-110% of those obtained by light-scattering before one proceeds with the analysis of samples by GPC (98). Fisons' calibration 315Z (earlier experimental samples of this research work were analysed

Fig. 6.4.1 The Results of Aston's GPC Calibration CD5E

Batch Numbers	Weight Average Molecular Weights		$\frac{GPC}{L.S.} \times 100$
	L.S.	GPC	
3202	490000	493715	100.76
1343	231000	229485	99.34
921	154000	153382	99.60
5403	72000	71594	99.44
2540	44400	44588	100.42
2514	41800	42595	101.90
7968	22300	22280	99.91
3205	9300	9171	98.61
Stachyose	667	671	100.60
Glucose	180	180	100.00

Calibration Constants				
b_1	b_2	b_3	b_4	b_5
-16.634	21.702	-16.606	16.067	87.798

FIG 6.4.2 GPC CALIBRATION CURVE (CD5E) AT ASTON'S TSK-PW COLUMNS

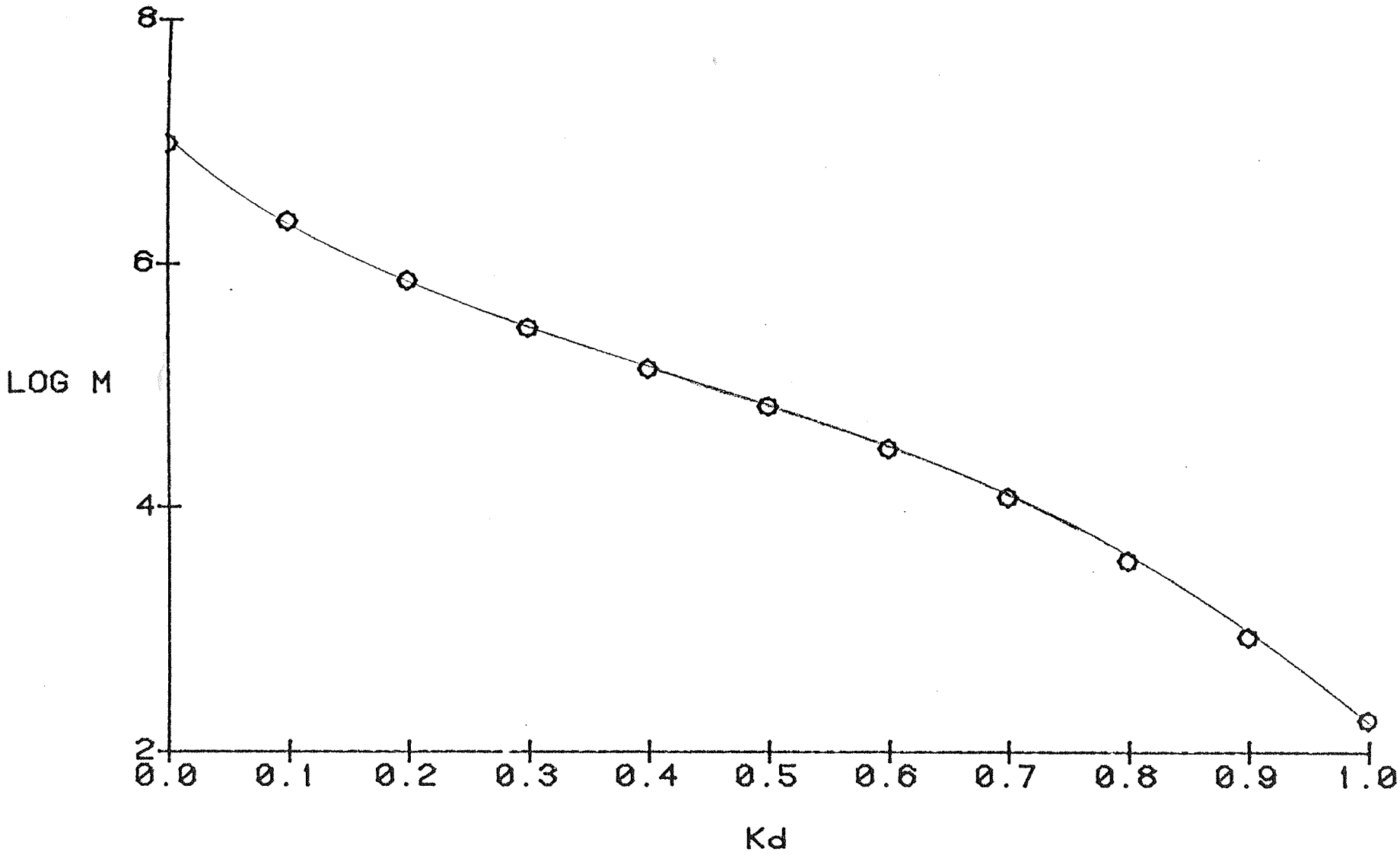

Fig. 6.4.3 The Results of Aston's GPC Calibration CD6E

Batch Numbers	Weight Average Molecular Weights		$\frac{GPC}{L.S.} \times 100$
	L.S.	GPC	
PT 3636	239825	244153	101.80
PH 1078	149600	144398	96.52
PG 7427	104450	103450	99.04
PF 1601	73625	74003	100.51
PB 5227	42150	42457	100.73
PE 5382	21975	23451	106.72
PA 0094	11500	10892	94.71
JD 2985	8825	8377	94.92
DK 8868	5250	5140	97.90
PD 2335	4100	4331	105.63
Glucose	180	180	100.00

Calibration Constants				
b_1	b_2	b_3	b_4	b_5
-13.663	12.758	-9.547	15.987	-73.385

FIG 6.4.4 GPC CALIBRATION CURVE (CD6E) AT ASTON'S TSK-PW COLUMNS

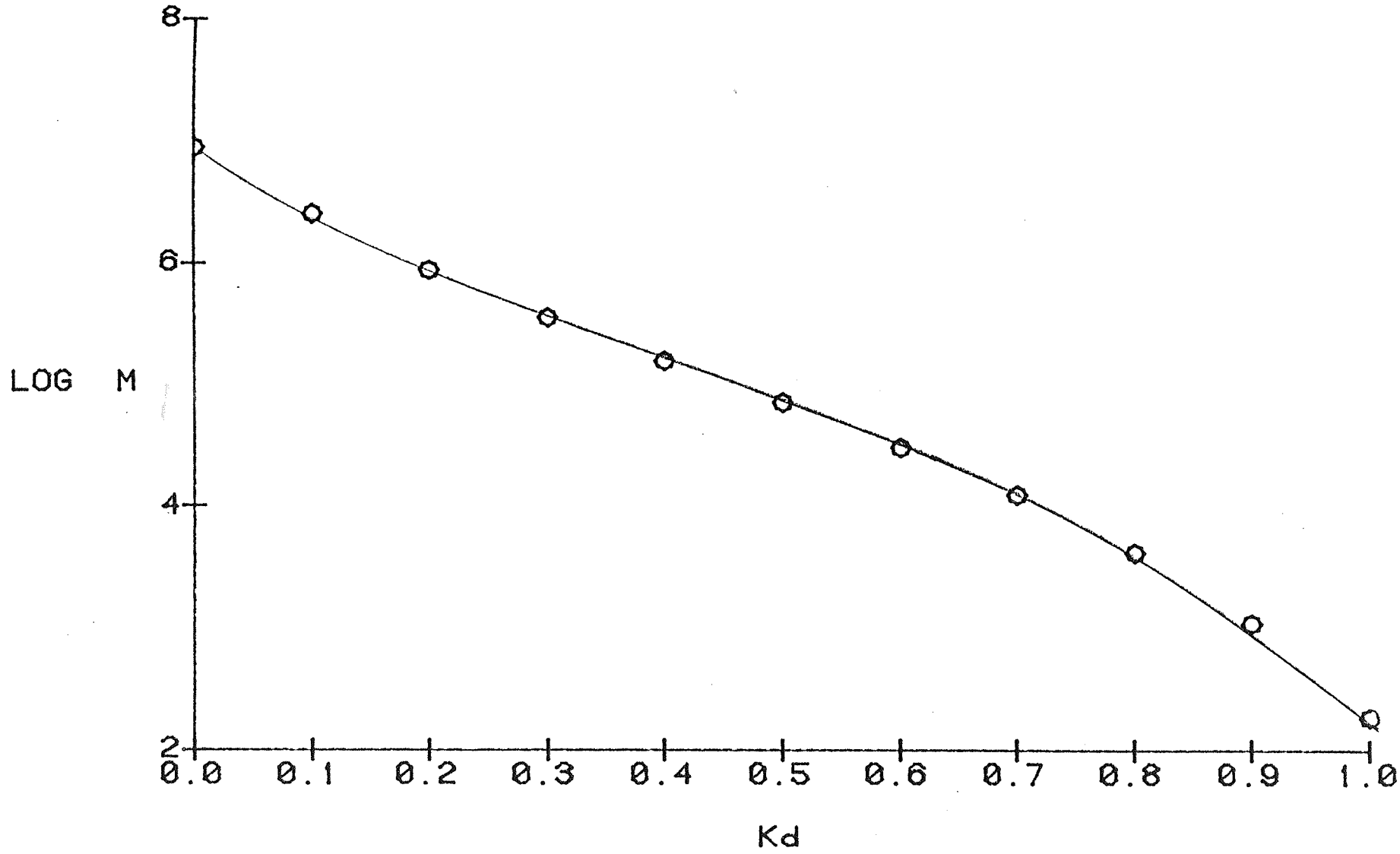

during this calibration) provided a much better agreement, individual molecular weights obtained by GPC were within 98-102% of those obtained by light-scattering with a standard deviation of 0.77.

Aston's calibration CD5E (identical calibration standards as Fisons' 315Z calibration) provided results of individual molecular weights within 98-102% with a standard deviation of 0.92. Different calibration standards were used for 'CD6E' giving results of individual molecular weights within 94-107% with a standard deviation of 3.9.

The reproducibility of the GPC system can be illustrated by the analysis of BT1J for thirty runs over a period of eight months. The standard deviation on the $\bar{M}_W$ was 814 with a mean value of 39,990, a difference of 3.6% over the light-scattering value of 41,500.

6.4.2 DETERMINATION OF THE AVERAGE MOLECULAR WEIGHTS

To convert the chromatogram of a sample to average molecular weights it was required that:

(a) The heights measured at regular intervals of thirty seconds along the chromatogram, the elution times of i) very high molecular weight dextran peak (for calculation of the void volume), ii) glucose peak (for calculation of the total liquid volume), iii) the start of chromatogram, iv) the end of a chromatogram and finally the calibration constants b_1-b_5 be entered into the computer program (Appendix A2).

(b) This computer program calculated the number ($\bar{M}_N$), weight ($\bar{M}_W$) average molecular weights, polydispersity ($\bar{D}$) and weight fractions from the chromatogram using equations:

a) $$K_d = \frac{V_R - V_o}{V_i} \quad \ldots\ldots\ldots\ldots\ldots\ldots\ldots\ldots \quad 3.3.1$$

b) $$M_i = b_5 + \exp\{b_4 + b_1(K_{di}) + b_2(K_{di})^2 + b_3(K_{di})^3\} \quad \ldots\ldots \quad 3.3.16$$

c) $$\text{Normalised height, } h_i = \frac{\text{Chromatogram height, } h_i'}{\text{Total chromatogram heights } \Sigma h_i'} \quad \ldots\ldots\ldots\ldots\ldots\ldots \quad 6.4.1$$

d) $$\bar{M}_W = \frac{\Sigma h_i M_i}{\Sigma h_i} \quad \ldots\ldots\ldots\ldots\ldots\ldots\ldots\ldots \quad 3.3.20$$

e) $$\bar{M}_N = \frac{\Sigma h_i}{\Sigma h_i / M_i} \quad \ldots\ldots\ldots\ldots\ldots\ldots\ldots\ldots \quad 3.3.21$$

f) $$\bar{D} = \frac{\bar{M}_W}{\bar{M}_N} \quad \ldots\ldots\ldots\ldots\ldots\ldots\ldots\ldots\ldots\ldots \quad 3.3.10$$

C H A P T E R S E V E N

LABORATORY-SCALE ETHANOL FRACTIONATION OF DEXTRAN

7.0 LABORATORY-SCALE ETHANOL FRACTIONATION OF DEXTRAN

7.1 INTRODUCTION

The simplest and quickest method of testing the mathematical model (Chapter 5.0) was to simulate the Fisons plant fractionation procedure on the laboratory scale.

The Fisons plant fractionation procedure for producing the final syrup (clinical dextran) from syrup I is a two-stage process based on the solubility method of fractional precipitation by the addition of a non-solvent (ethanol).

The first stage is the production of syrup IR and super IR, the second stage is the production of final syrup and final super from the super IR (See Fig. 7.1.1).

7.2 EXPERIMENTAL METHOD

Dextran solution (Syrup I, Plant Batch RB 51K) having a concentration of 8% w/v was filtered using a Carlson pressure filter with Na 120 and G4 filter sheets (John C. Carlson Ltd., Aston-u-Lyne).

Plant ethanol (supplied by Fisons Ltd., Holmes Chapel) of known concentration was mixed with 400 cm^3 syrup I solution in a 1000 cm^3 separating funnel to fractionate some of the high molecular weight dextrans. As large dextran molecules are less soluble in aqueous ethanol than small ones, it precipitates from the solution as a syrup IR.

After 16-20 hours the syrup IR was separated, ethanol was distilled off from the syrup IR using a Quick-fit kit

Fig. 7.1.1 Block Diagram of the Plant Fractionation; Double Fractionation

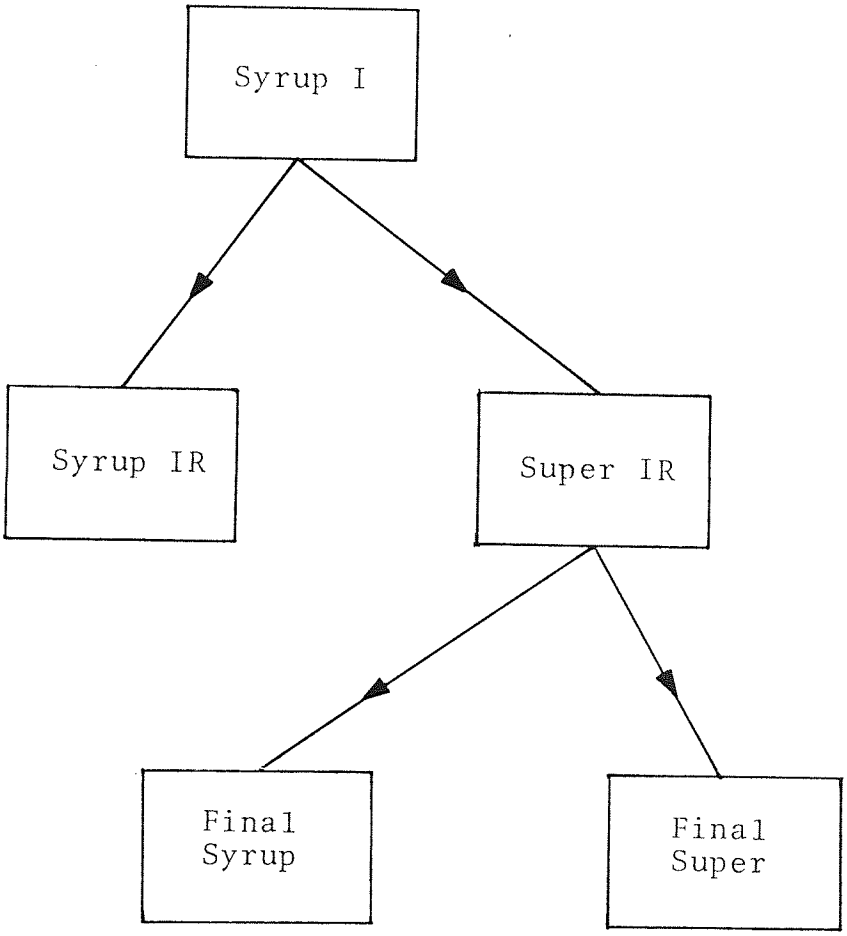

(Gallenkamp & Co. Ltd., Birmingham) and from the remaining solution (super IR). Concentrations measured by a constant temperature ABBE optical refractometer (Bellingham and Stanley Ltd., London N19) using a calibration curve and the volumes of these two solutions were recorded.

Ethanol was mixed with the super IR to fractionate the medium molecular weight dextrans (final syrup) leaving the very low molecular weight dextrans in the final super. After 16-20 hours the final syrup was separated and ethanol was distilled off from the two dextran solutions. Concentrations and volumes of the solutions were recorded.

The other measurements recorded were:

(i) Volumes of the syrup IR, super IR, final syrup and final super (prior to ethanol distillation),

(ii) The volumes of ethanol used in the fractionation stages,

(iii) The volumes of the distilled ethanol, and

(iv) The fractionation temperature.

A total of thirty one laboratory experiments were carried out during this research work. For run 10 and onwards fractionation was performed at 25^{o}C in a constant temperature water bath controlled by a thermoregulator (TE-4, Techne, Cambridge, U.K.).

Three calibrations were carried out on the ABBE optical refractometer at 20^{o}C during this research work; the calibrations were found to be linear with respect to dextran concentration. Tabulation of the results are given in Figs. 7.2.1-7.2.3. The data was fitted by the least squares linear regression method. The correlation coefficient (β) is a measure of how well the straight

Fig. 7.2.1 ABBE Optical Refractometer Calibration Results

Dextran Conc. (%w/v) y	Refractometer Reading (Decimal Degrees) x
2	3.517
4	3.703
5	3.862
8	4.247
10	4.517
12	4.765
15	5.120
20	5.688

$y = 8.100x - 26.361$

Correlation Coefficient = 0.9993

Fig. 7.2.2 ABBE Optical Refractometer Calibration Results

Dextran Conc. (%w/v) y	Refractometer Reading (Decimal Degrees) x
2	3.467
4	3.717
5	3.850
8	4.217
10	4.467
12	4.700
15	5.017

$y = 8.307x - 26.930$

Correlation Coefficient = 0.9995

Fig. 7.2.3 ABBE Optical Refractometer Calibration Results

Dextran Conc. (%w/v) y	Refractometer Reading (Decimal Degrees) x
2	3.417
4	3.683
5	3.817
8	4.183
10	4.450
12	4.667
15	5.017
20	5.567

$y = 8.353x - 26.837$

Correlation Coefficient = 0.9993

line fitted to the data approximates the data. The value will be between -1 and +1 with either + or -1 being a perfect correlation.

7.3 COMPARISON OF EXPERIMENTAL RESULTS WITH PREDICTIONS OF THE MODEL

Experimental conditions and results are listed in Figs. 7.2.4-7.2.10 whereas the model predictions are listed separately in Figs. 7.2.11-7.2.17.

For runs 1-11 experimental results of the weight percentage (Wt%) dextran fractions are plotted against model results in Fig. 7.2.18. It can be seen that for the first fractionation (Surup IR) the two sets of results are in good agreement. For the second fractionation (final syrup) the model is predicting approximately twelve weight per cent more than the experimental values.

To try and explain the offset in the second stage it was proposed to carry out more laboratory experiments, with a few variations in the experimental method.

Runs 13-18 were slightly different in procedure to runs 1-11. Previously after the separation of the Syrup IR and super IR, ethanol was distilled off from the latter. In this case no distillation was carried out on the Super IR. To precipitate the final syrup ethanol was simply added to the super IR (similar procedure of the Fisons' plant, Holmes Chapel (22)). Experimental results are compared with the model predictions in Fig. 7.2.19 for runs 13-18.

Fig. 7.2.19 shows that for the first stage the two

Fig. 7.2.4 Experimental Conditions and Results; Runs 1-5

Run	1	2	3	4	5
Vol. of Syrup I (cm^3)	650	400	400	400	400
Conc. of Syrup I (%w/v)	8	9	9	8	8
Fractionation Temp(^oC)	19	19	19	18	18
Conc. of Ethanol (wt%)	88.5	88.5	88.5	88.5	88.5
Vol. of Ethanol Used in First Stage (cm^3)	-	330	310	275	275
Vol. of Ethanol Used in Second Stage (cm^3)	-	340	330	300	250
Was Ethanol in Super IR Distilled	YES	YES	YES	YES	YES
Were Stages Stirred for 4 Hours	NO	NO	NO	NO	NO
Vol. of Syrup IR (cm^3)	-	70	60	15	10
Vol of Super IR (cm^3)	-	660	650	655	665
Vol.of Final Super(cm^3)	-	590	480	561	460
Vol.of Final Syrup(cm^3)	-	20	20	67	56
$D = \frac{\text{Vol. of Super IR}}{\text{Vol. of Syrup IR}}$	-	9.43	10.83	43.67	66.50
$F = \frac{\text{Vol. of Final Super}}{\text{Vol. of Final Syrup}}$	-	29.50	24.00	8.37	8.21
Wt% Syrup IR	49.60	58.00	60.00	4.90	3.80
Wt% Super IR	44.00	41.00	39.00	92.44	95.30
Wt% Final Super	20.00	13.20	16.60	27.63	23.75
Wt% Final Syrup	26.20	26.40	22.00	63.78	68.75

Fig. 7.2.5 Experimental Conditions and Results; Runs 6-10

Run	6	-	8	9	10
Vol. of Syrup I (cm^3)	400		400	400	400
Conc. of Syrup I (%w/v)	7.5		8.6	8.55	7.3
Fractionation Temp (^oC)	20		19	20	25
Conc. of Ethanol (wt%)	84		84	84	66.5
Vol. of Ethanol Used in First Stage (cm^3)	300		310	310	510
Vol. of Ethanol Used in Second Stage (cm^3)	330		230	230	385
Was Ethanol in Super IR Distilled	YES		YES	YES	YES
Were Stages Stirred for 4 Hours	NO		NO	NO	NO
Vol. of Syrup IR (cm^3)	40		55	36	33
Vol. of Super IR (cm^3)	647		650	665	877
Vol.of Final Super(cm^3)	590		380	367	615
Vol.of Final Syrup(cm^3)	40		30	40	35
$D = \frac{\text{Vol. of Super IR}}{\text{Vol. of Syrup IR}}$	16.18		11.82	18.47	26.58
$F = \frac{\text{Vol. of Final Super}}{\text{Vol. of Final Syrup}}$	14.75		12.67	9.18	17.57
Wt% Syrup IR	29.60		51.00	29.00	23.30
Wt% Super IR	68.70		49.00	71.00	78.50
Wt% Final Super	10.70		8.70	7.40	33.60
Wt% Final Syrup	55.00		39.50	63.60	43.00

Fig. 7.2.6 Experimental Conditions and Results; Runs 11-15

Run	11	-	13	14	15
Vol. of Syrup I (cm^3)	400		400	400	400
Conc. of Syrup I (%w/v)	7.3		8	8	8
Fractionation Temp (^oC)	25		25	25	25
Conc. of Ethanol (Wt%)	66.5		99.5	99.5	99.5
Vol. of Ethanol Used in First Stage (cm^3)	500		300	290	280
Vol. of Ethanol Used in Second Stage (cm^3)	435		144	150	120
Was Ethanol in Super IR Distilled	YES		NO	NO	NO
Were Stages Stirred for 4 Hours	NO		NO	NO	NO
Vol. of Syrup IR (cm^3)	23		43	41	36
Vol. of Super IR (cm^3)	877		630	620	620
Vol. of Final Super (cm^3)	650		750	745	710
Vol. of Final Syrup (cm^3)	40		-	-	18
$D = \frac{\text{Vol. of Super IR}}{\text{Vol. of Syrup IR}}$	38.13		14.65	15.12	17.22
$F = \frac{\text{Vol. of Final Super}}{\text{Vol. of Final Syrup}}$	16.25		-	-	39.44
Wt% Syrup IR	20.50		60.47	53.27	43.16
Wt% Super IR	81.92		39.53	46.73	56.84
Wt% Final Super	22.00		6.81	6.63	17.89
Wt% Final Syrup	58.90		33.59	40.98	36.66

Fig. 7.2.7 Experimental Conditions and Results; Runs 16-20

Run	16	17	18	19	20
Vol. of Syrup I (cm^3)	400	400	400	400	400
Conc. of Syrup I (%w/v)	8	8	8	8	8
Fractionation Temp (^oC)	25	25	25	25	25
Conc. of Ethanol (wt%)	99.5	99.5	99.5	80	80
Vol. of Ethanol Used in First Stage (cm^3)	270	250	240	330	340
Vol. of Ethanol Used in Second Stage (cm^3)	90	66	70	74	60
Was Ethanol in Super IR Distilled	NO	NO	NO	NO	NO
Were Stages Stirred for 4 Hours	NO	NO	NO	NO	NO
Vol. of Syrup IR (cm^3)	28	7	3	3.5	6.5
Vol. of Super IR (cm^3)	615	620	615	710	713
Vol.of Final Super(cm^3)	670	640	630	740	735
Vol.of Final Syrup(cm^3)	28	42	45	37	33
$D = \frac{\text{Vol. of Super IR}}{\text{Vol. of Syrup IR}}$	21.96	88.57	205	203	110
$F = \frac{\text{Vol.of Final Super}}{\text{Vol.of Final Syrup}}$	23.93	15.24	14.00	20.00	22.27
Wt% Syrup IR	31.44	5.92	1.80	2.10	5.18
Wt% Super IR	68.56	94.08	98.20	97.90	94.82
Wt% Final Super	18.52	27.81	31.44	49.61	44.55
Wt% Final Syrup	51.44	67.97	67.56	47.48	50.39

Fig. 7.2.8 Experimental Conditions and Results; Runs 21-25

Run	21	22	23	24	25
Vol. of Syrup I (cm^3)	400	400	400	400	400
Conc. of Syrup I (%W/V)	8	8	8	8	8
Fractionation Temp. (^oC)	25	25	25	25	25
Conc. of Ethanol (wt%)	80	80	80	80	80
Vol. of Ethanol Used in First Stage (cm^3)	350	360	370	380	390
Vol. of Ethanol Used in Second Stage (cm^3)	70	55	100	90	80
Was Ethanol in Super IR Distilled	NO	NO	NO	NO	NO
Were Stages Stirred for 4 Hours	NO	NO	NO	NO	NO
Vol. of Syrup IR (cm^3)	10.8	17	28	32	38
Vol. of Super IR (cm^3)	715	720	720	728	730
Vol.of Final Super(cm^3)	740	747	788	790	787
Vol.of Final Syrup(cm^3)	37	29	25	22	16
$D = \frac{\text{Vol. of Super IR}}{\text{Vol. of Syrup IR}}$	66.20	42.35	25.71	22.75	19.21
$F = \frac{\text{Vol.of Final Super}}{\text{Vol.of Final Syrup}}$	20.00	25.76	31.52	35.91	49.19
Wt% Syrup IR	9.36	16.64	30.05	37.55	46.55
Wt% Super IR	90.64	83.36	69.95	62.45	53.45
Wt% Final Super	42.97	44.86	25.59	25.68	24.76
Wt% Final Syrup	48.69	38.81	43.03	35.19	26.90

Fig. 7.2.9 Experimental Conditions and Results; Runs 26-30

Run	26	27	28	29	30
Vol. of Syrup I (cm^3)	400	400	400	400	400
Conc. of Syrup I (%W/V)	8	8	8	8	8
Fractionation Temp (^oC)	25	25	25	25	25
Conc. of Ethanol (Wt%)	80	80	80	80	80
Vol. of Ethanol Used in First Stage (cm^3)	400	370	380	390	370
Vol. of Ethanol Used in Second Stage (cm^3)	70	100	90	80	60
Was Ethanol in Super IR Distilled	NO	NO	NO	NO	NO
Were Stages Stirred for 4 Hours	NO	YES	YES	YES	YES
Vol. of Syrup IR (cm^3)	40	28	32	38	76
Vol. of Super IR (cm^3)	735	720	728	730	675
Vol.of Final Super(cm^3)	790	790	790	789	725
Vol.of Final Syrup(cm^3)	12	25	21	16	6
$D = \frac{\text{Vol. of Super IR}}{\text{Vol. of Syrup IR}}$	18.38	25.71	22.75	19.21	8.88
$F = \frac{\text{Vol. of Final Super}}{\text{Vol. of Final Syrup}}$	65.83	31.60	37.62	49.31	121
Wt% Syrup IR	52.73	30.07	37.50	44.47	87.13
Wt% Super IR	47.27	69.93	62.50	55.53	12.88
Wt% Final Super	25.78	24.94	25.31	24.91	3.60
Wt% Final Syrup	20.40	42.66	35.00	26.78	9.24

Fig. 7.2.10 Experimental Conditions and Results; Runs 31-33

Run	31	32	33	-	-
Vol. of Syrup I (cm^3)	400	400	400		
Conc. of Syrup I (%w/v)	8	8	8		
Fractionation Temp(^oC)	25	25	25		
Conc. of Ethanol (Wt%)	80	80	80		
Vol. of Ethanol Used in First Stage (cm^3)	370	360	360		
Vol. of Ethanol Used in Second Stage (cm^3)	300	110	320		
Was Ethanol in Super IR Distilled	YES	NO	YES		
Were Stages Stirred for 4 Hours	YES	YES	YES		
Vol. of Syrup IR (cm^3)	76	25	25		
Vol. of Super IR (cm^3)	675	720	715		
Vol.of Final Super(cm^3)	550	790	560		
Vol.of Final Syrup(cm^3)	5.5	31	33		
$D = \frac{\text{Vol. of Super IR}}{\text{Vol. of Syrup IR}}$	8.88	28.80	28.6o		
$F = \frac{\text{Vol.of Final Super}}{\text{Vol.of Final Syrup}}$	100	25.48	16.97		
Wt% Syrup IR	86.63	20.75	20.78		
Wt% Super IR	13.38	79.25	79.22		
Wt% Final Super	7.28	24.06	24.98		
Wt% Final Syrup	7.70	52.31	48.64		

Fig. 7.2.11 Results of the Mathematical Model Predictions

Run	1	2	3	4	5
C X 10^5	2.77	4.86	3.19	-120	-41
D	3.83	6.94	3.38	0.0009	0.13
E x 10^4	1.56	2.56	2.12	0.88	0.81
F	6.15	17.03	13.02	6.24	4.83
P	0.37	0.34	0.33	0.70	0.71
Fixed Value of P	-	-	-	-	-
Wt% Syrup IR	52.30	55.72	57.61	4.60	4.49
Wt% Super IR	47.70	44.28	42.39	95.40	95.51
Wt% Final Super	10.50	9.74	9.71	23.09	22.30
Wt% Final Syrup	37.20	34.54	32.68	72.31	73.21

Fig. 7.2.12 Results of the Mathematical Model Predictions

Run	6	-	8	9	10
C x 10^5	4.03		3.60	2.76	1.90
D	122		6.57	14.06	10.45
E x 10^4	2.39		3.57	4.33	1.09
F	110		18.46	30.13	9.42
P	0.57		0.49	0.67	0.51
Fixed Value of P	-		-	-	-
Wt% Syrup IR	19.96		45.25	27.16	24.41
Wt% Super IR	80.04		54.75	72.84	75.59
Wt% Final Super	23.47		6.02	5.97	24.54
Wt% Final Syrup	56.57		48.73	66.87	51.05

Fig. 7.2.13 Results of the Mathematical Model Predictions

Run	11	-	13	14	15
$C \times 10^5$	2.04		6.36	4.51	3.10
D	16.37		5.67	2.55	4.46
$E \times 10^4$	1.19		-0.21	-0.06	3.20
F	2.66		-0.05	-0.3	6.88
P	0.68		-	-	-
Fixed Value of P	-		0.42	0.51	0.47
Wt% Syrup IR	19.87		61.05	66.06	47.33
Wt% Super IR	80.13		38.95	33.94	52.67
Wt% Final Super	11.91		-3.92	-17.93	6.08
Wt% Final Syrup	68.22		42.87	51.87	46.59

Fig. 7.2.14 Results of the Mathematical Model Predictions

Run	16	17	18	19	20
C x 10^5	2.53	0.81	-1.53	-0.88	0.88
D	8.24	84.44	12.94	2.88	28.80
E x 10^4	2.99	1.26	1.26	0.75	0.81
F	5.61	3.18	3.13	5.60	7.26
P	-	-	-	-	-
Fixed Value of P	0.61	0.78	0.78	0.57	0.60
Wt% Syrup IR	33.13	5.62	4.10	17.50	10.50
Wt% Super IR	66.87	94.38	95.90	82.50	89.50
Wt% Final Super	6.69	16.73	15.79	22.75	29.35
Wt% Final Syrup	60.18	77.65	80.11	59.75	60.15

Fig. 7.2.15 Results of the Mathematical Model Predictions

Run	21	22	23	24	25
C x 10^5	0.37	1.00	2.86	3.23	3.78
D	13.84	8.37	10.10	7.82	5.96
E x 10^4	0.75	0.81	1.50	1.45	1.50
F	6.79	8.39	5.64	6.65	8.10
P	-	-	-	-	-
Fixed Value of P	0.59	0.49	0.53	0.45	0.37
Wt% Syrup IR	11.38	22.85	33.03	39.57	47.72
Wt% Super IR	88.62	77.15	66.97	60.43	52.28
Wt% Final Super	29.32	28.05	14.82	15.94	15.78
Wt% Final Syrup	59.30	49.10	52.15	44.49	36.50

Fig. 7.2.16 Results of the Mathematical Model Predictions

Run	26	27	28	29	30
C x 10^5	4.02	3.03	3.45	3.90	2.17
D	4.13	13.94	8.51	7.13	1.42
E x 10^4	1.46	1.48	1.48	1.31	2.20
F	8.78	6.96	6.49	7.62	196
P	-	-	-	-	-
Fixed Value of P	0.30	0.53	0.45	0.37	0.18
Wt% Syrup IR	55.63	29.13	38.77	44.43	81.68
Wt% Super IR	44.37	70.87	61.23	55.57	18.32
Wt% Final Super	15.15	18.38	16.70	19.39	0.91
Wt% Final Syrup	29.22	52.49	44.53	36.18	17.41

Fig. 7.2.17 Results of the Mathematical Model Predictions

Run	31	32	33	-	-
C x 10^5	2.42	2.23	2.04		
D	1.54	21.33	13.81		
E x 10^4	2.11	1.53	1.48		
F	59.41	7.84	6.08		
P	-	-	-		
Fixed Value of P	0.17	0.63	0.61		
Wt% Syrup IR	82.95	22.59	25.83		
Wt% Super IR	17.05	77.41	74.17		
Wt% Final Super	0.56	15.09	13.37		
Wt% Final Syrup	16.49	62.32	60.80		

FIG 7.2.18 COMPARISON OF MODEL RESULTS WITH EXPERIMENTAL RESULTS RUNS 1-11

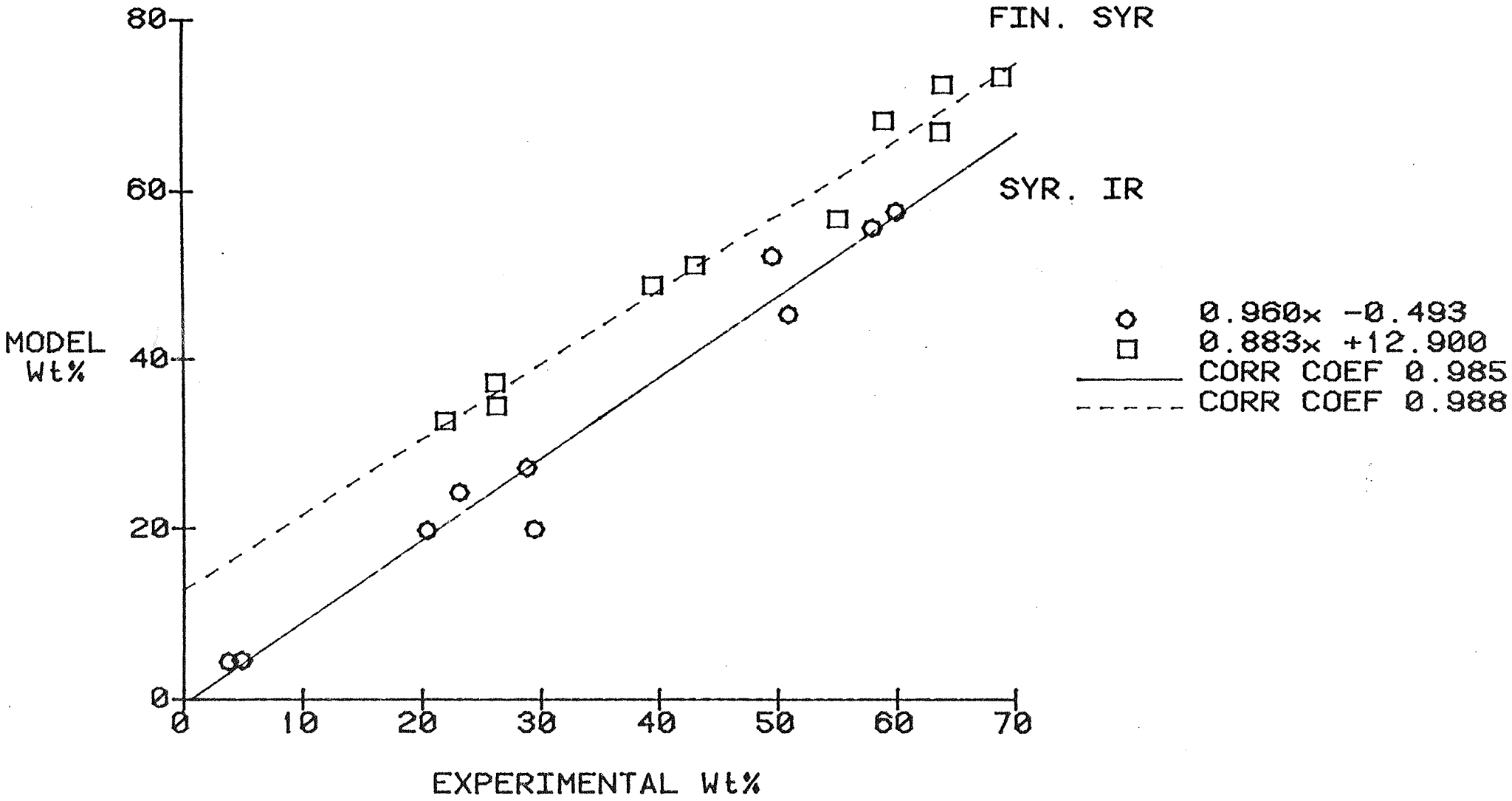

FIG 7.2.19 COMPARISON OF MODEL RESULTS WITH EXPERIMENTAL RESULTS RUNS 13-18

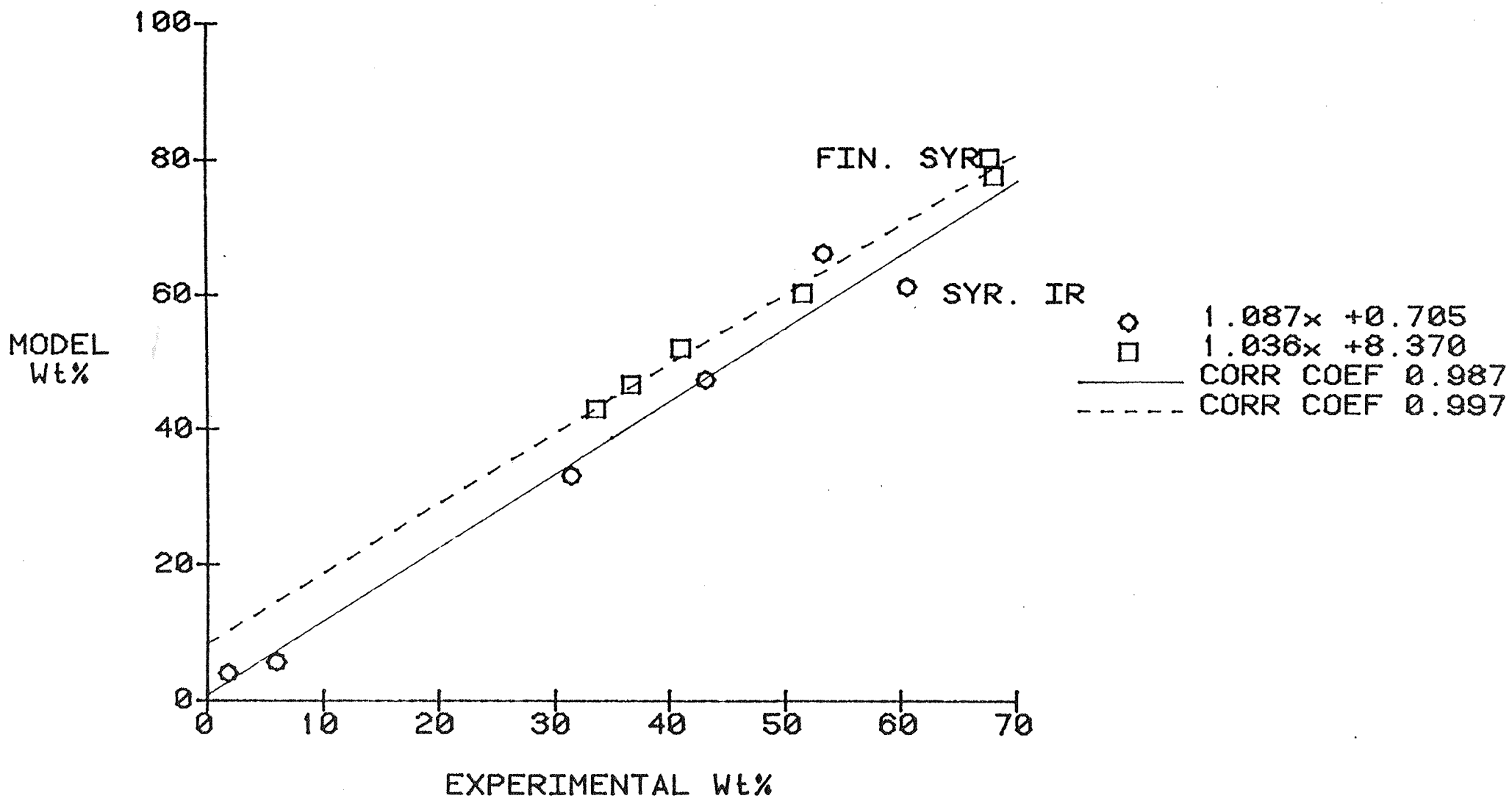

sets of results are in good agreement but an offset of similar magnitude found in previous runs is present in the second stage.

A further fifteen laboratory experiments were carried out using the above procedure with the exception of runs 31 and 33 where the ethanol distillation was carried out on the super IR. The objective was to perform two sets of experiments, namely runs 30, 31 and 32, 33 similar in the experimental conditions, except that in runs 31 and 33 ethanol was distilled from the super IR.

For runs 30 and 31 Pharmacia dextran T110 (Lot No. 5404) standard was used as the syrup I because of its i) similar weight average molecular weight to Fisons' syrup I plant Batch RB 51K, ii) narrow molecular weight distribution.

For runs 27 and onward the first and second separating stages were stirred for four hours continuously (shaken by hand previously) before leaving the solutions to stand for 16-20 hours so that equilibrium could be established.

Runs 23, 24 and 25 were similar to 27, 28 and 29 respectively in all respects with the exception of four hours stirring on runs 27, 28 and 29. The objective of this was to determine i) whether or not the longer stirring time made any difference to the amount of dextrans precipitated out, ii) if reproducibility of the results were obtainable.

Fig. 7.2.9 (runs 23-29) shows that i) the four hours stirring time has made no difference on the dextran

precipitations, ii) the reproducibility of the results is excellent. This is also supported by runs 30, 31 and 32, 33.

Fig. 7.2.20 is an overall comparison of the experimental results and model predictions. As before the first stage is in good agreement but an offset of about ten per cent is present in the second stage.

7.4 COMPARISON OF GPC AND MODEL PREDICTED MWD'S

For the laboratory experimental runs 8-11 a comparison of the MWD's obtained from GPC and the model equations was made.

The MWD's predicted by the model are defined by the weight fraction of species i μ_{if}, μ_{it}, μ_{ib} and μ_{is}, the equations are:

For the Final Syrup (μ_{if})

$$\mu_{if} = \frac{D.\exp(EM_i)}{P(F+\exp(EM_i))(D+\exp(CM_i))} \cdot \mu_{io} \quad \ldots\ldots 5.29$$

For the Super IR (μ_{it})

$$m_{it} = \frac{D}{D+\exp(CM_i)} \cdot m_{io} \quad \ldots\ldots 5.8$$

$$m_{io} = m_o \mu_{io} \quad \ldots\ldots 5.13$$

similarly

$$m_{it} = m_t \mu_{it} \quad \ldots\ldots 7.4.1$$

on substitution of equations 5.13 and 7.4.1 into 5.8 gives

FIG 7.2.20 COMPARISON OF MODEL RESULTS WITH EXPERIMENTAL RESULTS RUNS 1-33

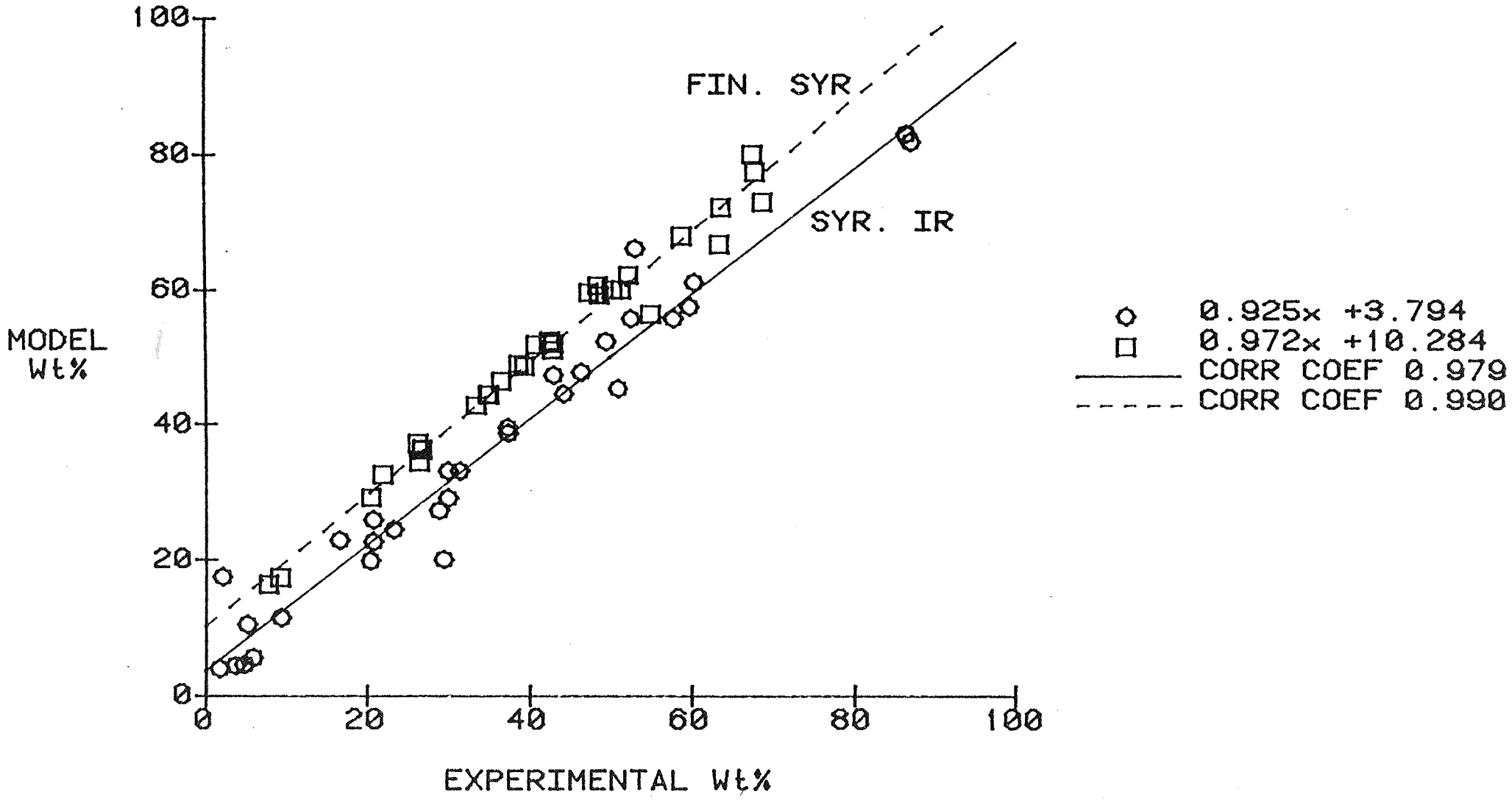

$$\mu_{it} = \frac{D}{(D+\exp(CM_i))(m_t/m_o)} \cdot \mu_{io} \quad \ldots\ldots\ldots\ldots \quad 7.4.2$$

For the Syrup IR (μ_{ib})

Equation 5.7 can alternatively be written as

$$\mu_{ib} = \frac{1}{m_b}(m_o\mu_{io} - m_t\mu_{it}) \quad \ldots\ldots\ldots\ldots\ldots\ldots \quad 7.4.3$$

rearranging equation 7.4.2 gives

$$m_t\mu_{it} = \frac{D}{D+\exp(CM_i)} \cdot m_o\mu_{io} \quad \ldots\ldots\ldots\ldots\ldots \quad 7.4.4$$

from the mass balance on the first stage

$$m_b = m_o - m_t \quad \ldots\ldots\ldots\ldots\ldots\ldots\ldots\ldots \quad 7.4.5$$

On substitution of the above two equations into 7.4.3 gives

$$\mu_{ib} = \{\mu_{io} - \frac{D}{D+\exp(CM_i)} \cdot \mu_{io}\} \frac{m_o}{m_o-m_t} \quad \ldots\ldots\ldots \quad 7.4.6$$

For the Final Super (μ_{is})

Equation 5.20 can alternatively be written as

$$\mu_{is} = \frac{1}{m_s} \cdot (m_t\mu_{it} - m_f\mu_{if}) \quad \ldots\ldots\ldots\ldots\ldots \quad 7.4.7$$

from the mass balance on the second stage

$$m_s = m_t - m_f \quad \ldots\ldots\ldots\ldots\ldots\ldots\ldots\ldots \quad 7.4.8$$

On substitution of equations 7.4.4 and 7.4.8 into 7.4.7 gives

$$\mu_{is} = \{\frac{D}{D+\exp(CM_i)} \cdot m_o\mu_{io} - m_f\mu_{if}\} \frac{1}{m_t-m_f} \quad \ldots\ldots \quad 7.4.9$$

The computer program using these equations for predicting the model MWD's is given in Appendix A5.

Comparison of GPC and model predicted MWD's are given in graphical form for runs 8-11 (see Figs. 7.4.1 - 7.4.16).

For runs 8-11 the final syrup MWD curves are in excellent agreement. This reflects the power of the modified Marquardt optimisation program (Appendix A3), as it relies on the minimisation of the difference between the GPC and model predicted weight fractions squared (see equation 5.30).

For the final super's the agreement is not very good. There is though a closer fit of the MWD's on the lower molecular weight range.

The MWD's of the super IR are also in very good agreement. This was to be excepted as Fig. 7.2.20 shows that the first stage is well predicted and from equation 5.14 it is seen that this prediction is based on the percentage dextrans present in the super IR.

For the syrup IR's the agreement is poor on the very high molecular weight range.

7.5 A TEST OF THE BOLTZMANN EQUATION USING EXPERIMENTAL DATA

For the first stage fractionation the Boltzmann expression is given by:

$$\frac{m_{ib}}{m_{it}} = \frac{V_b}{V_t} \exp\left(\frac{\lambda M_i}{KT}\right) \quad \ldots\ldots\ldots\ldots\ldots\ldots\ldots\ldots \quad 5.4$$

Fig. 7.4.1 Comparison of GPC and Model MWD's

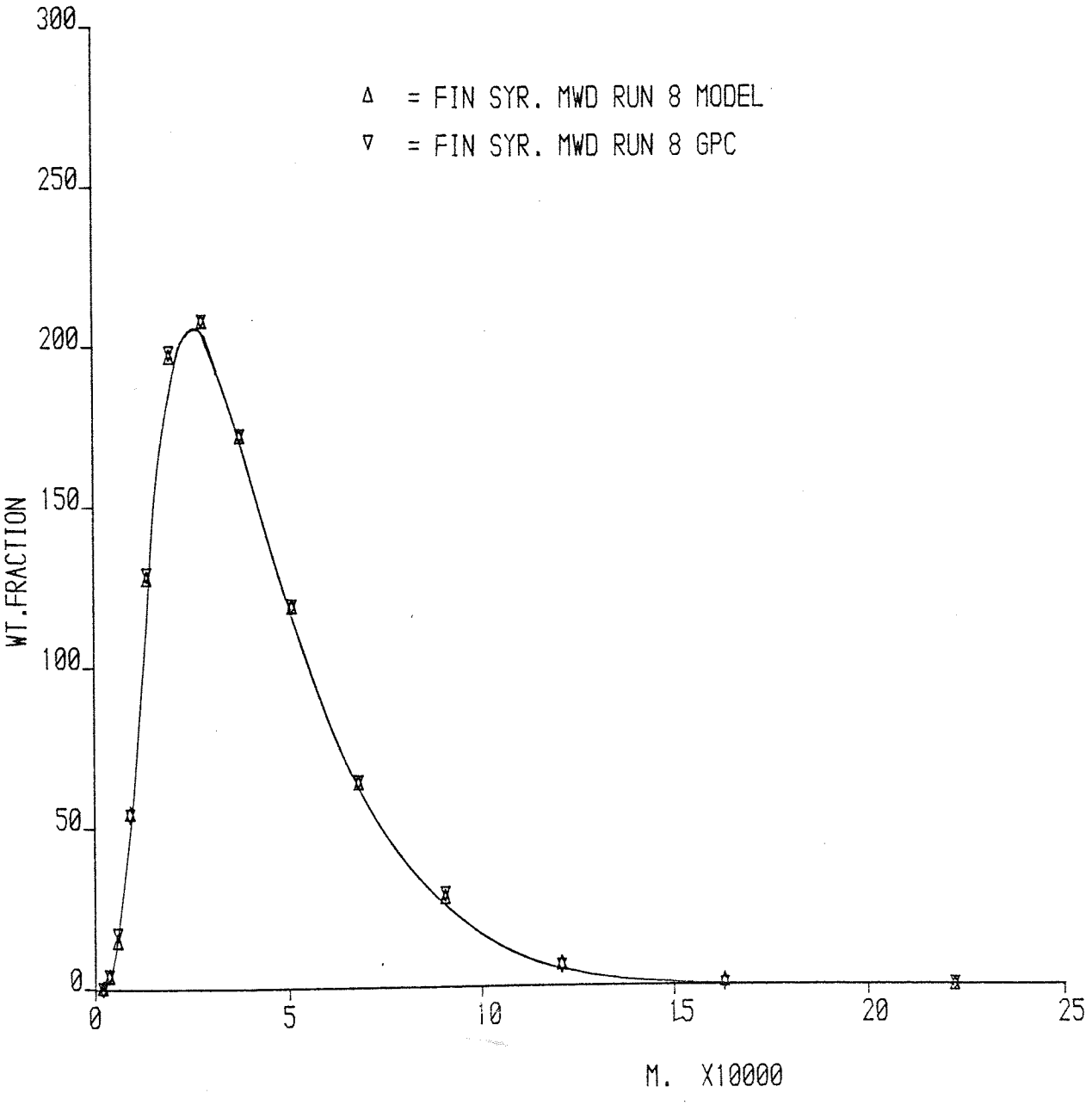

Fig. 7.4.2 Comparison of GPC and Model MWD's

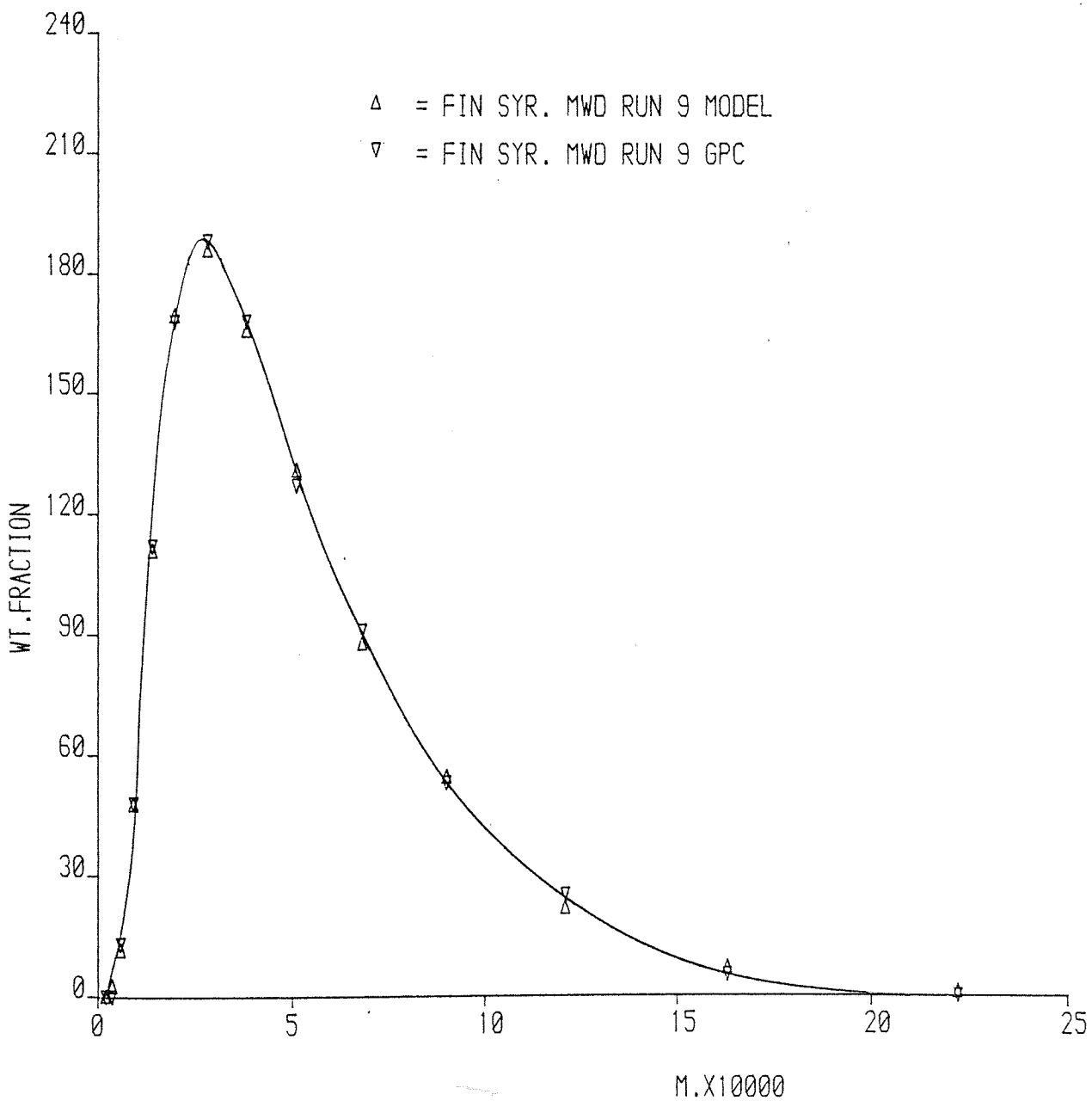

Fig. 7.4.3 Comparison of GPC and Model MWD's

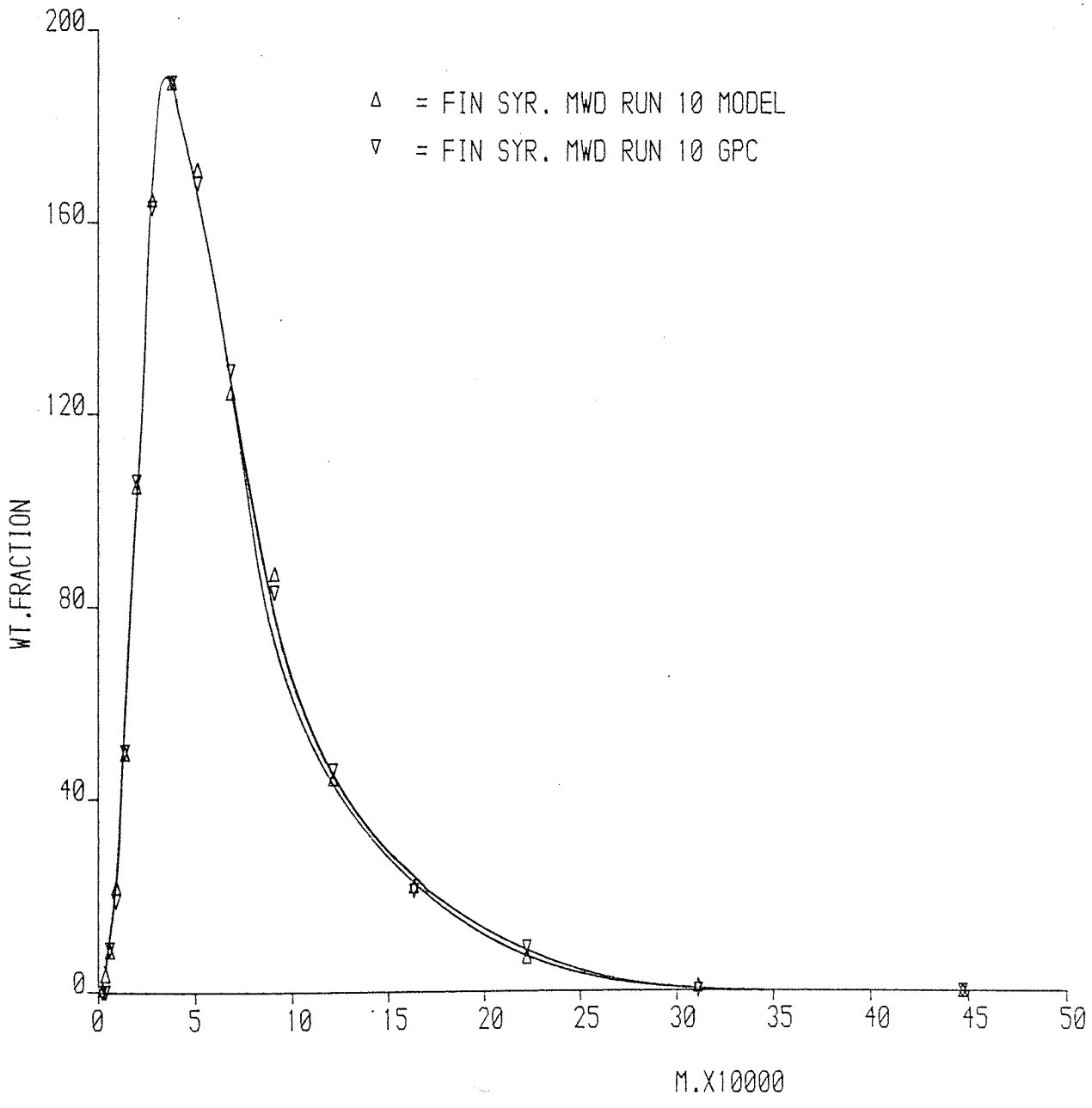

Fig. 7.4.4 Comparison of GPC and Model MWD's

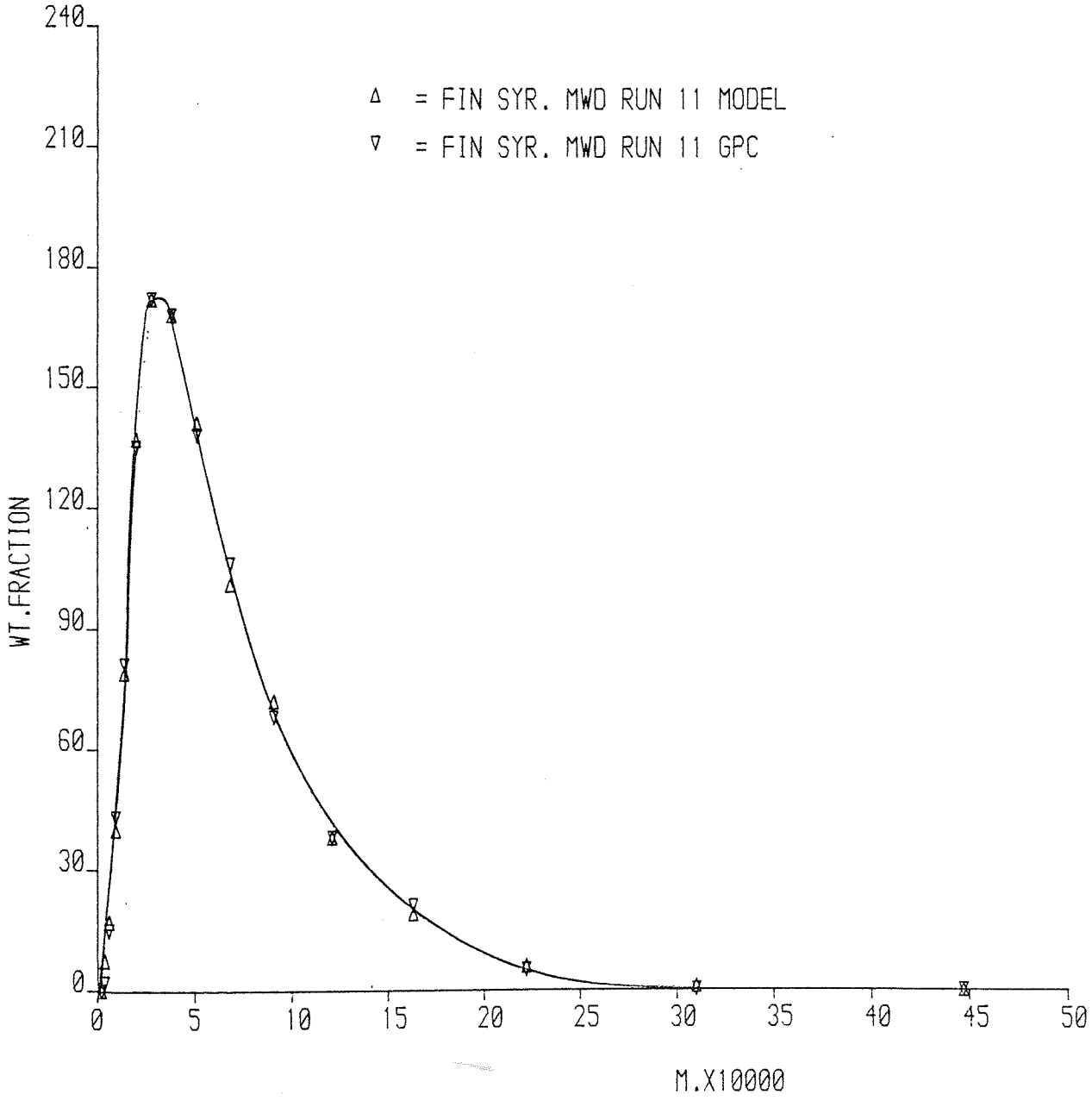

Fig. 7.4.5 Comparison of GPC and Model MWD's

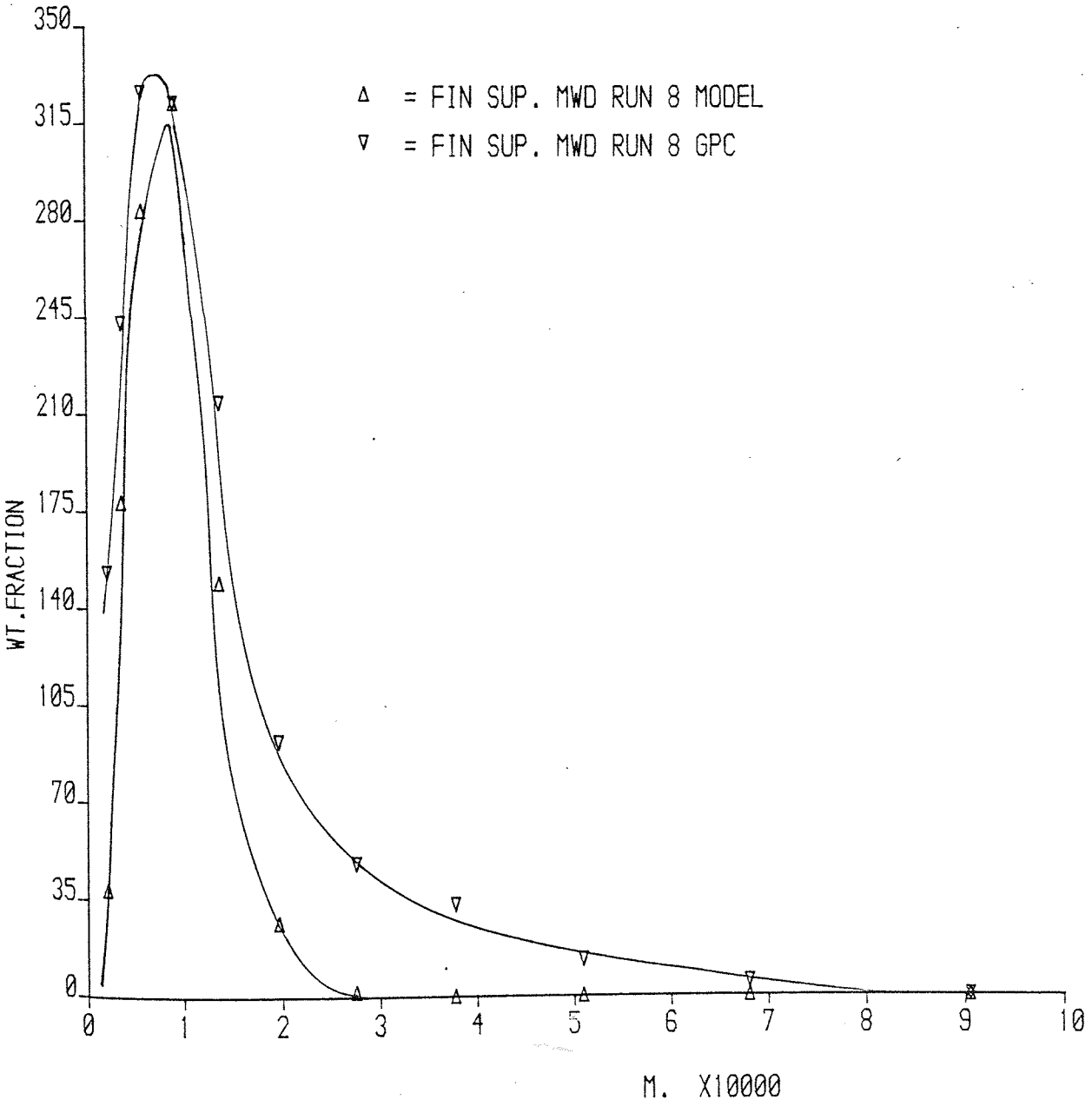

Fig. 7.4.6 Comparison of GPC and Model MWD's

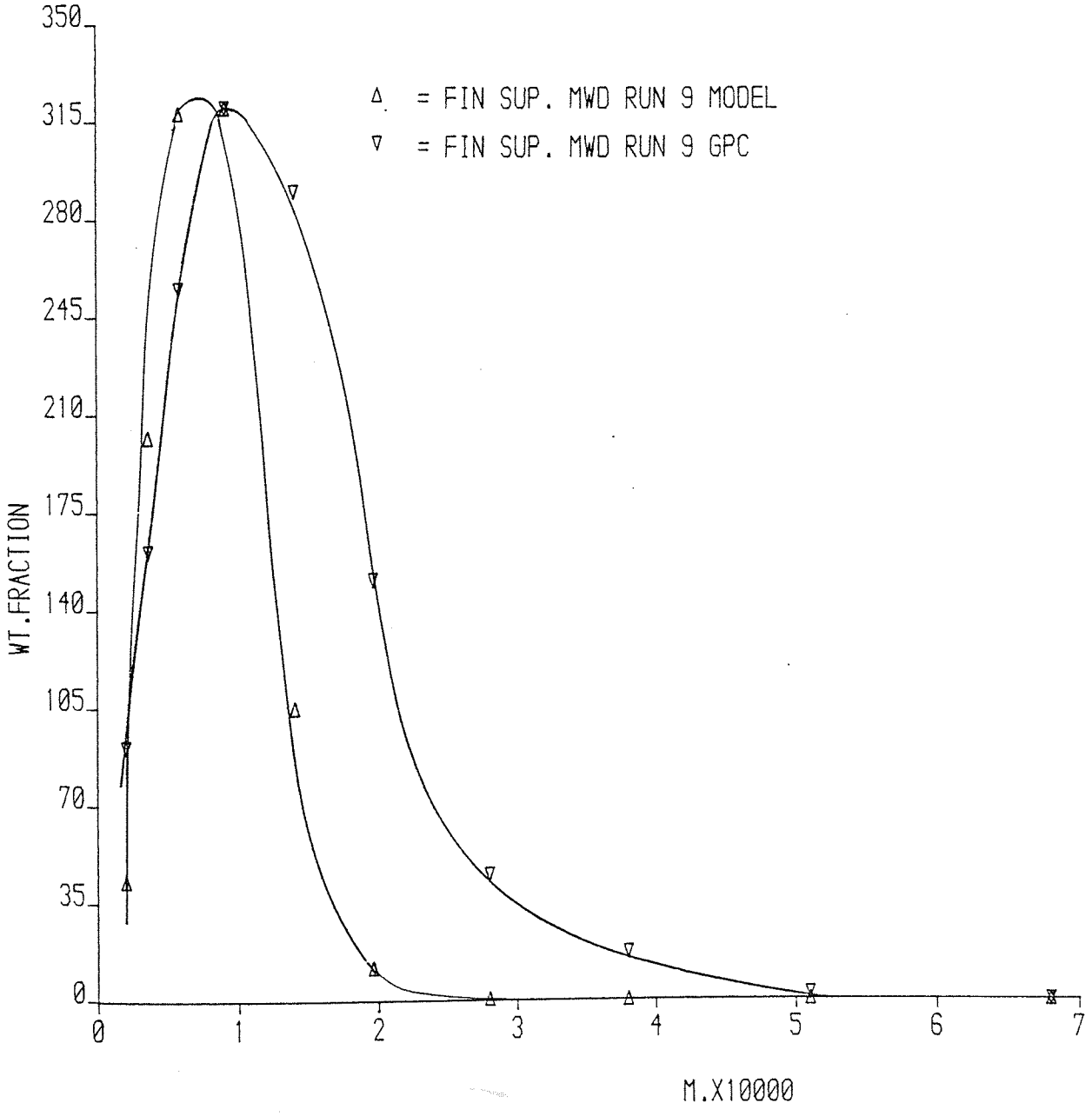

Fig. 7.4.7 Comparison of GPC and Model MWD's

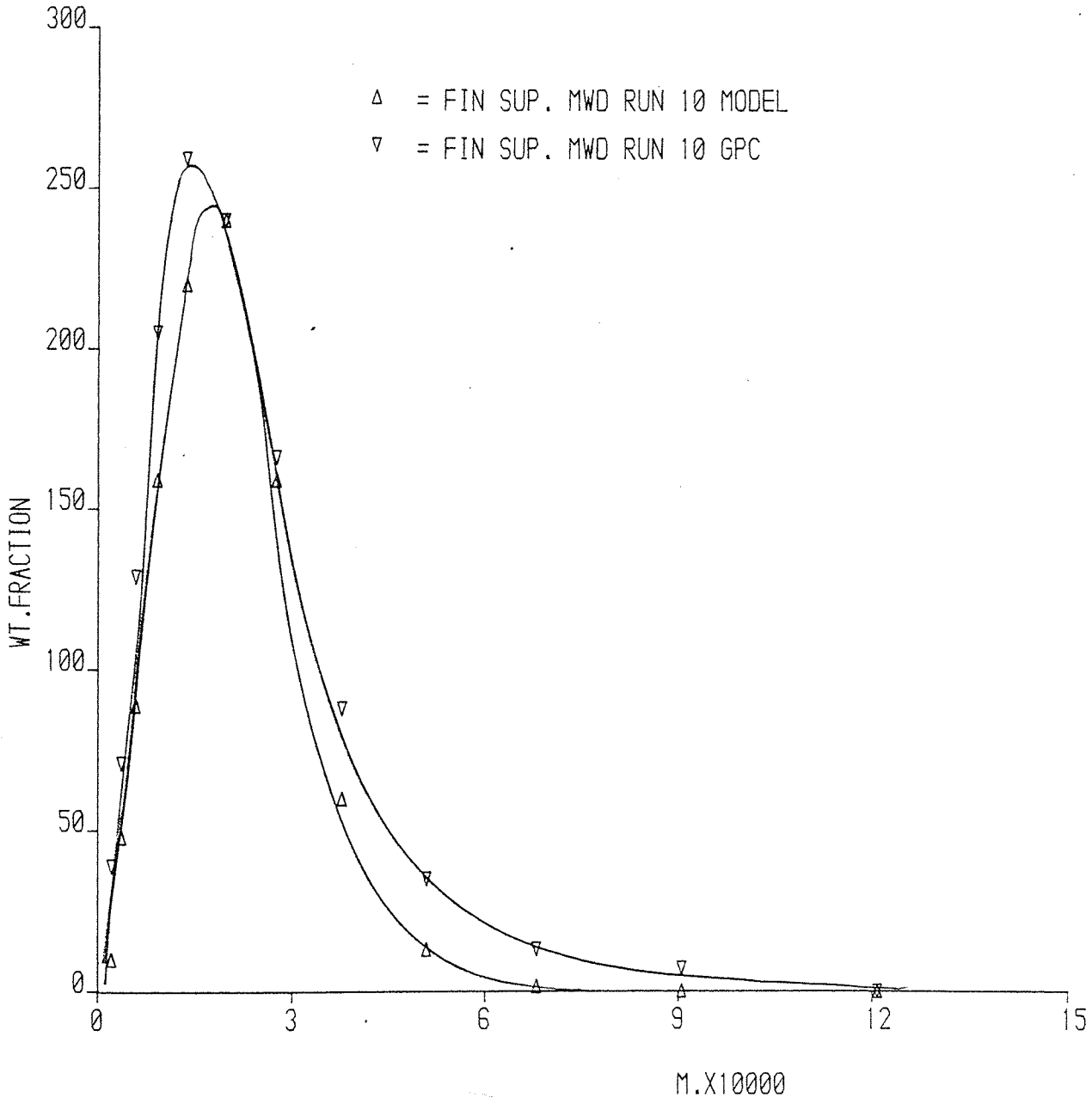

Fig. 7.4.8 Comparison of GPC and Model MWD's

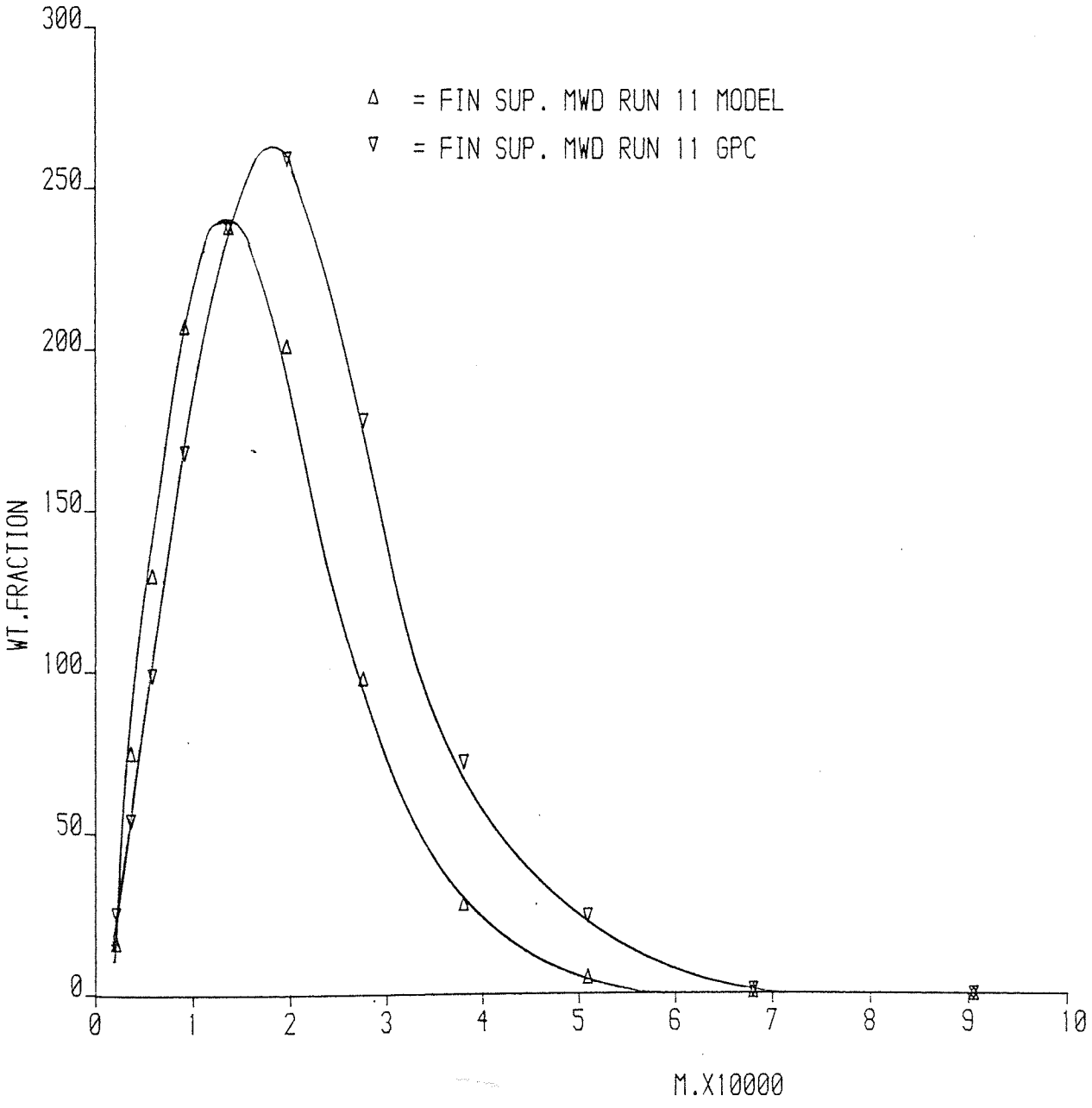

Fig. 7.4.9 Comparison of GPC and Model MWD's

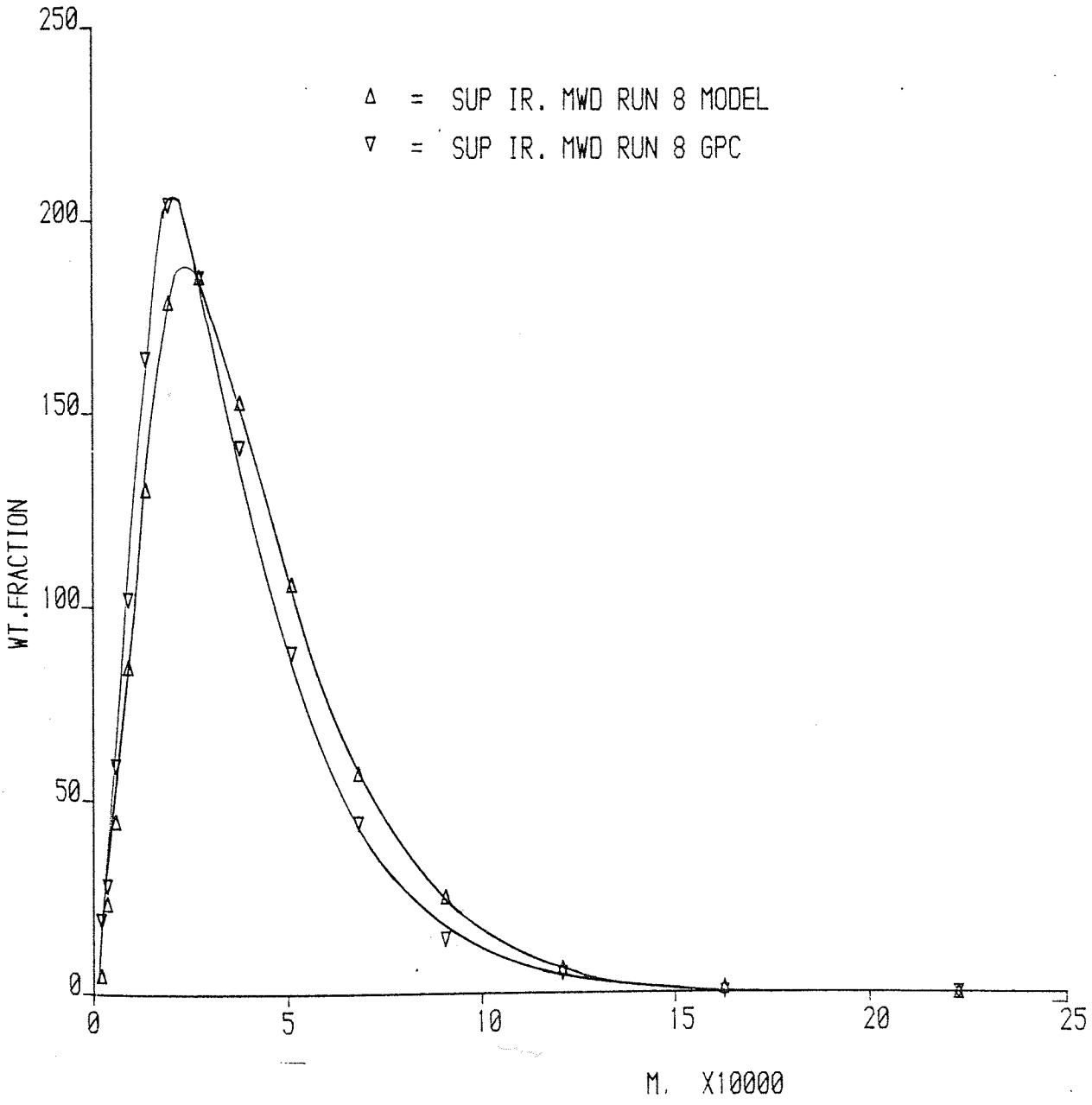

Fig. 7.4.10 Comparison of GPC and Model MWD's

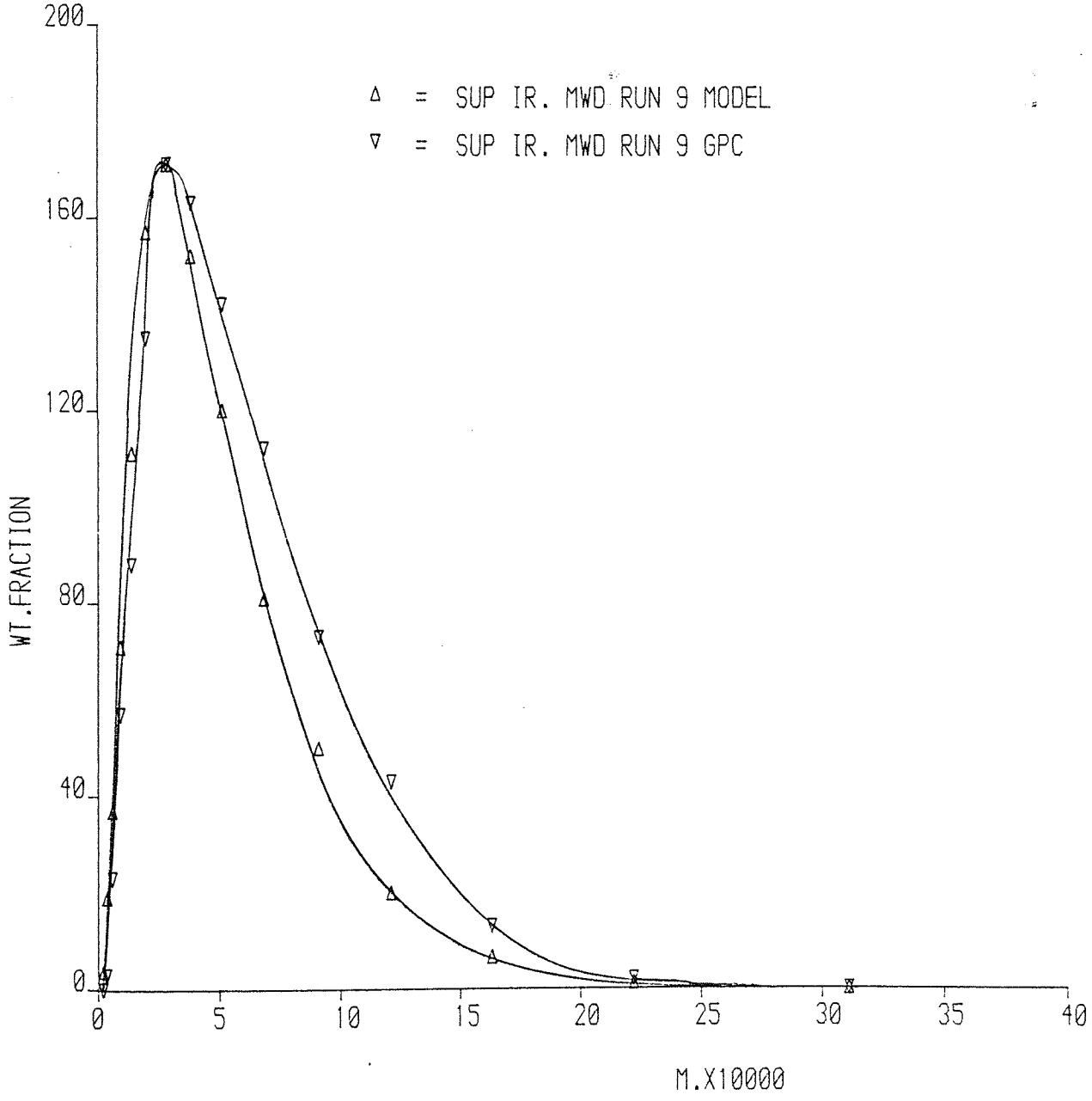

Fig. 7.4.11 Comparison of GPC and Model MWD's

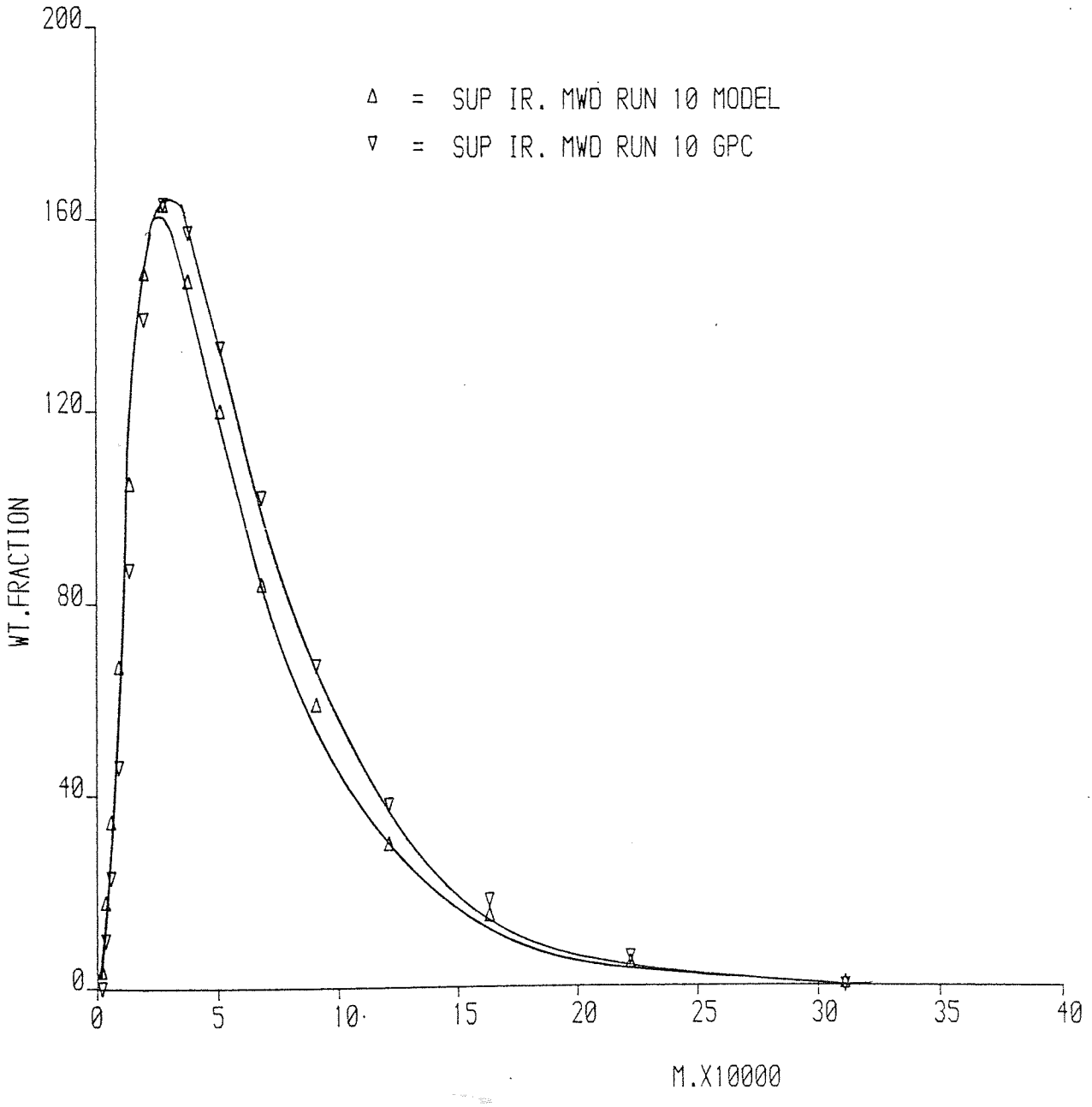

Fig. 7.4.12 Comparison of GPC and Model MWD's

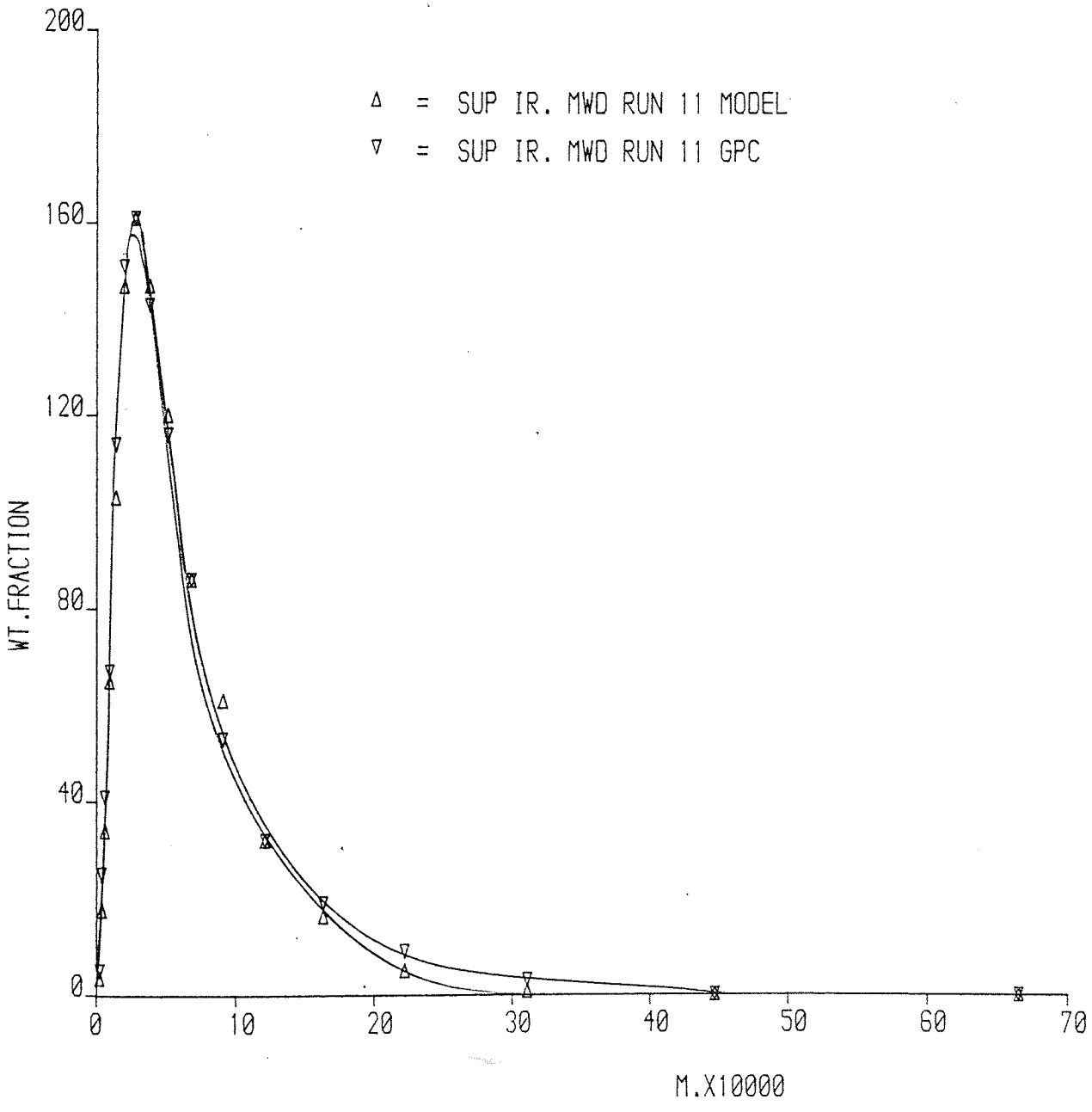

Fig. 7.4.13 Comparison of GPC and Model MWD's

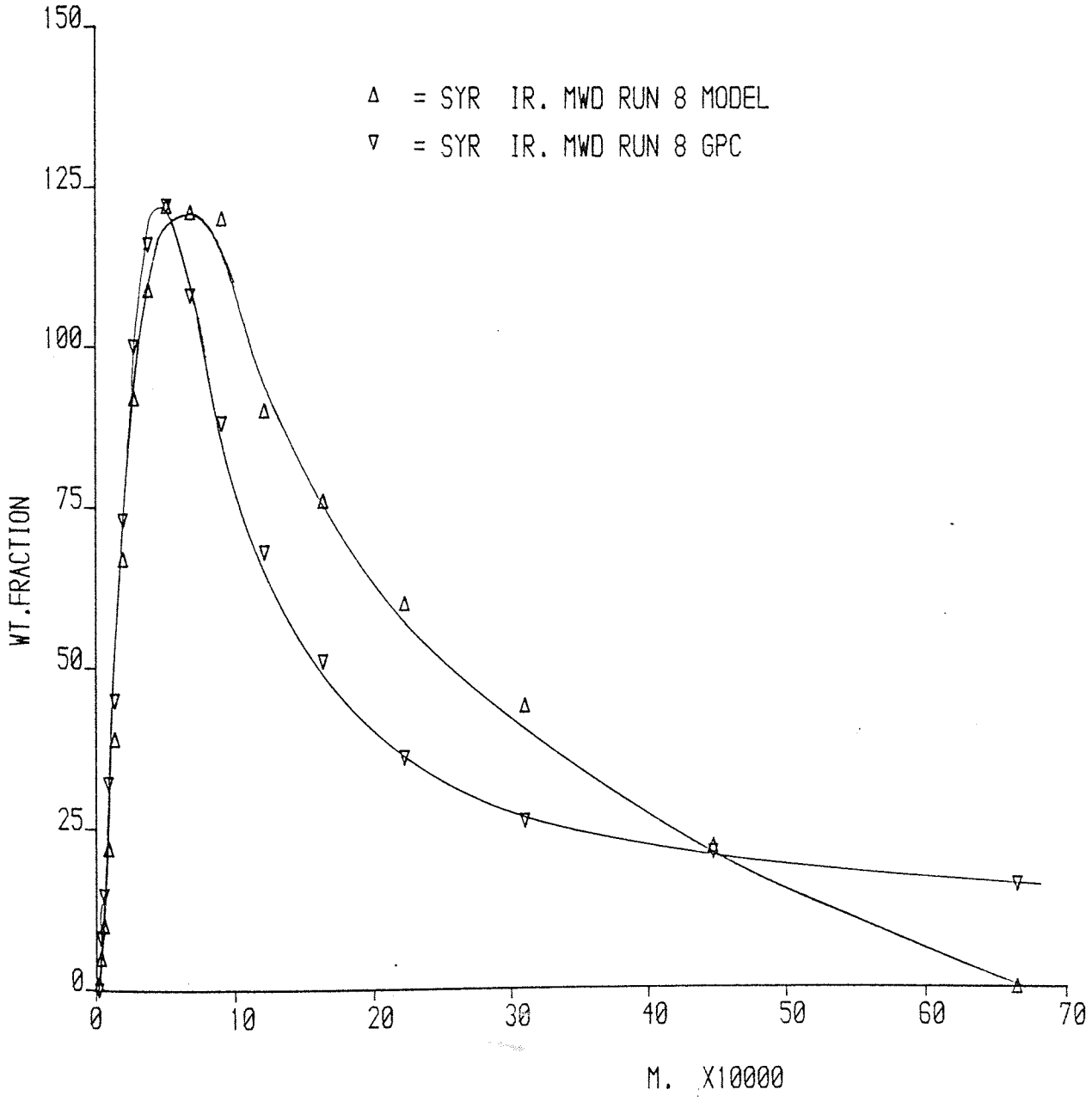

Fig. 7.4.14 Comparison of GPC and Model MWD's

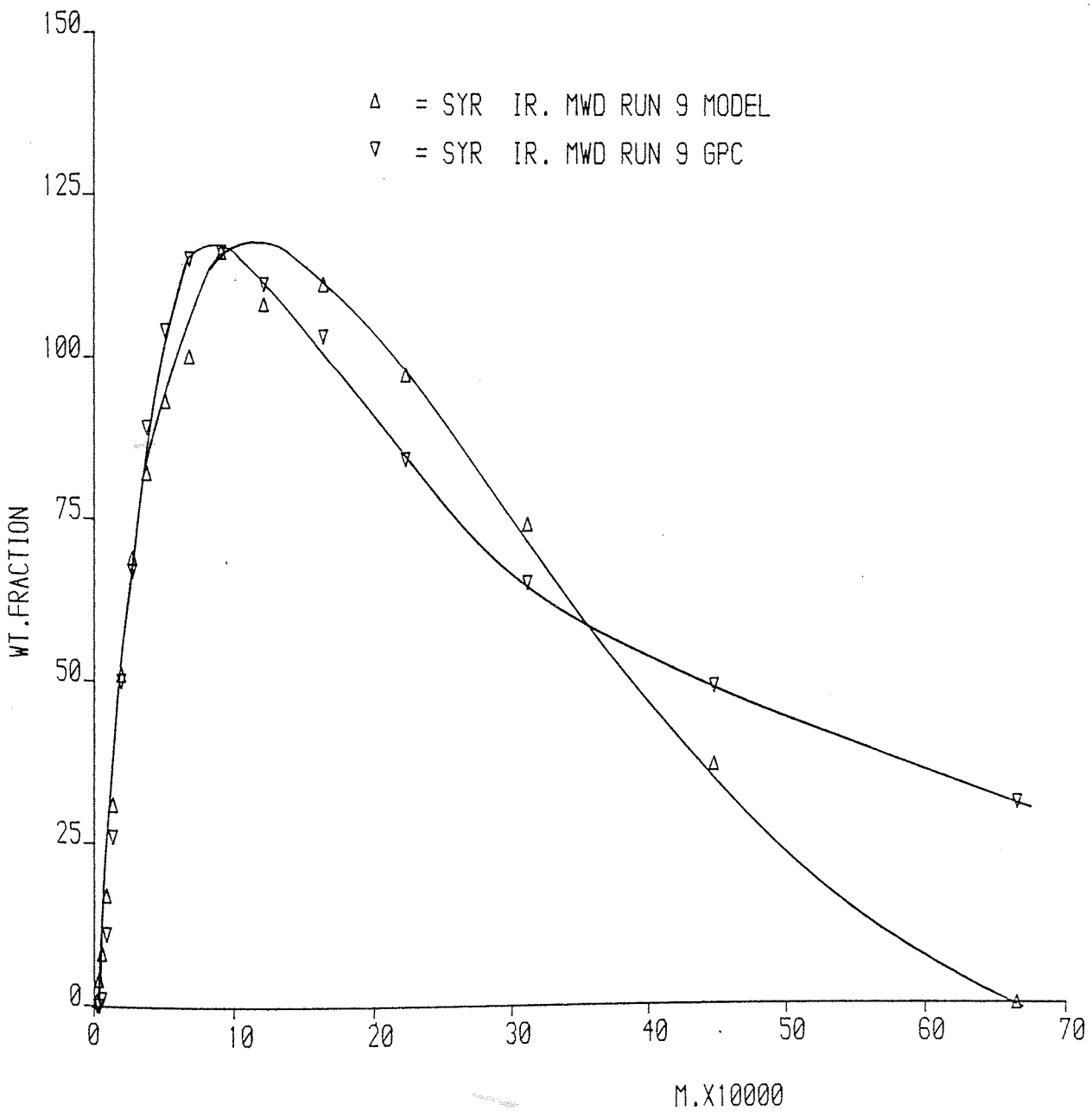

Fig. 7.4.15 Comparison of GPC and Model MWD's

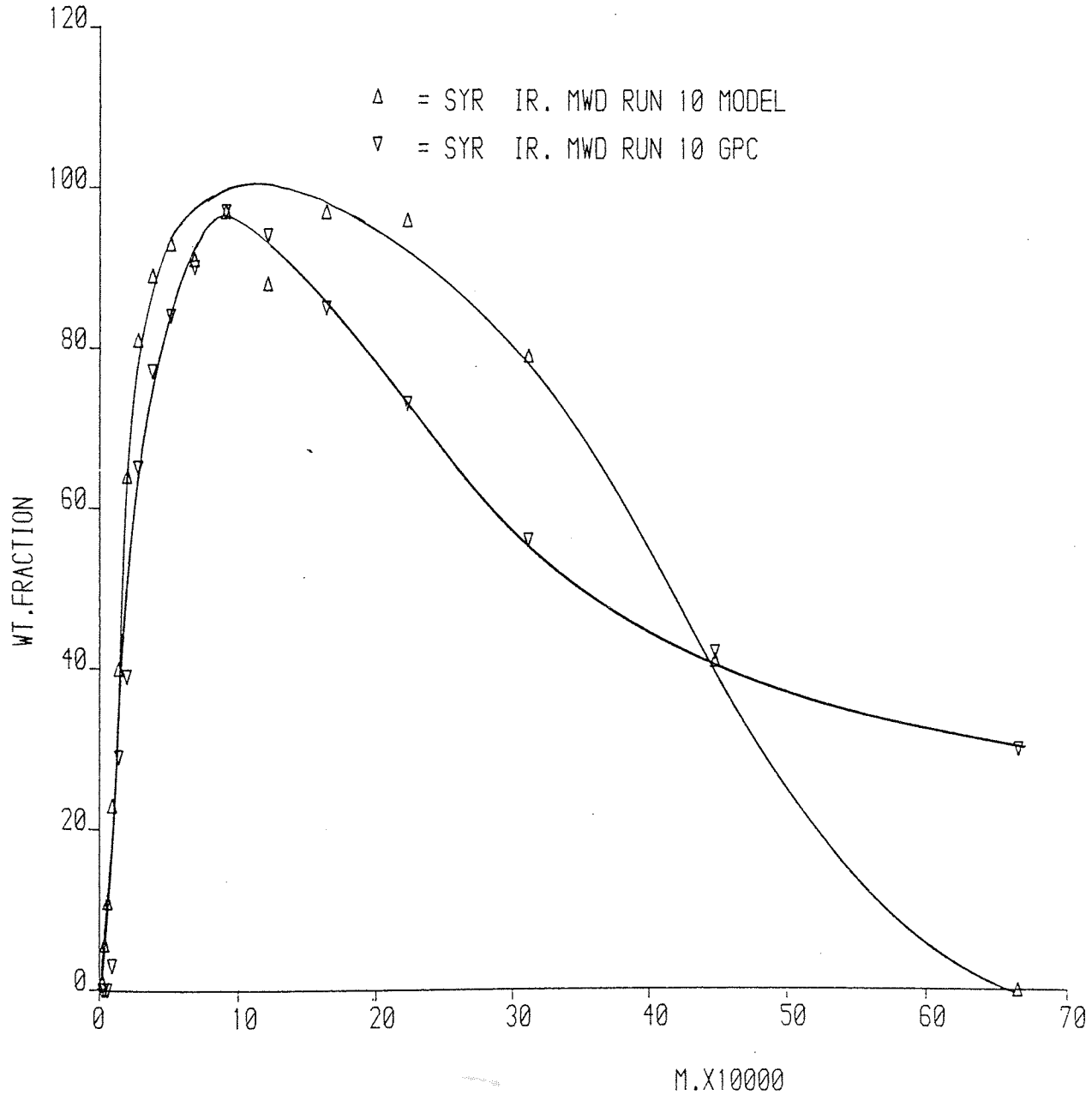

Fig. 7.4.16 Comparison of GPC and Model MWD's

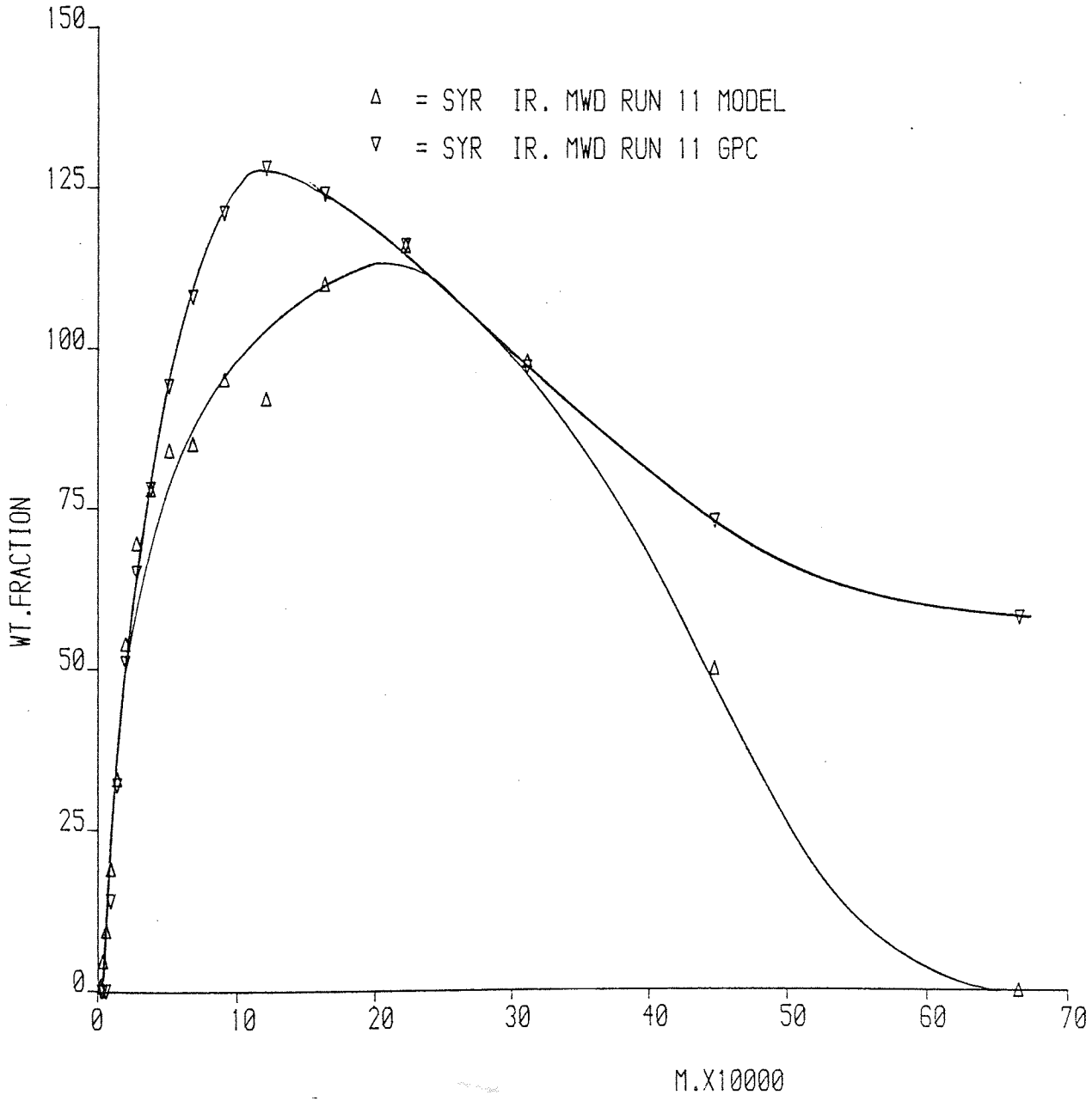

On substitution of the constants C and D (equations 5.5 and 5.6 respectively) gives:

$$\frac{m_{ib}}{m_{it}} = \frac{1}{D} \exp(CM_i) \quad \ldots\ldots\ldots\ldots\ldots\ldots\ldots\ldots \quad 7.5.1$$

and taking logarithms of the above equation gives:

$$\ln\left(\frac{m_{ib}}{m_{it}}\right) = CM_i + \ln\left(\frac{1}{D}\right) \quad \ldots\ldots\ldots\ldots\ldots\ldots\ldots \quad 7.5.2$$

This is a straight line relationship if $\ln(m_{ib}/m_{it})$ is plotted against M_i, giving C as the slope and $\ln(1/D)$ as the intercept.

Similarly for the second stage fractionation, the expression obtained after repeating the above steps is:

$$\ln\left(\frac{m_{if}}{m_{is}}\right) = EM_i + \ln\left(\frac{1}{F}\right) \quad \ldots\ldots\ldots\ldots\ldots\ldots\ldots \quad 7.5.3$$

This equation would yield E as the slope and $\ln(1/F)$ as the intercept when $\ln(m_{if}/m_{is})$ is plotted against M_i.

Runs 8-11 were again used for this test. Raw data was provided by the GPC analyses. The Boltzmann graphs for the above runs are given in Figs. 7.5.1-7.5.8.

For the first stage fractionation (Figs. 7.5.1-7.5.4) it is seen that the correlation coefficients are extremely good, run 11 having a slightly lower value. For the second stage runs 9 and 11 (Figs. 7.5.6 and 7.5.8) again show good correlation coefficients, runs 8 and 10 (Figs. 7.5.5-7.5.7) have lower values.

Fig. 7.5.9 shows that C values obtained from the Boltzmann plots and model predictions are in very good

FIG 7.5.1 BOLTZMANN PLOT FOR FIRST STAGE FRACTIONATION RUN 8

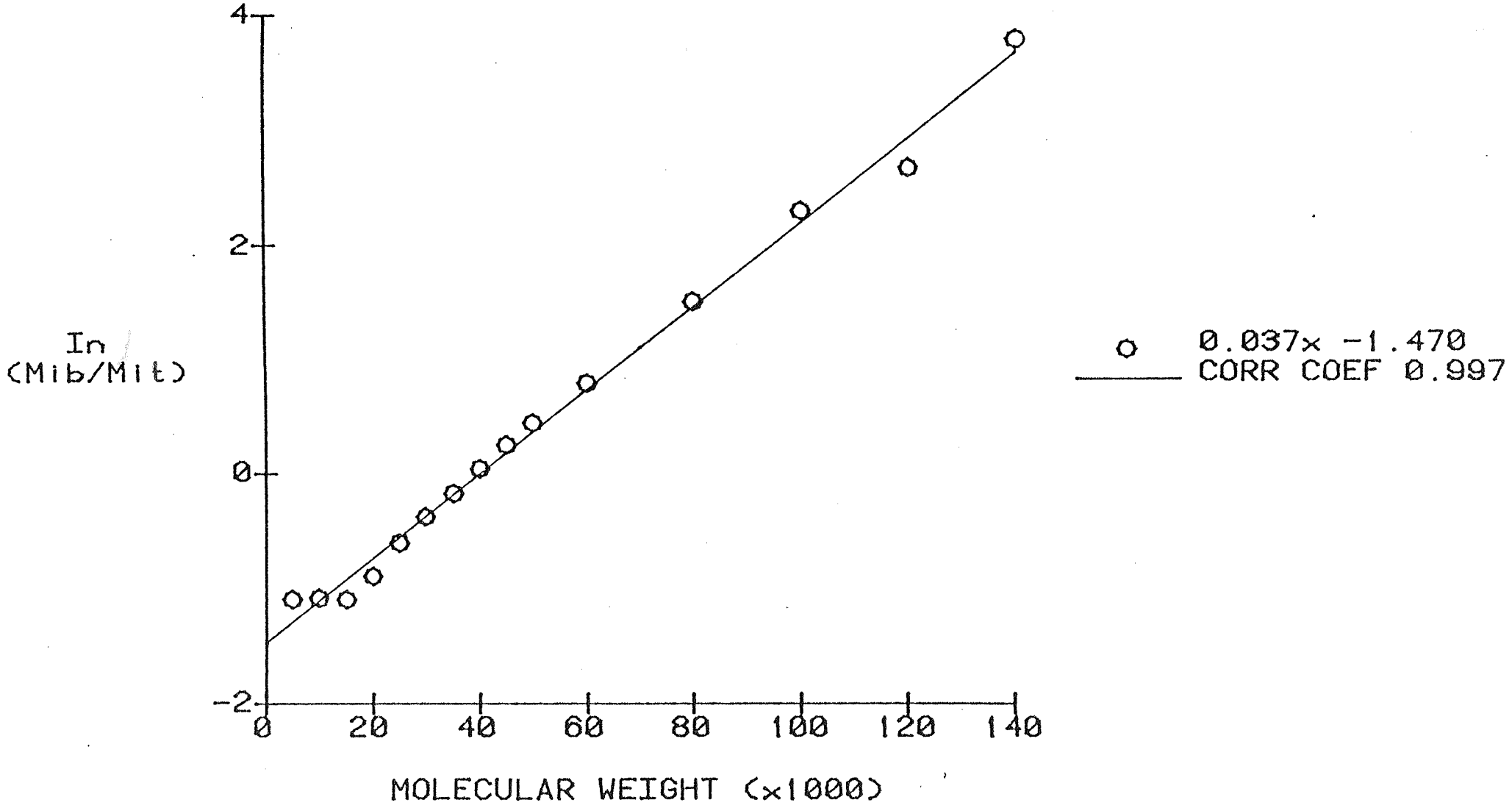

FIG 7.5.2 BOLTZMANN PLOT FOR FIRST STAGE FRACTIONATION RUN 9

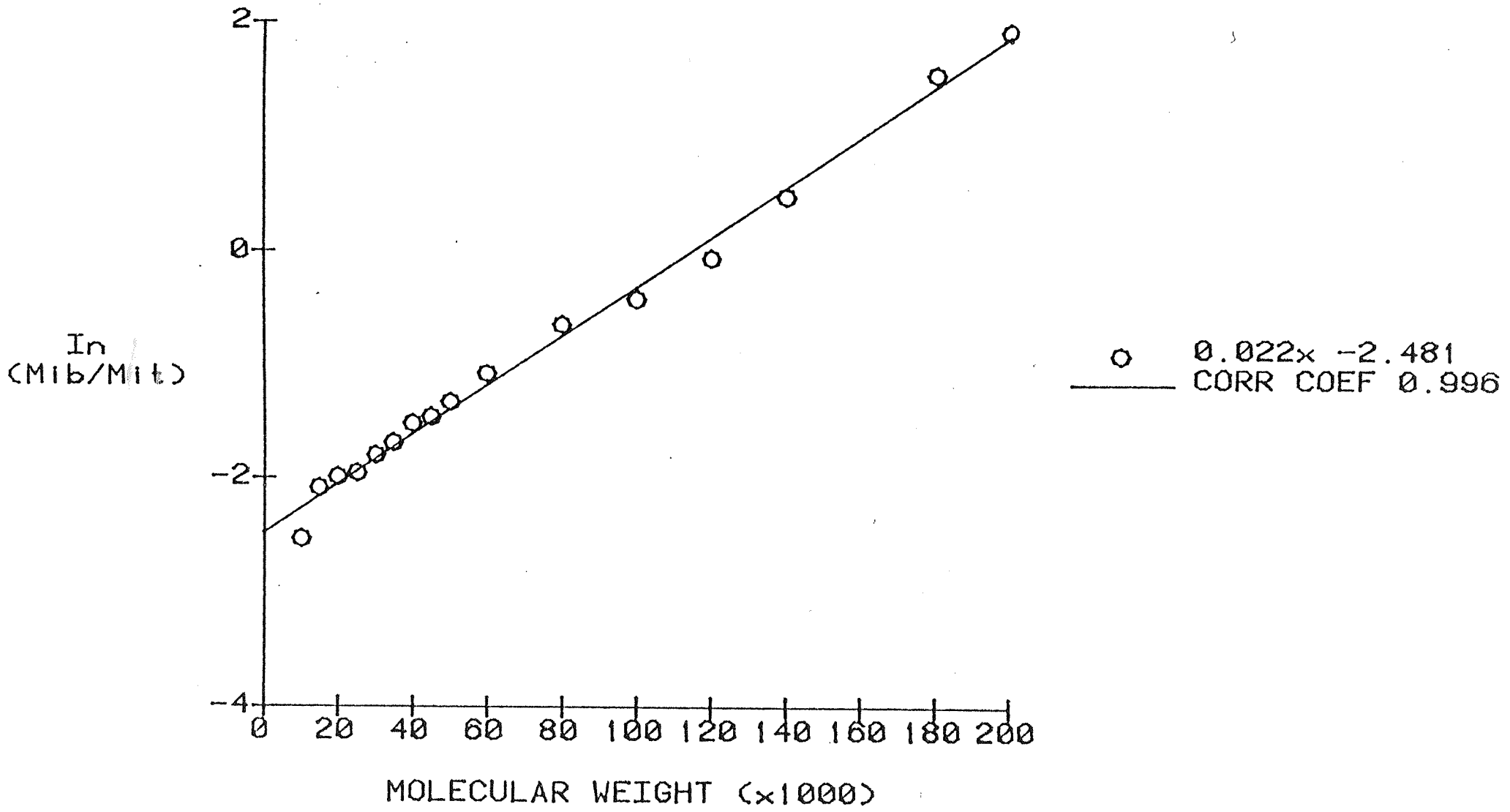

FIG 7.5.3 BOLTZMANN PLOT FOR FIRST STAGE FRACTIONATION RUN 10

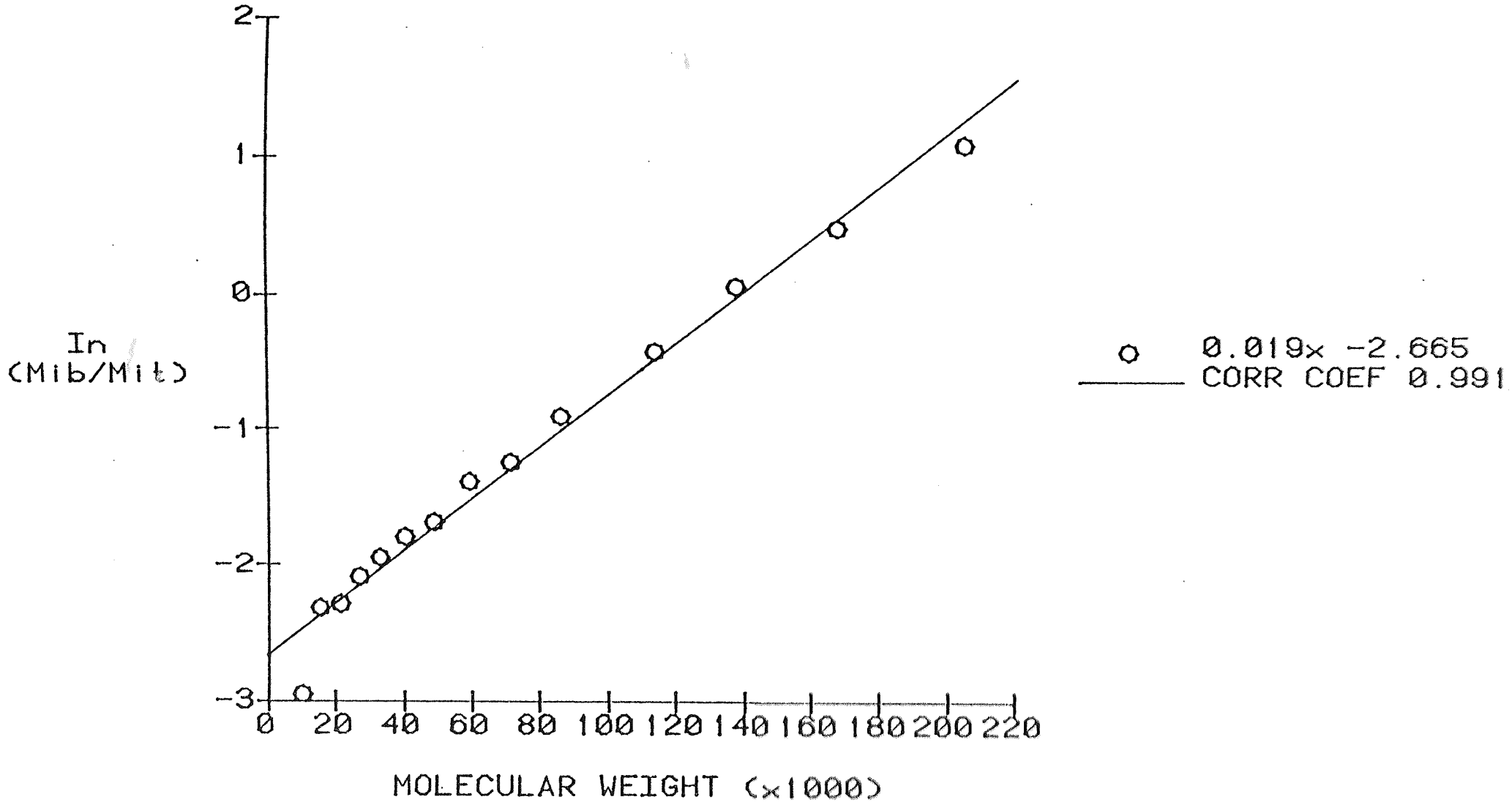

FIG 7.5.4 BOLTZMANN PLOT FOR FIRST STAGE FRACTIONATION RUN 11

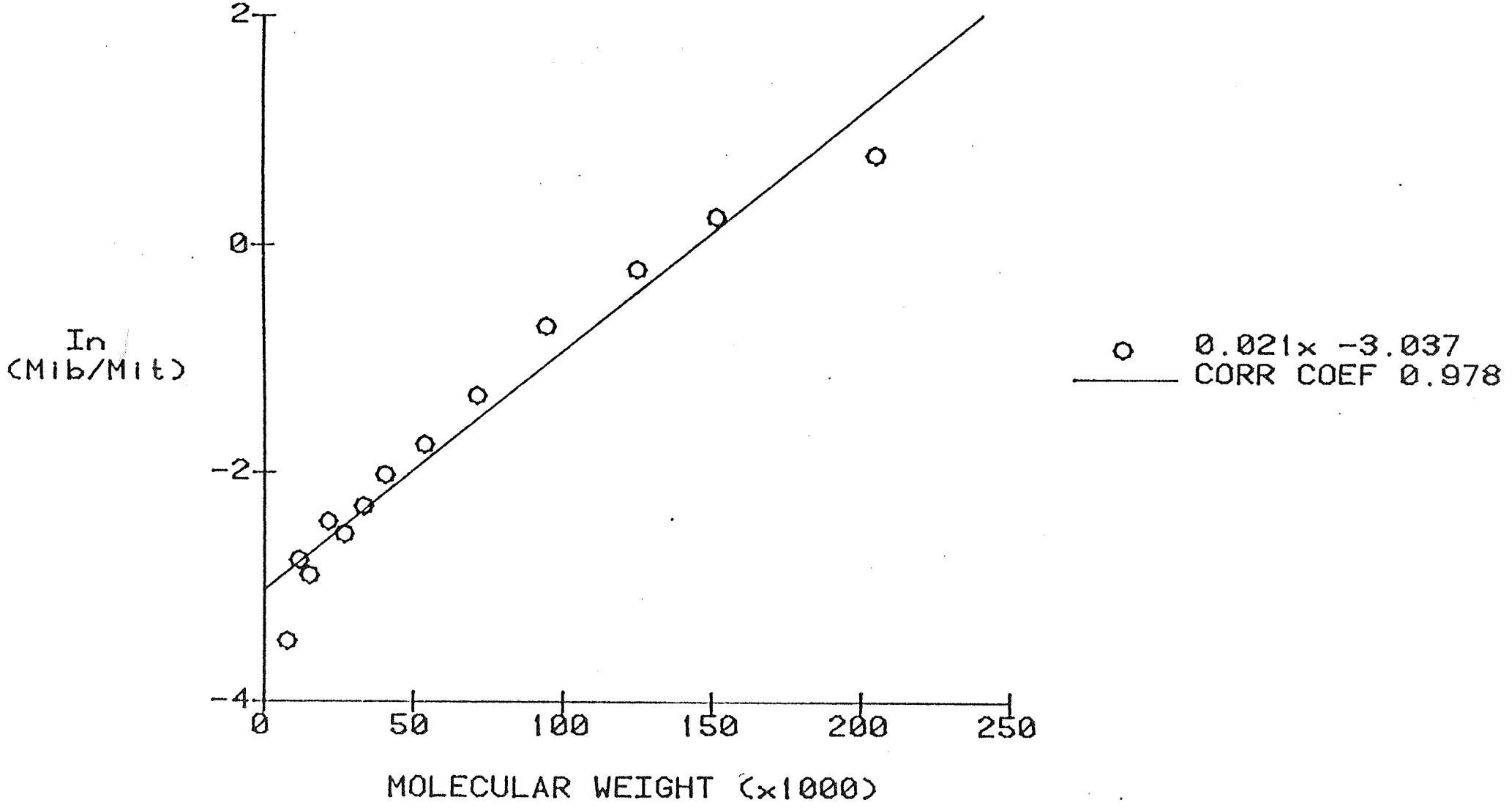

FIG 7.5.5 BOLTZMANN PLOT FOR SECOND STAGE FRACTINATION RUN 8

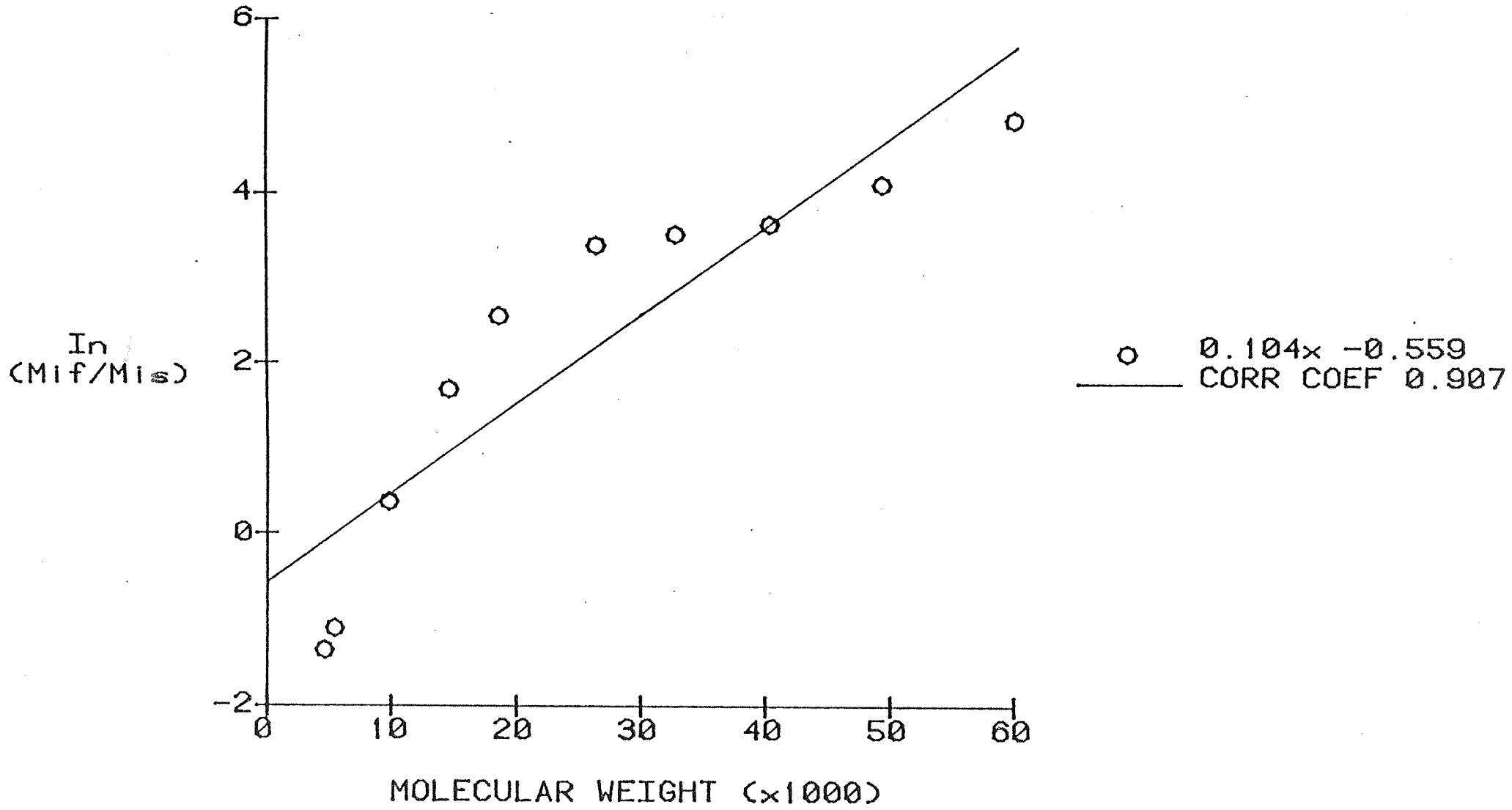

FIG 7.5.6 BOLTZMANN PLOT FOR SECOND STAGE FRACTIONATION RUN 9

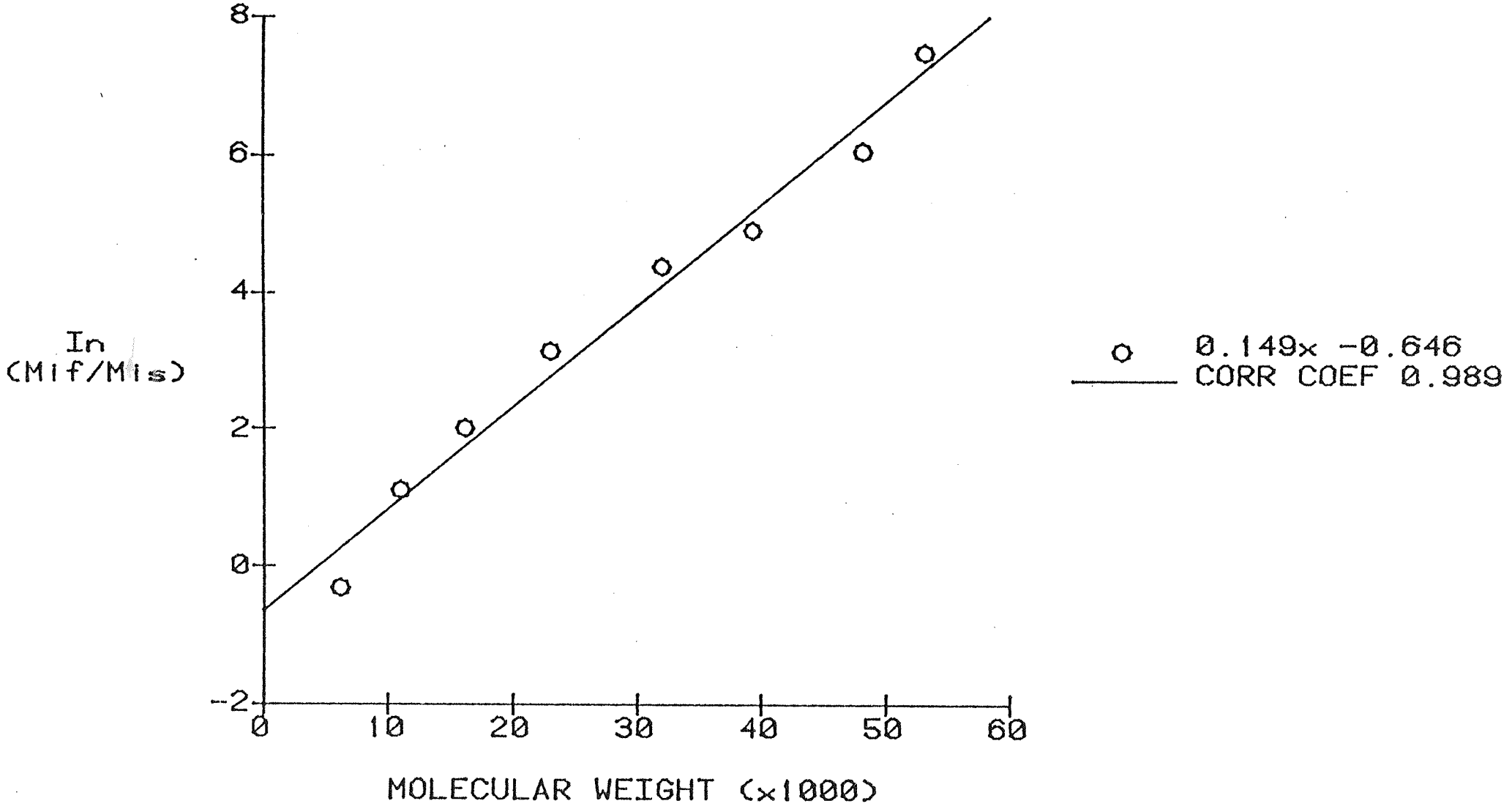

FIG 7.5.7 BOLTZMANN PLOT FOR SECOND STAGE FRACTIONATION RUN 10

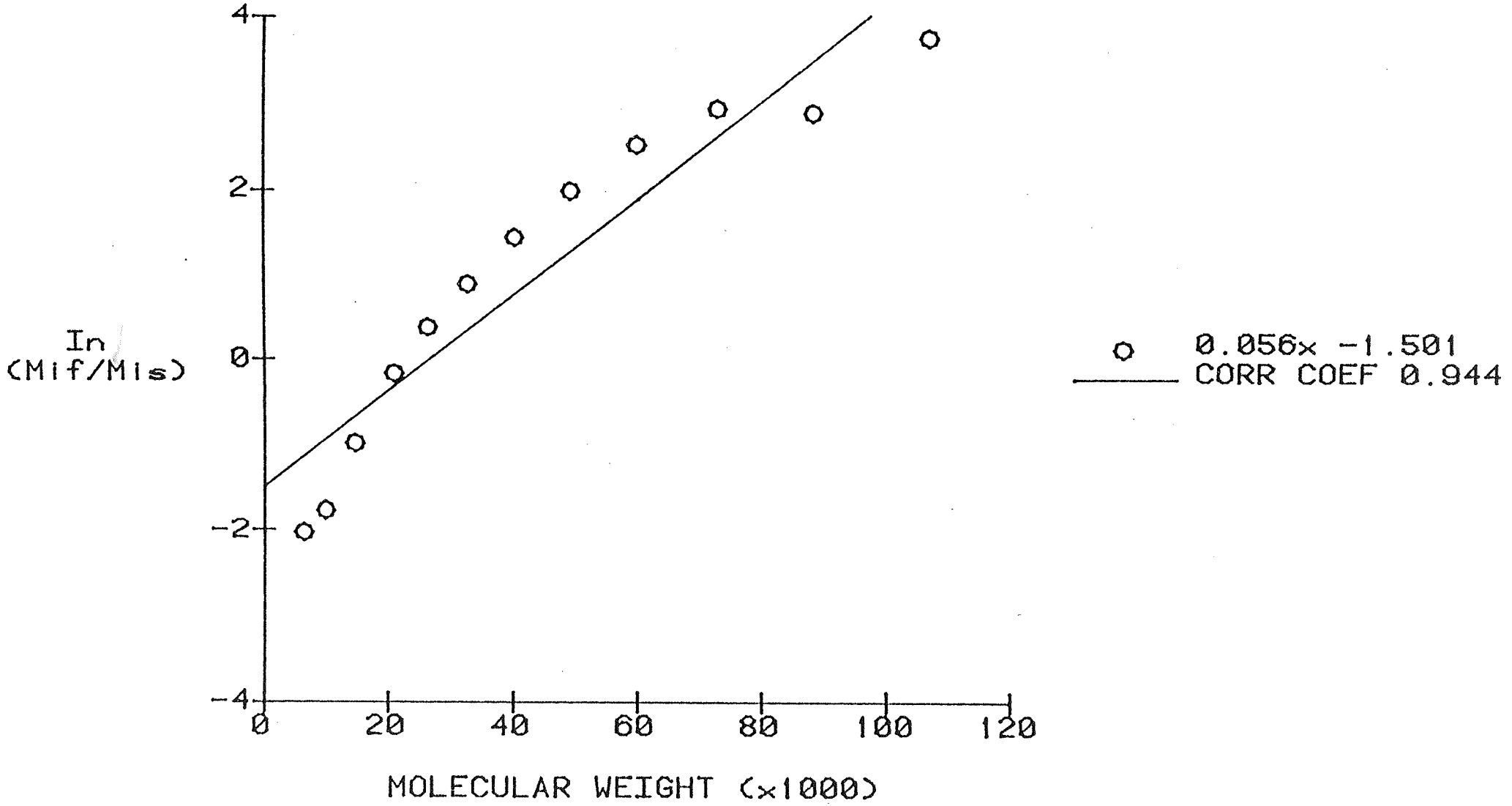

FIG 7.5.8 BOLTZMANN PLOT FOR SECOND STAGE FRACTIONATION RUN 11

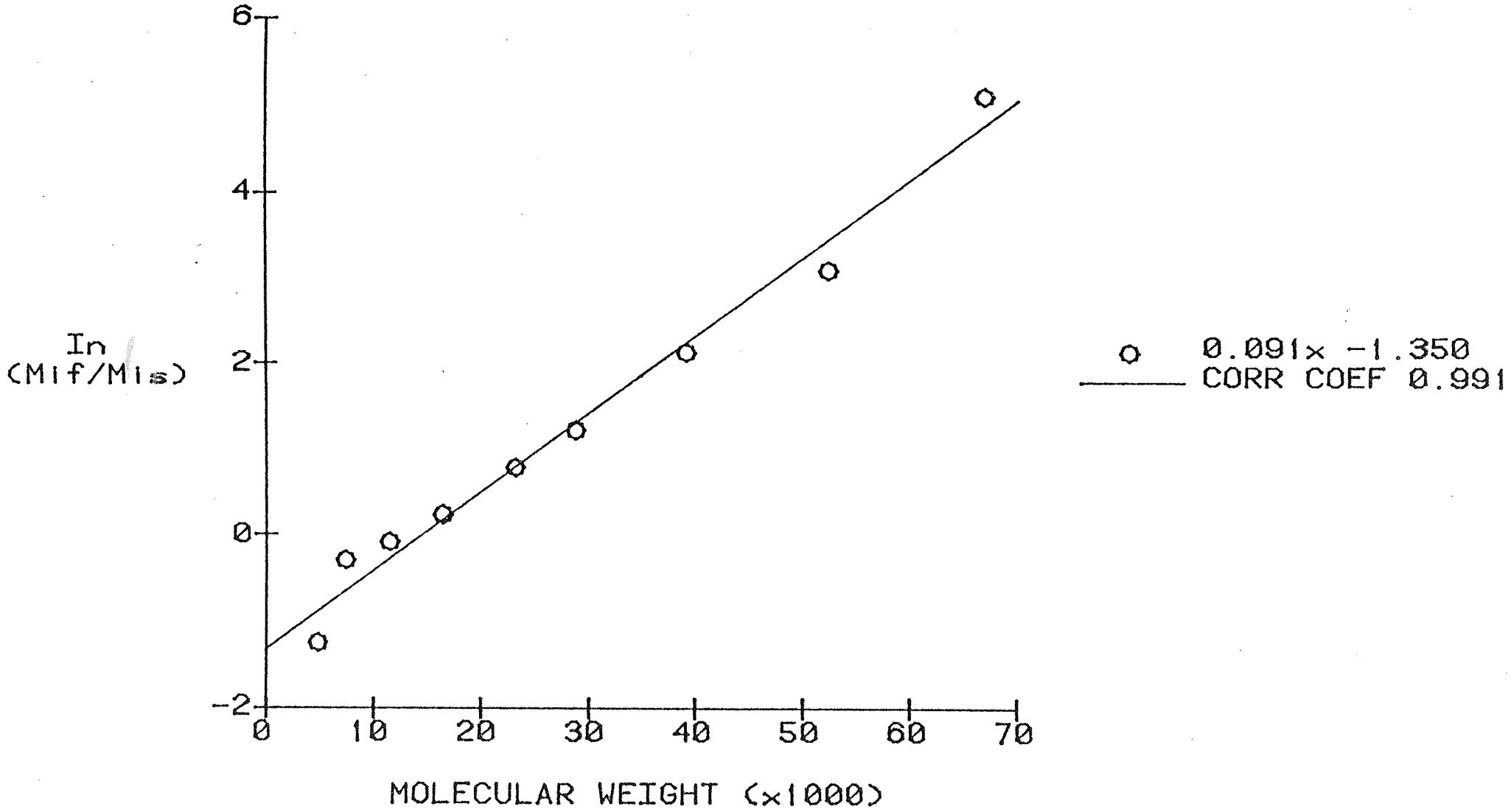

Fig. 7.5.9 Comparison of the C,D,E and F Constants

Run	8	9	10	11
C x 10^5 Boltzmann Plot	3.68	2.18	1.92	2.10
C x 10^5 Model Prediction	3.60	2.76	1.90	2.04
D Boltzmann Plot	4.39	11.95	14.37	20.84
D Model Prediction	6.57	14.06	10.45	16.37
D Experimental	11.82	18.47	26.60	38.10
E x 10^5 Boltzmann Plot	10.41	14.86	5.65	9.13
E x 10^5 Model Prediction	35.70	43.30	10.90	11.90
F Boltzmann Plot	1.75	1.91	4.49	3.86
F Model Prediction	18.46	30.13	9.42	2.66
F Experimental	12.67	9.18	17.60	16.30

agreement. However no comparison can be made for the other three constants.

7.6 EFFECT OF P-PARAMETER ON THE MODEL PROGRAM

This work was carried out to investigate why the five-parameter optimising program (Appendix A3) was predicting poor results for run 13 and onwards, whereas it predicted good results for the previous runs.

The laboratory experiments considered were runs 3,23,24,25,26 and 29.

Investigation was based on the values of the residual sum of squares (R.S.S.) that were obtained when the P-parameter was kept fixed between values of 0.05 and 0.9. This was achieved by altering the program (Appendix A3) from a five to a four-parameter optimisation keeping the fifth parameter P fixed throughout the program.

Graphical plots of the R.S.S. against P values are given in Figs. 7.6.1-7.6.6 for the above runs.

Fig. 7.6.1 shows a minimum around 0.3, the program predicted a value of 0.33 which is comparable to the experimental value, a minimum was also found in Fig. 7.6.3 around 0.1 but this value differs from the experimental value. The other figures show no minimum, explaining why the program had difficulty optimising.

It was therefore necessary to use the four-parameter optimisation program by keeping P fixed. Experience from previous runs showed that parameter P was approximately equal to the weight fraction of dextrans in the final syrup plus 0.1. For runs 13-33 the P value was thus

FIG 7.6.1 GRAPH OF R.S.S AGAINST P FOR LABORATORY EXPERIMENT RUN 3

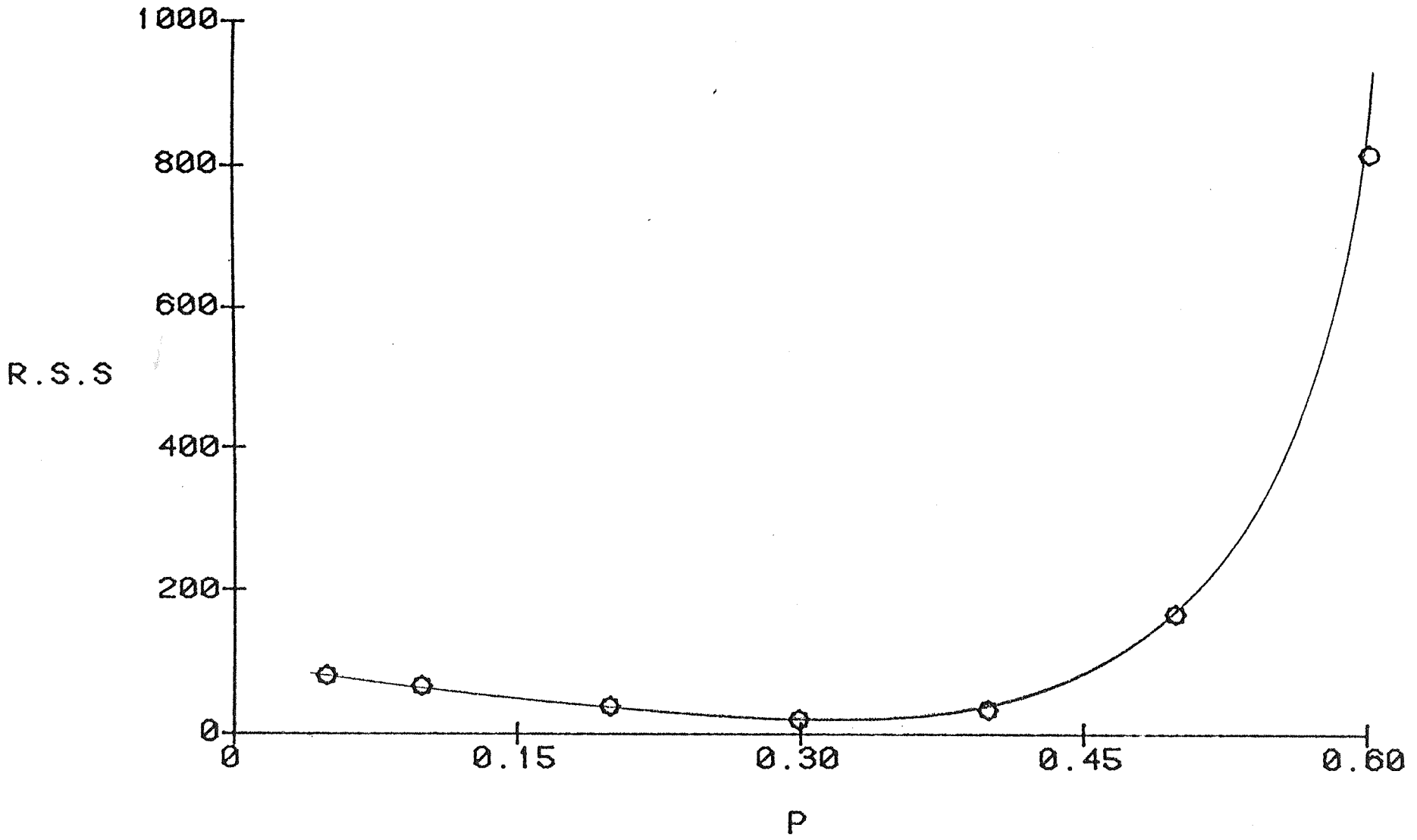

FIG 7.6.2 GRAPH OF R.S.S AGAINST P FOR LABORATORY EXPERIMENT RUN 23

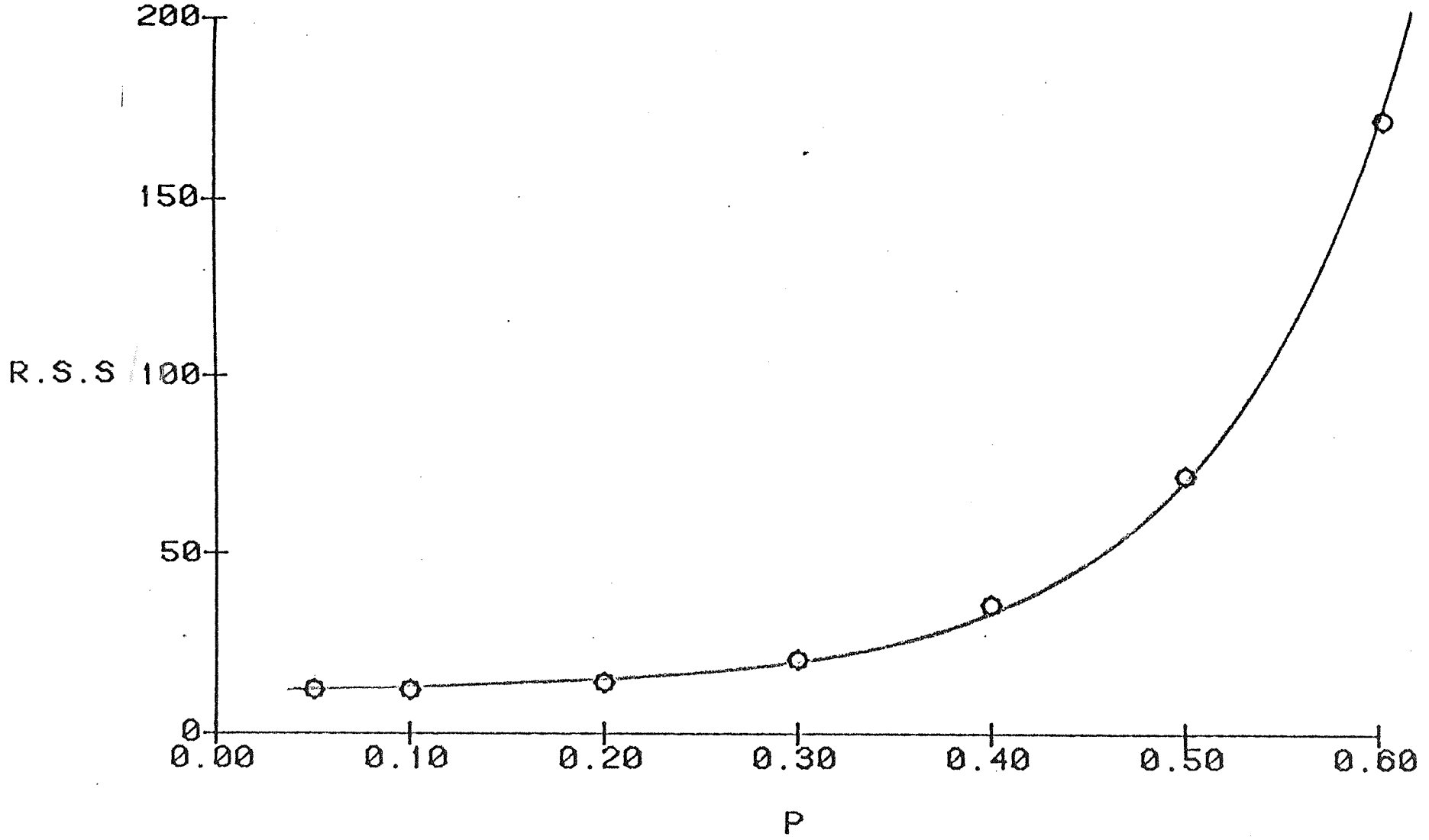

FIG 7.6.3 GRAPH OF R.S.S AGAINST P FOR LABORATORY EXPERIMENT RUN 24

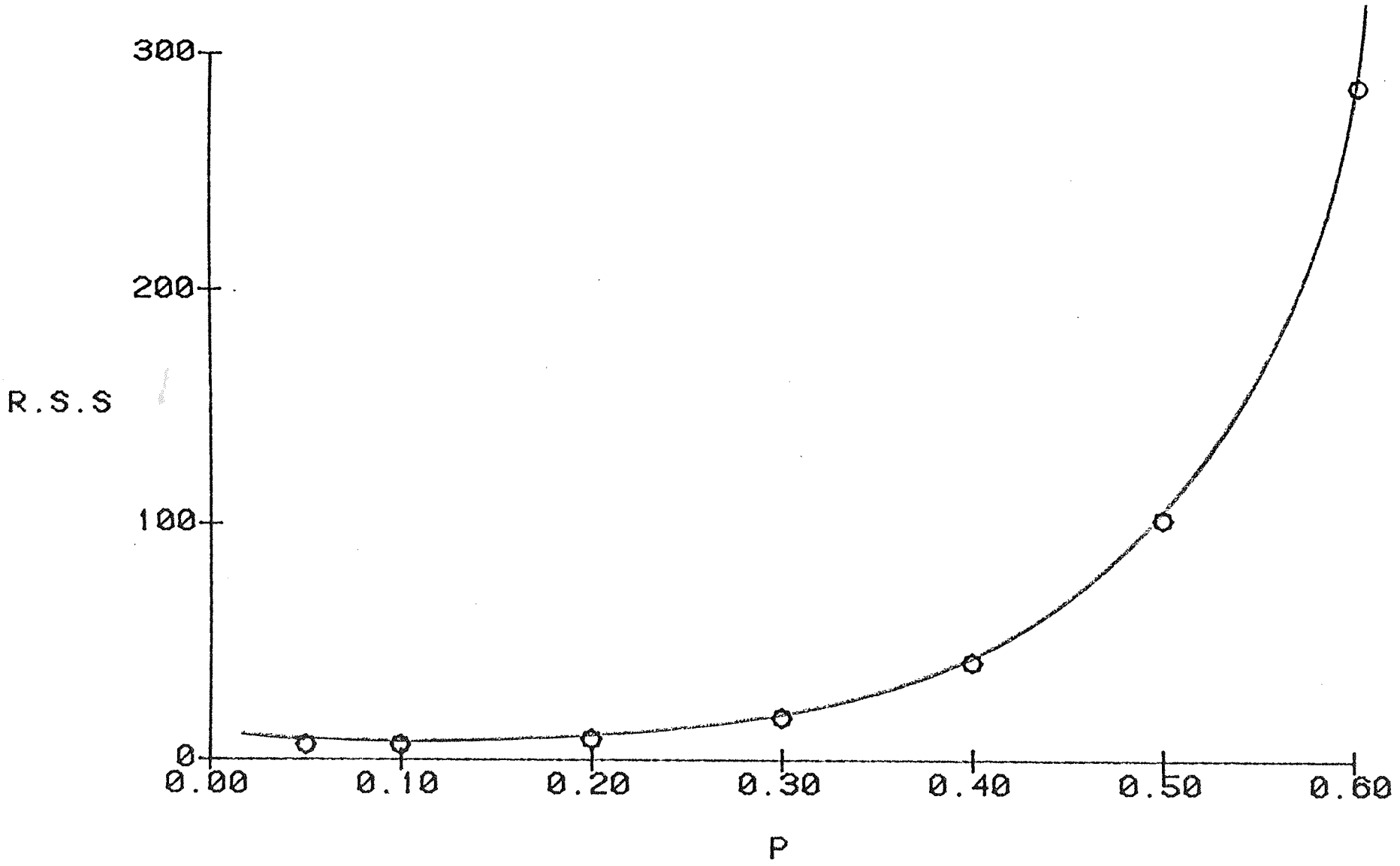

FIG 7.6.4 GRAPH OF R.S.S AGAINST P FOR LABORATORY EXPERIMENT RUN 25

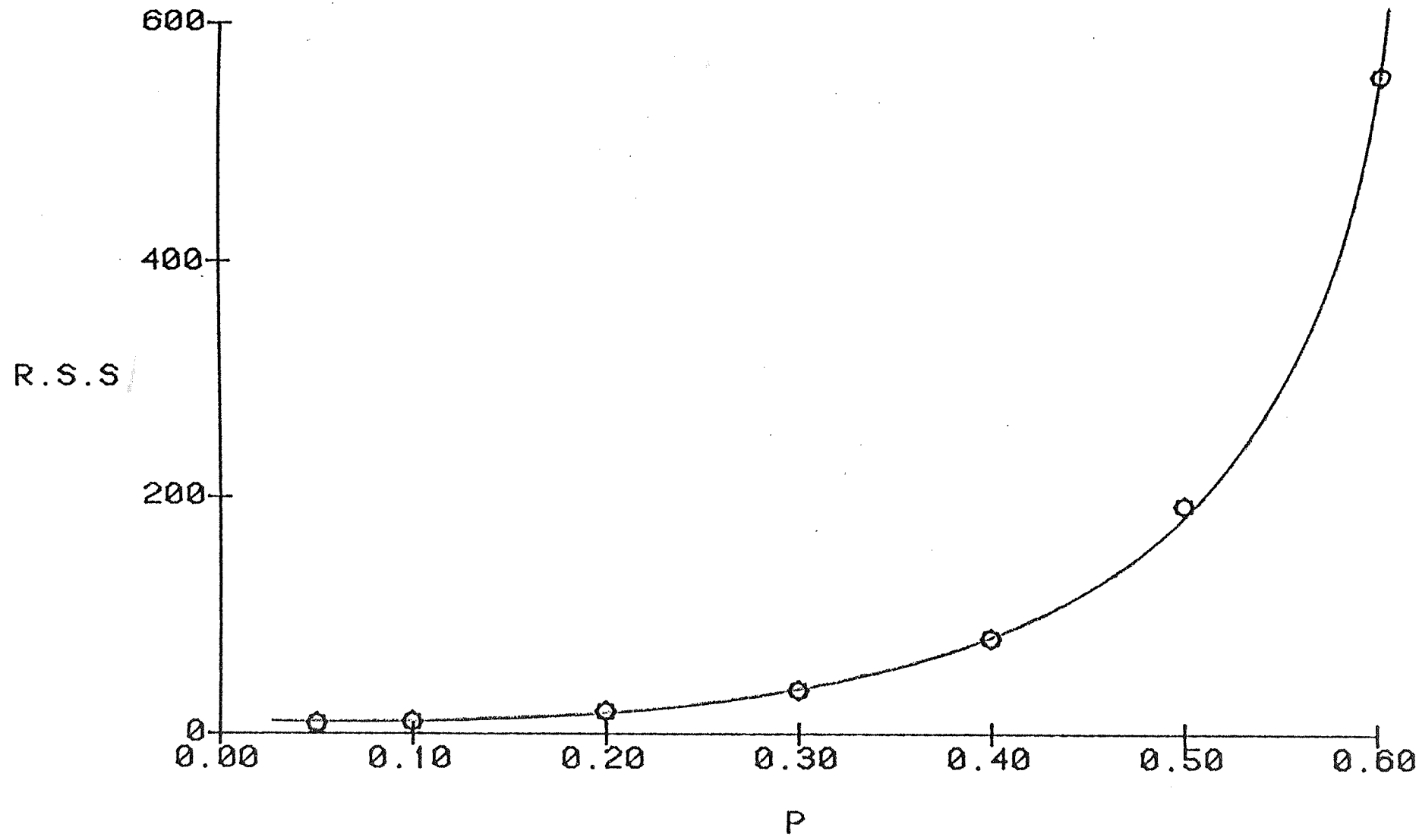

FIG 7.6.5 GRAPH OF R.S.S AGAINST P FOR LABORATORY EXPERIMENT RUN 26

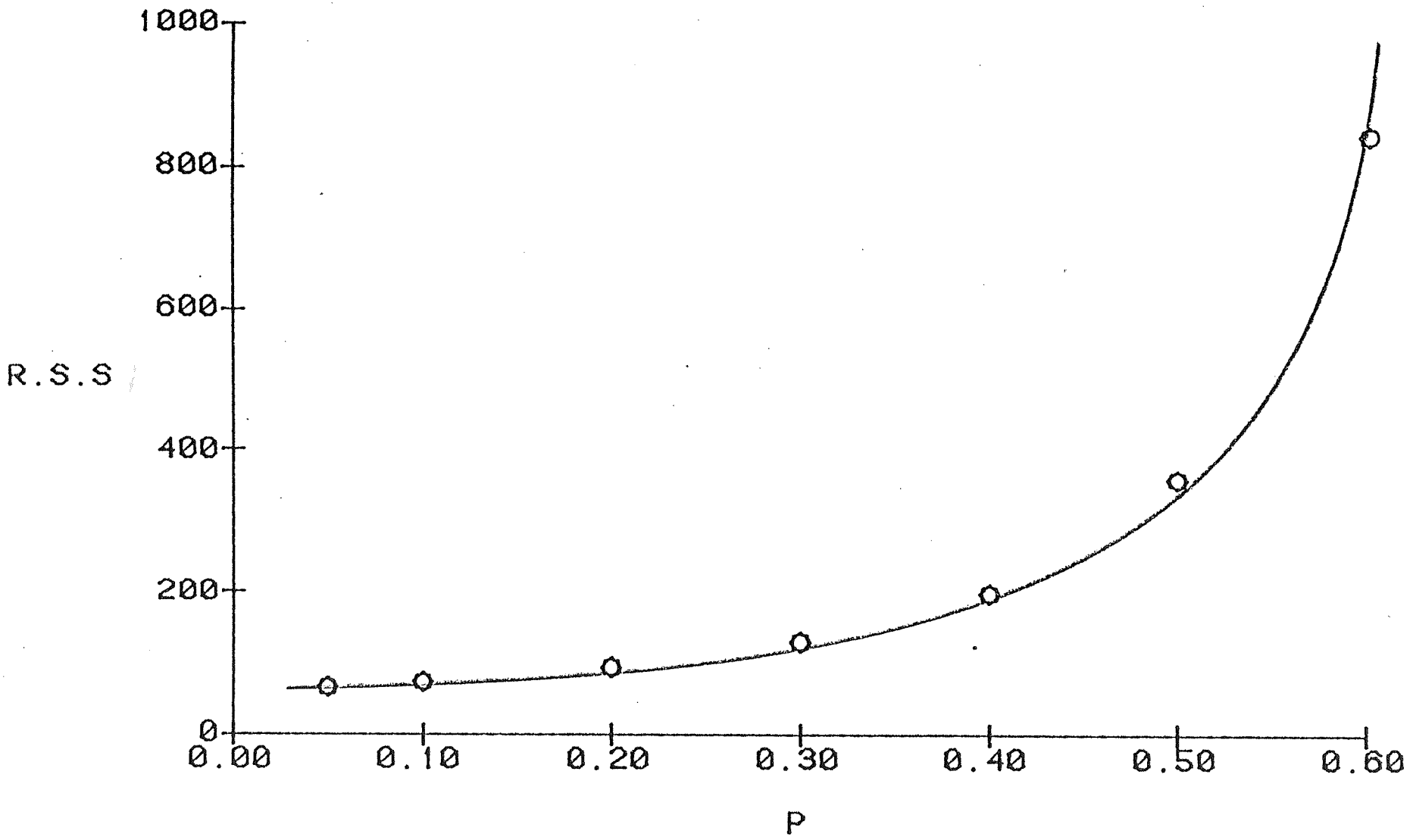

FIG 7.6.6 GRAPH OF R.S.S AGAINST P FOR LABORATORY EXPERIMENT RUN 29

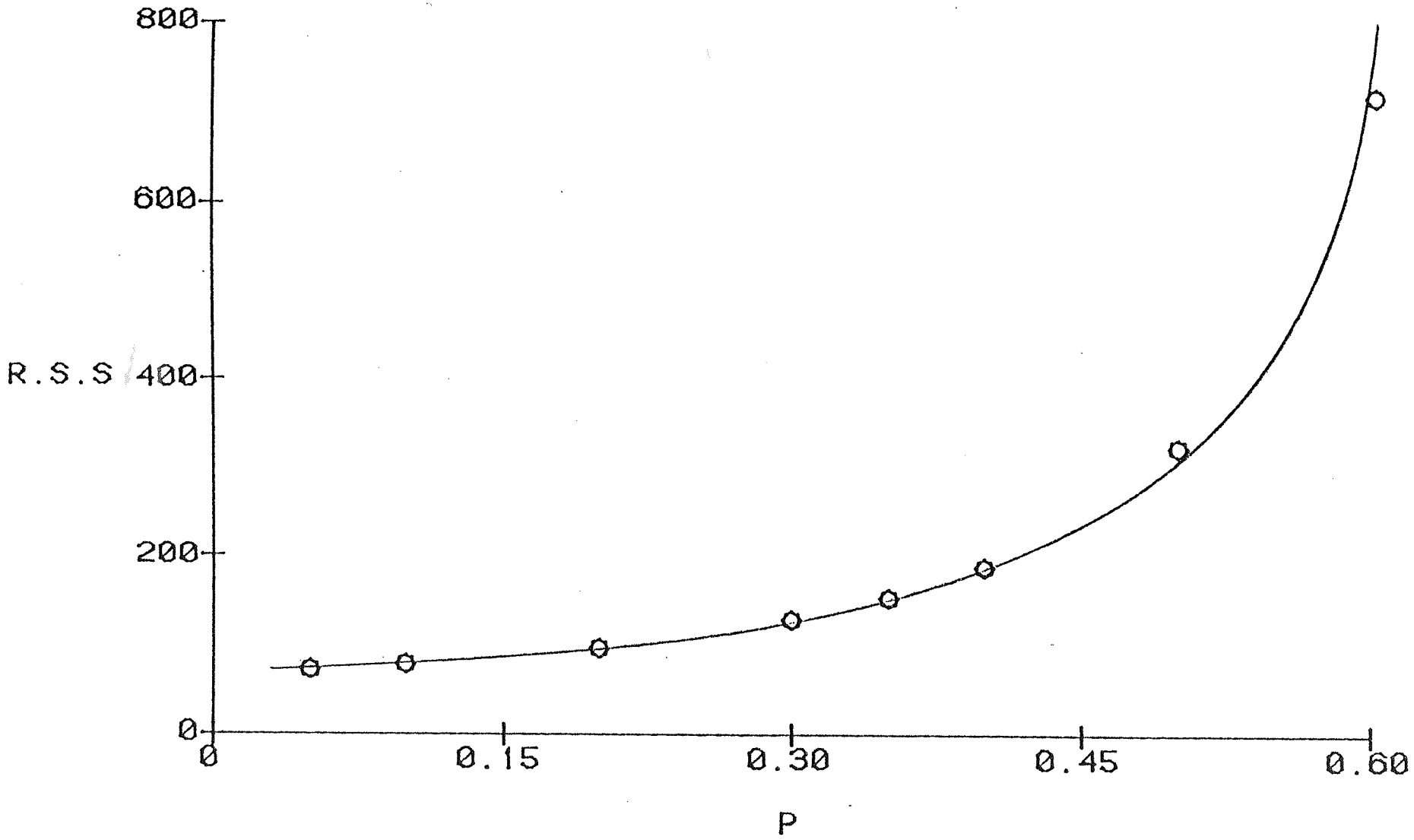

accordingly chosen.

7.7 EFFECT OF MOLECULAR WEIGHT RAISED TO DIFFERENT POWERS IN THE MATHEMATICAL MODEL

Albertsson (108) showed that the particle surface area was also responsible for distribution of protein particles between two phases. Assuming in the case of dextran that the Stokes' radius or the volume was responsible for precipitation, then from equation 3.1.33 the former would be approximately proportional to $M^{0.5}$ and the latter to $M^{1.5}$.

This work was therefore carried out to investigate what Wt% dextran fractions the model would predict if M in equation 5.2 was replaced by i) $M^{0.5}$ and ii) $M^{1.5}$.

The five-parameter program (Appendix A3) was used with data from run 3.

Fig. 7.7.1 lists the initial value of P, the syrup IR and final syrup Wt% fractions and the R.S.S. for i) $M^{1.0}$, ii) $M^{0.5}$ and iii) $M^{1.5}$.

For $M^{1.0}$ the results are similar for the three different P values. For $M^{0.5}$ two different P values give the same results with offset present in both stages when compared with experimental results, the other two P values giving high values of the R.S.S. For $M^{1.5}$ the results are very poor.

7.8 CONCLUSIONS

(i) On the laboratory-scale ethanol fractionation the results between the model predictions and experimental

Fig. 7.7.1 Effect of Molecular Weight Raised to Different Powers in the Mathematical Model

	Initial Value of p	Wt% Syrup IR	Wt% Final Syrup	R.S.S.
$M^{1.0}$	0.20	57.61	32.68	19.50
	0.60	57.61	32.68	19.50
	0.70	57.61	32.68	19.50
$M^{0.5}$	0.20	66.64	22.51	2245
	0.22	46.99	39.19	22.70
	0.33	46.99	39.19	22.70
	0.50	61.68	34.59	22866
$M^{1.5}$	0.20	77.03	18.35	50.50
	0.25	-5734	3998	543
	0.50	-0.19	93.00	17380

values are in very good agreement for both stages, apart from the offset that is obtained in the final syrup of about ten per cent.

(ii) The non-distillation of ethanol in the super IR did not affect the offset obtained in the final syrup; this is shown by the results of runs 13-18 (see Fig. 7.2.19).

(iii) There was no change in the offset again. When dextran T110 (Pharmacia Lot No.5404) was used as syrup I instead of Fisons plant syrup I (Batch No. RB 51K), refer to runs 30 and 31.

(iv) The four hours stirring on the two stages has shown no difference in the amount of dextrans precipitated. This is shown by runs 23-29 (Fig. 7.2.9).

(v) The reproducibility of the experimental results is excellent. This is shown by the above runs and also supported by runs 30,31 and 32,33.

(vi) Comparison of GPC and Model predicted MWD's for the final syrup and super IR are in good agreement. For the final super and syrup IR the agreement is poor on the high molecular weight side (see Section 7.4).

(vii) For the first stage fractionation, plots of the Boltzmann equation are extremely good but runs 8 and 10 on the second stage show slightly poorer results. There is also a good agreement between C values obtained from the Boltzmann plot and model prediction (see Section 7.5).

(viii) It was found that the parameter P had a significant effect on the optimisation program. It was therefore necessary to keep P fixed and optimise the remaining four parameters. The model predictions were in good agreement with experimental results (see runs 13-33).

(ix) On the effect of molecular weight raised to powers of 0.5 and 1.5, it can be concluded that $M^{0.5}$ would present an offset in both stages as well as difficulty in optimising the model equation. The relationship of $M^{1.5}$ has not produced any encouraging results.

C H A P T E R E I G H T

INDUSTRIAL-SCALE ETHANOL FRACTIONATION OF DEXTRAN

8.0 INDUSTRIAL-SCALE ETHANOL FRACTIONATION OF DEXTRAN

8.1 INTRODUCTION

The objective of this work was to compare the mathematical model predictions obtained from analytical analyses of twenty three industrial plant batches with the actual plant results.

Dextran samples were collected from ten batches processed during the early months of 1982, thirteen more batches processed a few months later were also collected.

The industrial hydrolysis and fractionation procedures will be mentioned briefly in this Chapter.

All the samples in this Chapter were analysed on Aston's GPC system.

8.2 INDUSTRIAL HYDROLYSIS AND FRACTIONATION

(i) Hydrolysis

Native dextran is subjected to partial acid hydrolysis to split the high molecular weight material into smaller fragments. The hydrolysis is carried out by adding hydrochloric acid in a two-phase system according to U.K. patent 1,143,784.

When the specific gravity (SG) falls below 1.0 indicating the lower phase has been completely hydrolysed with the bulk temperature of the settling vessel contents at 25^{o}C, hydrolysis is stopped.

After the contents have been stirred for 20 minutes, a sample is submitted for an average intrinsic viscosity (AIV) check to ensure hydrolysis is complete to the

desired end point. Hydrolysis is continued if necessary until AIV is reduced to a satisfactory value for the required clinical dextran.

The entire contents are then circulated from the hydrolysis vessel to a mixing vessel fitted with a suitable stirrer.

The hydrolysate is then neutralised with 5N sodium hydroxide solution in the mixing vessel to give a pH value of about 5.5.

The hydrolysate is then transferred to one of two fractionators A (or B) by a pump (Fig. 8.2.1). The considerable quantity of hydrolysate trapped in the vertical pipe lines is easily cleared by using compressed air. A small quantity of pyrogen-free (P/F) water is metered into the hydrolysis vessel and then transferred to the fractionator, in order to further clear out the transfer line. The hydrolysate volume is recorded.

(ii) Fractionation

A sample of the hydrolysate is taken into the laboratory to measure its SG and optical rotation. From this the weight of dextran present is calculated.

The batch is fractionated in order to discard unwanted high molecular weight and low molecular weight material present in the hydrolysate leaving a narrow MWD product suitable for clinical use.

The scheme and nomenclature employed is shown in Fig. 8.2.2. Also shown are the approximate Wt% fractions required for a dextran $\bar{M}_w$ 40,000 final product.

Fig. 8.2.1 FLOW DIAGRAM OF DEXTRAN PLANT FRACTIONATION

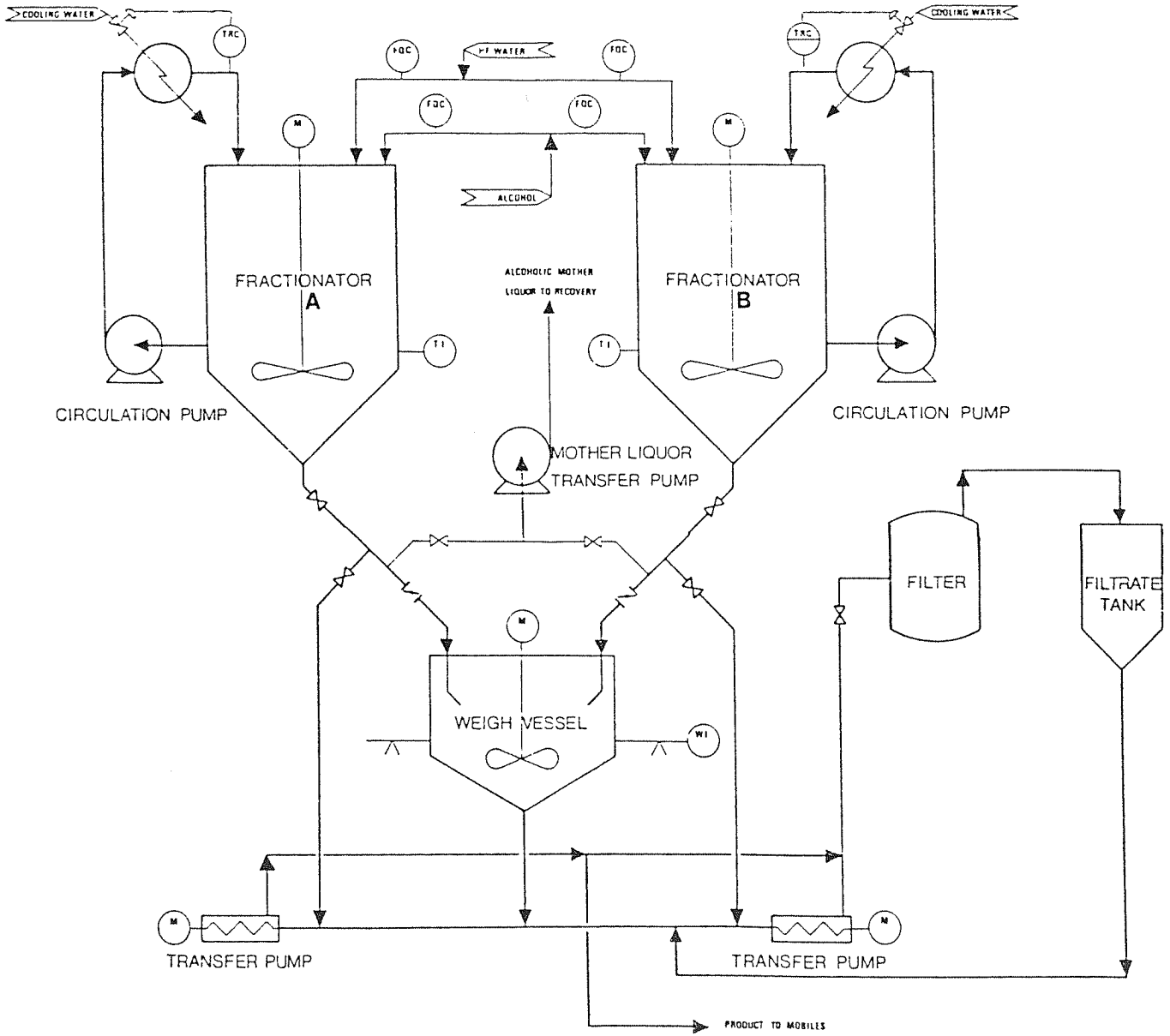

Fig. 8.2.2 Plant Fractionation Scheme

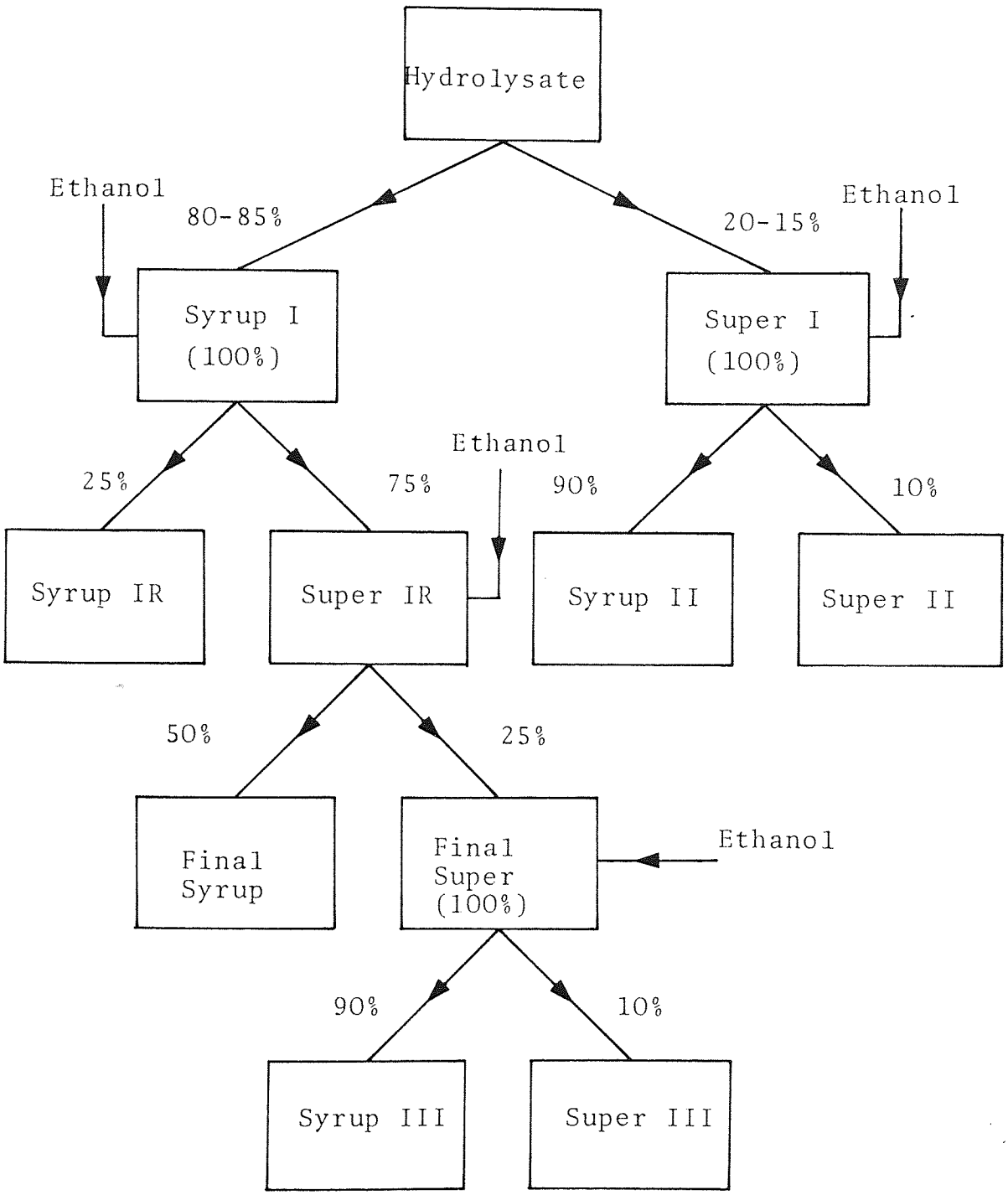

Syrup IR → Transferred to hydrolyser
Syrup II & III → Transferred to iron dextran plant
Super II & III → Transferred to distillation plant for ethanol recovery
Final Syrup → Final product → Spray drying plant

80-85% of the hydrolysate dextrans have to be fractionated to give the syrup I. This is achieved by adding 85% w/v ethanol to the hydrolysate whilst being stirred, a two-phase mixture results. The fractionation is carried out at a constant temperature of 25°C.

A sample of the above solution in a two litre flask is taken into the laboratory and kept for half an hour in a water tank also at 25°C. After half an hour a clear supernatant (top layer) sample can be taken (equivalent to super I) to measure its SG and optical rotation so that the weight of dextrans which will be in the main bulk of super I can be predicted.

If necessary, more ethanol (or P/F water) is added to achieve the target fractionation.

A known weight of water is pumped into the weigh vessel (Fig. 8.2.1); this is normally about 10% of the expected syrup I weight. This is about 2.5 (taking ethanol/water into account) times the syrup I dextran weight. The weigh vessel water is used to reduce the viscosity of syrup I when drawn from the fractionator. The lower viscosity reduces the tendency of the syrup I to stick to the weigh vessel side walls and makes it more readily transferable by pump.

After four hours the syrup I is drawn into the weigh vessel via a quick release valve. An inspection hatch in the weigh vessel lid gives access to a chute down which the syrup I is discharged; this enables detection of the syrup I/super I interface and subsequent use of the quick release valve to shut off the flow.

Measurements of the syrup I weight are taken, the actual amount of dextrans fractionated as syrup I is then calculated from SG and optical rotation measurements.

The syrup I is then pumped to the second fractionator and diluted with P/F water, Hyflow Supercell (filter aid) is also added at this stage. The syrup I is pumped through a Calmic filter (of the candle type) and then back to a fractionator.

The filtered solution of the syrup I dextran is adjusted to 8% w/v by the addition of a calculated amount of P/F water.

Ethanol is added until a visual "cloud point" is reached which based on operative experience will yield the called for amount of syrup IR from syrup I. A sample is taken in a two litre flask and allowed to settle for 45 minutes in a constant water bath at 25°C. Measurements of the SG and optical rotation are taken for the sample super IR to determine the weight of dextrans present, to assess if the fractionation process is yielding the target amounts of dextran in each phase.

If necessary, more ethanol (or P/F water) is added to the bulk to achieve the target fractionation. The syrup IR is drawn off into the weigh vessel after allowing 8-10 hours settling time.

The other fractionations are carried out in a similar way, i.e. a sample is taken into the laboratory, then after 45 minutes measurements of the SG and optical rotation on the supernatant are made to calculate the percentage dextrans fractionated.

The dextrans of syrup II and III are used in the manufacture of other dextran based products.

8.3 COMPARISON OF PLANT RESULTS WITH PREDICTIONS OF THE MODEL

8.3.1 PLANT SAMPLES RB 8L/40-SL 17L/70

During this research work instead of using a double fractionation procedure to obtain clinical dextrans, the samples collected were processed by performing triple fractionations, i.e. the optional extra fractionation of a syrup IR and super IR stage II was introduced (see Fig. 8.3.1) defined as a triple fractionation.

The ten batches processed during early 1982 were all triple fractionations.

The mathematical model is based on a double fractionation process (Fig. 7.1.1) and therefore needs modification before applying to triple fractionation data. A simple solution to the problem was instead of using the input data of syrup I and final syrup analyses (as for double fractionation), input data from syrup I and syrup IR stage II analyses can be used; it is also possible to use the data from super IR stage I and final syrup analyses; this is easily justified by referring to Fig. 8.3.1 since they are separated by two stages.

For the above ten batches the sample super IR stage I was not collected. Model predictions could therefore only be made by using input data from syrup I and syrup IR stage II analyses.

Fig. 8.3.1 Block Diagram of the Improved Plant Fractionation: Triple Fractionation

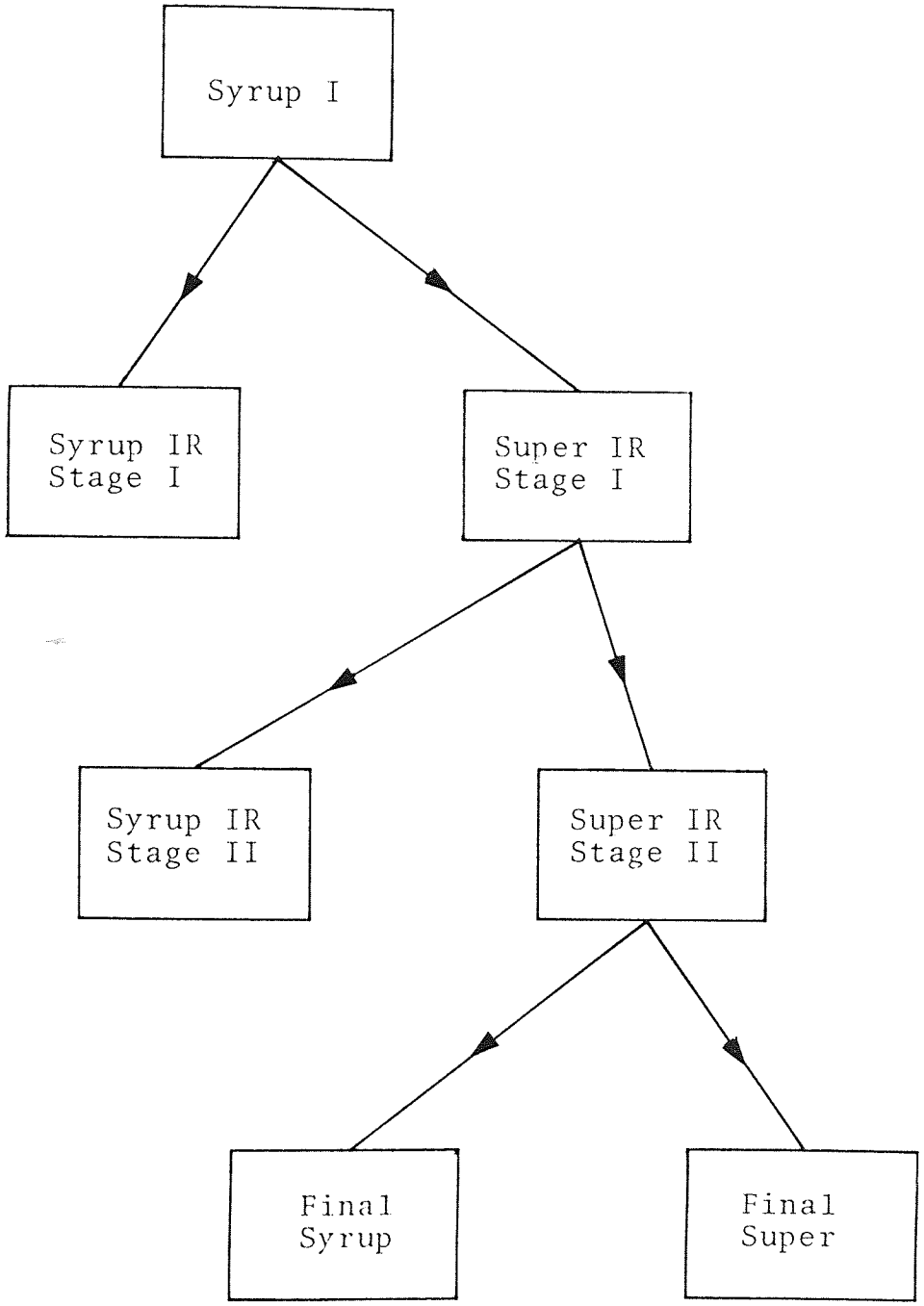

The results of the weight average molecular weights and polydispersity of the ten batches analysed at Aston are given in Figs. 8.3.2 and 8.3.3.

Figs. 8.3.4 and 8.3.5 lists the batch numbers, the volume ratios of super to syrup and the Wt% fractions achieved for syrup IR St I, super IR St I, super IR St II and syrup IR St II. The model predictions are listed in Figs. 8.3.6 and 8.3.7.

Model predictions could not be made on batches SL 9L/70 and RB 10L/40 due to the lack of sample syrup IR St II.

Of the ten batches only RB 8L/40 agreed reasonably well with the model predictions. The model prediction for this batch on the Wt% syrup IR stage II separated is about 11% greater than the actual plant result. This degree of offset is similar to that found in the laboratory-scale experiments (see Section 7.3).

For some of the other batches, the model has predicted yields of up to 200% and negative volume ratios; this is theoretically not possible. Four possible explanations for this discrepancy could be i) not enough time may have been allowed for the syrup IR stage I to settle in the fractionator before being drawn off; ii) the incapability of the GPC packing to accurately analyse the very high molecular weight dextrans. It should be noted here that the samples syrup I and syrup IR stage II have large proportions of these very high molecular weight dextrans; iii) due to the partially deteriorated GPC columns; iv) due to the leaking pump-head on the analytical GPC system.

Fig. 8.3.2 Results of the Analytical GPC Analyses

Batch Number		RB 8L/ 40	SL 9L/ 70	RB 10L/ 40	SL 11L/ 70	RB 12L/ 40
Syrup I	$\bar{M}w$	163383	267882	157942	250307	164718
	$\bar{D}$	9.15	12.20	9.88	8.76	10.63
Syrup IR St I	$\bar{M}w$	1119048	1039890	986015	926367	863238
	$\bar{D}$	49.99	15.25	44.16	19.05	32.87
Syrup IR St II	$\bar{M}w$	364207	-	-	375553	107792
	$\bar{D}$	10.70	-	-	6.61	2.58
Super IR St II	$\bar{M}w$	33142	59252	-	55340	34336
	$\bar{D}$	2.73	3.61	-	2.76	2.27
Final Super	$\bar{M}w$	7827	16505	10215	16335	14751
	$\bar{D}$	2.08	3.01	2.00	3.08	2.42
Final Syrup	$\bar{M}w$	38693	66598	36013	66863	37471
	$\bar{D}$	1.76	2.00	1.78	2.32	1.61

Fig. 8.3.3 Results of the Analytical GPC Analyses

Batch Number		RB 13L/ 40	RB 14L/ 40	SL 15L/ 70	SL 16L/ 70	SL 17L/ 70
Syrup I	$\bar{M}w$	79193	122304	238936	92674	333984
	$\bar{D}$	5.09	7.59	7.33	3.35	10.26
Syrup IR St I	$\bar{M}w$	642779	1016319	1413914	701652	1375328
	$\bar{D}$	28.03	24.75	20.31	8.85	19.12
Syrup IR St II	$\bar{M}w$	98392	74013	137139	254266	548340
	$\bar{D}$	3.38	2.70	2.38	6.45	7.29
Super IR St II	$\bar{M}w$	33584	34432	61974	-	68703
	$\bar{D}$	2.51	2.17	2.85	-	2.85
Final Super	$\bar{M}w$	21903	12694	17151	24499	18070
	$\bar{D}$	2.78	2.19	2.29	2.99	1.67
Final Syrup	$\bar{M}w$	35686	34172	64584	68601	75198
	$\bar{D}$	1.63	1.78	1.90	1.94	1.99

Fig. 8.3.4 Actual Plant Results

Batch Number	RB 8L/ 40	SL 9L/ 70	RB 10L/ 40	SL 11L/ 70	RB 12L/ 40
$\frac{D}{\text{Vol.of Super IR St I}}$ / Vol.of Syrup IR St I	26.78	23.00	13.14	22.90	29.34
$\frac{F}{\text{Vol.of Super IR St II}}$ / Vol.of Syrup IR St II	35.25	45.81	49.89	15.69	29.31
Wt% Syrup IR St I	11.06	16.21	13.33	14.70	13.87
Wt% Super IR St I	88.94	83.79	86.67	85.30	86.13
Wt% Super IR St II	76.21	76.36	73.94	68.88	71.45
Wt% Syrup IR St II	12.73	7.43	12.73	16.42	14.68

Fig. 8.3.5 Actual Plant Results

Batch Number	RB 13L/ 40	RB 14L/ 40	SL 15L/ 70	SL 16L/ 70	SL 17L/ 70
$\frac{D}{\text{Vol.of Super IR St I}}$ / Vol.of Syrup IR St I	11.92	29.85	19.03	39.48	19.01
$\frac{F}{\text{Vol.of Super IR St II}}$ / Vol.of Syrup IR St II	74.98	61.76	45.40	235.90	115.80
Wt% Syrup IR St I	14.06	15.42	15.64	10.77	16.83
Wt% Super IR St I	85.94	84.58	84.36	89.23	83.17
Wt% Super IR St II	80.32	77.46	66.91	87.37	70.37
Wt% Syrup IR St II	5.62	7.12	17.45	1.86	12.80

Fig. 8.3.6 Results of the Mathematical Model Predictions

Batch Number	RB 8L/ 40	SL 9L/ 70	RB 10L/ 40	SL 11L/ 70	RB 12L/ 40
C x 10^5	- 1.51	-	-	- 1.61	- 2.10
D	6.39	-	-	0.08	0.13
E x 10^4	0.20	-	-	0.003	0.86
F	10.64	-	-	- 0.82	2.85
P	0.24	-	-	1.20	0.23
Wt% Syrup IR St I	8.01	-	-	71.04	70.56
Wt% Super IR St I	91.99	-	-	28.96	29.44
Wt% Super IR St II	68.03	-	-	-91.93	3.90
Wt% Syrup IR St II	23.96	-	-	120.89	25.54

Fig. 8.3.7 Results of the Mathematical Model Predictions

Batch Number	RB 13L/ 40	RB 14L/ 40	SL 15L/ 70	SL 16L/ 70	SL 17L/ 70
C x 10^5	- 2.56	- 3.28	- 3.13	- 1.38	
D	0.03	0.04	22.32	0.08	
E x 10^4	0.007	0.005	0.32	0.54	↑
F	- 0.91	- 0.95	7.64	- 0.58	ERROR
P	0.73	1.97	0.46	0.22	
Wt% Syrup IR St I	88.11	79.05	1.12	79.01	EXECUTION
Wt% Super IR St I	11.89	20.95	98.88	20.99	
Wt% Super IR St II	-63.64	-181.23	46.87	- 1.33	PROGRAM
Wt% Syrup IR St II	75.53	202.18	52.01	22.32	↓

8.3.2 A TEST OF THE BOLTZMANN EQUATION USING PLANT DATA

Fig. 8.3.8 shows the results of the Boltzmann equation; the method and equations used to derive the results are given in Section 7.5.

Values of the parameters C and D could not be obtained from the Boltzmann equation due to absence of the sample super IR St I, i.e. Boltzmann plots for the first stage were not possible.

For the second stage, Boltzmann plots for batches SL 9L/70, RB 10L/40 and SL 16L/70 were again not possible due to the absence of samples syrup IR St II and super IR St II. For the remaining batches the correlation coefficient values are quite good with the exception of batch SL 15L/70 having a marginally lower value. The slope of the second stage Boltzmann plot is equal to the parameter E. When comparison is made with the model predicted E value only batch RB 8L/40 has similar values. The intercept of the Boltzmann plot is equal to $\ln(1/F)$; the F values obtained from the Boltzmann plot, model prediction and the plant do not agree with each other (see Fig. 8.3.9).

Four batches showed good correlation coefficients for the third stage (final syrup and final super). Some of the β values were not so good (see Fig. 8.3.8).

8.3.3 PLANT SAMPLES RB 35L/40 - RB 59L/40

These thirteen batches processed during late 1982 were also all triple fractionations with the exception of a double fractionation on batch RB 35L/40.

Fig. 8.3.8 Results of the Boltzmann Equation Plots

Batch Number	Syrup IR St II and Super IR St II			Final Syrup and Final Super		
	β	Slope x 10^5	Inter-cept	β	Slope x 10^5	Inter-cept
RB 8L/ 40	0.996	1.978	-3.056	0.977	16.161	-0.861
SL 9L/ 70	-	-	-	0.914	7.348	-1.104
RB 10L/ 40	-	-	-	0.979	9.989	-0.940
SL 11L/ 70	0.991	1.076	-2.608	0.912	7.187	-0.564
RB 12L/ 40	0.983	2.197	-2.867	POOR	-	-
RB 13L/ 40	0.990	1.451	-3.490	POOR	-	-
RB 14L/ 40	0.994	1.679	-3.319	0.924	10.076	-0.941
SL 15L/ 70	0.942	0.738	-2.228	0.956	9.705	-1.758
SL 16L/ 70	-	-	-	POOR	-	-
SL 17L/ 70	0.960	0.649	-2.709	0.984	7.56	-0.978

Fig. 8.3.9 Comparison of the E and F Constants

Batch Number	E x 10^4 Boltzmann Plot	E x 10^4 Model Prediction	F Boltzmann Plot	F Model Prediction	F Plant
RB 8L/ 40	0.198	0.200	21.24	10.64	35.25
SL 9L/ 70	-	-	-	-	45.81
RB 10L/ 40	-	-	-	-	49.89
SL 11L/ 70	0.108	0.003	13.57	- 0.82	15.69
RB 12L/ 40	0.220	0.860	17.58	2.85	29.31
RB 13L/ 40	0.145	0.007	32.79	- 0.91	74.98
RB 14L/ 40	0.168	0.005	27.63	- 0.95	61.76
SL 15L/ 70	0.074	0.320	9.28	7.64	45.40
SL 16L/ 70	-	0.540	-	- 0.58	235.90
SL 17L/ 70	0.065	-	15.01	-	115.80

The samples collected were super IR St I (syrup I for batch RB 35L/40) and final syrup. Model predictions could now be obtained by using input data from super IR St I and final syrup analyses (see Section 8.3.1).

Fig. 8.3.10 lists the results of the weight average molecular weight of final syrups analysed at both the Quality Control Department (96) and on Aston's analytical GPC system using calibration "CD5E". A reasonable agreement is obtained between the two GPC systems with the exception of batch SL 56L/70.

Fig. 8.3.11 lists the batch numbers, weight average molecular weights and polydispersity of syrup I, super IR St I and final syrup. For batch RB 35L/40 there was no IR St II performed as this was a double fractionation batch.

For simplicity the sample syrup I of batch RB 35L/40 will be referred to as super IR St I.

Figs. 8.3.12-8.3.14 lists the batch numbers, the volume ratios of super to syrup and Wt% fractions achieved for syrup IR St II, super IR St II, final super and final syrup.

The model predictions are listed separately in Figs. 8.3.15-8.3.17. Due to the optimising difficulty of the five-parameter optimisation program (Appendix A3), model predictions were obtained by keeping P fixed and optimising the remaining constants (C,D,E and F).

The plant results of the Wt% dextran fractions are plotted against model predictions in Fig. 8.3.18, for the first fractionation (syrup IR St II) the two sets of

Fig. 8.3.10 Results of Final Syrup $\bar{M}_W$ Analysed at Aston and Fisons GPC Systems

Batch Number	Final Syrup $\bar{M}_W$		% Difference
	Aston Analyses	Fisons Q.C. Analyses	
RB 35L/40	42529	42216	+ 0.74
RB 36L/40	46031	46487	- 0.98
RB 37L/40	37912	41192	- 7.96
Repeat	38327	41192	- 6.96
RB 38L/40	46363	45396	+ 2.13
RB 50L/40	40619	42028	- 3.35
RB 51L/40	41746	43909	- 4.93
SL 53L/70	65064	66037	- 1.47
RB 54L/40	44376	46665	- 4.91
RB 55L/40	42320	43741	- 3.25
SL 56L/70	74582	90742	-17.81
Repeat	76868	90742	-15.29
RB 57L/40	40428	43271	- 6.57
Repeat	41370	43271	- 4.39
RB 58L/40	41558	42471	- 2.15
RB 59L/40	42255	42489	- 0.55

Fig. 8.3.11 Results of GPC Analyses on Plant Batches RB 35L/40 - RB 59L/40

Batch Number	Syrup I		Super IR St I		Final Syrup	
	$\bar{M}_w$	$\bar{D}$	$\bar{M}_w$	$\bar{D}$	$\bar{M}_w$	$\bar{D}$
RB 35L/40	119166	6.86	-	-	42529	1.84
RB 36L/40	-	-	45828	2.26	46031	1.68
RB 37L/40	-	-	41508	2.48	37912	1.70
RB 38L/40	-	-	62424	3.56	46363	1.78
RB 50L/40	-	-	42572	2.40	40619	1.68
RB 51L/40	-	-	50559	2.78	41746	1.75
SL 53L/70	-	-	89856	3.18	65064	1.80
RB 54L/40	-	-	50160	2.77	44376	1.83
RB 55L/40	-	-	78301	4.31	42320	1.84
SL 56L/70	-	-	124786	4.38	74582	2.05
RB 57L/40	-	-	53059	2.80	40428	1.71
RB 58L/40	-	-	45595	2.66	41558	1.82
RB 59L/40	-	-	41312	2.38	42255	1.77

Fig. 8.3.12 Actual Plant Results

Batch Number	RB 35L/ 40	RB 36L/ 40	RB 37L/ 40	RB 38L/ 40	RB 50L/ 40
$\frac{D}{\text{Vol. of Super IR St II}}$ / Vol. of Syrup IR St II	50.04	76.19	75.66	65.98	47.27
$\frac{F}{\text{Vol. of Final Super}}$ / Vol. of Final Syrup	14.44	13.06	13.75	13.24	18.00
Wt% Syrup IR St II	10.45	6.10	5.98	7.65	13.59
Wt% Super IR St II	89.55	93.90	94.02	92.35	86.41
Wt% Final Super	19.50	27.60	23.97	27.12	21.00
Wt% Final Syrup	70.05	66.30	70.05	65.23	65.41

Fig. 8.3.13 Actual Plant Results

Batch Number	RB 51L/ 40	SL 53L/ 70	RB 54L/ 40	RB 55L/ 40	SL 56L/ 70
$\frac{D}{\text{Vol. of Super IR St II}}$ / Vol. of Syrup IR St II	49.80	37.73	36.94	30.51	45.36
$\frac{F}{\text{Vol. of Final Super}}$ / Vol. of Final Syrup	13.06	14.18	15.88	15.77	10.47
Wt% Syrup IR St II	10.79	15.03	15.47	19.05	11.42
Wt% Super IR St II	89.21	84.97	84.53	80.95	88.58
Wt% Final Super	8.10	11.99	17.93	9.68	11.15
Wt% Final Syrup	81.11	72.98	66.60	71.27	77.43

Fig. 8.3.14 Actual Plant Results

Batch Number	RB 57L/ 40	RB 58L/ 40	RB 59L/ 40	-	-
$\frac{\text{D}}{\text{Vol. of Super IR St II}}$ / Vol. of Syrup IR St II	48.15	90.88	23.96		
$\frac{\text{F}}{\text{Vol. of Final Super}}$ / Vol. of Final Syrup	16.94	14.28	14.41		
Wt% Syrup IR St II	25.47	9.52	20.70		
Wt% Super IR St II	74.53	90.48	79.30		
Wt% Final Super	9.84	11.93	15.81		
Wt% Final Syrup	64.69	78.55	63.49		

Fig. 8.3.15 Results of the Mathematical Model Predictions

Batch Number	RB 35L/ 40	RB 36L 40	RB 37L/ 40	RB 38L/ 40	RB 50L/ 40
C x 10^5	2.18	1.79	2.18	1.57	2.27
D	99.50	30.56	31.03	34.67	22.74
E x 10^4	1.87	1.60	2.88	1.30	2.20
F	5.43	5.63	8.54	5.56	8.30
Fixed Value of P	0.78	0.76	0.80	0.70	0.73
Wt% Syrup IR St II	7.38	8.90	10.01	7.56	13.18
Wt% Super IR St II	92.62	91.10	89.99	92.44	86.82
Wt% Final Super	14.84	14.99	10.03	22.28	13.81
Wt% Final Syrup	77.78	76.11	79.96	70.16	73.01

Fig. 8.3.16 Results of the Mathematical Model Predictions

Batch Number	RB 51L/ 40	SL 53L/ 70	RB 54L/ 40	RB 55L/ 40	SL 56L/ 70
C x 10^5	3.67	1.50	1.94	3.41	0.97
D	533.73	31.32	19.41	111.17	31.39
E x 10^4	5.46	2.34	1.91	4.34	1.14
F	31.47	12.49	6.22	19.21	1.22
Fixed Value of P	0.90	0.80	0.71	0.81	0.82
Wt% Syrup IR St II	5.94	12.86	14.90	13.19	10.71
Wt% Super IR St II	94.06	87.14	85.10	86.81	89.29
Wt% Final Super	6.14	7.52	14.11	7.54	5.16
Wt% Final Syrup	87.92	79.62	70.99	79.27	84.13

Fig. 8.3.17 Results of the Mathematical Model Predictions

Batch Number	RB 57L/40	RB 58L/40	RB 59L/40	-	-
C x 10^5	2.92	2.86	0.77		
D	24.41	248.17	5.33		
E x 10^4	3.74	3.01	2.25		
F	15.76	9.75	6.08		
Fixed Value of P	0.73	0.85	0.69		
Wt% Syrup IR St II	20.26	4.64	20.81		
Wt% Super IR St II	79.74	95.36	79.19		
Wt% Final Super	7.59	10.84	9.73		
Wt% Final Syrup	72.15	84.52	69.46		

FIG 8.3.18 COMPARISON OF MODEL RESULTS WITH PLANT RESULTS
BATCH No's RB 35L- RB 59L

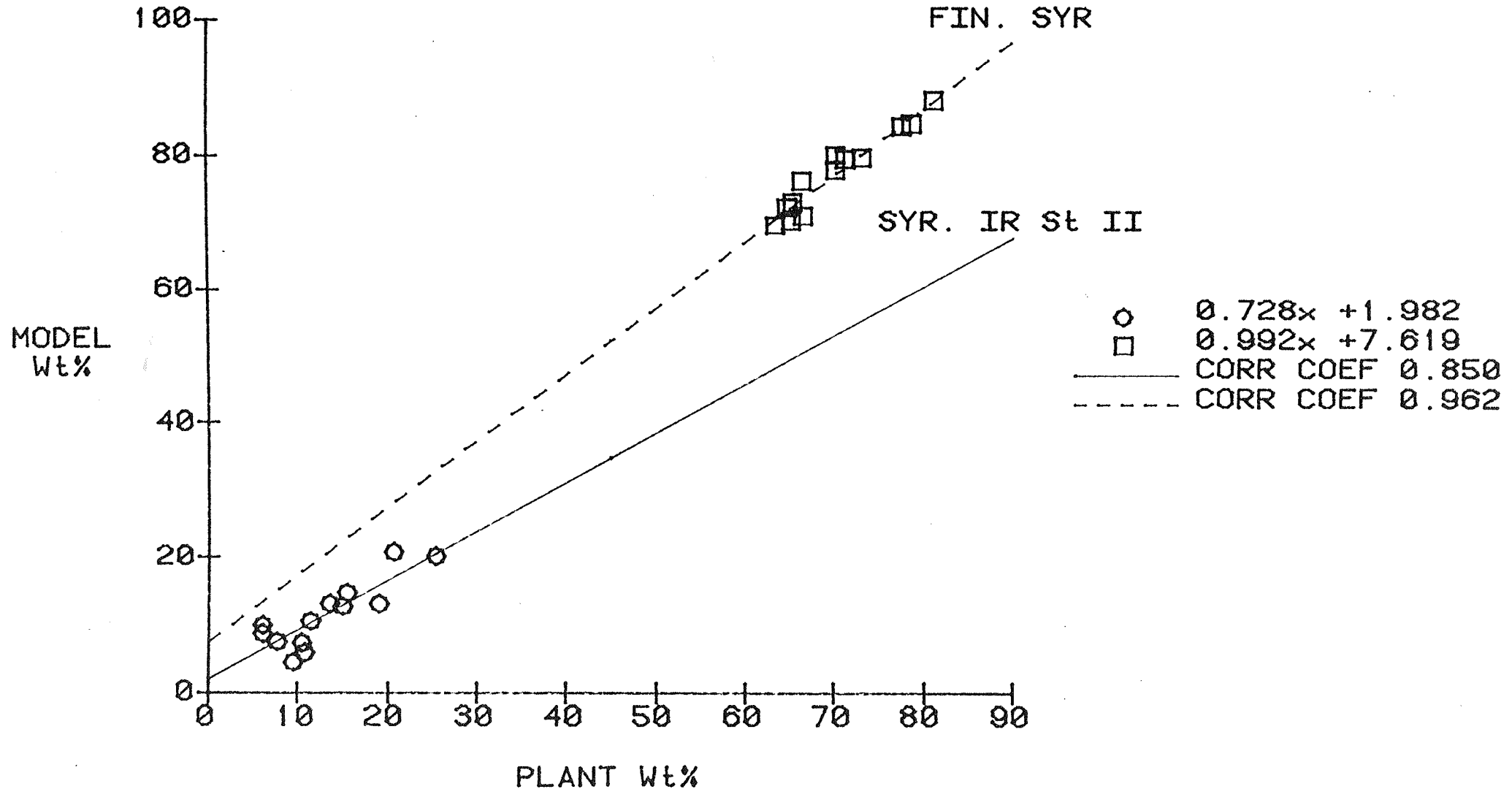

results are in reasonable agreement. The slope and the correlation coefficient values are marginally lower than the ones found in the laboratory experiments (see Section 7.3).

For the second stage (final syrup) the two sets of results are in very good agreement but an offset of approximately eight per cent is present, the model predicting more than the actual plant results. This degree of offset was also found in the laboratory experiments (see Fig. 7.2.20).

8.4 CONCLUSIONS

(i) On the plant batches RB 8L/40-SL 17L/70 the comparison of model predictions with the actual plant results was poor with the exception of batch RB 8L/40.

Possible explanations for the poor agreement could be that not enough time may have been allowed for the syrup IR St I to settle in the fractionator before being drawn off (this will be discussed in Chapter 9.0). Also there were problems with the analytical GPC system (see Section 8.3.1).

Another possible explanation could be the large amount of very high molecular weight dextrans present especially in the syrup IR St II sample.

(ii) For the second stage fractionation (batches RB 8L/40 - SL 17L/70), results of the Boltzmann equation plots are very good. For the third stage (final super and final syrup) only four batches had reasonable correlation coefficient values.

(iii) For the plant batches RB 35L/40 - RB 59L/40 the comparison of model predictions with the actual plant results on the first fractionation (syrup IR St II) is reasonable. The comparison on the second stage (final syrup) between the results is very good.

One of the disadvantages of these plant samples is that the Wt% dextran fractions are grouped together in their prospective regions. This can be seen from Fig. 8.3.18. The Wt% syrup IR St II is grouped together in the 5-20 Wt% region whereas the Wt% final syrup is grouped together in 60-80 Wt% region making a true comparison difficult over the entire region.

CHAPTER NINE

SETTLING OF DEXTRAN MOLECULES

9.0 SETTLING OF DEXTRAN MOLECULES

9.1 INTRODUCTION

On the chemical plant bulk drawing of syrup IR St I is made after 6 hours and the final drawing 2 hours later; the syrup IR St II is drawn after 16 hours.

This work was carried out to investigate the settling of dextran molecules on precipitation and whether equilibrium was achieved in the set time.

The following fractionation processes were sampled.

(i) Syrup I precipitation of batch SL 28M/70.

(ii) Super IR St I precipitation of batch SL 36M/70.

(iii) Syrup I precipitation of batch RB 56M/40.

It should be noted here that the first two batches were aimed at producing a clinical dextran of 70,000 weight average molecular weight whereas the last batch is aimed for 40,000 $\bar{M}_w$ clinical dextran.

All the samples in this chapter were analysed on the Aston University GPC system.

9.2 SETTLING OF BATCH SL 28M/70

Samples were collected during syrup I ethanol fractionation using a sampling can (Griffin and George Ltd; Alperton, Middlesex).

The samples were collected from three different depths, these were 1.1, 2.1 and 2.6 m below the liquid surface. At 1.1 and 2.1 m sampling was done every hour until the syrup IR St I was drawn into the weigh vessel after 6 hours. For the 2.6 m depth sampling was done every half hour for the first 3 hours, then every hour for the

remaining 3 hours.

The dimensions of the fractionator and sampling points are shown in Fig. 9.2.1. Fig. 9.2.2 shows the $\bar{M}_W$ results of the GPC analysis. Fig. 9.2.3 is a graphical plot of the weight average molecular weights for the samples collected against settling time. It can be seen from Fig. 9.2.3 that the samples have not settled to equilibrium with respect to molecular weight, i.e. fractionation had not been completed and that some of the high molecular weight syrup was still present in the supernatant phase when the syrup was drawn.

The sharp increase in the $\bar{M}_W$ after 5 hours for the 2.6 m depth was due to the syrup/super interface. This is also supported by the following calculation:

Syrup IR St I drawn into weigh vessel = 2650 kg

Assuming density of syrup as 1150 kg/m^3

Volume of syrup = $\frac{2650}{1150}$ m^3 = 2.3 m^3

Since the volume of the cone section is 15 m^3, the syrup was entirely contained in the 45^o cone. Equating the syrup volume with the volume equation for a 45^o cone, the syrup height was calculated to be 1.3 m, i.e. 2.7 m below the liquid surface, which is very close to the deepest sampling point.

Fig. 9.2.4 is a graphical plot for the Wt % above a molecular weight of 150,000 against settling time. The Wt % above a molecular weight of 400,000 graph is shown in Fig. 9.2.5.

Fig. 9.2.1 Diagram of Sampling Points for Batch SL 28M/70

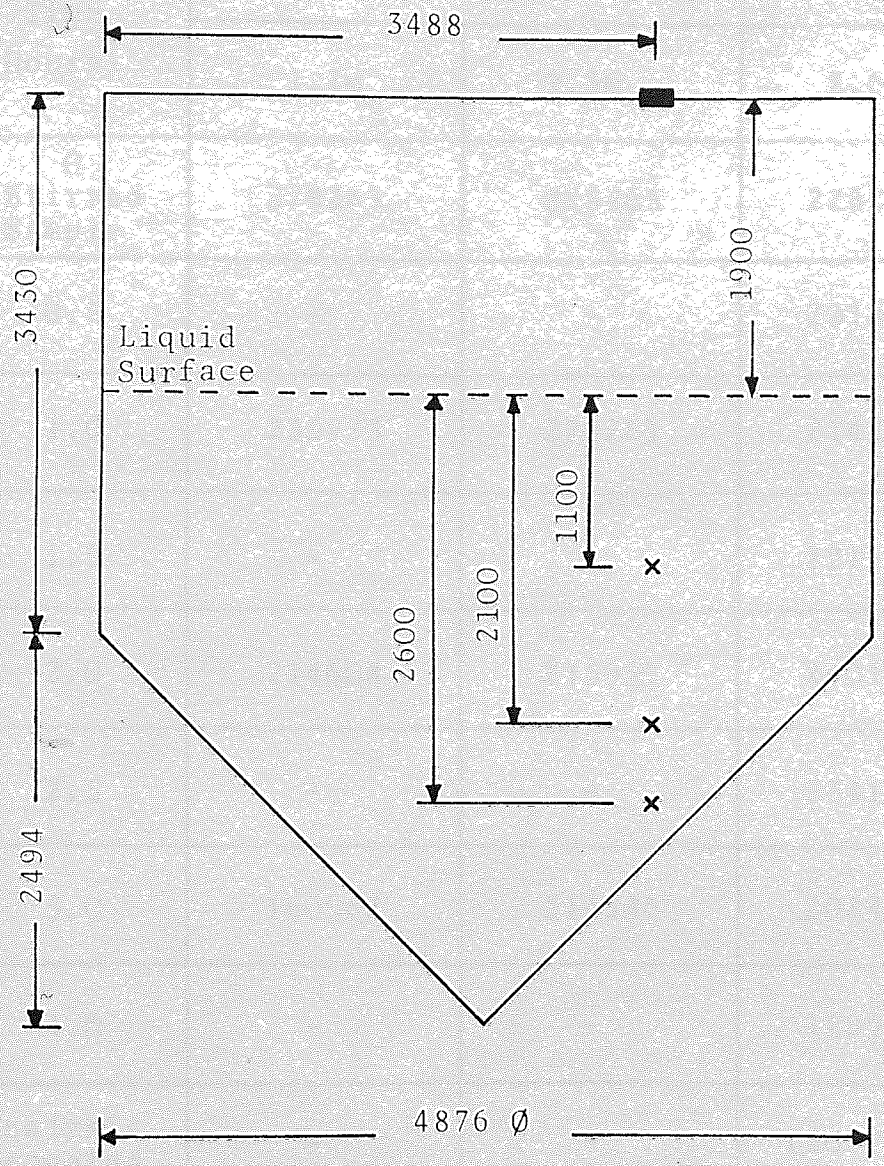

All Dimensions in mm
Scale 1:50

Fig. 9.2.2 $\bar{M}_W$'s for Batch SL 28M/70 Measured by TSK-GPC System at Aston

Sample Time (Hours)	Weight Average Molecular Weight of Samples at Depth		
	1.1m	2.1m	2.6m
0 Stirred Sample	228265	228265	228265
0.5	-	-	231816
1.0	235923	228251	214275
1.5	-	-	221553
2.0	214608	218937	240109
2.5	-	-	224181
3.0	160962	214546	208467
4.0	-	-	189955
Analysis Repeated	-	-	(203243)
5.0	128114	175578	178346
Analysis Repeated	-	-	(194891)
6.0	92936	97190	493531
Analysis Repeated	-	-	(547738)

$\bar{M}_W$ of Syrup IR St I = 776054

FIG 9.2.3 WEIGHT AVERAGE MOLECULAR WEIGHTS FOR BATCH SL 28M AGAINST SETTLING TIME

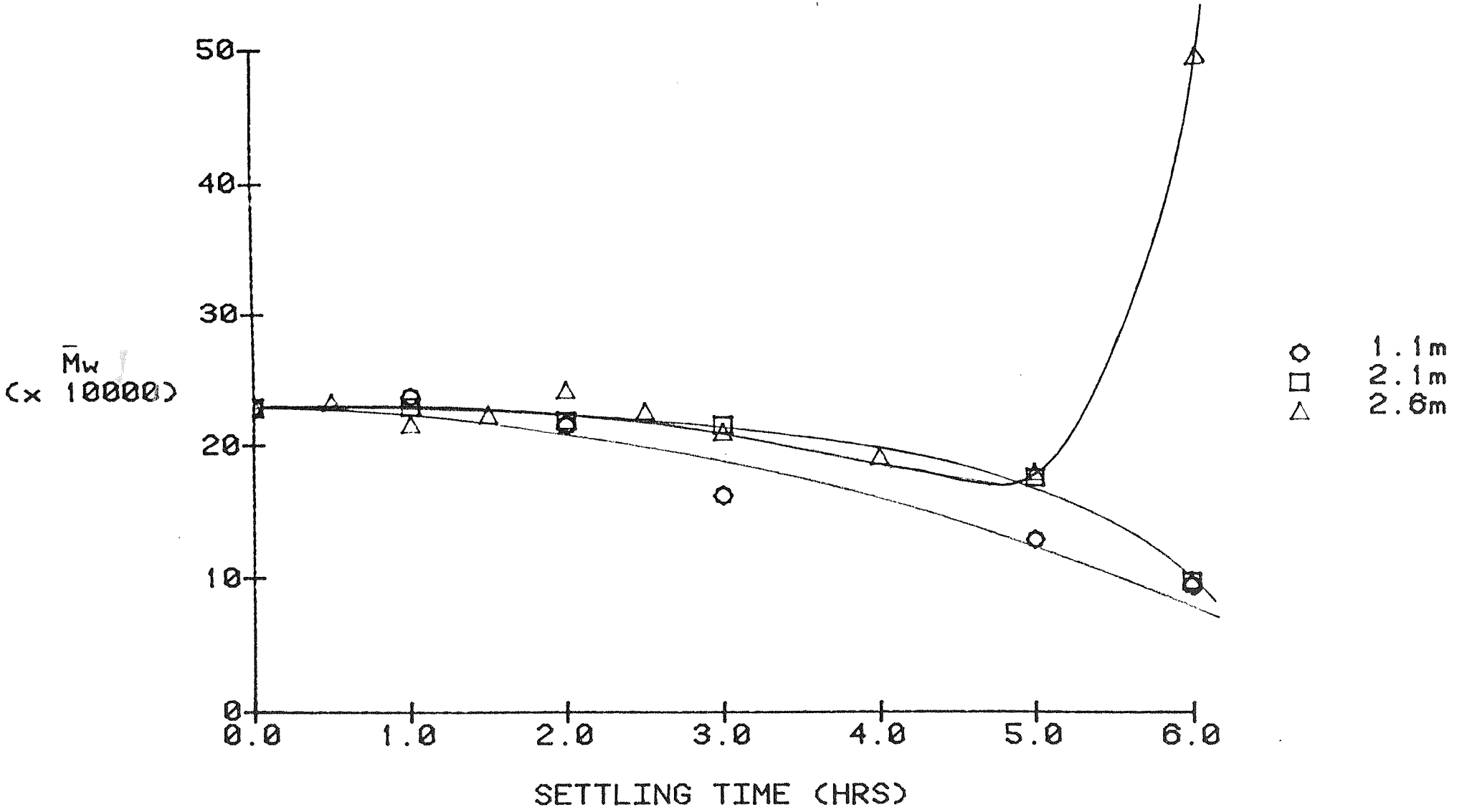

FIG 9.2.4 CUMULATIVE Wt% PRESENT ABOVE 150,000 M
IN SUPER IR St I (Bx SL 28M)

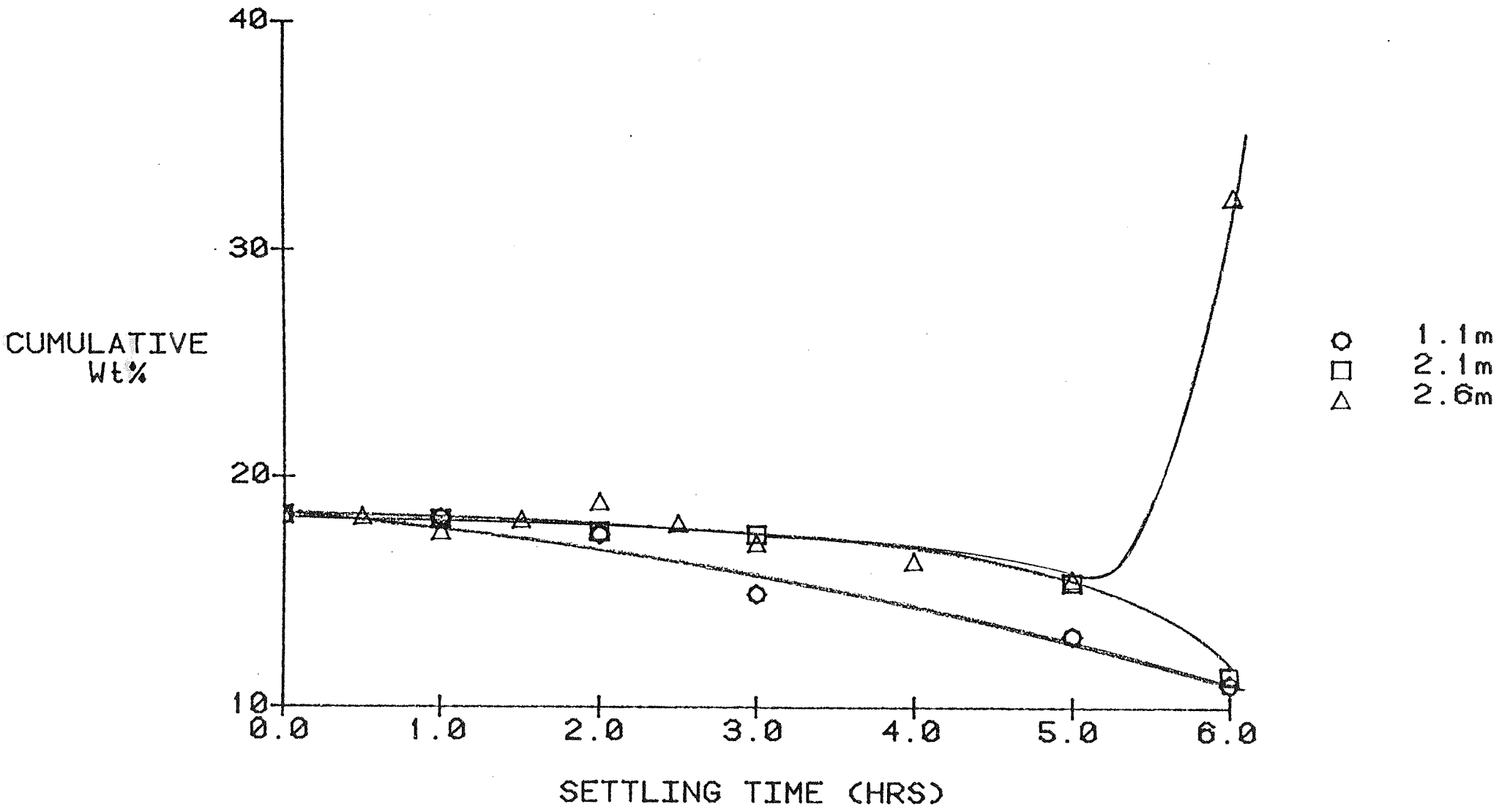

FIG 9.2.5 CUMULATIVE Wt% PRESENT ABOVE 400,000 M
IN SUPER IR St I (Bx SL 28M)

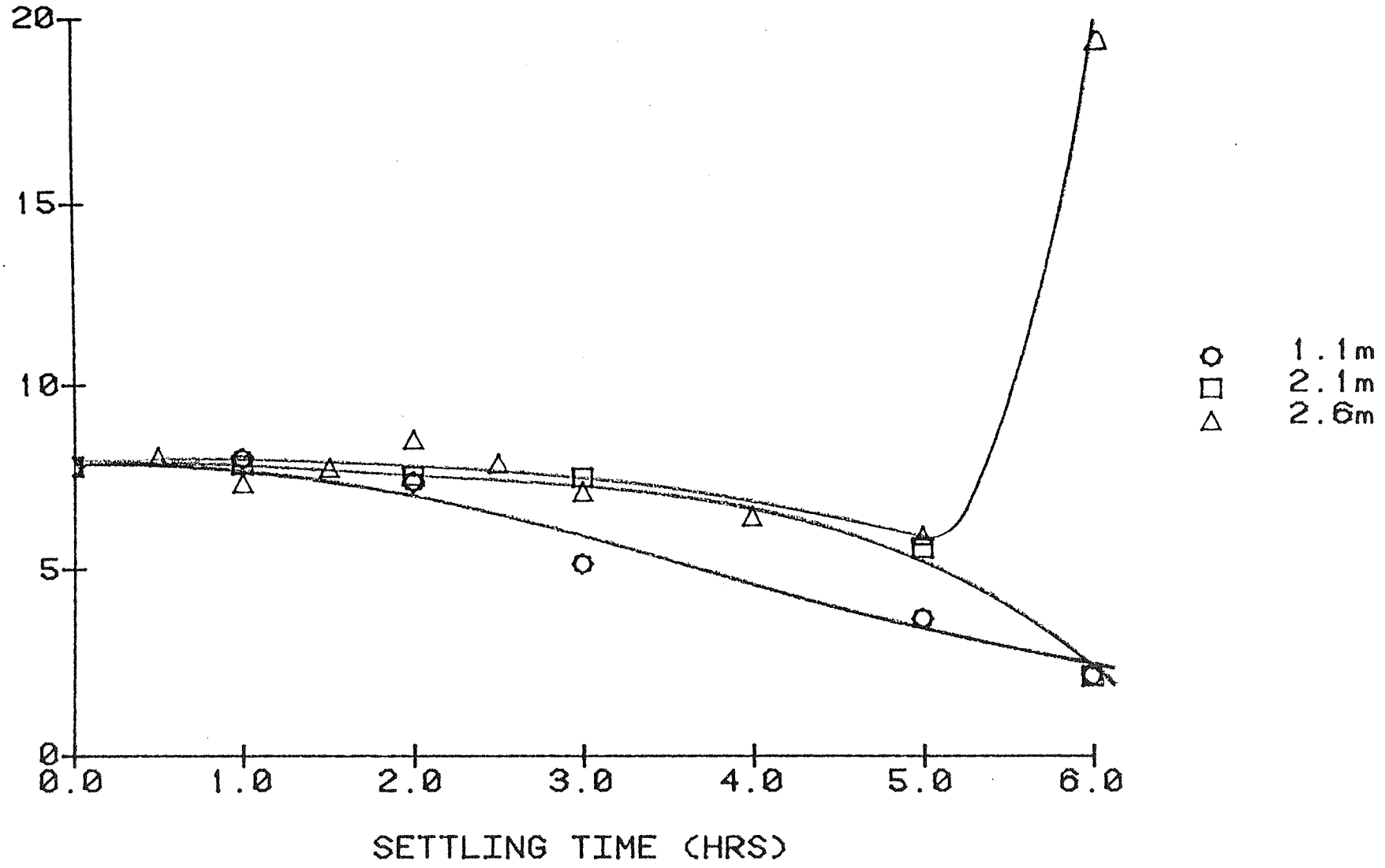

From the above two figures it can be seen that the supernatant has not come to equilibrium after 6 hours even at the 1.1 m depth.

To provide further information two more fractionations were sampled which were allowed longer settling times (see Sections 9.3 and 9.4).

9.3 SETTLING OF BATCH SL 36M/70

Samples were collected during super IR St I ethanol fractionation; a settling time of 24 hours was allowed.

Samples were collected from two different depths, 0.5 and 2 m below the liquid surface. At 0.5 m sampling was performed every hour for the first 4 hours, then every 2 hours until the syrup IR St II was drawn into the weigh vessel. For the 2 m depth sampling was performed every hour for the first 4 hours, then every 4 hours for the remaining 20 hours. The sampling points are shown in Fig. 9.3.1.

Fig. 9.3.2 shows the $\bar{M}_W$ results of the GPC analysis. Fig. 9.3.3 is a graphical plot of the $\bar{M}_W$'s for the samples collected against settling time. This figure shows that equilibrium has been established after approximately 13 hours at both depths. Fig. 9.3.3 shows that at equilibrium there is a small difference between the $\bar{M}_W$'s for the two different depths. This difference will be looked at statistically by considering what is the probability that the results obtained could arise by chance from the same parent source, i.e."is there a significant difference between the two results?"

Fig. 9.3.1 Diagram of Sampling Points for Batch SL 36M/70

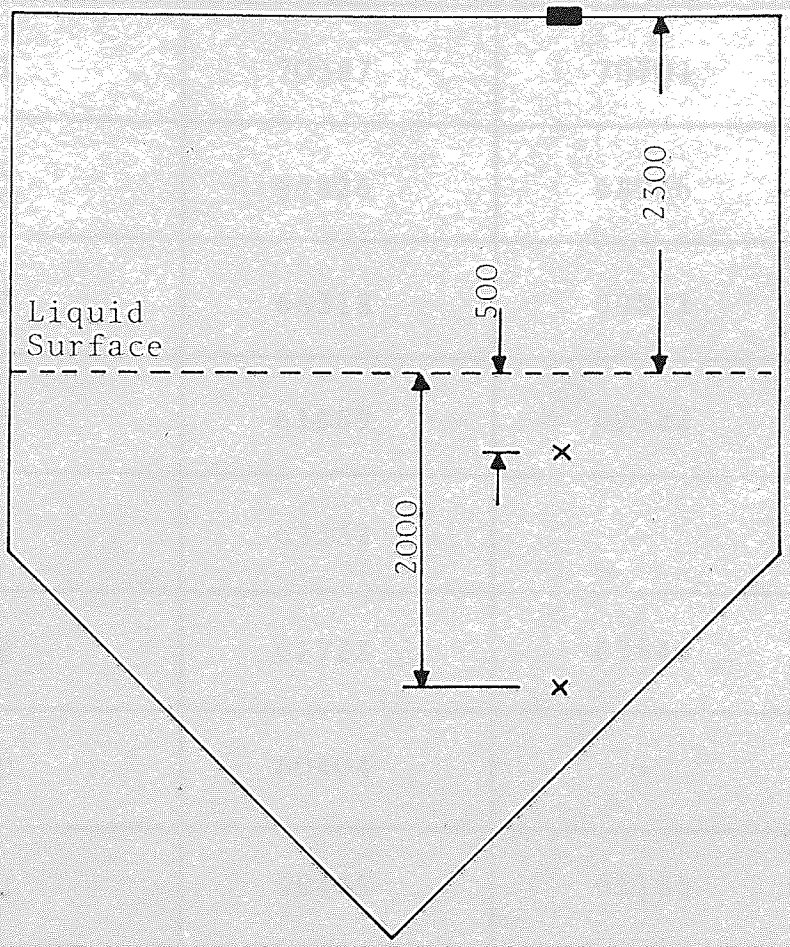

All Dimensions in mm.

Scale 1:50

Fig. 9.3.2 $\bar{M}_W$'s for Batch SL 36M/70 Measured by TSK-GPC System at Aston

Sample Time (Hours)	Weight Average Molecular Weight of Samples at Depth	
	0.5m	2m
0 Stirred Sample	70517	70517
1	70387	70701
2	69826	68936
3	66318	69821
4	61589	69522
6	62332	-
8	61722	67846
10	60404	-
12	59445	61135
16	60286	60635
18	59617	-
20	60536	61287
22	60289	-
24	59509	61029

$\bar{M}_W$ of Super IR St II = 58971
$\bar{M}_W$ of Syrup IR St II = 197630

FIG 9.3.3 WEIGHT AVERAGE MOLECULAR WEIGHTS FOR BATCH SL 36M AGAINST SETTLING TIME

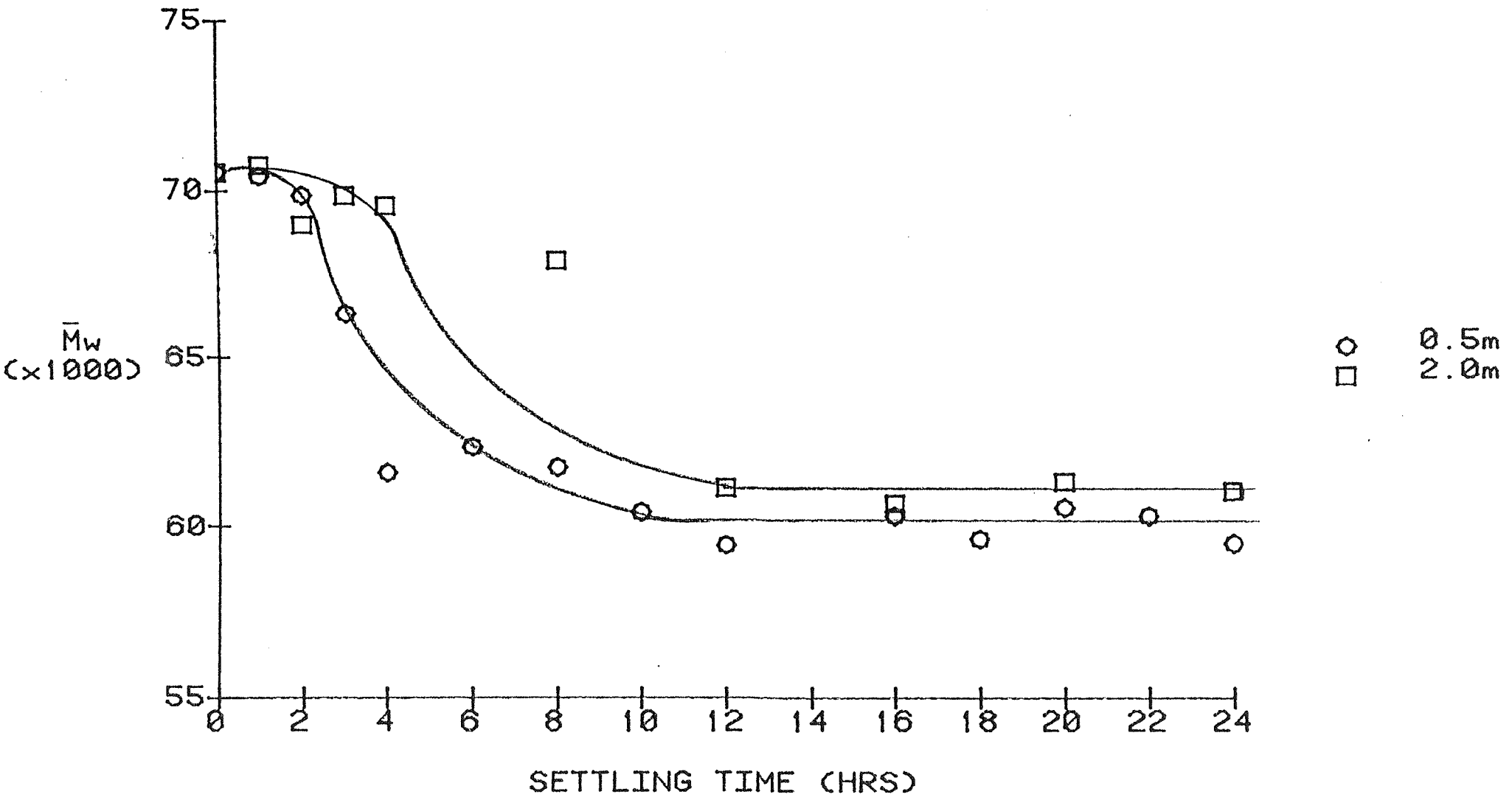

There are a very large number of different statistical tests (130), each test being designed to deal with a certain type of situation. For this experiment the 'Student's' t Test was chosen since this has the purpose of comparing a random sample consisting of 3 or more measurements with a large parent group whose mean is known, but whose standard deviation is not known.

The method is based on making a tentative negative assumption that there is no significant difference between the mean of the sample group and the mean of the large parent group, and the probability of this being the case is determined by calculating the value of 'Student's' t, and referring this answer to the 'Student's' t Table.

The 'Student's' t value is calculated from the following formula:

$$t = \frac{\sqrt{n}.|\bar{a}_1 - \bar{a}_2|}{s.d} \quad \ldots\ldots\ldots\ldots\ldots\ldots\ldots\ldots \quad 9.3.1$$

where

n = number of measurements in the sample group

$\bar{a}_1$ = mean of the large parent group

$\bar{a}_2$ = mean of the sample measurement

$s.d$ = standard deviation of the sample measurements

Over many years, the following probability levels have been used satisfactorily by statisticians.

If the observed difference is likely to occur by chance with a frequency of more than once in 20 times, it is not accepted as being a significant difference. Any probability larger than 5% is considered insufficient to deny the tentative assumption that the results have

stemmed from the same source. This situation can be described as 'significant difference not proven'.

If the observed difference could be expected to occur by chance only once in 20 times, which is a probability of 5%, this is considered to be unlikely to be due to chance. Differences showing this probability level are generally said to be probably significant.

If the observed difference is only to be expected as a result of chance once in 100 times, which is a probability of 1%, it must be admitted that the likelihood of the no-difference assumption being correct is, in fact, very unlikely. The verdict here is that the difference is significant.

For this batch the 'Student's' t value was calculated as follows:

n	Time (hours)	$\bar{M}_W$ 0.5m	2m	2m-0.5m (a_2)
1	16	60286	60635	349
2	20	60536	61287	751
3	24	59509	61029	1520

The parent mean discrepancy value $\bar{a}_1$ is assumed to be zero.

$$n = 3$$

$$\bar{a}_1 = 0$$

$$\bar{a}_2 = 873.33$$

$$s.d = 595.01$$

From equation 9.3.1

$$t = \frac{\sqrt{3}.|0-873.33|}{595.01} = 2.54$$

From the 'Student's' t Table, the probability value obtained is greater than 10%. The observed difference is now likely to occur by chance with a frequence of more than once in 10 times. It is therefore accepted that there is no significant difference in the two results.

Fig. 9.3.4 is a graphical plot for the Wt% above molecular weight of 60,000 against settling time. The Wt% above molecular weight of 150,000 graph is shown in Fig. 9.3.5.

The above two figures also show that equilibrium is established after 13 hours at both depths. As before there is a small difference at equilibrium for the two depths in Figs. 9.3.4 and 9.3.5.

Applying the 'Student's" t test to calculate the probability of no significant difference between $\bar{a}_1$ and $\bar{a}_2$, the results of Fig. 9.3.4 will be looked at first and Fig. 9.3.5 secondly.

n	Time (hours)	Wt% above molecular weight 60,000 0.5m	2m	2m-0.5m (a_2)
1	16	33.02	33.35	0.33
2	20	33.20	33.20	0
3	24	32.57	33.28	0.71

The parent mean discrepancy value $\bar{a}_1$ is assumed to be zero.

$n = 3$

$\bar{a}_1 = 0$

$\bar{a}_2 = 0.347$

$s.d = 0.355$

FIG 9.3.4 CUMULATIVE Wt% PRESENT ABOVE 60,000 M
IN SUPER IR St II (Bx SL 36M)

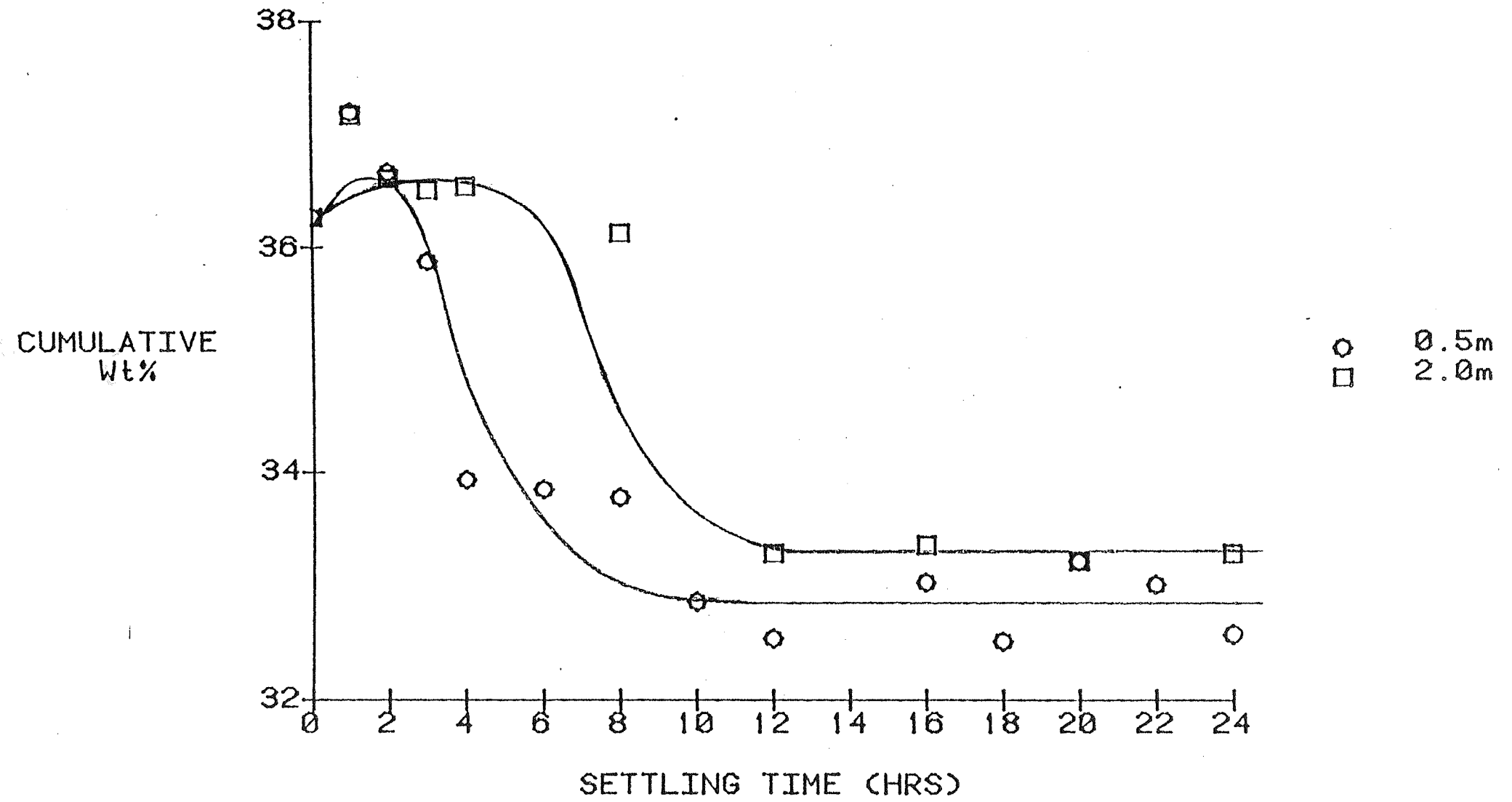

FIG 9.3.5 CUMULATIVE Wt% PRESENT ABOVE 150,000 M IN SUPER IR St II (Bx SL 36M)

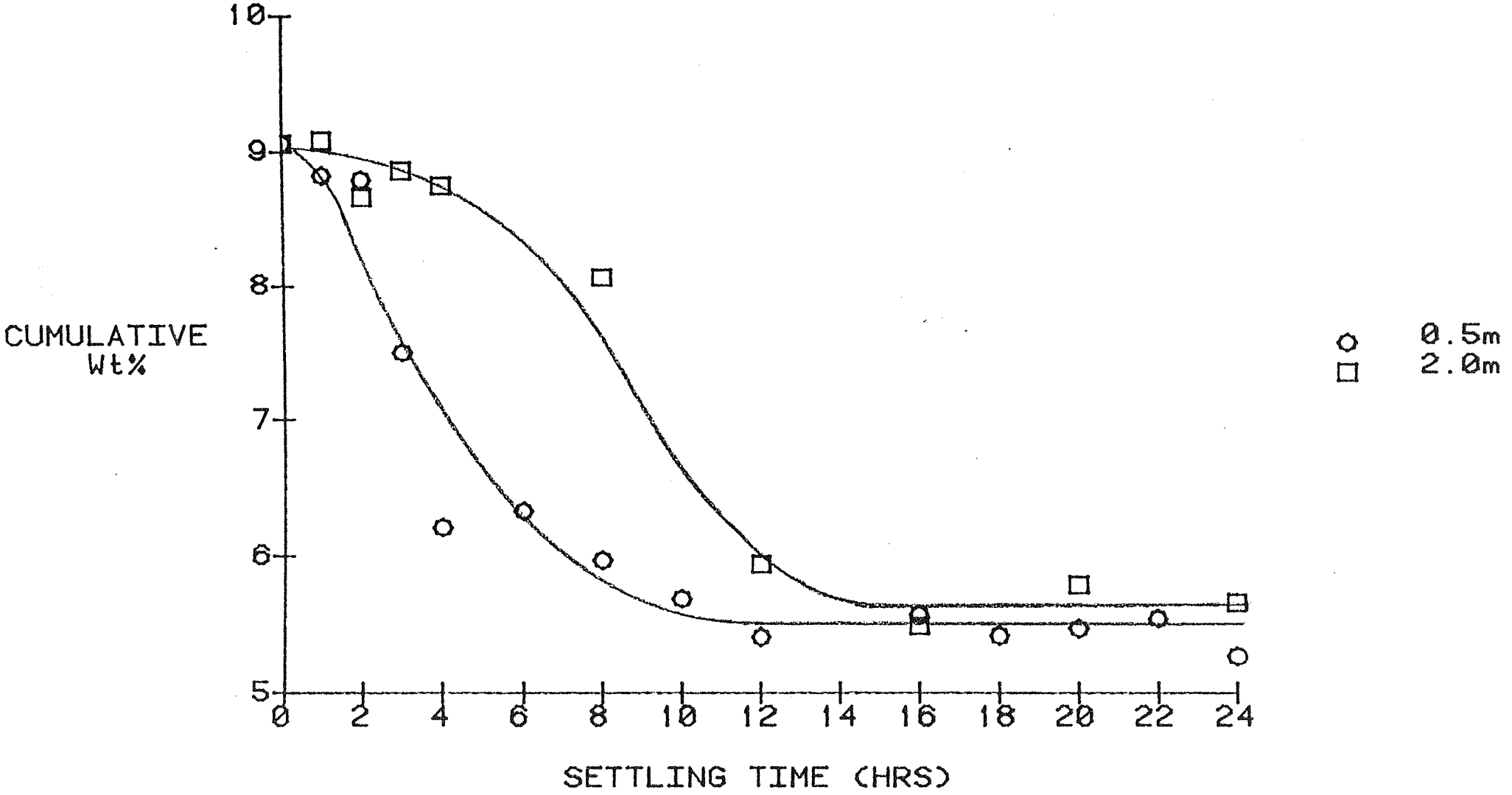

From equation 9.3.1

$$t = \frac{\sqrt{3}.|0-0.3471|}{0.355} = 1.69$$

From the 'Student's' t Table, the probability value obtained is greater than 10%, the two results are therefore not accepted as being significantly different.

For the results of Fig. 9.3.5.

n	Time (hours)	Wt% above molecular weight 150,000 0.5m	2m	2m-0.5m (a_2)
1	16	5.57	5.49	-0.08
2	20	5.47	5.79	0.32
3	24	5.27	5.66	0.39

The parent mean discrepancy value $\bar{a}_1$ is assumed to be zero.

$n = 3$

$\bar{a}_1 = 0$

$\bar{a}_2 = 0.21$

$s.d = 0.254$

From equation 9.3.1

$$t = \frac{\sqrt{3}.|0-0.21|}{0.254} = 1.43$$

The probability value obtained is again greater than 10%, i.e. the two results are not accepted as being significantly different.

9.4 SETTLING OF BATCH RB 56M/40

Samples were collected during syrup I ethanol fractionation; a settling time of 24 hours was allowed.

Samples were collected from two different depths, 0.5 and 2m below the liquid surface. At 0.5m sampling

was performed every hour for the first 4 hours, then every 2 hours until the syrup IR St I was drawn into the weigh vessel. For the 2m depth sampling was performed every hour for the first 4 hours, then every 4 hours for the remaining 20 hours. The sampling points are shown in Fig. 9.4.1.

Fig. 9.4.2 shows the $\bar{M}_W$ results of the GPC analysis. A graphical plot of the $\bar{M}_W$'s for the samples collected against settling time is shown in Fig. 9.4.3, This figure shows that equilibrium has been established after approximately 6 hours at both depths.

A small difference between the $\bar{M}_W$'s for the two depths is again present in Fig. 9.4.3. The probability value calculated by the statistical method of 'Student's' is as follows:

n	Time (hours)	$\bar{M}_W$ 0.5m	2m	2m-0.5m (a_2)
1	8	39205	40833	1628
2	12	39587	40942	1355
3	16	39177	40627	1450
4	20	39875	39495	-380
5	24	39954	39909	- 45

$n = 5$

$\bar{a}_1 = 0$

$\bar{a}_2 = 801.60$

$s.d = 938.42$

$$t = \frac{\sqrt{5}|0-801.60|}{938.42} = 1.91$$

Fig. 9.4.1 Diagram of Sampling Points for Batch RB 56M/40

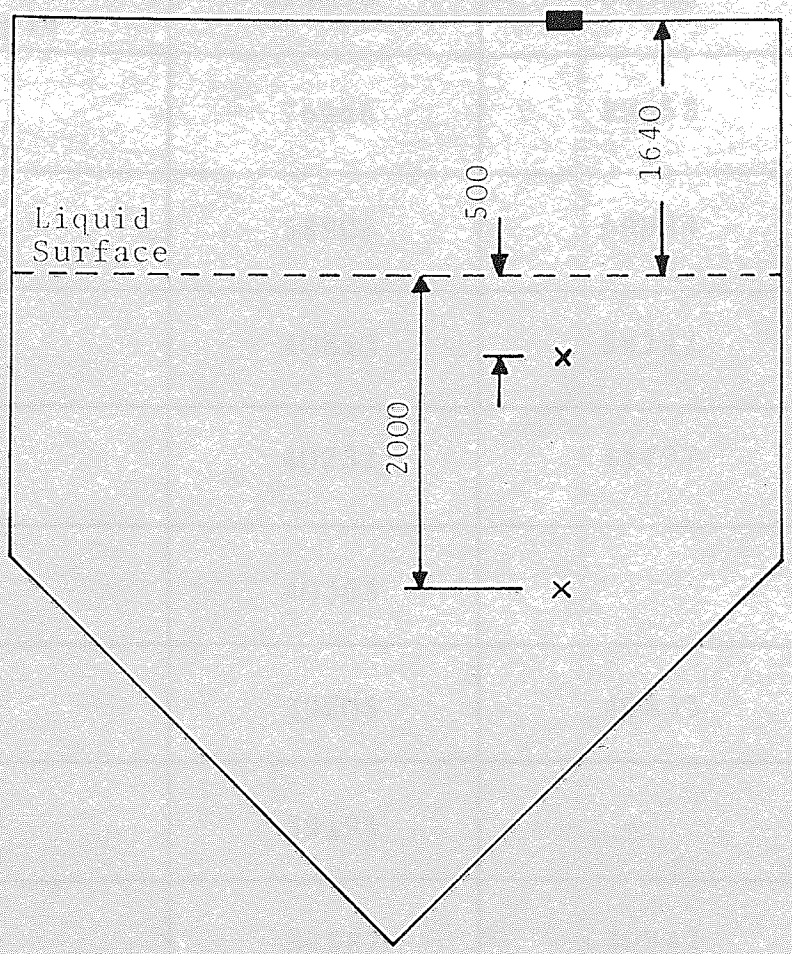

All Dimensions in mm.

Scale 1:50

Fig. 9.4.2 $\bar{M}_w$'s for Batch RB 56M/40 Measured by TSK-GPC System at Aston

Sample Time (Hours)	Weight Average Molecular Weight of Samples at Depth	
	0.5m	2m
0 Stirred Sample	134046	134046
1	76966	89653
2	58905	69984
3	40810	58142
4	40232	41797
6	40363	-
8	39205	40833
10	39191	-
12	39587	40942
14	39242	-
16	39177	40627
20	39875	39495
24	39954	39909

$\bar{M}_w$ of Super IR St I = 39809
$\bar{M}_w$ of Syrup IR St I = 541412

FIG 9.4.3 WEIGHT AVERAGE MOLECULAR WEIGHTS FOR BATCH RB 56M AGAINST SETTLING TIME

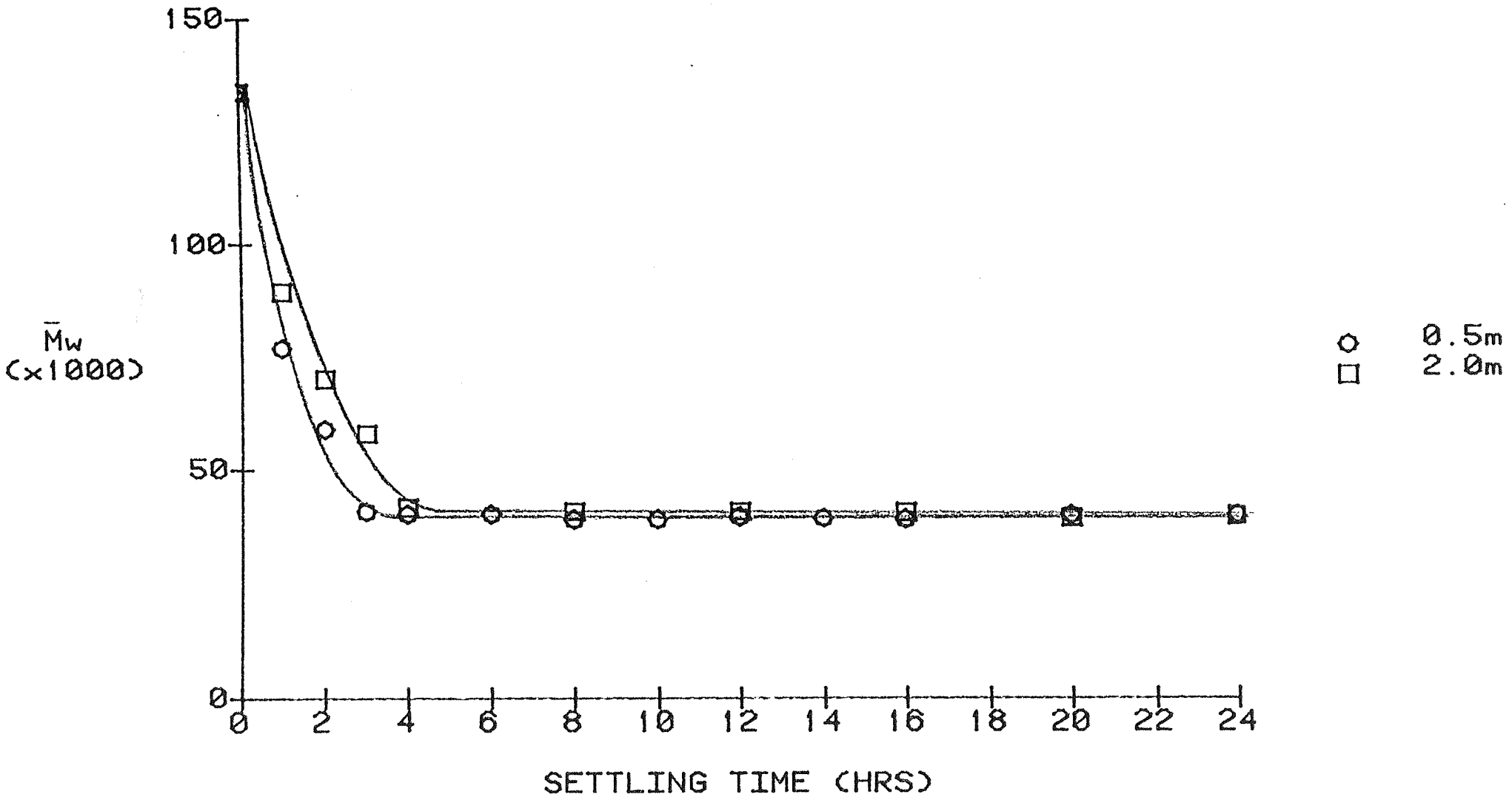

The probability value obtained from the 'Student's' t Table is greater than 10%. It is therefore accepted that there is no significant difference in the two results.

A graphical plot for the Wt% above molecular weight 60,000 against settling time is shown in Fig. 9.4.4. The Wt% above molecular weight of 150,000 graph is shown in Fig. 9.4.5.

The above two figures also show that equilibrium is established after 6 hours at both the 0.5 and 2m depths. As before there is again a small difference at equilibrium for the two depths.

Applying the 'Student's' t Test firstly to the results of Fig. 9.4.4 and then to the results of Fig. 9.4.5.

n	Time (hours)	Wt% above molecular weight 60,000 0.5m	2m	2m-0.5m (a_2)
1	8	16.63	17.75	1.12
2	12	16.99	17.56	0.57
3	16	16.67	17.67	1.00
4	20	17.17	16.97	-0.20
5	24	17.15	17.07	-0.08

$n = 5$

$\bar{a}_1 = 0$

$\bar{a}_2 = 0.482$

$s.d = 0.605$

From equation 9.3.1

$$t = \frac{\sqrt{5}|0-0.482|}{0.605} = 1.78$$

FIG 9.4.4 CUMULATIVE Wt% PRESENT ABOVE 60,000 M IN SUPER IR St I (Bx RB 56M)

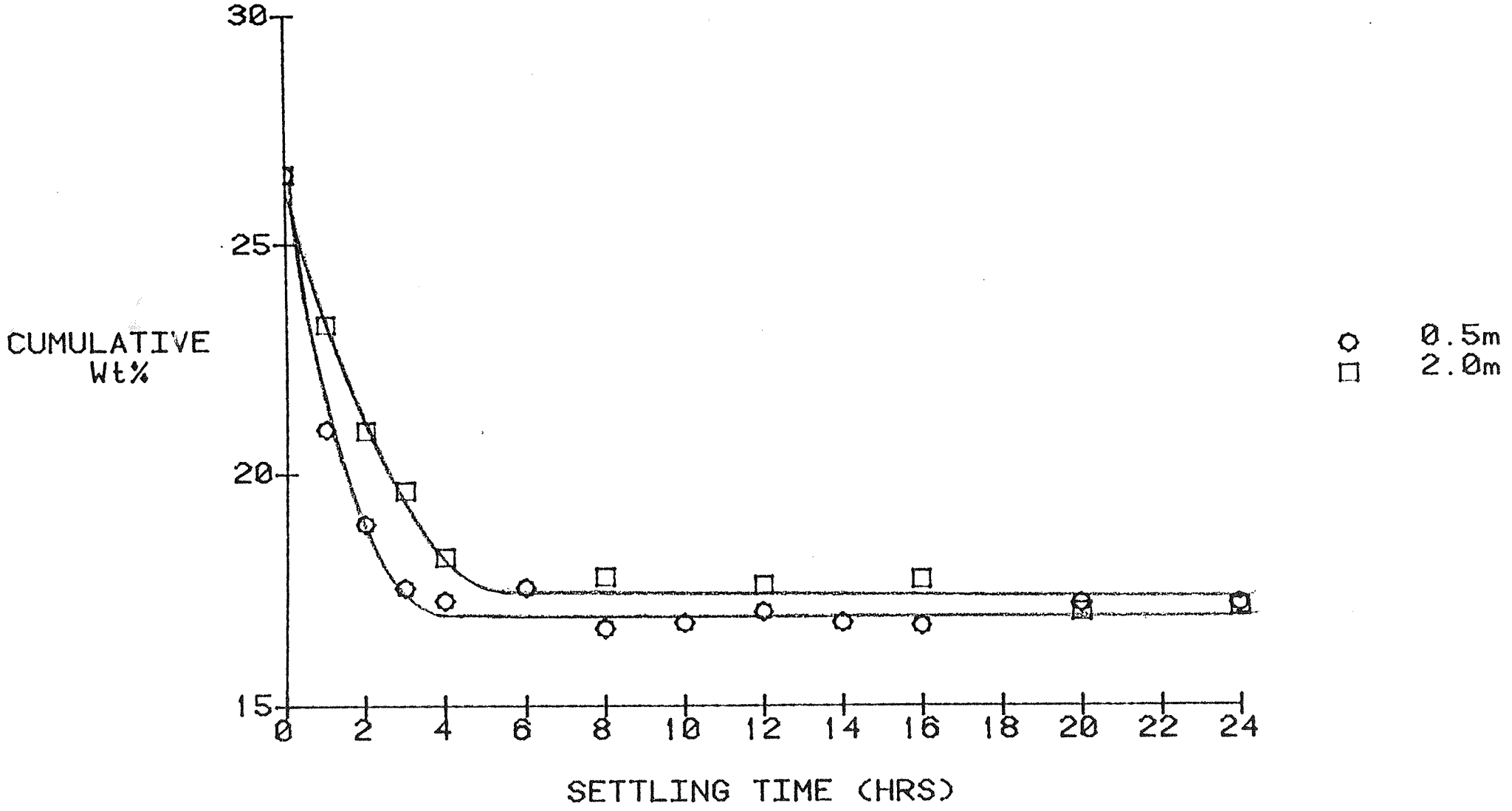

FIG 9.4.5 CUMULATIVE Wt% PRESENT ABOVE 150,000 M IN SUPER IR St I (Bx RB 56M)

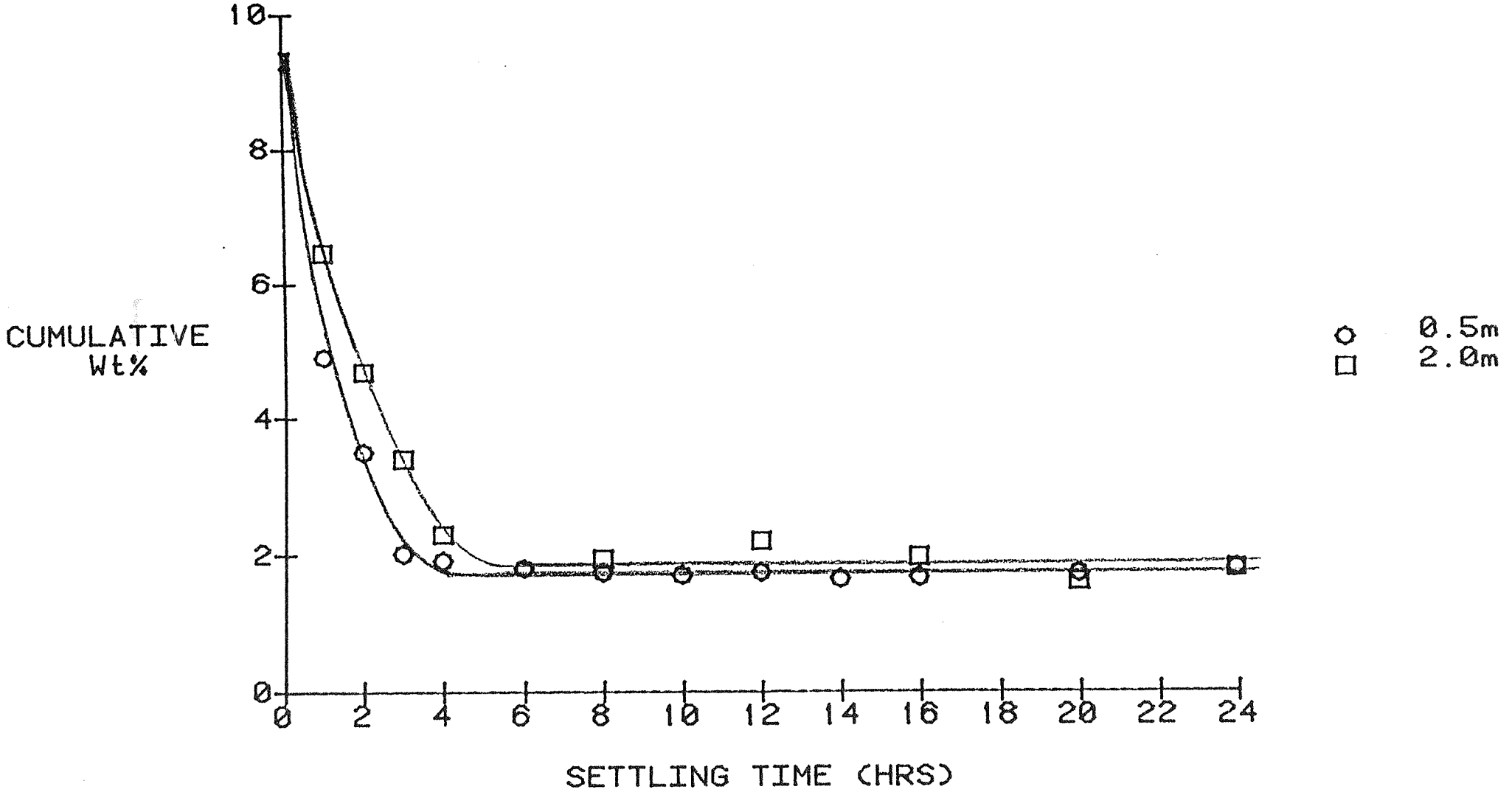

From the 'Student's' t Table, the probability value obtained is greater than 10%. The two results are therefore not accepted as being significantly different.

For the results of Fig. 9.4.5.

n	Time (hours)	Wt % above molecualr weight 150,000 0.5m	2m	2m-0.5m (a_2)
1	8	1.74	1.95	0.21
2	12	1.75	2.21	0.46
3	16	1.66	1.97	0.31
4	20	1.72	1.60	-0.12
5	24	1.81	1.81	0

$n = 5$

$\bar{a}_1 = 0$

$\bar{a}_2 = 0.172$

$s.d = 0.234$

From equation 9.3.1

$$t = \frac{\sqrt{5}|0-0.172|}{0.234} = 1.65$$

The probability value obtained is again greater than 10%, i.e. the two results are not accepted as being significantly different.

9.5 CONCLUSIONS

i) In the case of syrup IR St I where 6 hours settling was given on batch SL 28M/70 the $\bar{M}_W$ results show that fractionation had not been completed; also that some high molecular weight syrup was still present in the supernatant

phase when the syrup was drawn.

Similarly the Figs. 9.2.4 and 9.2.5 for 'Wt% above' various molecular weights show that the supernatant has not come to equilibrium after 6 hours even at the 1.1m depth.

ii) A syrup IR St II from batch SL 36m/70 was sampled with a settling time of 24 hours. On the plant stage II syrup IR's are allowed a settling time of 16 hours.

The $\bar{M}_W$ results show that fractionation was completed after approximately 13 hours. This is also supported by the graphs of 'Wt% above'.

iii) For batch RB 56M/40 the $\bar{M}_W$ results show that fractionation was completed after only 6 hours. Figs. 9.4.4 and 9.4.5 also agree with this settling time.

It is important to remember here that the above batch is aimed at producing a clinical dextran of $\bar{M}_W$ 40,000 when comparing the results with batch SL 28M/70 which refers to a clinical dextran of $\bar{M}_W$ 70,000. It should also be noted that the $\bar{M}_W$ of syrup I (batch RB 56M/40) is about half the $\bar{M}_W$ value of batch SL 28M/70 syrup I.

iv) The last 6 graphs presented showed slight differences at equilibrium for the different depths.

It has been shown statistically that there is no significant difference between the results at equilibrium for the 6 graphs.

v) Some of the anomalies found in the mathematical model predictions on the plant samples may have been caused by samples taken on the plant which had not settled to

equilibrium; sample super IR St I especially (see Section 8.4).

CHAPTER TEN

LIKELY ECONOMIC AND OPERATIONAL BENEFITS OF USING THE MODEL TO PREDICT PLANT FRACTIONATIONS

10.0 LIKELY ECONOMIC AND OPERATIONAL BENEFITS OF USING THE MODEL TO PREDICT PLANT FRACTIONATIONS

Out of the twenty three industrial plant batches mentioned in Chapter 8.0 only batches SL 9L/70, SL 11L/70, RB 37L/40, RB 38L/40, RB 51L/40, RB 54L/40 and RB 58L/40 (see Fig. 10.1) were fractionated completely. In Fig. 10.1 percentage in excess is defined as the Wt% fractionated above the target value and percentage less as the Wt% that should have been fractionated to reach the target value.

For the remaining batches the syrup IR stage I and IR stage II was over fractionated; this is obviously not economical due to the use of excess ethanol. Additional costs occur when distillation has to be carried out to remove the excess ethanol and over fractionation lowers the yield of clinical dextrans.

For batches RB 35L/40, RB 50L/40 and RB 55L/40 the final syrup was under fractionated. This is again uneconomical due to the valuable product left in the supernatant solution.

The syrup IR stage II for batches RB 8L/40, SL 15L/70 and RB 59L/40 had to be refractionated to get the MWD within the target set.

The use of the mathematical model to predict the plant fractionation would remove the necessity to refractionate and therefore save time and processing costs. The fractionation process cost for producing one batch of clinical dextran is approximately £3,300 including the

Fig. 10.1 Some of the Operational Results for the Plant Batches

Batch Number	Wt% Syrup IR St I Fractionated	Wt% Syrup IR St II Fractionated	Wt% Final Syrup Fractionated
RB 8L/40	2.4% in excess	refractionated	Within target
SL 9L/70	Within target	Within target	Within target
RB 10L/40	Within target	7.6% in excess	Within target
SL 11L/70	Within target	Within target	Within target
RB 12L/40	4.0% in excess	3.7% in excess	Within target
RB 13L/40	5.5% in excess	Within target	Within target
RB 14L/40	Within target	3.0% in excess	Within target
SL 15L/70	Within target	refractionated	Within target
SL 16L/70	4.7% in excess	Within target	Within target
SL 17L/70	3.8% in excess	refractionated	Within target
RB 35L/40	Within target	-	1.1% less
RB 36L/40	6.0% in excess	Within target	Within target
RB 37L/40	Within target	Within target	Within target
RB 38L/40	Within target	Within target	Within target
RB 50L/40	3.1% in excess	Within target	2.3% less
RB 51L/40	Within target	Within target	Within target
SL 53L/70	4.2% in excess	4.4% in excess	Within target
RB 54L/40	Within target	Within target	Within target
RB 55L/40	Within target	Within target	1.1% less
SL 56L/70	Within target	2.9% in excess	Within target
RB 57L/40	Within target	5.9% in excess	Within target
RB 58L/40	Within target	Within target	Within target
RB 59L/40	3.8% in excess	refractionated	Within target

cost of ethanol and labour. The likely cost of having to refractionate one stage is about £500. Four out of these twenty three batches had to be refractionated; a chemical company producing 100 batches per year would save about £8,500 per annum by not having to refractionate say by using the model.

The clinical dextran yields can also be improved by up to 5% with the use of this model. From the twenty three industrial batches mentioned earlier in this chapter a total of 30,312 kg of clinical dextran was produced; for 100 batches per annum the production of clinical dextran is likely to be 131,791 kg. It is anticipated that an extra 6,590 kg of clinical dextran could be produced from 100 batches by using this model. Since dextran sells at approximately £30,000 per tonne, the afore-mentioned chemical company would improve their cash flow by £197,700 in addition to the £8,500 per annum savings previously mentioned per 100 batches.

The use of the model would also remove the need to determine the MWD's of samples other than syrup I and final syrup and the skilled analysts time who decides when it is justifiable to proceed to the next fractionation.

The other likely economic and operational benefits of using the mathematical model are given in Chapter 2.0.

C H A P T E R E L E V E N

CONCLUSIONS AND RECOMMENDATIONS FOR FUTURE WORK

11.0 CONCLUSIONS AND RECOMMENDATIONS FOR FUTURE WORK

11.1 CONCLUSIONS

During this research project the mathematical model (Chapter 5.0) based on the Boltzmann equation was tested on both the laboratory-scale and industrial-scale. The settling of dextran molecules on precipitation was also investigated on an industrial-scale.

In the laboratory-scale ethanol fractionation of dextran, the comparison of results on the first stage between the model predictions and experimental values is in very good agreement. On the second stage there is an offset present between the two comparable sets of results over the entire experimental range of values. The model predicting values that are approximately 10 Wt% higher than the experimental values.

To investigate the reason for the offset on the second stage more laboratory experiments were carried out with slight differences in their experimental procedures. Runs 13-18 were performed with the non-distillation of ethanol in the super IR; Fig. 7.2.19 shows that on the second stage an offset of similar magnitude is again present between the two sets of results. There was again no change in the offset for runs 30 and 31 when dextran T 110 (Pharmacia Lot No. 5404) was used instead of the plant batch RB 51K as syrup I.

The exceptionally good agreement between the laboratory-scale experimental results and the model predictions on the first stage is also shown by plots of the Boltzmann equation (see Section 7.5). For the first stage there is

good agreement between the C values obtained from the Boltzmann plots and model predictions. However there was no agreement between the two sets of E values for the second stage.

In the research field a great deal of emphasis is laid on the reproducibility of experimental results. In this research work the reproducibility of experimental results is excellent even though the experimental methods were slightly different in procedures; this can be seen by referring to runs 23,27; 24,28; 25,29; 30,31 and 32,33.

On the industrial-scale (Chapter 8.0) fractionation, plant batches RB 8L/40 - SL 17L/70 gave poor comparisons between the model predictions and the actual plant results. Possible explanations for the poor agreement between the model predictions and the actual plant results are given in Section 8.4.

For the second lot of plant batches RB 35L/40 - RB 59L/40, comparison of the model predictions with the actual plant results on the first fractionation (syrup IR St II) is reasonable. Comparison between the two sets of results on the second stage (final syrup) produced an off-set of approximately 8 Wt% over the entire range, the model again predicting higher values (see Fig. 8.3.18).

One of the disadvantages of these plant samples is that the Wt% dextran fractions are grouped together in their prospective regions. Fig. 8.3.18 shows that the Wt% syrup IR St II is grouped in the 5-20 Wt% region whereas the Wt% final syrup is grouped in the 60-80 Wt% region. This therefore makes a true comparison difficult over the

entire region. It would be very advantageous for the model if the plant samples syrup IR St II and final syrup were available, representing the entire Wt% region, so that a truly accurate comparison between the two sets of results could be made.

The settling behaviour of dextran molecules on precipitation was studied on three different plant batches (Chapter 9.0).

(i) Batch SL 28M/70 where settling of syrup IR St I was performed for 6 hours, Figs. 9.2.3-9.2.5 show that equilibrium had not been established at any one of the three depths in the set time. It was therefore necessary to allow a settling time of 24 hours for the remaining two batches.

(ii) For batch SL 36M/70 where settling of syrup IR St II was performed, equilibrium was established after approximately 13 hours at both depths (see Fig. 9.3.3). This is also supported by Figs. 9.3.4 and 9.3.5.

(iii) For batch RB 56M/40 where settling of syrup IR St I was performed, Figs. 9.4.3-9.4.5 show that equilibrium was established after only 6 hours at both depths. This seems to contradict the results of batch SL 28M/70 but it is important to remember that batch RB 56M/40 is aimed at producing a clinical dextran of 40,000 $\bar{M}_w$, whereas the batch SL 28M/70 was aimed at producing a clinical dextran of 70,000 $\bar{M}_w$. It should also be noted that the syrup I $\bar{M}_w$ value of batch SL 28M/70 is about twice the syrup I $\bar{M}_w$ value of batch RB 56M/40.

Bulk drawing of the syrup IR St I is made after 6 hours and the final drawing 2 hours later on the plant. This could explain some of the anomalies found in the model predictions that may have been caused by samples taken on the plant which had not settled to equilibrium, especially the sample super IR St I (see Section 8.4).

The current practice on the plant studied is to settle the stage I for 8 hours and stage II for 16 hours. It is proposed that stages I and II be left to settle for 11 hours each since two efficient fractionations would be better in removing traces of very high molecular weight material and producing a sharp 'cut off' than the current process.

The use of the mathematical model to predict the plant fractionation would have several advantages as mentioned in earlier chapters but above all it would improve the cash flow of a company producing 100 batches per annum by over £200,000 per annum.

11.2 RECOMMENDATIONS FOR FUTURE WORK

The future work on this project can be divided into the following four categories.

(a) More laboratory experiments can be carried out on the ethanol fractionation of dextran. These experiments could be of the following type:

(i) Temperature constant at 25°C, concentration and volumes of ethanol constant but with different starting dextran concentrations say 1%, 4%, 6% and 10% w/v.

(ii) Starting concentration of dextran constant at 8% w/v, concentration and volumes of ethanol constant but carried out at different temperatures say $35^{o}C$, $45^{o}C$ and $65^{o}C$.

(b) More plant batches with longer settling times allowed on the first stage could be used to test the model further.

(c) Different optimisation strategies could be attempted to maximise the benefits of using the model. For example, the yield could be maximised subject to product quality constraints (e.g. $\bar{M}_w$ = 40,000; <7.5% with molecular weight <12,000; <7.5% with molecular weight >98,000).

(d) The mathematical model could be modified for a triple fractionation so that it can be tested on the entire plant fractionation process with the optional IR stage II included.

APPENDICES

A P P E N D I X A1

COMPUTER PROGRAM FOR CALIBRATING THE ANALYTICAL COLUMNS

```
C     THIS PROGRAM CARRIES OUT THE CALIBRATION OF GEL-PERMEATION
C     CHROMATOGRAPHIC COLUMNS USING "BROAD" FRACTIONS OF KNOWN
C     WEIGHT AVERAGE MOLECULAR WEIGHTS.
C
      IMPLICIT DOUBLE PRECISION (A-H,O-Y)
      DOUBLE PRECISION M1,M2,KD,Z
      DIMENSION NY(32),M1(32),M2(32),
     CY(32,60),KD(32,60),SUM(32,5),
     CB(5),C(5),RO(5),R1(5),R2(5),
     CXMAT(25),Q(4),ZZ(4)
      READ (1,102) (B(K),K=1,5)
      READ (1,105) NNI
      WRITE (2,200)
      WRITE (2,255)
      WRITE (2,265) (K,B(K),K=1,5)
      WRITE (2,210)
      NP=0
      T=10000.0
      B(4)=B(4)-DLOG(T)
      B(5)=B(5)/T
      DO 30 I=1,11
      READ (1,110) M1(I),P,VO,VT,VE,VDE,DIFF,VM,YM,SD
      NY(I)=P
      READ (1,120) (Y(I,J),J=1,NY(I))
      WRITE(2,557)(Y(I,J),J=1,NY(I))
  557 FORMAT(84F0.0)
      M1(I)=M1(I)/T
      VP=VT-VO
      SY=0.0
      IF (DIFF.NE.0.0) YG=-1/(2*SD**2)
      DO 25 J=1,NY(I)
      IF (DIFF.EQ.0.0) GOTO 20
      IF (VE.EQ.VM) GOTO 20
      YA=YG*(VE-VM)**2
      YE=DLOG(Y(I,J)/YM)
      YE=YM*EXP(YA*YE/(YA-YE))
      IF (YE.LT.Y(I,J)) Y(I,J)=YE
   20 SY=SY+Y(I,J)
      KD(I,J)=(VE-VO)/VP
      VE=VE+VDE
      WRITE(2,765)SY,KD(I,J),VE
  765 FORMAT(3F20.6)
   25 CONTINUE
      DO 28 J=1,NY(I)
      Y(I,J)=Y(I,J)/SY
      WRITE(2,876)Y(I,J)
  876 FORMAT(F10.5)
   28 CONTINUE
      NP=NP+1
   30 CONTINUE
C
C     ITERATION PHASE
C
   32 IF (NNI.EQ.0) GOTO 85
```

```
   DO 34 K=1,3
34 ZZ(K)=K*10.0E10
   DO 80 NI=1,NNI
   DO 40 I=1,NP
   M2(I)=0.0
   DO 35 K=2,5
35 SUM(I,K)=0.0
   SUM(I,1)=1.0
   DO 40 J=1,NY(I)
   Z=DEXP(B(4)+B(1)*KD(I,J)+B(2)*KD(I,J)**2+B(3)*KD(I,J)**3)
   M2(I)=M2(I)+(B(5)+Z)*Y(I,J)
   SUM(I,2)=SUM(I,2)+Y(I,J)*Z
   SUM(I,3)=SUM(I,3)+Y(I,J)*Z*KD(I,J)
   SUM(I,4)=SUM(I,4)+Y(I,J)*Z*KD(I,J)**2
   SUM(I,5)=SUM(I,5)+Y(I,J)*Z*KD(I,J)**3
40 CONTINUE
   DO 45 K=1,5
   RO(K)=0.0
   DO 45 I=1,NP
45 RO(K)=RO(K)+(M1(I)-M2(I))/M1(I)**2*SUM(I,K)
   JK=0
   DO 50 K=1,5
   DO 50 J=1,5
   JK=JK+1
   XMAT(JK)=0.0
   DO 50 I=1,NP
   XMAT(JK)=XMAT(JK)+SUM(I,K)*SUM(I,J)/M1(I)**2
50 CONTINUE
   CALL MATINV (XMAT)
   JK=0
   DO 55 K=1,5
   R1(K)=0.0
   DO 55 J=1,5
   JK=JK+1
   R1(K)=R1(K)+RO(J)*XMAT(JK)
55 CONTINUE
   R2(5)=R1(1)
   R2(4)=R1(2)
   R2(1)=R1(3)
   R2(2)=R1(4)
   R2(3)=R1(5)
   DO 70 N=1,3
   Q(N)=0.0
   DO 60 K=1,5
   IF (N.EQ.1) C(K)=B(K)
   IF (N.EQ.2) C(K)=B(K)+0.5*R2(K)
60 IF (N.EQ.3) C(K)=B(K)+R2(K)
   DO 70 I=1,NP
   M2(I)=0.0
   DO 65 J=1,NY(I)
   Z=DEXP(C(4)+C(1)*KD(I,J)+C(2)*KD(I,J)**2+C(3)*KD(I,J)**3)
65 M2(I)=M2(I)+(C(5)+Z)*Y(I,J)
   Q(N)=Q(N)+((M1(I)-M2(I))/M1(I))**2
70 CONTINUE
```

```
   72 NII1=NI-1
      WRITE (2,25Ø) NII1,B(1),B(2),B(3),B(4),B(5),Q(1)
      Q(4)=Ø.5+Ø.25*(Q(1)-Q(3))/(Q(3)-2.Ø*Q(2)+Q(1))
      DO 75 K=1,5
   75 B(K)=B(K)+Q(4)*R2(K)
      DO 77 KK=2,4
      K=6-KK
   77 ZZ(K)=ZZ(K-1)
      ZZ(1)=SNGL(Q(1))
      IF (ZZ(4).NE.ZZ(3)) GOTO 8Ø
      IF (ZZ(3).NE.ZZ(2)) GOTO 8Ø
      IF (ZZ(2).NE.ZZ(1)) GOTO 8Ø
      NI=NI+1
      GOTO 85
   8Ø CONTINUE
C
C     FINAL RESULTS OUTPUT
C
   85 Q(1)=Ø.Ø
      DO 95 I=1,NP
      M2(I)=Ø.Ø
      DO 9Ø J=1,NY(I)
      Z=EXP(B(4)+B(1)*KD(I,J)+B(2)*KD(I,J)**2+B(3)*KD(I,J)**3)
   9Ø M2(I)=M2(I)+(B(5)+Z)*Y(I,J)
   95 Q(1)=Q(1)+((M1(I)-M2(I))/M1(I))**2
      NII1=NI-1
      WRITE (2,25Ø) NII1,B(1),B(2),B(3),B(4),B(5),Q(1)
      B(4)=B(4)+DLOG(T)
      B(5)=B(5)*T
   98 WRITE (2,26Ø)
      WRITE (2,265) (K,B(K),K=1,5)
      WRITE (2,27Ø)
      WRITE (2,275)
      DO 3 I=1,NP
      M1(I)=M1(I)*T
      M2(I)=M2(I)*T
    3 CONTINUE
      WRITE (2,28Ø) (M1(I),M2(I),I=1,NP)
      STOP
C
C     FORMAT STATEMENTS
C
  1Ø2 FORMAT (5FØ.Ø)
  1Ø5 FORMAT (I3)
  11Ø FORMAT (12FØ.Ø)
  12Ø FORMAT (14ØFØ.Ø)
  2ØØ FORMAT (' GPC CALIBRATION PROGRAM')
  21Ø FORMAT(//11X,'B1',8X,'B2',8X,'B3',8X,'B4',
     C8X,'B5',9X,'RES SS'/)
  25Ø FORMAT(I3,3X,5F1Ø.5,D15.6)
  255 FORMAT (//'    INITIAL VALUES OF CALIBRATION CONSTANTS :-')
  26Ø FORMAT (//'    FINAL VALUES OF CALIBRATION CONSTANTS :-')
  265 FORMAT (12X,'B',I1,'=',F11.3)
  27Ø FORMAT (//' COMPARISON OF MOLECULAR WEIGHTS:-')
```

```
  275 FORMAT (11X, 'MW(LS)',4X,'MW(GPC)')
  28Ø FORMAT (7X,F1Ø.Ø,1X,F1Ø.Ø)
      END
      SUBROUTINE MATINV (A)
C     MATRIX INVERSION ROUTINE
      DOUBLE PRECISION A,R,AA,AH
      DIMENSION A(25),L(5),M(5)
      R=1.Ø
      N=5
      NK=-N
      DO 8Ø K=1,N
      NK=NK+N
      L(K)=K
      M(K)=K
      KK=NK+K
      AA=A(KK)
      DO 2Ø J=K,N
      IJ=N*(J-1)
      DO 2Ø I=K,N
      II=IJ+I
      IF (DABS(AA).GE.DABS(A(II))) GOTO 2Ø
      AA=A(II)
      L(K)=I
      M(K)=J
   2Ø CONTINUE
      J=L(K)
      IF (J.LE.K) GOTO 35
      KI=K-N
      DO 3Ø I=1,N
      KI=KI+N
      JI=KI-K+J
      AH=-A(KI)
      A(KI)=A(JI)
   3Ø A(JI)=AH
   35 I=M(K)
      IF (I.LE.K) GOTO 45
      JJ=N*(I-1)
      DO 4Ø J=1,N
      JN=NK+J
      JI=JJ+J
      AH=-A(JN)
      A(JN)=A(JI)
   4Ø A(JI)=AH
   45 IF (AA.NE.Ø.Ø) GOTO 5Ø
      R=Ø.Ø
      GOTO 15Ø
   5Ø DO 55 I=1,N
      IF (I.EQ.K) GOTO 55
      IK=NK+I
      A(IK)=A(IK)/(-AA)
   55 CONTINUE
      DO 65 I=1,N
      IK=NK+I
      AH=A(IK)
```

```
      IJ=I-N
      DO 65 J=1,N
      IJ=IJ+N
      IF (I.EQ.K)GOTO 65
      IF (J.EQ.K)GOTO 65
      KJ=IJ-I+K
      A(IJ)=AH*A(KJ)+A(IJ)
   65 CONTINUE
      KJ=K-N
      DO 75 J=1,N
      KJ=KJ+N
      IF (J.EQ.K) GOTO 75
      A(KJ)=A(KJ)/AA
   75 CONTINUE
      R=R*AA
      A(KK)=1.Ø/AA
   8Ø CONTINUE
      K=N
  1ØØ K=K-1
      IF (K.LE.Ø.Ø) GOTO 15Ø
      I=L(K)
      IF (I.LE.K) GOTO 12Ø
      KK=N*(K-1)
      II=N*(I-1)
      DO 11Ø J=1,N
      JK=KK+J
      JI=II+J
      AH=A(JK)
      A(JK)=-A(JI)
      A(JI)=AH
  11Ø CONTINUE
  12Ø J=M(K)
      IF (J.LE.K) GOTO 1ØØ
      KN=K-N
      DO 13Ø I=1,N
      KN=KN+N
      JN=KN-K+J
      AH=A(KN)
      A(KN)=-A(JN)
      A(JN)=AH
  13Ø CONTINUE
      GOTO 1ØØ
  15Ø RETURN
      END
      FINISH
****
```

INPUT VARIABLES IN THE PROGRAM FOR CALIBRATING THE ANALYTICAL COLUMNS

B1,5	initial guess of the calibration constants
NNI	number of iterations
M1(I)	$\bar{M}_w$ of the sample by light-scattering
P	number of heights
VO	void volume
VT	total liquid volume
VE	elution volume at the start of a chromatogram
VDE	step-change in elution volume
DIFF	0.0
VM	elution volume at maximum height
YM	maximum height
SD	0.0
Y	height of chromatogram

A P P E N D I X A2

COMPUTER PROGRAM FOR CALCULATING THE AVERAGE MOLECULAR WEIGHTS AND MWD

```
1     DIM H(170),VIN(170),AMIN(170),S(170),S5(170)
2     PRINT"TYPE IN THE BATCH NUMBER"
3     INPUT KR$
4     PRINT"TYPE IN DATE"
5     INPUT K$
7     PRINT"TYPE IN NMAX,V0,VE1,VI,VT"
8     INPUT NMAX,D0,D1,D2,D3
9     PRINT"TYPE IN THE HEIGHTS"
10    FOR I=1 TO NMAX:INPUT H(I):NEXT I
20    GO SUB 1000:GO SUB 5000
25    OPEN1,4
26    OPEN2,4,1
27    OPEN3,4,2
28    F$="999 99999.999 9999999999. 9999.99 999999.999 9999.99"
29    PRINT#3,F$
30    PRINT#1,CHR$(1)"BATCH NUMBER";KR$
31    PRINT#1:PRINT#1
33    PRINT#1,CHR$(1)"DATE OF ANALYSIS";K$
34    PRINT#1:PRINT#1
35    PRINT#1,"FLOWRATE=";RATE
36    PRINT#1,"      V0=";D0
37    PRINT#1,"     VE1=";D1
38    PRINT#1,"      VI=";D2
39    PRINT#1,"      VT=";D3
40    PRINT#1
42    PRINT#1,"WEIGHT AVERAGE MOLECULAR WEIGHT=";AAAW
43    PRINT#1,"NUMBER AVERAGE MOLECULAR WEIGHT=";AVMN
44    PRINT#1,"                        Mw/Mn RATIO=";SPR
45    PRINT#1:PRINT#1:PRINT#1
50    HD$="POINT"+"      "+"KD VALUE"+"      "
51    GH$="MOL.WEIGHT"+"     "
52    FH$="HEIGHT"+"      "+"WGHT FRAC"+"  CUMM%"
53    EH$=HD$+GH$+FH$
54    PRINT#1,EH$
60    FOR I=NMAX TO 1 STEP -1
62    PRINT#2,I,VIN(I),AMIN(I),H(I),S(I),S5(I)
80    NEXT I
81    PRINT#1:PRINT#1:PRINT#1
82    PRINT#1,"ASTON GPC CALIBRATION CONSTANTS"
83    PRINT#1,"   B1=";B1
84    PRINT#1,"   B2=";B2
85    PRINT#1,"   B3=";B3
86    PRINT#1,"   B4=";B4
87    PRINT#1,"   B5=";B5
90    CLOSE1:CLOSE2:CLOSE3
100   END
663   OS$=OP$+OJ$
1000  RATE=57.000/D3
1010  VIE=D1*RATE
1020  VFE=D2*RATE
1030  VI=(VIE-28.586)/28.415
1040  VF=(VFE-28.586)/28.415
1050  VH=(VF-VI)/(NMAX-1)
1100  RETURN
```

```
5000 REM CALCULATE M.W.D.
5010 B1=-16.634:B2=21.702:B3=-16.606:B4=16.067:B5=87.798
5020 S1=0.0:S2=0.0:S3=0.0
5030 FOR I=1 TO NMAX
5040 VIN(I)=VI+VH*(I-1)
5050 IF VIN(I)>1.0 THEN 5080
5060 IF VIN(I)<0.0 THEN 5090
5065 AKIN(I)=B4+B1*VIN(I)+B2*(VIN(I)**2)+B3*(VIN(I)**3)
5070 AMIN(I)=B5+EXP(AKIN(I))
5072 GO TO 5100
5080 AMIN(I)=B5+EXP(B4+B1+B2+B3)
5085 GO TO 5100
5090 AMIN(I)=B5+EXP(B4)
5100 S1=S1+H(I):S2=S2+(AMIN(I)*H(I))
5110 S3=S3+(H(I)/AMIN(I)):NEXT I
5120 AAAW=S2/S1
5125 AVMN=S1/S3
5130 SPR=AAAW/AVMN
5180 PRINT"WEIGHT AVERAGE MOLECULAR WEIGHT=";AAAW
5190 PRINT"NUMBER AVERAGE MOLECULAR WEIGHT=";AVMN
5195 PRINT"                          Mw/Mn RATIO=";SPR
5200 S4=0.0
5210 FOR I=1 TO NMAX:S4=S4+H(I):NEXT I
5220 FOR I=1 TO NMAX:S(I)=H(I)*100/S4:NEXT I
5225 S5(NMAX+1)=0.0
5230 FOR I=NMAX TO 1 STEP -1
5235 S5(I)=S5(I+1)+S(I)
5240 NEXT I
5500 RETURN
```

INPUT VARIABLES IN THE PROGRAM FOR CALCULATING THE AVERAGE MOLECULAR WEIGHTS AND MWD

KR$	batch number
K$	date of analysis
NMAX	number of heights
DØ	elution time of high molecular weight dextran
D1	initial elution time of chromatogram
D2	final elution time of chromatogram
D3	elution time of glucose
H(I)	heights of chromatogram

A P P E N D I X A3

THE MATHEMATICAL MODEL PROGRAM

```
C     THIS PROGRAM CALCULATES THE WEIGHT PERCENTAGES
C     OF DEXTRANS PRESENT IN EACH PHASE AT THE END
C     OF THE ETHANOL FRACTIONATION USING THE OPTIMUM
C     VALUES OF THE MODEL PARAMETERS C,E,F,D AND P.
C
      READ(1,800)RUN
      WRITE(2,810)RUN
      CALL HOLMES(C,E,F,D)
      WRITE(2,890)
      WRITE(2,900)C,E,F,D
      READ(1,901)P,Q
      S=0.0
      T=0.0
 60   READ(1,902)AM,W
      IF (W.EQ.0.0) GO TO 80
      G=E*(AM**P)
      IF (G.LT.170.0) GO TO 61
      G=170.0
 61   A=D*EXP(G)*W
      B1=F+EXP(G)
      Y=C*(AM**Q)
      IF (Y.LT.170.0) GO TO 619
      Y=170.0
 619  R=D+EXP(Y)
      B=A/B1
      S=S+B/R
      T=T+W
      GO TO 60
 80   U=0.0
      V=0.0
 100  READ(5,902)AM,W
      IF (W.EQ.0.0) GO TO 180
      A=D*W
      Y=C*(AM**Q)
      IF (Y.LT.170.0) GO TO 140
      Y=170.0
 140  B=D+EXP(Y)
      U=U+(A/B)
      V=V+W
      GO TO 100
 180  SYRUP1R=100.0-(U/V)*100.0
      SUPER1R=(U/V)*100.0
      FINSYP=(S/T)*100.0
      FINSUP=((U/V)*100.0)-((S/T)*100.0)
      WRITE(2,903)SYRUP1R,SUPER1R,FINSYP,FINSUP
 800  FORMAT(1F0.0)
 810  FORMAT(22X,'DEXTRAN FRACTIONATION RUN NO :'F3.0,/,
     122X,'-----------------------------------',//)
 890  FORMAT(//,26X,'PARAMETERS ARE :',/)
 900  FORMAT(1H ,24X,' C = ',E15.8,//,
     125X,' E = ',E15.8,//,
     225X,' F = ',E15.8,//,
     325X,' D = ',E15.8,/////)
 901  FORMAT(2F0.0)
```

```
902  FORMAT(2F0.0)
903  FORMAT(15X,'FRACTIONATION REPORT FOR DEXTRAN AT ASTON',/,
    115X,'XXXXXXXXXXXXXXXXXXXXXXXXXXXXXXXXXXXXXXXXXX',////,
    228X,'%SYRUP1=100',/,
    333X,'I',/,
    420X,'-------------------------',/,
    520X,'I',25X,'I',/,
    613X,'%SYRUP1R=',F8.5,9X,'%SUPER1R=',F8.5,/,
    746X,'I',/,
    832X,'-------------------------',/,
    932X,'I',27X,'I',/,
    923X,'%FINAL SYRUP=',F8.5,6X,'%FINAL SUPER=',F8.5)
     STOP
     END
C
C    THIS PROGRAM CALCULATES THE OPTIMUM MODEL
C    PARAMETERS C,E,F,D AND P
C
     SUBROUTINE HOLMES(C1,E1,F1,D1)
   C PROGRAM TO USE SUBROUTINE VB01A
     IMPLICIT DOUBLE PRECISION (A-H,O-Z)
     DIMENSION X(100,10),AF(9),Y(100),W(100),Z(100),V(25),E(25)
     DIMENSION SF(15),A(15,15)
     COMMON //SF,IDVH
     READ(1,100) N, M, L, MAXFN
 100 FORMAT(5I0  )
     IA=M
     READ(1,110) (V(I), I = 1, M)
 110 FORMAT(20F0.0)
     READ(1,170) IWT
 170 FORMAT(1I0  )
     DO 777 LL = 1, N
     IF(IWT.EQ.0)  GO  TO  30
     READ(1,110) (X(LL,J), J = 1, L), Y(LL), W(LL)
     GO  TO  777
  30 READ(1,110) (X(LL,J), J = 1, L), Y(LL)
     W(LL)=1.0D00
 777 CONTINUE
     READ(1,170) IEC
     IF(IEC.EQ.0) GOTO 60
     READ(1,110) V(M+1), V(M+2)
  60 DO 20 I=1,M
     SF(I)=DABS(1.0D0/V(I))
  20 V(I)=V(I)*SF(I)
     WRITE(2,180)(X(1,J),J=1,L),Y(1),W(1)
     WRITE(2,180)(X(N,J),J=1,L),Y(N),W(N)
 180 FORMAT(1H0,8(D15.5,1X))
     CALL VB01A(X,Y,W,Z,N,V,E,M,L,A,IA,MAXFN)
     C1=V(1)
     E1=V(2)
     F1=V(3)
     D1=V(4)
     RETURN
     END
```

```
      SUBROUTINE MA1ØAD(A,B,M,NR,N,M1,IA,IB)
      IMPLICIT REAL*8(A-H,O-Z)
      DIMENSION A(IA,IA),B(IB,IA)
      IF(M-1)2Ø,41,42
   41 IF(A(1,1))9Ø,9Ø,43
   43 IF(M1)4Ø,37,4Ø
   4Ø A(1,1)=1.ØDØ/A(1,1)
      IF(NR)39,39,819
  819 DO 61 I=1,NR
   61 B(1,I)=B(1,I)*A(1,1)
      GO TO 2Ø
   37 IF(NR)39,39,15
   15 DO 62 I=1,NR
   62 B(1,I)=B(1,I)/A(1,1)
   39 GO TO 2Ø
   42 IF(M1)11,38,38
   38 MM1=M-1
      DO 44 I=1,MM1
      IP1=I+1
      DO 45 J=IP1,M
      A(I,J)=A(J,I)
   45 CONTINUE
   44 CONTINUE
      DO 1 I=1,M
      DO 6 J=I,M
      I1=I-1
      IF(I1)6,5,9
    9 IQA=IA*IA
      IQB=IQA
      CALL MCØ3AD(A,A,(I-1)*IA+1,(I-1)*IA+I1,(J-1)*IA+1,(J-1)
     2*IA+I1,A(I,J),A(I,J),I1,1,IQA,IQB)
    5 IF(J-I)6,7,8
    7 IF(A(I,I))9Ø,9Ø,93
   93 A(I,I)=DSQRT(A(I,I))
      GO TO 6
    8 A(I,J)=A(I,J)/A(I,I)
    6 CONTINUE
      IF(NR)1,1,99
   99 IF(M1)1,1Ø,1Ø
   1Ø DO 2 J=1,NR
      IF(I1)2,3,4
    4 IQA=IA*IA
      IQB=IB*IA
      CALL MCØ3AD(A,B,(I-1)*IA+1,(I-1)*IA+I1,(J-1)*IB+1,(J-1)
     2*IB+I1,B(I,J),B(I,J),I1,1,IQA,IQB)
    3 B(I,J)=B(I,J)/A(I,I)
    2 CONTINUE
    1 CONTINUE
      IF(NR)18,18,19
   19 DO 227 J=1,NR
      DO 127 I1=1,M
      I=M+1-I1
      IF(I1.EQ.1)GO TO 327
   28 IQA=IA*IA
```

```
      IQB=IB*IA
      CALL MCØ3AD(A,B,I*IA+I,(I+I1-2)*IA+I,(J-1)*IB+I+1,
     2(J-1)*IB+I+I1-1,B(I,J),B(I,J),I1-1,1,IQA,IQB)
  327 B(I,J)=B(I,J)/A(I,I)
  127 CONTINUE
  227 CONTINUE
   18 IF(M1)2Ø,2Ø,11
   11 DO 22 I=1,M
      A(I,I)=1.ØDØ/A(I,I)
   22 CONTINUE
      DO 24 I2=1,M
      I=M+1-I2
      I1=I+1
      DO 31 J2=1,I
      J=I+1-J2
      J1=J+1
      IF(I-J)2Ø,23,25
   23 W=A(I,I)
      IF(M-I)2Ø,32,26
   25 W=Ø.ØDØ
      IQA=IA*IA
      IQB=IQA
      CALL MCØ3AD(A,A,(J1-1)*IA+I,(I-1)*IA+I,(J1-1)*IA+J,
     2(I-1)*IA+J,W,W,I-J1+1,1,IQA,IQB)
   26 IQA=IA*IA
      IQB=IQA
      CALL MCØ3AD(A,A,(I-1)*IA+I1,(I-1)*IA+M,(I1-1)*IA+J,(M-1)
     1*IA+J,W,W,M-I1+1,1,IQA,IQB)
   32 A(I,J)=W*A(J,J)
   31 CONTINUE
   24 CONTINUE
      I1=M-1
      DO 29 I=1,I1
      J1=I+1
      DO 3Ø J=J1,M
      A(I,J)=A(J,I)
   3Ø CONTINUE
   29 CONTINUE
   2Ø N=Ø
   7Ø RETURN
   9Ø WRITE(2,91)
      N=1
      GO TO 7Ø
   91 FORMAT(32H MATRIX IS NOT POSITIVE DEFINITE)
      END
      SUBROUTINE MCØ3AD(A,B,KA1,KA2,KB1,KB2,C,S,N,IFLAG,IQA,IQB)
      DOUBLE PRECISION A,B,C,S,SUM
      DIMENSION A(IQA),B(IQB)
      KA=Ø
      KB=Ø
      IF(N.EQ.1) GO TO 6
      KA=(KA2-KA1)/(N-1)
      KB=(KB2-KB1)/(N-1)
    6 S=C
```

```
      IF(IFLAG.GT.1)S=-S
      IF(N.EQ.Ø) GO TO 8
      SUM=Ø.Ø
      DO 1Ø J=1,N
      IA=(J-1)*KA+KA1
      IB=(J-1)*KB+KB1
      SUM=SUM+A(IA)*B(IB)
   1Ø CONTINUE
      IF(IFLAG.EQ.1.OR.IFLAG.EQ.3)SUM=-SUM
      S=S+SUM
    8 RETURN
      END
      SUBROUTINE VBØ1A(X1,YY,WW,W,M,X,E,N,L,A,IA,MAXFN)
      IMPLICIT DOUBLE PRECISION (A-H,O-Z)
      DIMENSION XX(1ØØ),YY(M),WW(M),W(M),X(25),E(25),A(15,15)
      DIMENSION SF(15),C(15,15),X1(1ØØ, L), QQ(15)
      DIMENSION D(15),S(15),T(15),U(15),V(15),F(15),VV(15),
     1AA(15,15)
      COMMON //SF,IDVH
      NDF=M-N
      DF=FLOAT(NDF)
      RHO=.25DØ
      SIG=.75DØ
      Q=Ø.ØDØ
      QC=1.ØDØ
      SS=Ø.ØDØ
      DO 4 J=1,N
      V(J)=Ø.ØDØ
      DO 4 K=1,J
    4 A(J,K)=Ø.ØDØ
      IFL=Ø
      TSS=Ø.ØDØ
      TY=Ø.ØDØ
      TTY=Ø.ØDØ
      DO 97 I=1,M
   97 TY=TY+YY(I)
      DO 5 I=1,M
      DO 15Ø J=1,L
  15Ø XX(J)=X1(I,J)
      CALL DERIV(XX,X,F,FUNC,N,L)
      IF(IFL.EQ.Ø)GOTO3
      WRITE(2,1ØØØ)
 1ØØØ FORMAT('ØINITIAL DATA CAUSES IFL TO BE SET BY DERIV')
      RETURN
    3 SS=SS+WW(I)*(FUNC-YY(I))**2
      TSS=TSS+WW(I)*YY(I)*YY(I)
      TTY=TTY+WW(I)*(YY(I)-TY/M)**2
      DO 5 J=1,N
      V(J)=V(J)+WW(I)*(FUNC-YY(I))*F(J)
      DO 5 K=1,J
    5 A(J,K)=A(J,K)+WW(I)*F(J)*F(K)
      DO 6 J=1,N
      DO 6 K=1,J
    6 AA(J,K)=A(J,K)
```

```
      CALL MA1ØAD(AA,D,N,Ø,NR,1,15,1)
      DO 7 I=1,N
    7 E(I)=AA(I,I)/(DF*1.ØD2)
      IR=1
      IT=Ø
      DO 1Ø I=1,N
      D(I)=A(I,I)
      IF(D(I).LE.Ø.)D(I)=1.
   1Ø CONTINUE
      DO 18 I=1,N
   18 T(I)=DSQRT(D(I))
   2Ø CONTINUE
C     WRITE(2,1ØØ1)IT,IR
C1ØØ1 FORMAT('Ø',3Ø14)
C      WRITE(2,1ØØ2)SS
 1ØØ2  FORMAT(1X,8D15.7)
      DO 888 IQX = 1, N
      QQ(IQX)=X(IQX)/SF(IQX)
  888 CONTINUE
      WRITE(2,1ØØ2) (QQ(I), I = 1, N)
      WRITE(2,1ØØ2)(X(I),I=1,N)
      WRITE(2,1ØØ2)(V(I),I=1,N)
      IT=IT+1
      DO 31 I=1,N
      U(I)=A(I,I)
      IF(U(I).GE.Ø.ØDØ)GOTO31
      WRITE(2,1ØØ3) I,I
 1ØØ3 FORMAT('ØERROR IN A(',I3,',',I3,')')
      RETURN
   31 CONTINUE
   35 CONTINUE
      DO 36 I=1,N
      S(I)=V(I)
   36 A(I,I)=U(I)+Q*D(I)
      CALL MA1ØAD(A,S,N,1,NR,Ø,15,1)
      IF(NR.EQ.Ø)GOTO4Ø
      Q=2.ØDØ*Q
      IF(Q.EQ.Ø.ØDØ)Q=1.ØDØ
      GOTO35
   4Ø CONTINUE
      DO 37 I=1,N
   37 W(I)=S(I)
      CALL MCØ3AD(V,W,1,N,1,N,Ø.,VW,N,Ø,15,M)
      IF(VW.LE.Ø.ØDØ)GOTO87
      DO 42 I=1,N
      Z=U(I)*W(I)
      IF(I.GT.1) CALL MCØ3AD(A,W,I,(I-2)*15+I,1,I-1,Z,Z,I-1,
     1Ø,225,M)
      IF(I.LT.N)
     1CALL MCØ3AD(A,W,(I-1)*15+I+1,(I-1)*15+N,I+1,N,Z,Z,
     1N-I,Ø,225,M)
   42 S(I)=2.ØDØ*V(I)-Z
      CALL MCØ3AD(S,W,1,N,1,N,Ø.,DQ,N,Ø,15,M)
      JJ=Ø
```

```
      IFL=Ø
      DO 5Ø I=1,N
      IF(W(I)**2.GT.E(I)*SS/1.ØD4)JJ=JJ+1
      S(I)=X(I)
   5Ø X(I)=X(I)-W(I)
      SSP=Ø.ØDØ
      DO 5Ø1 J=1,N
      VV(J)=Ø.ØDØ
      DO 5Ø1 K=1,J
  5Ø1 AA(J,K)=Ø.ØDØ
      DO 5Ø2 I=1,M
      DO 16Ø J=1,L
  16Ø XX(J)=X1(I,J)
      CALL DERIV(XX,X,F,FUNC,N,L)
      IF(IFL.EQ.Ø)GOTO51
      Y=.1DØ
      DS=Ø.ØDØ
      GOTO52
   51 CONTINUE
      SSP=SSP+WW(I)*(FUNC-YY(I))**2
      DO 5Ø2 J=1,N
      VV(J)=VV(J)+WW(I)*(FUNC-YY(I))*F(J)
      DO 5Ø2 K=1,J
  5Ø2 AA(J,K)=AA(J,K)+WW(I)*F(J)*F(K)
      IR=IR+1
      DS=SS-SSP
      WRITE(2,4567) JJ,DQ
 4567 FORMAT(1HØ,I1Ø,D15.8)
      IF((JJ.EQ.Ø.OR.DQ.LE.Ø.ØDØ.OR.IR.GE.MAXFN).AND.DS.GE.RHO
     1*DQ)GOTO8Ø
      IF(DS.GE.RHO*DQ)GOTO6Ø
      Y=.5DØ
      Z=2.ØDØ*VW-DS
      IF(Z.GT.Ø.ØDØ)Y=VW/Z
      IF(Y.GT..5DØ)Y=.5DØ
      IF(Y.LT..1DØ)Y=.1DØ
   52 CONTINUE
      IF(Q.NE.Ø.ØDØ)GOTO58
      Y=2.ØDØ*Y
      DO 521 I=1,N
  521 A(I,I)=1.ØDØ/A(I,I)
      DO 522 I=2,N
      II=I-1
      DO 522 J=1,II
      CALL MCØ3AD(A,A,(J-1)*15+J,(I-2)*15+J,(I-1)*15+J,(I-1)
     1*15+I-1,Ø.ØDØ,Z,I-J,3,225,225)
  522 A(J,I)=Z*A(I,I)
      DO 533 I=1,N
      DO 53 J=I,N
      CALL MCØ3AD(A,A,(J-1)*15+I,(N-1)*15+I,(J-1)*15+J,(N-1)
     1*15+J,Ø.ØDØ,Z,N-J+1,Ø,225,225)
   53 A(I,J)=ABS(Z)
  533 E(I)=A(I,I)/(DF*1ØØ.)
      Q=Ø.ØDØ
```

```
      TR=Ø.ØDØ
      DO 54 I=1,N
      TR=TR+A(I,I)*D(I)
      Z=Ø.ØDØ
      DO 55 J=1,I
   55 Z=Z+A(J,I)*T(J)
      IF(I.EQ.N)GOTO56
      II=I+1
      DO 57 J=II,N
   57 Z=Z+A(I,J)*T(J)
   56 CONTINUE
      Z=Z*T(I)
      IF(Z.GT.Q)Q=Z
   54 CONTINUE
      IF(TR.LT.Q)Q=TR
      Q=1.ØDØ/Q
      QC=Q
   58 CONTINUE
      Q=Q/Y
      IF(DS.GT.Ø.ØDØ)GOTO7Ø
      DO 59 I=1,N
   59 X(I)=S(I)
      GOTO35
   6Ø CONTINUE
      IF(DS.LE.SIG*DQ)GOTO7Ø
      Q=Q*.5DØ
      IF(Q.LT.QC)Q=Ø.ØDØ
   7Ø CONTINUE
      SS=SSP
      DO 72 I=1,N
      V(I)=VV(I)
      DO 72 J=1,I
   72 A(I,J)=AA(I,J)
      GOTO2Ø
   8Ø CONTINUE
      IF(DS.LE.Ø.ØDØ)GOTO83
      SS=SSP
      DO 81 I=1,N
      V(I)=VV(I)
      DO 81 J=1,I
   81 A(I,J)=AA(I,J)
      GOTO84
   83 CONTINUE
      DO 85 I=1,N
   85 X(I)=S(I)
   87 CONTINUE
      DO 86 I=1,N
   86 A(I,I)=U(I)
   84 CONTINUE
C     WRITE(2,1ØØ1)IT,IR
C     WRITE(2,1ØØ2)SS
C     WRITE(2,1ØØ2)(X(I),I=1,N)
C     WRITE(2,1ØØ2)(V(I),I=1,N)
      DO 9Ø I=1,M
```

```
      DO 17Ø J=1,L
 17Ø XX(J)=X1(I,J)
  9Ø CALL DERIV(XX,X,F,W(I),N,L)
      CALL MA1ØAD(A,D,N,Ø,NR,1,15,1)
      VAR=SS/DF
      SEST=DSQRT(VAR)
      CF=TY*TY/M
      RSQ=(TSS-SS)/TSS
      RSQ1=(TTY-SS)/TTY
      DO 91 I=1,N
      DO 92 J=1,N
  92 A(I,J)=A(I,J)*VAR
  91 E(I)=DSQRT(A(I,I))
      WRITE(2,2ØØØ)
2ØØØ FORMAT(1HØ,4X,1HI,1ØX,'V(I)',16X,'S.E. OF V(I)',//)
      DO 93 I=1,N
      X(I)=X(I)/SF(I)
      E(I)=E(I)/SF(I)
  93 WRITE(2,2Ø01)I,X(I),E(I)
2Ø01 FORMAT(1X,I5,2D2Ø.8)
      WRITE(2,2Ø02)SS,NDF,SEST
2Ø02 FORMAT(///,1X,'RESIDUAL SUM OF SQUARES=',D16.8,//
     11X,'DEGREES OF FREEDOM=',I4,//
     11X,'S.E. OF RESIDUAL.=',D16.8,//)
      WRITE(2,7Ø03) TSS,RSQ,RSQ1
7Ø03 FORMAT(1H ,'UNCORRECTED SUM OF SQUARES IS',D15.6/1X,
     2'R-SQUARED IS',F8.4/1X,'R-SQUARED ABOUT MEAN IS',F8.4//1X,
     3'CORRELATION MATRIX',//)
      DO 99 I=1,N
      DO 99 J=1,N
  99 C(I,J)=A(I,J)/DSQRT(A(J,J))/DSQRT(A(I,I))
      CALL OAØ1A(C,N,N,15)
      IF(L.GT.3) L=3
      WRITE(2,2Ø03)(I,I=1,L)
2Ø03 FORMAT(8X,'OBS Y',1ØX,'FITTED Y',11X,'X',I1,15X,'X',I1,
     115X,'X',I1)
      WRITE(2,2Ø05)
2Ø05 FORMAT(1HØ)
      DO 94 I=1,M
      IF(IDVH.EQ.1)WRITE(9,1958)YY(I),W(I),(X1(I,J),J=1,L)
  94 WRITE(2,2Ø04)YY(I),W(I),(X1(I,J),J=1,L)
1958 FORMAT(G19.1Ø)
2Ø04 FORMAT(5D16.5)
      RETURN
      END
      SUBROUTINE OAØ1A(A,M,N,IA)
      IMPLICIT REAL*8(A-H,O-Z)
      DIMENSION A(1ØØ)
C     INITIALISE MATRIX COUNT.
      INTEGER * 4 IM
      DATA IM/Ø/
      IM=IM+1
      IP=1
      J3=(N-1)/6+1
```

```
      DO 101 J=1,J3
      J1=6*J-5
      J2=6*J
      IF(J2-N)6,6,7
    7 J2=N
    6 IP=IP+1
      WRITE(2,4)(J4,J4=J1,J2)
    4 FORMAT (6I11)
      WRITE(2,3)
    3 FORMAT (1X)
      M1=1
      M2=1
      M3=0
      DO 1 I=1,M
      K1=IA*(J1-1)+I
      K2=IA*(J2-1)+I
      WRITE(2,5)I,(A(K),K=K1,K2,IA)
    5 FORMAT (I5,6F11.5)
      IF (M1-6)9,10,9
   10 WRITE(2,8)
    8 FORMAT (1X)
      M1=0
    9 IF (M2-30)11,12,11
   12 IF (M2-M) 13,1,1
   13 WRITE(2,4)(J4,J4=J1,J2)
      IP=IP+1
      M2=0
   11 M1=M1+1
      M2=M2+1
    1 CONTINUE
  101 CONTINUE
      RETURN
      END
C  TO CALL USER SUBROUTINE AND CALCULATE PARTIAL DERIVATIVES
      SUBROUTINE DERIV(X,V,F,Z,M,L)
      IMPLICIT DOUBLE PRECISION(A-H,O-Z)
      DIMENSION X(L),V(15),F(M),SF(15),VU(15)
      COMMON SF
      DO 20 I=1,M
   20 VU(I)=V(I)/SF(I)
      Z=FUNC(X,VU)
      C=.0000001
      DO 10 J=1,M
      H=C/SF(J)
      VU(J)=VU(J)+H
      Z1=FUNC(X,VU)
      F(J)=(Z1-Z)/H
      F(J)=F(J)/SF(J)
C     WRITE(2,100) Z,Z1,H,SF(J),F(J)
C 100 FORMAT(1H ,6D24.16)
   10 VU(J)=VU(J)-H
      RETURN
      END
C
```

```
C
      DOUBLE PRECISION FUNCTION FUNC(X,P)
      IMPLICIT DOUBLE PRECISION (A-H,O-Z)
      DIMENSION X(2), P(5)
      G=P(2)*DEXP(1.ØDØ*DLOG(X(1)))
      IF(G.GT.7Ø.ØDØ)  G=7Ø.ØDØ
      IF(G.LT.-7Ø.ØDØ)  G=-7Ø.ØDØ
      H=P(1)*DEXP(1.ØDØ*DLOG(X(1)))
      IF(H.GT.7Ø.ØDØ)   H=7Ø.ØDØ
      IF(H.LT.-7Ø.ØDØ)  H=-7Ø.ØDØ
      A=DEXP(G)
      C=P(3)+DEXP(G)
      D=P(4)+DEXP(H)
      FUNC=(P(4)*A*X(2))/(P(5)*C*D)
      RETURN
      END
C
C
      FINISH
```

INPUT VARIABLES IN THE MATHEMATICAL MODEL PROGRAM

RUN	experimental run number
N	number of data points to optimise
M	number of parameters
L	number of independent variables
MAXFN	maximum number of iterations
V(I)	initial guesses of the parameters
IWT	0
X(LL,J)	molecular weight and weight fraction of original sample
Y(LL)	weight fraction of final sample
IEC	0
P	1.0
Q	1.0
AM	molecular weight of original sample
W	weight fraction of original sample

A P P E N D I X A4

DATA STORING PROGRAM FOR THE ANALYTICAL COLUMNS

```
1Ø   DIM A(4ØØ),Z(5)
6ØØØ I=1:T1=TI:Y=1
6Ø1Ø GO SUB 7ØØØ
6Ø2Ø E=TI-T1
6Ø3Ø IF E<12Ø THEN 6Ø2Ø
6Ø4Ø IF Y=5 THEN 6Ø9Ø
6Ø5Ø Y=Y+1:T1=TI
6Ø6Ø GO TO 6Ø1Ø
6Ø9Ø T1=TI
61ØØ A(I)=Z(I)+Z(2)+Z(3)+Z(4)+Z(5))/5
61Ø5 PRINT"READING";I/6;"=";A(I),A(I)/4
651Ø IF I<36Ø THEN 675Ø
655Ø FOR Q=156 TO I
656Ø OPEN 1,4,1
657Ø OPEN 2,4,2
658Ø F$="9999.99      S9999.99         S9999.99"
659Ø PRINT#2,F$
66ØØ PRINT#1,Q/6,A(Q),A(Q)/4
661Ø CLOSE1:CLOSE2
662Ø NEXT Q
665Ø END
675Ø Y=1.Ø:I=I+1
676Ø GO TO 6Ø1Ø
7ØØØ OPEN 1,9,1
7Ø1Ø GET#1,J$,K$
7Ø2Ø IF K$="" THEN K=-224:GO TO 7Ø4Ø
7Ø3Ø K=ASC(K$)-224
7Ø4Ø IF K<Ø THEN D=(K+32)*-1
7Ø5Ø IF K>=Ø THEN D=K
7Ø6Ø D=D*256
7Ø7Ø IF J$="" THEN J=Ø:GO TO 7Ø9Ø
7Ø8Ø J=ASC(J$)
7Ø9Ø IF K<Ø THEN J=J*-1
71ØØ Z(Y)=J+D
71Ø5 PRINT Z(Y),Z(Y)/4
711Ø CLOSE1
712Ø RETURN
```

A P P E N D I X A5

COMPUTER PROGRAM FOR CALCULATING THE MWD's PREDICTED BY THE MATHEMATICAL MODEL

```
1     DIM AM(1ØØ),W(1ØØ)
2     DIM U3(1ØØ),U4(1ØØ),V5(1ØØ),V2(1ØØ)
3     DIM U(1ØØ),U1(1ØØ),V(1ØØ),V1(1ØØ)
1Ø    I=1
15    PRINT"TYPE IN M.W."
2Ø    INPUT AM(I)
3Ø    PRINT"TYPE IN WGT"
4Ø    INPUT W(I)
45    IF W(I)=Ø.Ø THEN 6Ø
5Ø    I=I+1
55    GO TO 15
6Ø    OPEN 1,4
65    PRINT#1:PRINT#1:PRINT#1
7Ø    PRINT#1," M.W  SYR.I SYR.IR  SUP.IR  FIN.SUP  FIN.SYR"
75    CLOSE1
8Ø    PRINT"TYPE IN C,D,E,F,P,Q,WSU,WFSY"
85    INPUT C,D,E,F,P,Q,WSU,WFSY
86    S=Ø.Ø:S1=Ø.Ø:S2=Ø.Ø:S3=Ø.Ø
9Ø    FOR J=1 TO I
95    Y=C*(AM(J)**Q)
1ØØ   IF Y<75 THEN 11Ø
1Ø5   Y=75
11Ø   R=((D+EXP(Y))*WSU)
115   A1=D*W(J)
13Ø   G=E*(AM(J)**P)
135   IF G<75 THEN 145
14Ø   G=75
145   A=D*EXP(G)*W(J)
15Ø   B1=(F+EXP(G))*WFSY
155   B2=(D+EXP(Y))
156   V3=A/B1
16Ø   V5(J)=V3/B2
161   U3(J)=A1/R
162   U4(J)=(W(J)-(WSU*U3(J)))/(1-WSU)
163   V2(J)=((WSU*U3(J))-(WFSY*V5(J)))/(WSU-WFSY)
164   S=S+U3(J)
165   S1=S1+U4(J)
166   S2=S2+V5(J)
167   S3=S3+V2(J)
168   NEXT J
169   FOR J=1 TO I
17Ø   U(J)=(U3(J)/S)*1ØØØ
171   U1(J)=(U4(J)/S1)*1ØØØ
172   V(J)=(V5(J)/S2)*1ØØØ
173   V1(J)=(V2(J)/S3)*1ØØØ
19Ø   OPEN 2,4,1
195   OPEN 3,4,2
2ØØ   PRINT#3,"9999999.9 9999.99 9999.99 9999.99 9999.99 9999.99"
2Ø5   PRINT#2,AM(J),W(J),U1(J),U(J),V1(J),V(J)
21Ø   CLOSE2:CLOSE3
22Ø   NEXT J
23Ø   OPEN 1,4
24Ø   PRINT#1:PRINT#1:PRINT#1
25Ø   PRINT#1,"  C*1Ø**Ø5   D   E*1Ø**Ø5  F  "
```

```
260  C=INT(C*100000000+0.5)/1000
265  E=INT(E*100000000+0.5)/1000
270  D=INT(D*1000+0.5)/1000
275  F=INT(F*1000+0.5)/1000
280  OPEN 2,4,1
285  OPEN 3,4,2
290  PRINT#3,"  9999.999 9999999.999 9999999.999 9999999.999"
300  PRINT#2,C,D,E,F
310  CLOSE1:CLOSE2:CLOSE3
```

INPUT VARIABLES IN THE PROGRAM FOR CALCULATING THE MWD's PREDICTED BY THE MODEL

AM(I)	molecular weight of original sample
W(I)	weight fraction of original sample
C	mathematical model constant (predicted)
D	mathematical model constant (predicted)
E	mathematical model constant (predicted)
F	mathematical model constant (predicted)
P	1.0
Q	1.0
WSU	Wt% of super IR
WFSY	Wt% of final syrup

NOMENCLATURE

NOMENCLATURE

a	calibration constant in equation 3.3.11
$\bar{a}_1$	mean of the large parent group
$\bar{a}_2$	mean of the sample measurement
A	constant in equation 3.1.3
A_s	asymmetry factor
b	calibration constant in equation 3.3.11
$b_{1,5}$	calibration constants in equation 3.3.16
B	constant in equation 3.1.3
B_1	constant in equation 3.1.30
B_2	constant in equation 3.1.30
C	mathematical model constant
C_1	concentration of polymer in bottom phase
C_2	concentration of polymer in top phase
D	mathematical model constant
$\bar{D}$	polydispersity
E	difference in potential energy
E	mathematical model constant
F	mathematical model constant
$\overline{\Delta G_i}$	partial molal free energy of mixing of the ith fraction of the polymer
$\overline{\Delta G_1}$	partial molal free energy of mixing of the solvent
$\overline{\Delta G_2}$	partial molal free energy of mixing of the polymer
h_i	normalised chromatogram heights
h_i'	chromatogram heights
HETP	height of an equivalent theoretical plate
k	molecular weight dependence coefficient
K	Boltzmann constant
K_d	distribution coefficient
L	length of packed column

L.S.	light-scattering
m_b	mass of dextrans in syrup IR
m_f	mass of dextrans in final syrup
m_o	mass of dextrans in starting solution
m_s	mass of dextrans in final super
m_t	mass of dextrans in super IR
m_{ib}	mass of species i in syrup IR
m_{if}	mass of species i in final syrup
m_{io}	mass of species i in starting solution
m_{is}	mass of species i in final super
m_{it}	mass of species i in super IR
M	molecular weight
M_i	molecular weight of species i
$\bar{M}_N$	number average molecular weight
$\bar{M}_w$	weight average molecular weight
n	number of measurements in sample group
n_i	number of molecules of M_i
N	number of theoretical plates
N_o	Avogadro's constant
p	concentration dependence of μ
P	mathematical model constant
r	Stokes' radius
R	gas constant
R.S.S.	residual sum of squares
s.d.	standard deviation
S	residual sum of squares
t	Student's t value
T	temperature
V_b	volume of syrup IR dextran solution

V_f	volume of final syrup dextran solution
V_i	pore volume
V_i	volume fraction of the ith fraction of the polymer
V_{iAcc}	pore volume accessible to the species
V_n	hydrodynamic volume
V_o	void volume
V_o	volume of original dextran solution
V_R	elution or retention volume
V_s	volume of final super dextran solution
V_t	total liquid volume
V_t	volume of super IR dextran solution
V_2	volume fraction of all polymer molecules
W	weight fraction
W_b	baseline width
Wt%	weight percentage
$W_{\frac{1}{2}}$	peak width at one-half the peak height
W_i	weight of molecules of M_i
x	ratio of the molecular volumes of polymer molecule and solvent
$\bar{x}_n$	number average molecular size
β	correlation coefficient
γ^*	critical liquid composition
γ	Simha constant
$\{\eta\}$	intrinsic viscosity
λ	energetic parameter
μ	polymer/solvent interaction parameter
μ_o	constant in equation 3.1.22
μ_{oo}	constant in equation 3.1.27
μ_{ib}	weight fraction of species i in the syrup IR

μ_{io} weight fraction of species i in the original solution

μ_{if} weight fraction of species i in the final syrup

μ'_{if} weight fraction of species i in the final syrup from GPC analysis

μ_{is} weight fraction of species i in the final super

μ_{it} weight fraction of species i in the super IR

σ partition coefficient

σ standard deviation of the peak

ϕ number of peaks resolved in a column

REFERENCES

REFERENCES

1. Thoren, L., Dextran as a Plasma Substitute, Blood Substitutes and Plasma Expanders. Progress in Clinical and Biological Research, Vol.19, Alan R. Liss, Inc. (1978), 265-282.

2. Martin, L.E., Dextran: A Plasma Volume Expander, Chemistry and Industry, 8, (1955), 184-191.

3. Foster, F.H., Dextran - Manufacture and Use, Part 1, Process Biochemistry, Feb.1968, 15-19.

4. Foster, F.H., Dextran - Manufacture and Use, Part 2, Process Biochemistry, March 1968, 55-62.

5. Atik, M., Dextran 40 and Dextran 70, Arch Surg., 94, (1967), 664-671.

6. Maycock, W., Ricketts, C.R., Stability of Dextran During Prolonged Storage, Nature (London), 213, (1967), 88.

7. Hehre, E.J., Studies on the Enzymatic Synthesis of Dextran from Sucrose, Jou. of Biol. Chem., 163, (1946), 221-233.

8. Ingelman, B., Chemistry of Dextrans and Some Dextran Products. Acta.Acad.Regiae Sci., 12, (1969), 9-23.

9. Kobayashi, M., Shishido, K., Kikuchi, T., Fractionation of the Leuconostoc Mesenteroides NRRL B-1299 Dextran and Preliminary Characterisation of the Fractions. Agr.Biol.Chem., 37(2), (1973), 357-365.

10. Nemes-Namasi, E., Investigation of the Structure of Dextrans by Physical Methods Infrared Spectroscopic Investigations, Acta Biologica Debrecina, 5, (1967), 67-70.

11. Senti, F.R., Hellman, N.N., Ludwig, N.H., Babcock, G.E., Tobin, R., Glass, C.A., Lamberts, B.L., Viscosity, Sedimentation and Light-Scattering Properties of Fractions of an Acid-Hydrolysed Dextran, Jou. of Poly.Sci., 17, (1955), 527-546.

12. Jeanes, A., Haynes, W.C., Wilham, C.A., Rankin, J.C., Melvin, E.H., Marjorie, J.A., Cluskey, J.E., Fisher, B.E., Tsuchiya, H.M., Rist, C.E., Characterisation and Classification of Dextrans from Ninety-Six Strains of Bacteria, Jou.Am.Chem.Soc., 76, (1954), 5041-5052.

13. Jeanes, A., Haynes, W.C., Wilham, C.A., Characterisation of Dextrans from Four Types of Leuconostoc Mesenteroides. Jou. Bacteriol., 71, (1956), 167-173.

14. Nilsson, K., Söderlund, G., Clinical Dextrans. Specifications and Quality of Preparations on the Market, Acta Pharm.Suec., 15, (1978), 439-454.

15. Bixler, G.H., Hines, G.E., McGhee, R.M. Shurter, R.A., Dextran, Ind. and Eng.Chem., 45(4), (1953), 692-705.

16. Wolff, I.A., Mehltretter, C.L., Mellies, R.L., Watson, P.R., Hofreiter, B.T., Patrick, P.L., Rist, C.E., Production of Clinical-Type Dextran, Ind. and Eng.Chem., 46(2), (1954), 370-377.

17. Wolff, I.A., Mellies, R.L., Lohmar, R.L., Hellman, N.N., Rogovin, S.P., Watson, P.R., Sloan, J.W., Hofreiter, B.T., Fisher, B.E., Rist, C.E., Production of Clinical Type Dextran, Ind. and Eng.Chem., 46(2), (1954), 2605-2610.

18. Granath, K.A., Solution Properties of Branched Dextrans, Jou. of Colloid Sci., 13, (1958), 308-328.

19. Booth, G.C., Gold, V., Molecular Weight Studies of Dextran, Jou.Chem.Soc., (1956), 3380-3385.

20. Zief, M., Brunner, G., Metzendorf, J., Fractionation of Partially Hydrolysed Dextran, Ind. and Eng.Chem., 48(1), (1956), 119-121.

21. Zebec, M., Dezelic, G., Dezelic, N., Kratohvil, J.P., Schulz, K.F., Physicochemical Studies of Dextran. I. Characterisation of Clinical Samples, Croatica Chemical Acta, 36, (1964), 13-26.

22. Gibbs, R., Fisons Pharmaceutical Division, Holmes Chapel, Cheshire, Personal Communication.

23. Moore, J.C., Gel Permeation Chromatography I. A New Method for Molecular Weight Distribution of High Polymers, Jou.Poly.Sci., A(2), (1964), 835-843.

24. Alsop, R.M., Byrne, G.A., Done, J.N., Earl, I.E., Gibbs, R., Quality Assurance in Clinical Dextran Manufacture by Molecular Weight Characterisation, Proc.Biochem., Dec.1977, 15-22.

25. Snyder, L.R., Kirkland, J.J., Introduction to Modern Liquid Chromatography. John Wiley and Sons, New York (1974).

26. Gidding, J.C., Maximum Number of Components Resolvable by Gel Filtration and Other Elution Chromatographic Media, Anal Chem., 39, (1967), 1027-1028.

27. Granath, K.A., Kvist, B.E., Molecular Weight Distribution Analysis by Gel Chromatography on Sephadex, Jou. of Chromatography, 28, (1967), 69-81.

28. Laurent, T.C., Granath, K.A., Fractionation of Dextran and Ficoll by Chromatography on Sephadex G-100, Biochim. Biophys. Acta, 136, (1967), 191-198.

29. Epton, R., Holloway, C., McLaren, J.V., Characterisation of Cross-Linked Poly (Accrylomorphines) as Matrices for Aqueous GPC,, Jou. of Chromatography, 90, (1974), 249-258.

30. Hagel, L., Comparison of Some Soft Gels for the Molecular Weight Distribution Analysis of Dextran, Jou. of Chromatography, 160, (1978), 59-71.

31. Bombaugh, K.J., Dark, W.A., King, R.N., Gel Permeation Chromatography: New Applications and Techniques. Jou. of Poly.Sci., Part C., 21, (1968), 131-142.

32. Kuga, S., New Cellulose Gel for Chromatography, Jou. of Chromatography, 195, (1980), 221-230.

33. England, K., A Comparison of Batch and Continuous Chromatography Equipment for the Separation of Organic Mixtures, Ph.D. Thesis, University of Aston in Birmingham, U.K., (1979).

34. Barker, P.E., Properties Associated with the Column Packings Used in the Characterisation of Dextran by Aqueous GPC., Jou. of Chromatography, 174, (1979), 143-151.

35. TSK-Gel, Technical Data Bulletin, Toyo Soda Manufacturing Co. Ltd., Tokyo, Japan, Toyo-Soda Publication (1980).

36. Barker, P.E., Hatt, B.W., Vlachogiannis, G.J., Suitability of TSK-Gel Toyopearl Packing for Gel Permeation Chromatographic Analysis of Dextran, Jou. of Chromatography, 208, (1981), 74-77.

37. Vlachogiannis, G.J., Dextran Polymer Fractionation by Production Scale Chromatography and Ultrafiltration, Ph.D. Thesis, University of Aston in Birmingham, U.K., (1982).

38. Hashimoto, T., Sasaki, H., Aiura, M., Kato, Y., High Speed Aqueous Gel Permeation Chromatography, Jou.Polym.Sci.Polym.Phys.Ed., 16, (1978), 1789-1800.

39. Kato, Y., Sasaki, H., Aiura, M., Hashimoto, T., High Performance Aqueous Gel Permeation Chromatography of Oligomers, Jou. of Chromatography, 153, (1978), 546-549.

40. Hashimoto, T., Sasaki, H., Aiura, M., Kato, Y., High Speed Aqueous Gel Permeation Chromatography of Proteins, Jou. of Chromatography, 160, (1978), 301-305.

41. Kato, Y., Komiya, K., Sasaki, H., Hashimoto, T., Comparison of TSK-Gel PW Type and SW Type in High Speed Aqueous Gel Permeation Chromatography, Jou. of Chromatography, 193, (1980), 311-317.

42. Kuga, S., Pore Size Distribution Analysis of Gel Substances by Size Exclusion Chromatography, Jou. of Chromatography, 206, (1981), 449-454.

43. Himmel, M.E., Squire, P.G., High Performance Size Exclusion Chromatography of Sea Warm Chlorocruorin on a TSK G5000 PW Preparative Column, Jou. of Chromatography, 210, (1981), 443-452.

44. De Vries, A.J., Le Page, M., Beau, R., Guillemin, C.L., Evaluation of Porous Silica Beads as a New Packing Material for Chromatographic Columns, Anal.Chem., 39, (1967), 935-939.

45. Barker, P.E., Barker, S.A., Hatt, B.W., Somers, P.J., Separation by Continuous Chromatography, Chem. and Process Eng., Jan. 1971, 1-3 (Reprint).

46. Barker, P.E., Ellison, F.J., Hatt, B.W., A New Process for the Continuous Fractionation of Dextran, Ind.Eng.Chem.Process Des.Dev., 17, (1978), 302-309.

47. Barker, P.E., Hatt, B.W., Williams, A.N., Fractionation of a Polymer Using a Preparative-Scale Continuous Chromatography, Chromatographia, 11, (1978), 487-493.

48. Williams, A.N., Fractionation and Separation by Continuous Liquid-Liquid Chromatography, Ph.D. Thesis, University of Aston in Birmingham, U.K. (1977).

49. Buytenhuys, F.A., Van der Maeden, F.P.B., Gel Permeation Chromatography on Unmodified Silica Using Aqueous Solvents, Jou. of Chromatography, 149, (1978), 489-500.

50. Vermont, J., Deleuil, M., De Vries, A.J., Guillemin, C.L., Modern Liquid Chromatography on Spherosil, Anal.Chem., 47, (1975), 1329-1337.

51. Le Page, M., Beau, R., De Vries, A.J., Evaluation of Analytical Gel Permeation Chromatography Columns Packed with Porous Silica Beads, Jou.Polym.Sci., Part C, 21, (1968), 119-130.

52. Beau, R., Le Page, M., De Vries, A.J., Exclusion Chromatography Using Columns Packed with Silica Beads, Appl.Polym.Sympos., 8, (1969), 137-155.

53. Cooper, A.R., Barrall, E.M., Gel Permeation Chromatography: Physical Characterisation and Chromatographic Properties of Porasil, Jou.Appl. Polym.Sci., 17, (1973), 1253-1268.

54. Bombaugh, K.J., Dark, W.A., Little, J.N., Fractionation of Polyvinyl Alcohol and Deactivated Porous Silica Beads by Gel Permeation Chromatography, Anal.Chem., 41, (1969), 1337-1339.

55. Dintzis, F.R., Tobin, R., Molecular Sieve Chromatography of Amylose and Dextran Over Porous Glass, Jou. of Chromatography, 88, (1974), 77-85.

56. Omorodion, S.N.E., Hamielec, A.E., Brash, J.L., Optimisation of Peak Separation and Broadening in Aqueous GPC Dextrans, Jou.Liq.Chromatogr., 4, (1981), 41-50.

57. Basedow, A.M., Ebert, K.H., Ederer, H.J., Fosshag, E., Fractionation of Polymer by Gel Permeation Chromatography: An Experimental and Theoretical Approach, Jou. of Chromatography, 192, (1980), 259-274.

58. Basedow, A.M., Ebert, K.H., Production, Characterisation and Solution Properties of Dextran Fractions of Narrow Molecular Weight Distributions, Jou.Polym. Sci.Polym.Sympos., 66, (1979), 101-115.

59. Haller, W., Basedow, A.M., Konig, B., General Permeation Chromatography Equation and its Application to Taylor Made Controlled Pore Glass Columns, Jou. of Chromatography, 132, (1977), 387-397.

60. Talley, C.P., Bowman, L.M., Quaternised Porous Beads for Exclusion Chromatography of Water-Soluble Polymers, Anal.Chem., 51, (1979), 2239-2244.

61. Barker, P.E., Hatt, B.W., Holding, S.R., Dissolution of Silaceous Chromatographic Packings in Various Aqueous Eluents, Jou. of Chromatography, 206, (1981), 27-34.

62. Unger, K.K., Kern, R., Ninou, M.C., Krebs, K.F., High-Performance Gel Permeation Chromatography with a New Type of Silica Packing Material, Jou. of Chromatography, 99, (1974), 435-443.

63. Applications of Aquapore Columns, Chromatix, California, U.S.A.

64. Dreher, T.W., Hawthorne, D.B., Grant, B.R., Comparison of Open-Column and High Performance GPC in the Separation and Molecular Weight Estimation of Polysaccharides, Jou. of Chromatography, 174, (1979), 443-446.

65. Fukano, K., Komiya, K., Sasaki, H., Hashimoto, T., Evaluation of New Supports for High-Pressure Aqueous Gel Permeation Chromatography: TSK-Gel SW Type Columns, Jou. of Chromatography, 166, (1978), 47-54.

66. Kato, Y., Komiya, K., Sawada, Y., Sasaki, H., Purification of Enzymes by High-Speed Gel Filtration on TSK-Gel SW Columns, Jou. of Chromatography, 190, (1980), 305-310.

67. Kato, Y., Komiya, K., Sasaki, Y., Hashimoto, T., Separation Range and Separation Efficiency in High-Speed Gel Filtration on TSK-Gel SW Columns, Jou. of Chromatography, 190, (1980), 297-303.

68. Alsop, R.M., Progress in Industrial Microbiology, Vol.18, (1983), 1-44.

69. Bristow, P.A., LC in Practice, HETP, (1976), 32-38.

70. Simpson, C.F., Practical High Performance Liquid Chromatography, Heyden and Son Ltd., (1976).

71. Yau, W.W., Kirkland, J.J., Bly, D.D., Modern Size Exclusion Liquid Chromatography, John Wiley and Sons, (1979).

72. Polesuk, J., Howery, D.G., Chromatographic Detection, Jou. Chromatographic Sci., 11, (1973), 226-233.

73. Altgelt, K.H., Segal, L., Gel Permeation Chromatography, Marcel Dekker, Inc., (1971).

74. McNair, H.M., Chandler, C.D., High Performance Liquid Chromatography Equipment III, Jou. Chromatographic Sci., 14, (1976), 477-487.

75. Hassel, J.A., Computer Manipulation and Substraction of GPC Chromatograms, Jou.Polym.Sci.Polym.Lett.Ed., 17, (1979), 111-113.

76. Mukherji, A., An Inexpensive On-Line Data Processing System for GPC, Jou.Liq.Chromatography, 4, (1981), 71-84.

77. Jordan, R.C., Christ, P.J., A Data System for Polymer Characterisation, Application to GPC, Am.Lab., 11, (1979), 71-72,74,76,78-81.

78. Hester, R.D., Mitchell, P.H., A New Universal Calibration Method, Jou.Polym.Sci.Polym.Chem.Ed., 18, (1980), 1727-1738.

79. Ouano, A.C., Quantitative Data Interpretation Techniques in GPC, Jou.Macromol.Sci., - Revs.Macromol. Chem., C9(1), (1973), 123-148.

80. Hatt, B.W., Polymer Molecular Weight Distribution by Gel Permeation Chromatography, Developments in Chromatography-1, Knapman, C.E.H., Applied Science Publ., Essex (1979), 157-199.

81. Grabistic, Z., Rempp, R., Benoit, H., A Universal Calibration for Gel Permeation Chromatography, Jou.Polym.Sci., Part B, 5, (1967), 753-759.

82. Frank, F.C., Ward, I.M., Williams, T., Calibration Procedure for Gel Permeation Chromatography, Jou. Polym.Sci., A-2, 6, (1968), 1357-1369.

83. Balke, S.T., Hamielec, A.E., Gel Permeation Chromatography Calibration Curve from Polydisperse Standards, Ind.Eng.Prod.Res.Dev., 8, (1969), 54-57.

84. Wilde, D.J., Optimum Seeking Methods, Prentice-Hall, Englewood Cliffs, New Jersey, (1964), 151.

85. Tung, L.H., Runyon, J.R., Calibration of Instrumental Spreading for Gel Permeation Chromatography, Jou. Appl.Polym.Sci., 13, (1969), 2397-2409.

86. Cervenka, A., Bates, T.W., Characterisation of Polydisperse Branched Polymers by Means of Gel Permeation Chromatography, Jou. of Chromatography, 53, (1970), 85-93.

87. Smit, J.A.M., Hoogervorst, C.J.P., Staverman, A.J., Dispersion in Gel Permeation Chromatography. A Rapid Numerical Solution to Tungs Integral Equation, Jou.Appl.Polym.Sci., 15, (1971), 1479-1492.

88. Nilsson, G., Nilsson, K., Molecular Weight Distribution Determination of Clinical Dextran by GPC, Jou. of Chromatography, 101, (1974), 137-153.

89. Basedow, A.M., Ebert, K.H., Ederer, H., Hunger, H., Die Bestimmung der Molekulargewichtsverteilung von Polymer en Durch Permeationschromatographie an Porösem glas, 1, Makromol.Chem., 177, (1976), 1501-1524 (GER).

90. Lansing, W., Kraemer, E., A New Method of GPC Calibration Using Dextran Fractions of Low Polydispersity, Jou.Am.Chem.Soc., 57, (1935), 1369-1385.

91. Hartley, H.O., The Modified Gauss-Newton Method for Fitting of Non-Linear Regression Functions by Least Squares, Technometrices, 3, (1961), 269-280.

92. McCrackin, F.L., Calibration of GPC Columns Using Polydisperse Polymer Standards, Jou.Appl.Polym. Sci., 21, (1977), 191-198.

93. Chaplin, R.P., Ching, W., Accurate Calibration of GPC by Use of Broad Molecular Weight Distribution Standards, Jou.Macromol.Sci.Chem., A14, (1980), 257-263.

94. Soeteman, A.A., Separation of Dextrans by GPC, Jou. Polym.Sci., Polym.Phys.Ed., 16, (1978), 2147-2155.

95. Malower, E.G., Montana, A.J., Algorithm for the Determination of Linear GPC Calibration Curve of a Polydisperse Standard, Jou.Polym.Sci., Polym. Phys.Ed., 118, (1980), 2303-2305.

96. Alsop, R.M., Fisons Pharmaceutical Division, Holmes Chapel, Cheshire, Personal Communication.

97. Butera, G., Fisons Pharmaceutical Division, Holmes Chapel, Cheshire, Personal Communication.

98. Alsop, R.M., Vlachogiannis, G.J., Determination of the Molecular Weight of Clinical Dextran by Gel Permeation Chromatography on TSK-PW Type Columns, Jou. of Chromatography, 246, (1982), 227-240.

99. Instructions Manual Servoscribe RE 541.20, Smiths Industries Ltd., Cricklewood, London, U.K.

100. Instructions Manual Differential Refractometer R401, Waters Associates Ltd., Hartford, Cheshire, U.K.

101. Schulz, G.V., Nordt, E., Fraktionierung Polymolekularer Stoffe Durch Verteilung Zwischen Zwei Flüssigen Phasen, Jou.Pract.Chem., 155, (1940), 115-128 (GER).

102. Bronsted, J.N., Molekulgrosse und Phasenverteilung.I., Zeit.Phys.Chem.Brodenstein Festband, 279, (1931), 257-266 (GER).

103. Cantow, M.J.R., Polymer Fractionation, Academic Press, (1967).

104. Schulz, G.V., Die Trennung Polymolekularer Gemische Durch Fraktionierte Fällung, Zeit.Phys.Chem., B46, (1940), 137-156 (GER).

105. Schulz, G.V., Die Verteilungsfunktionen Polymolekularer Stoffe und ihre Ermittelung Durch Zerlegung in Fraktionen, Zeit.Phys.Chem., B47, (1940), 155-193. (GER).

106. Albertsson, P.A., Partition of Cell Particles and Macromolecules, Wiley-Interscience, (1960).

107. Albertsson, P.A., Particle Fractionation in Liquid Two-Phase Systems, Biochimica Et Biophysica Acta, 27, (1958), 378-395.

108. Albertsson, P.A., Frick, G., Partition of Virus Particles in a Liquid Two-Phase System, Biochimica Et Biophysica Acta, 37, (1960), 230-237.

109. Albertsson, P.A., Partition in Polymer Two-Phase Systems - Some Recent Results, Prog.Sep.Purif., 2, (1969), 105-120.

110. Frick, G., Lif, T., Relation Between Size and Distribution of DNA Molecules in a Two-Phase Polymer System, Archives of Biochemistry and Biophysics, Supplement 1, (1962), 271-275.

111. Pharmacia Fine Chemicals, Molecular Weight and Molecular Size Determination, Separation News (March 1972).

112. Flory, P.J., Thermodynamics of High Polymer Solutions, Jou. of Chemical Physics, 9, (1941), 660-661.

113. Huggins, M.L., Solutions of Long Chain Compounds, Jou. of Chemical Physics, 9, (1941), 440.

114. Scott, R.L., Magat, M., The Thermodynamics of High-Polymer Solutions:I. The Free Energy of Mixing of Solvents and Polymers of Heterogeneous Distribution, Jou. of Chemical Physics, 13(5), (1945), 172-177.

115. Scott, R.L., The Thermodynamics of High-Polymer Solutions:II. The Solubility and Fractionation of a Polymer of Heterogeneous Distribution, Jou. of Chemical Physics, 13(5), (1945), 178-187.

116. Flory, P.J., Thermodynamics of High Polymer Solutions, Jou. of Chemical Physics, 10, (1942), 51-61.

117. Flory, P.J., Thermodynamics of Heterogeneous Polymers and their Solutions, Jou. of Chemical Physics, 12(11), (1944), 425-438.

118. Sayre, E.V., The Distribution of Polymer Fractions, Jou. of Polymer Science, 10(2) (1953), 175-183.

119. Okamoto, H., Sekikawa, K., Phase Equilibrium of Polydispersed Polymer Solution and Fractionation, Jou. of Polymer Science, 55, (1961), 597-607.

120. Flory, P.J., Principles of Polymer Chemistry, Cornell University Press, (1953).

121. Kamide, K., Sugamiya, K., Role of Concentration Dependence of Polymer/Solvent Interaction Parameter in the Polymer Fractionation by Successive Precipitational Method, Die Makromolekulare Chemie, 139, (1970), 197-220.

122. Kamide, K., Miyazaki, Y., Abe, T., Experimental Verification of Modern Theory of Molecular Weight Fractionation Based on Solubility Difference, Die Makromolekulare Chemie, 177, (1976), 485-522.

123. Kamide, K., Miyazaki, Y., Abe, A., An Additional Test of Modern Theory of Molecular Weight Fractionation Based on Solubility Difference, Polymer Jou., 9(4), (1977), 395-403.

124. Noda, I., Ishikawa, H., Miyazaki, Y., Kamide, K., Molecular Weight Fractionation of Binary Mixtures of Monodisperse Poly (α-methylstyrene) by the Solubility Difference : Comparison of Experiment with Theory, Polymer Jou., 12(2), (1980), 87-95.

125. Kamide, K., Miyazaki, Y., Effect of Molecular Weight Dependence of the μ-parameter on Phase Equilibrium of Multicomponent Polymer-Single Solvent System : Comparison of Theory with Experiment, Polymer Jou., 13(4), (1981), 325-341.

126. Kamide, K., Abe, T., Miyazaki, Y., Further Study on the Evaluation of Molecular Weight Dependence of μ-parameter by Phase Equilibrium Experiment on Polystyrene-Methylcyclohexane System, Polymer Jou., 14(5), (1982), 355-361.

127. Breitenbach, V.J.W., Wolf, B.A., Untersuchungen von Phasengleichgewichten an Polymerlösungen Mittels Säulenfraktionierung, Die Makromolekulare Chemie, 108, (1967), 263-280 (GER).

128. Alsop, R.M., Barker, P.E., Vlachogiannis, G.J., Fractionation, Purification and Concentration of Dextran Solutions by Ultrafiltration, Jou. Membrane Science, 20(1), (1984), 79-92.

129. Alsop, R.M., Barker, P.E., Vlachogiannis, G.J., Efficient Production of Clinical Dextran from Dextran Hydrolysate, The Chemical Engineer, Jan. (1984), 24-27.

130. Langley, R., Practical Statistics, Pan Books Ltd., (1970).